The elaborate interplay of natural killer cells and vaccinia virus

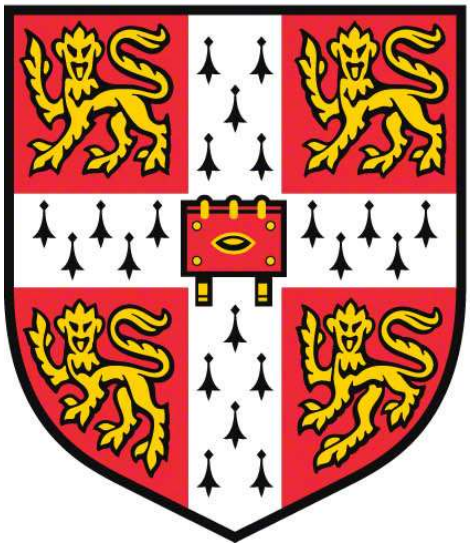

Delphine Marie-France C. Depierreux

University of Cambridge

Emmanuel College

Department of Pathology

Supervisors: Professor Geoffrey L. Smith & Doctor Brian J. Ferguson

This dissertation is submitted for the degree of *Doctor of Philosophy*

April 2020

Preface

This thesis is the result of my own work and includes nothing which is the outcome of work done in collaboration except as declared in the Preface and specified in the text. It is not substantially the same as any that I have submitted, or, is being concurrently submitted for a degree or diploma or other qualification at the University of Cambridge or any other University or similar institution except as declared in the Preface and specified in the text. I further state that no substantial part of my thesis has already been submitted, or, is being concurrently submitted for any such degree, diploma or other qualification at the University of Cambridge or any other University or similar institution except as declared in the Preface and specified in the text. It does not exceed the prescribed word limit for the relevant Degree Committee.

The NCR-Ig fusion proteins were previously generated by Dr Kafai Leung. Dr H. Ren performed the radioactive work for cytotoxic assays. NK cell FACS sorting was conducted by the phenotyping hub at Addenbrooke's. The PMP study is the result of a collaborative effort. The conception and experimental design were outlined by me, cell infection and labelling by me and A. Altenburg, TMT labelling and fractionation by M. Weekes laboratory members, mass spectrometry by CIMR proteomics facility (Robin Antrobus), raw data processing by M. Weekes laboratory. Subsequent data handling, bioinformatic analyses, graphs, interpretation, and FACS-based validation presented in this thesis were made by me. The transcriptomic study was performed in collaboration with the Cambridge Genomic Service (CGS) sequencing facility that prepared the libraries, carried out the sequencing and generated differential gene expression data files. The experimental design, animal work, sample preparation and RNA extraction were done by me. All subsequent data handling, bioinformatic analyses, graphs, interpretation and FACS-based validation presented in this thesis were made by me.

The elaborate interplay of natural killer cells and vaccinia virus

Delphine Marie-France C. Depierreux

Abstract

Vaccinia virus (VACV) is a poxvirus and is the vaccine used to eradicate smallpox. It is also an expression vector for heterologous antigens and an oncolytic virus for cancer therapy. VACV encodes multiple proteins that aid evasion of the host immune response. There is, however, an incomplete understanding of how this immune suppression by VACV is consistent with such a strong immune response and subsequent memory. There is especially little known about the relationship between natural killer (NK) cells and VACV. Previous studies showed that during VACV infection, NK cells proliferate, are activated, limit viral replication, kill VACV-infected cells and display memory-like qualities. However, how NK cells recognise and interact with VACV-infected cells, which ligand(s) trigger NK cell activation, which NK receptors (NKR) are involved, and whether VACV uses strategies to interfere with the NK cell response remains elusive. This thesis aimed to address such questions using screening methods in parallel to candidate-based approach to tackle the challenges caused by the high diversity of NKRs and NK ligands.

First, the responsiveness of murine NK cells to systemic VACV infection was studied *ex vivo*. Transcriptomic analysis, along with validation at the protein level, indicated NK cell activation and preparedness to mediate effector functions. Analysis of NK cell transcriptomic signature indicated that the stimuli triggering NK cell activation in the context of VACV infection correspond primarily with direct cell recognition but also cytokines such as Il-12 and -18, and IFNs. NKRs expression level in response to VACV was investigated, both at the transcript and protein level, and candidate NKRs involved specifically in the response to VACV were defined. Using a published dataset, the human and murine NK cell response to VACV was compared, revealing strong similarities.

Second, the modulation of the plasma membrane (PM) proteome after VACV infection was studied using a proteomic screen that allowed to i) determine how VACV affects NK ligands expression; ii) give insights into VACV host surface protein modulation mechanism; iii) highlight previously unrecognised VACV strategies to evade NK cell response, iv) establish for the first time, a comprehensive analysis of

VACV proteins expressed at the host PM and, v) suggest VACV surface proteins that potentially engage with NK cells.

Third, the impact of the absence of VACV A56, an NK ligand candidate, and the murine natural cytotoxicity receptor (NCR) NKp46, were studied, *in vitro* and *in vivo*, in the context of VACV infection. This confirmed that VACV A56 prevents cell fusion, anchors VACV K2 and VCP (virus complement control protein) at the cell surface and enhances the binding of human and murine NCRs to VACV-infected cells. Further, it revealed that A56 deletion did not affect plaque size or EEV (extracellular enveloped virus) release, did not alter NK ligands surface expression, but led to decreased VACV-infected cells killing by murine NK cells. Lastly, the impact of VACV A56 and NKp46 deletion, on VACV infection outcome were assessed *in vivo,* in the acute and the memory stage and did not reveal substantial differences.

Collectively, these data constitute a valuable resource concerning the interaction of VACV with NK cells and the factors influencing their interplay. These data can contribute to improve the development of VACV-based vaccines vectors and oncolytic viruses, and further our understanding of host-pathogen interactions.

Acknowledgements

I am immensely grateful towards my supervisors Geoff L. Smith and Brian J. Ferguson, for their support and guidance throughout my PhD. journey. I cannot thank you enough for offering me the opportunity to join your labs and consequently benefit from your advice and expertise. I originally undertook postgraduate studies to satisfy my scientific curiosity but have gained so much. Your knowledge in the field and enthusiasm for research never failed to impress me. Your precious advice and directions have shaped me as a researcher and will accompany me for the years to come. I thank you both whole-heartily for your support. Similarly, I sincerely thank my examiners, Louise Boyle and Carlos Maluquer de Motes, for patiently reading through my thesis, leading an enjoyable discussion, and kindly sharing their advice and expertise.

I extend my gratitude to all the present and past members of the Smith and the Ferguson lab. There have been over 30 people who shared part of my PhD journey between the two labs. You made all the bad days and failed experiments a lot more bearable. I knew that there would always be someone happy and ready to help in the lab. I thoroughly enjoyed our lab trips, competitive squash games, cardboard boat races, the endless tea times, birthday cakes, evenings at the cinema and the many pub trips. In particular, I would like to thank Dave for his unlimited kindness and patience during the early stages of my PhD. He was always there to answer all my “quick” questions. Equally, I would like to thank Zhenya for teaching me everything I know about FACS and mice. Without your support, the long hours in the animal facility would have been so much more difficult. You have been an example, in many regards, and I genuinely believe that science needs more people like you. I also owe countless laughing-induced muscle aches to the Fergie girls, Esra, JJ, Osh, Taylor, Jemma, Ben, Ana. Thank you so much for your positivity and for cheering up pathology at all times.

I am thankful for my mentor, Max Nibert, who gave me the opportunity to join his lab at Harvard while I was still a relatively inexperienced researcher. I am forever grateful for having had the privilege to work in your lab and for your continuous support and advice. My passion for scientific research stems from the fantastic time I had in your lab.

I am also grateful to Benoit Muylkens and Nathalie Kirschvink, my master’s thesis supervisors who introduced me to the world of virology with the virus of Schmallenberg. I made my very first steps in the world of research in your lab where I learned skills that have been key in the past few years and will continue to accompany me. Thank you for seeding my interest in science.

I could not have asked for a better environment than Emmanuel College in which to carry out my PhD. Throughout my four years, I have met incredible individuals and the graduate students of Emma have truly been a second family. The times we shared have made my experience at Cambridge a fun and enjoyable ride. I cannot wait to meet up with my alumni Emma fellow in the near future. In that regards, a very special thanks to Sarah who is the kindest and most altruistic person I have ever met; to Chiara for being my PhD buddy from the start to the end, spending long evenings in the library writing and practising the art of procrastination; to Rob and Elise for their wonderful company during the COVID-19 lockdown, to Louis, Maria, Alice, Jason, for your friendship and to all the others for making of Emmanuel college a warm and welcoming environment. In a similar tone, I would like to thank my Belgian friends, neither distance nor time has affected our friendship. I can't wait to visit you all and finally take the time to catch-up extensively.

I heartily thank Eardi, for patiently guiding me through the once mysterious world of statistics, demonstrating the beauty of π^2, fixing my laptop countless times, returning my many lost-properties, and so much more. Beyond all of this, you transformed my time in Cambridge from being outstanding to being exceptional. You made everything easier, funnier and simply better. Thank you for being who you are, and for always being there.

Finally, I would like to thank my family for supporting me, for being understanding about the many months spent away without visiting and making every return at home feel like a special occasion. Thank you for polishing up and putting on your best English accent when you visited and thank you for having my back, as always.

My PhD journey has been immensely rewarding, I gained so much more than simply another degree. The last four years in Cambridge have made my curiosity greater and shaped who I am. Although I am looking forward to the years to come, with all the new challenges and adventures ahead of me, I am deeply saddened to have to finish this beautiful adventure.

Table of contents

Contents

List of abbreviations

µ/mg	micro/milli gram
µ/ml	micro/milli litre
µ/mM	micro/milli molar
aa	Amino acid
Abs	Antibodies
ADCC	Antibody-dependent cellular cytotoxicity
AICL	Activation-induced C-type lectin
APC	Allophycocyanin antigen
B6	C57BL/6
BAT3	HLA-B-associated transcript 3
Bcl	B-cell lymphoma
BLCL	B lymphoblastoid cell lines
BrdU	Bromodeoxyuridine
BSA	Bovine serum albumin
CCL	Chemokine (C-C motif) ligand
CD	Cluster of differentiation
CEACAM1	Carcinoembryonic antigen-related cell adhesion molecule 1
CEV	Cell-associated enveloped virus
CFSE	Carboxyfluorescein succinimidyl ester
CGS	Cambridge Genomic Services
Clr	C-type lectin related
CMC	Carboxy methyl cellulose
CPE	Cytopathic effect
CPXV	Cowpox virus
CRACC	CD2-like receptor-activating cytotoxic cell
Crm	Cytokine response modifier
CRTAM	Class I-restricted T cell-associated molecule
CTL	Cytotoxic T lymphocyte
CTLA-4	Cytotoxic T-lymphocyte-associated antigen 4
CXCL	C-X-C motif chemokine
CXCL16	CXC chemokine 16
CXCR6	C-X-C motif chemokine receptor 6

cNK	Conventional NK cell
cpm	Count per million
CyTOF	Cytometry by time-of-flight
d.p.i.	Days post-infection
DAP	DNAX-activating protein (of molecular mass 10 or 12 kDa)
DAPI	4’,6-diamidino-2-phenylindole
DAVID	Database for Annotation, Visualization and Integrated Discovery
DC	Dendritic cell
DENV	Dengue virus
DMEM	Dulbecco modified Eagle’s medium
DMSO	Dimethyl sulphoxide
DN	Double negative
DNA	Deoxyribonucleic acid
DNAM-1	DNAX accessory molecule-1
DNase	Deoxyribonuclease
DP	Double positive
ds	Double-stranded
DTH	Delayed-type hypersensitivity
DTT	Dithiothreitol
EAT2	Ewing’s sarcoma-associated transcript 2
EBV	Epstein-Barr virus
ECTV	Ectromelia virus
EDTA	Ethylenediaminetetra-acetic acid
EEV	Extracellular enveloped virus
EFC	Entry fusion complex
ER	Endoplasmic reticulum
ERT	EAT-2–related transducer
FACS	Fluorescence-activated cell sorting
Fas	First apoptosis signal
FasL	Fas ligand
FBS	Foetal bovine serum
FC	Fold change
Fc	Fragment, crystallisable
FDR	False discovery rate

FGB	Fibrinogen beta chain
FGL1	Fibrinogen-like protein 1
FITC	Fluorescein isothiocyanate
GAG	Glycosaminoglycan
GFP	Green fluorescence protein
GO	Gene ontology
Gzm	Granzyme
h	hour(s)
HA	Haemagglutinin
HCMV	Human cytomegalovirus
HCV	Hepatitis C virus
HEK293T	Human embryonic kidney
HeLa	Henrietta Lacks
HEPES	4-(2-hydroxyethyl)-1-piperazineethanesulfonic acid
HFFF-TERTs	Human foetal foreskin fibroblast, telomerase reverse transcriptase-immortalised
HIV	Human immunodeficiency virus
HLA	Human leukocyte antigen
hNKp46	Human NKp46
HSV	Herpes simplex virus
HTLV-1	Human T-cell leukaemia virus type I
HVEM	Herpesvirus entry mediator
i.c.	Intracranial
i.d.	Intradermal
i.n.	Intranasal
i.p.	Intraperitoneal
ICAM-1	Intercellular adhesion molecule
IEV	Intracellular enveloped virus
IFI211	IFN induced protein 211
IFI44	IFN induced protein 44
IFIT1	IFN induced protein with tetratricopeptide repeats 1
IFIT3	IFN induced protein with tetratricopeptide repeats 3
IFN	Interferon
IHD-J	International Health Department-J

IL	Interleukin
ImmGen	Immunological genome project
IMV	Intracellular mature virus
IRF	IFN regulatory factor
ISG	IFN-stimulated gene
ITAM	Immunoreceptor tyrosine-based activation motif
ITIM	Immunoreceptor tyrosine-based inhibition motif
i.v.	Intravenous
JAK	Janus activated kinase
KACL	Keratinocyte-associated C-type lectin
kb	Kilobase
KIR	Killer immunoglobulin-like receptor
KLRG1	Killer cell lectin-like receptor G1
Lag3	Lymphocyte-activation gene 3
LAIR	Leukocyte-associated immunoglobulin-like receptor
LC-MS3	Liquid chromatography-tandem mass spectrometry 3
LDH	Lactate dehydrogenase
LFA	Lymphocyte function-associated antigen leukocyte
LLT-1	Lectin-like transcript 1
LTBR	Lymphotoxin B receptor
mAb	Monoclonal antibody
mCMV	Murine cytomegalovirus
MFI	Median fluorescence intensity
MHC-I	Major histocompatibility complex class I
MICA/B	MHC class-I-chain related protein A/B
mNKp46	Mouse NKp46
MOCV	Molluscum contagiosum virus
MOI	Multiplicity of infection
mRNA	Messenger ribonucleic acid
MULT1	Murine ULBP-like transcript 1
MVA	Modified vaccinia Ankara
MV-LAP	Myxoma virus leukaemia-associated protein
MYXV	Myxoma virus
NCR	Natural cytotoxicity receptor

ND50	Neutralisation dose 50
NF-κB	Nuclear factor-kappa B
NK	Natural killer
NKC	NK-gene complex
NKG2D	NK group 2, member D
NKG2DL	NKG2D ligands
NKR	NK receptor
NKRP1	NK cell receptor protein 1
NP-40	Nonidet-P40
NS	Not significant
NTB-A	NK-T-B-antigen
NYCBH	New York City Board of Health
OMCP	Orthopoxvirus MHC-I like protein
p.i.	Post-infection
P/S	Penicillin/streptomycin
PAGE	Polyacrylamide gel electrophoresis
PBMC	Peripheral blood mononuclear cell
PBS	Phosphate-buffered saline
PBS-T	PBS-Tween
PCNA	Exosomal proliferating cell nuclear antigen
PCR	Polymerase chain reaction
PD1	Programmed cell death protein 1
PD-L1	Programmed cell death ligand 1
PD-L2	Programmed cell death ligand 2
PE	Phycoerythrin
PFA	Paraformaldehyde
pfu	Plaque forming unit(s)
PM	Plasma membrane
PMP	Plasma membrane proteomics
PVRIG	PVR-related Ig domain
qPCR	Quantitative PCR
Rag	Recombination activating gene
Rev	Revertant
RK-13	Rabbit kidney cells

RNA	Ribonucleotide
RNA-seq	RNA sequencing
RPMI	Roswell Park Memorial Institute (medium) 1640
RT	Room temperature
SAP	SLAM-associated protein
Sca1	Stem cell antigen 1
SD	Standard deviation
SDS	Sodium dodecyl sulphate
SDS-PAGE	Sodium dodecyl sulphate – polyacrylamide gel
sec	Second(s)
SH2	SRC homology 2
SHIP	SH2-containing inositol polyphosphate 5-phosphatase
SHP	SH2 domain-containing protein
SIGLEC	Sialic acid-binding immunoglobulin-like lectins
SILAC	Stable isotope labelling of amino acid
SLAM	Signalling lymphocytic activation molecule
SRC	Short consensus repeats
ss	Single-stranded
STAT	Signal transducers and activators of transcription
Syk	Spleen tyrosine kinase
TACTILE	T cell–activated increased late expression
TAP	Transporter associated with antigen
TEMED	N, N, N‟, N‟-Tetramethylethylenediamine
TGN	Trans-Golgi network
Th	T helper
TIGIT	T cell immunoreceptor with Ig and ITIM domains
Tim-3	T-cell Ig and mucin-containing domain-3
TLA-1	TNF-like protein 1A
TLR	Toll-like receptor
TNF	Tumour necrosis factor
TRAIL	TNF-related apoptosis-inducing ligand
UL40	Unique long protein 40
ULBP	UL16-binding protein
UV	Ultraviolet

v/v	Volume/volume
VACV	Vaccinia virus
VARV	Variola virus
VCAM-1	Vascular cell adhesion molecule-1
VCP	Virus complement control protein
vGAAP	VACV Golgi anti-apoptotic protein
VZV	Vesicular stomatitis virus
w/v	Weight/volume
WB	Western blot
WCL	Whole-cell lysate
WHO	World Health Organisation
WR	Western Reserve
WT	Wild-type
β2m	β2-microglobulin
γ	Gamma

1 Chapter 1: Introduction

1.1 Natural killer cells: discovery and origin

Natural killer (NK) cells were first identified in 1975 when several independent groups found in nude mice (athymic) a lymphoid cell population capable of mediating cytotoxicity against tumour cell lines without prior exposure (Herberman *et al.* 1975; Kiessling *et al.* 1975). Later, NK cells were discovered to be a critical component of the immune system, particularly for fighting viral infections.

NK cells are lymphocytes and derive from the common lymphoid progenitor (CLP) (Figure 1). The CLP gives rise to two distinct lymphocyte populations, which vary by their size and the timing of their effector functions during infection: small lymphocytes and large granular lymphocytes (Parham 2015). B and T cells are small lymphocytes and require several days to exit their quiescent state and mediate the adaptive immune response. NK cells are large granular lymphocytes and are in a pre-active state, ready to eliminate abnormal cells such as cancer or virus-infected cells. Because of their rapid capacity to mediate these effector functions, NK cells have typically been described as part of the innate immune system, and because the cytokines and chemokines that they secrete shape the subsequent adaptive immune response, NK cells are considered as a bridge between the innate and adaptive immune system. Recently, NK cells were shown to display memory-like qualities that has challenged their long-standing classification as innate lymphocytes.

NK cell maturation stages are characterised by the expression of multiple surface receptors (Kim *et al.* 2002; Yu *et al.* 2013). NK cell maturation is highly dependent on interleukin-15 (IL-15) (Cooper *et al.* 2002) and multiple transcription factors such as GATA3, NFIL, Tbet (reviewed in (Hesslein & Lanier 2011; Luevano *et al.* 2012; Martín-Fontecha *et al.* 2011). Murine NK cell maturation occurs mostly in the bone marrow but also in lymph nodes, spleen, tonsils and thymus (Sojka *et al.* 2014; Yu *et al.* 2013), whilst human NK cell maturation starts in the BM and progress in secondary lymphoid tissues (Lanier *et al.* 1986a).

Because NK cells, B cells and T cells are derived from the CLP, they have in common the expression of many cell surface receptors. Typically, NK cells are identified by the absence of surface CD3 along with the presence of NK1.1 in B6 mice (Glimcher *et al.* 1977; Lanier *et al.* 1986b) or CD56 in humans (Lanier *et al.* 1986a). Once mature, NK cells are found in the bloodstream but also in most tissues. In both species, there are different subsets of mature NK cells, the conventional NK cells (cNK), which are mostly found in the blood and the spleen, and the tissue-resident NK cells, which are mostly found in

the liver, uterus, thymus and lymph nodes. In healthy individuals, cNK cells constitute up to 25 % of circulating lymphocytes in humans, and 2-7 % in mice (Paul & Lal 2017).

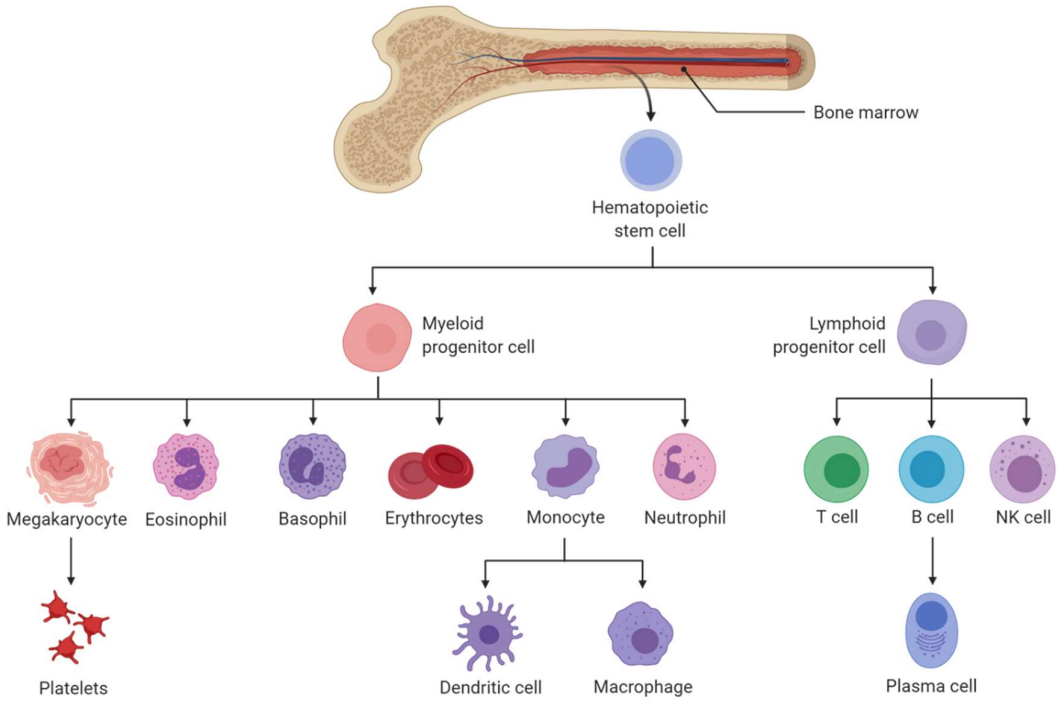

Figure 1 Stem cell differentiation from the bone marrow showing NK cell origin (Opensource diagram from Biorender)

1.2 NK cell functions

1.2.1 NK cell cytotoxic functions

NK cells can kill abnormal cells by two distinct mechanisms: the release of cytolytic granules and the engagement with death receptors. The release of NK cell lytic granules can be triggered via two pathways: classical receptor-mediated activation or antibody-dependent cellular-mediated cytotoxicity (ADCC) (Figure 2).

Classical activation occurs when the sum of inhibitory and activating signals transmitted by NK cell surface receptors leans towards activation. This occurs when such receptors engage with surface ligands whose expression has been altered, for example, after viral infection (Figure 3). ADCC occurs when the NK low-affinity receptor for the Fc fragment of IgG (also called CD16) engages with antibody (Ab) bound to the target cell surface. Upon activation by such mechanisms, NK cells release the content of pre-formed lytic granules at the immunological synapse; the contact zone between the NK cell and the target cell. The granules are released by fusion of the vesicle that contains them with the NK cell PM. This results in the transient surface expression of CD107, which is often used as a

degranulation marker to measure NK cell cytotoxicity (Alter *et al.* 2004). The granules contain cytolytic proteins such as perforin and granzyme (Gzm). Perforin leads to the formation of a pore in the membrane of the target cell, which allows the entrance of Gzm that triggers apoptosis of the target cell.

The other pathway used by NK cells to eliminate aberrant cells is to express ligands such as Fas ligand (FasL), TRAIL (TNF-related apoptosis-inducing ligand) and TNF (Tumour necrosis factor). These surface proteins engage with death receptors expressed by the target cell, and trigger signalling cascade leading to apoptosis of the target cell (Arase *et al.* 1995; Kayagaki *et al.* 1999; Montel *et al.* 1995a; Takeda *et al.* 2001).

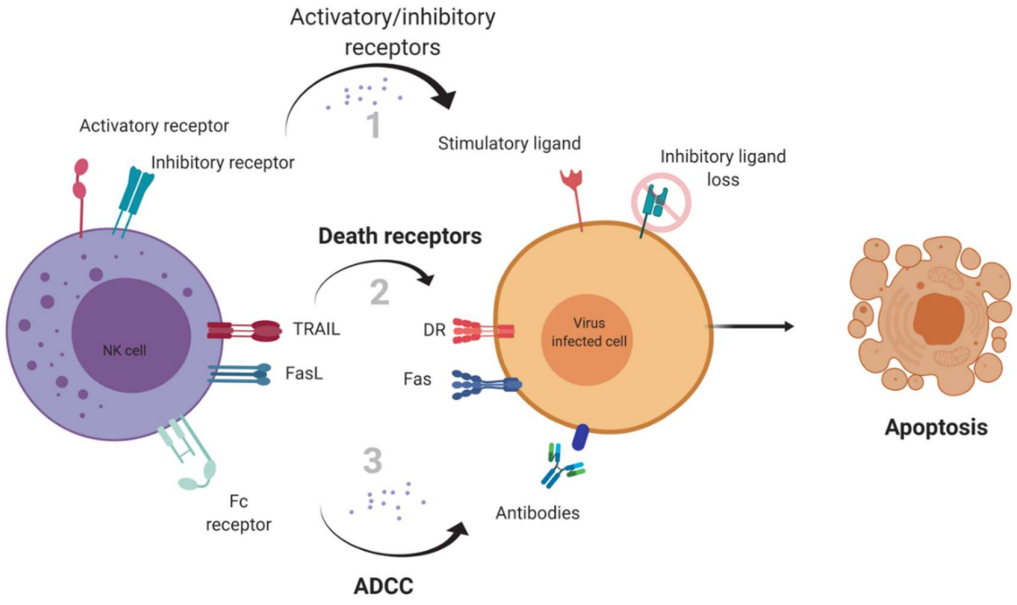

Figure 2 Schematic representing the three pathways by which NK cells trigger target cell apoptosis. 1) Classical receptor-mediated activation occurs when the sum of the activating and inhibitory signals transmitted by NK surface receptors leans toward activation, which leads to the release of cytotoxic granules. 2) Death receptor-mediated apoptosis occurs when the DR-ligand secreted or expressed at the surface of the NK cell engage with its specific DR, expressed by the target cell. 3) ADCC occurs when NK cell Fc receptor engages with the Fc portion of an Ab bound to its ligand on the surface of the target cell, which leads to the release of cytotoxic granules.

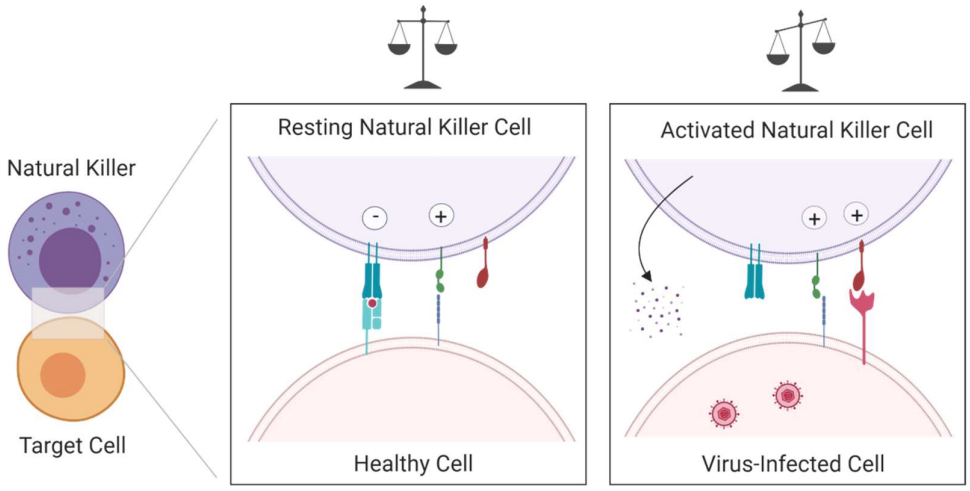

Figure 3 Schematic representing NK cell activation by classical surface receptor-mediated activation. Left panel: NK cells express surface receptors that transmit activating and inhibitory signals upon engagement with their ligands on healthy cells; leading to an overall null signal. Right panel: virus-infected cell surface ligands are altered, which leads to loss of engagement with NK cell inhibitory receptors and/or additional engagement with NK cell activating receptor. Overall, the sum of the signals results in NK cell activation.

1.2.2 NK cells shape the adaptive immune response

Besides their cytolytic capacities, activated NK cells secrete chemokines and cytokines, such as IFNγ or TNF-α, that contribute to inflammation and shape the subsequent adaptive immune response. IFNγ is a type II interferon (IFN) and is mainly secreted by NK cells early during the response to viral infection. Besides its direct antiviral effect, IFNγ can be sensed by innate immune cells such as macrophages. Macrophages are early responders to IFNγ, which enhances their activation and leads to a greater secretion of inflammatory cytokines such as lL-12. The latter then contributes to activate NK cells further in a positive feedback loop.

NK cell secretion of IFNγ and TNF-α, as well as direct cell-to-cell contact, can also trigger dendritic cell (DC) maturation (Piccioli *et al.* 2002). Mature DCs secrete IL-12 that contributes to NK activation in a positive feedback loop. Further, the interaction between DCs and NK cells can replace the function of CD4+ T cells to help to trigger a CD8+ T cell response (Adam *et al.* 2005; Mocikat *et al.* 2003). Importantly, NK cell secretion of IFNγ leads to Th1 polarisation of T cells (Martín-Fontecha *et al.* 2004; Morandi *et al.* 2006; Schuster *et al.* 2016), which is important for the anti-viral response (Maloy *et al.* 2000).

1.2.3 NK cell memory functions

More recently, NK cells were described to mediate protection via memory qualities (reviewed in (Holmes & Bryceson 2016; O'Sullivan *et al.* 2015; Pahl *et al.* 2018). In 2006, the concept of antigen-specific memory NK cells was introduced by O'Leary and colleagues after research based on the contact hypersensitivity response (CHS) model. This group observed that hapten-sensitised mice lacking T and B cells (recombination activation gene 2 (*Rag*2) -/-) could develop a CHS, which is an induced adaptive immunity model and is typically mediated by T and B cells (O'Leary *et al*.,2006). This immune response was abolished when NK cells were depleted and could not develop in a mouse model lacking mature NK, T and B cells (IL2rg -/-, *Rag*2-/-). Moreover, this group observed that the CHS persisted for more than four months, was specific to the hapten used for sensitisation and was transferable when hepatic NK cells were adoptively transferred to naïve mice (O'Leary *et al*.,2006).

The concept of antigen-dependent NK cell memory has been extended to different viral antigens. Sun and colleagues demonstrated that during mouse cytomegalovirus (mCMV) infection, the interaction between the activating NKR Ly49H and the mCMV glycoprotein m157 leads to a 100 (spleen) or 1000 (liver) fold expansion of antigen-specific NK cells (Sun *et al.,* 2009). These cells form a pool of memory NK cells capable of a recall response, characterized by enhanced IFNγ secretion and degranulation capacities, which confers protection upon re-challenge with mCMV (Sun *et al*., 2009).

Additionally, Paust and colleagues reported that adoptive transfer of hepatic NK cells from *Rag*1 -/- mice (lacking mature T and B cells) immunised with virus-like particles (influenza A virus, vesicular stomatitis virus or HIV-1) protects IL-2rg -/-, *Rag*2-/- mice (a model lacking mature NK, T and B cells) when challenged by the same virus (Paust *et al.,* 2010). Importantly, Gillard and colleagues identified a subset of NK cells expressing Thy1 that protects against vaccinia virus (VACV) challenge upon adoptive transfer in *Rag*-/- mice (Gillard *et al.,* 2011). Another group also reported that primate NK cells can mount memory response to simian immunodeficiency virus (SIV) infection and vaccination (Reeves *et al.* 2015), demonstrating that NK memory is not limited to rodents.

In humans, like murine Ly49H+ NK cells expand during mCMV infection, NKG2C+ NK cell frequency is increased during HCMV infection (Gumá *et al.* 2006). A clonal expansion of NKG2C+ NK cells is also observed during HCMV reactivation in HCMV seropositive individuals (Della Chiesa *et al.*, 2012; Lopez-Vergès *et al.*, 2011). This proliferation is specific since it does not occur in HCMV experienced individuals exposed to HSV (herpes simplex virus) or Epstein-Barr virus (EBV) (Björkström *et al.* 2011; Hendricks *et al.* 2014). Further, this interaction is thought to be driven by unique long protein 40

(UL40)-derived peptides presented by HLA-E, which could be recognised by NKG2C+ NK cells but not NKG2A (Hammer *et al.* 2018).

Recently, Nikzad and colleagues used humanised-mice vaccinated with HIV-envelope proteins to demonstrate that human hepatic NK cells mediate a recall response and kill cells in a vaccination-dependent and antigen-specific manner (Nikzad *et al.* 2019). These findings suggest that human NK cells display memory qualities and could potentially be trained by vaccination. In addition to the antigen-specific NK memory cells, Cooper and colleagues demonstrated that pro-inflammatory cytokines alone could induce memory-like features in NK cells. Indeed, splenic NK-cells activated by IL-12, IL-15 and IL-18 and transferred in naïve *Rag*1-/- mice persist up to three weeks and present an enhanced IFNγ production upon re-stimulation (Cooper *et al.* 2009).

Taken together, these observations show that NK cells possess the four typical characteristics of adaptive immune cells; the ability to mount a specific response to a pathogen, undergo clonal expansion, give rise to long-lived progeny and mediate a recall response to a pathogen encountered previously. However, a lot remains to be discovered about the factors that influence their development and the mechanisms responsible for their selection as memory cells.

1.3 NK cell activation regulation

NK cell homeostasis and activation are subject to two major regulators: i) cytokines and chemokines, ii) integration of signals emanating from germline-encoded cell surface receptors.

1.3.1 Cytokine-mediated regulation

Amongst the cytokines and chemokines sensed by NK cells, IL-2, IL-12, IL-15, IL-18 and IFNs are key regulators (Dokun *et al.* 2001). Such cytokines can be produced by the infected cell itself or by DCs and macrophages at the site of infection (Nguyen *et al.* 2002).

Upon viral infection, the infected target cells and DCs produce type I IFN such as IFN-α and -β. These cytokines cause NK cell proliferation and differentiation into more cytotoxic subsets by both direct action on NK cells (Mack *et al.* 2011; Martinez *et al.* 2008) and by triggering IL-15 production (Biron *et al.* 1999). Macrophage-derived IL-15 is critical for the generation, accumulation and survival of NK cells (Kennedy *et al.* 2000; Nguyen *et al.* 2002), and IL-15 presentation by DCs *in trans* leads to NK cell activation (Koka *et al.* 2004; Lucas *et al.* 2007).

Early after infection, DCs also produce IL-2, which promotes NK cell proliferation, lowers their activation threshold, and enhances their cytotoxic activity (Biron *et al.* 1990; Henney *et al.* 1981; Koka *et al.* 2004; Trinchieri 1989). Macrophages and DCs produce IL-12 that promotes NK cells recruitment, proliferation and enhance their cytotoxicity and IFNγ secretion (Nguyen *et al.* 2002; Parham 2015). IL-

12 and lL-18 act in concert to provide co-stimulatory signals to NK cells and this is necessary during viral infection for optimal NK cell activation (Gherardi 2003; Ortaldo *et al.* 2006; Sun *et al.* 2009a).

1.3.2 Receptor-mediated regulation

Unlike T cells, NK cells do not carry out germline receptor rearrangements. Instead, they express multiple germ-line encoded surface receptors whose engagement with cognate ligands leads to inhibitory or activator signals that determine NK cell activation status (Lanier *et al.* 1986b; Trinchieri 1989). Most of these receptors are C-type lectins or have immunoglobulin (Ig)-like folds.

Inhibitory receptors have in their cytoplasmic tails immunoreceptor tyrosine-based inhibitory motifs (ITIMS). Upon engagement of the receptor, these become phosphorylated and recruit SH2 domain-containing protein tyrosine phosphatase (SHP), which prevents NK activation (reviewed in (Billadeau & Leibson 2002; Lanier 2003; Vivier 2004)).On the other hand, NK cell activating receptors have immunoreceptor tyrosine-based activating motifs (ITAMS) in their cytoplasmic domain. Upon engagement of the receptor, these become phosphorylated, and recruit protein tyrosine kinases that trigger signalling cascades leading to NK activation (reviewed in (Billadeau & Leibson 2002; Lanier 2003; Vivier 2004)). Some activating receptors do not have ITAMS in their cytoplasmic tails and rely on the association with an adapter that contains ITAMS such as DNAX-activating protein of 12 kDa (DAP12) (Lanier *et al.* 1998).

NK cells encode many different self-surface receptors, some of which are conserved amongst mice and humans (reviewed in (Carrillo-Bustamante *et al.* 2016; Lanier 1998; Ravetch 2000) (Figure 4 and Figure 5). Each NK cell expresses only a subset of these receptors, which creates diversity amongst NK cells and explains why the NK cell response is clonally distributed (Parham 2015). All NK cells express a combination of activating and inhibitory receptors (Parham 2015). Such receptors are discussed in the subsequent sections. It is important to note that due to the high number of NK cell receptors, they cannot all be described in this thesis and that some NK cell receptors might not have been identified as such yet.

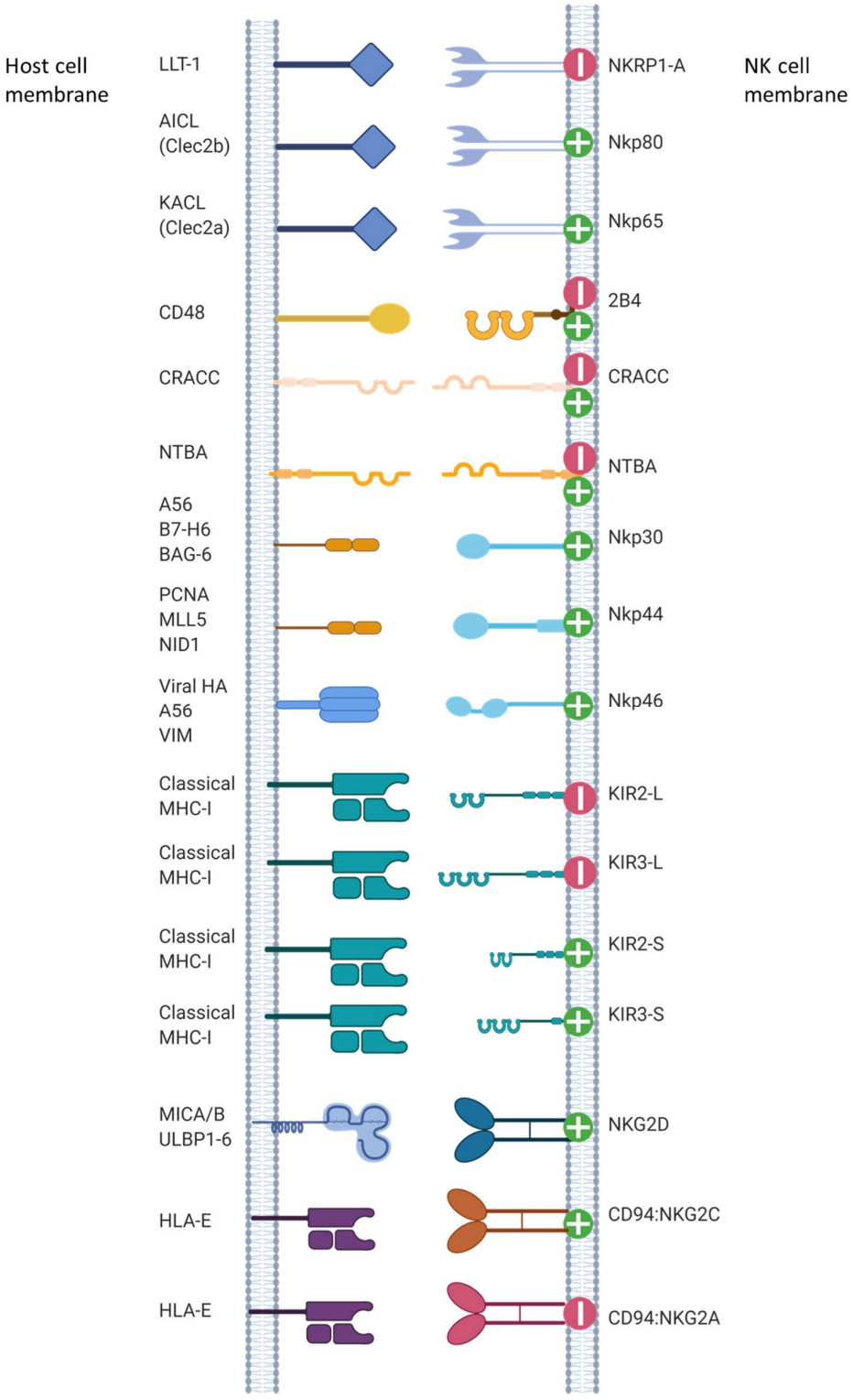

Figure 4 Human NK cell receptor-ligands couples. The main receptors that regulate NK cells activation status are shown with their respective ligands. The signal they transmit upon engagement is indicated by a "+" for activating signals and "–" for inhibitory signals.

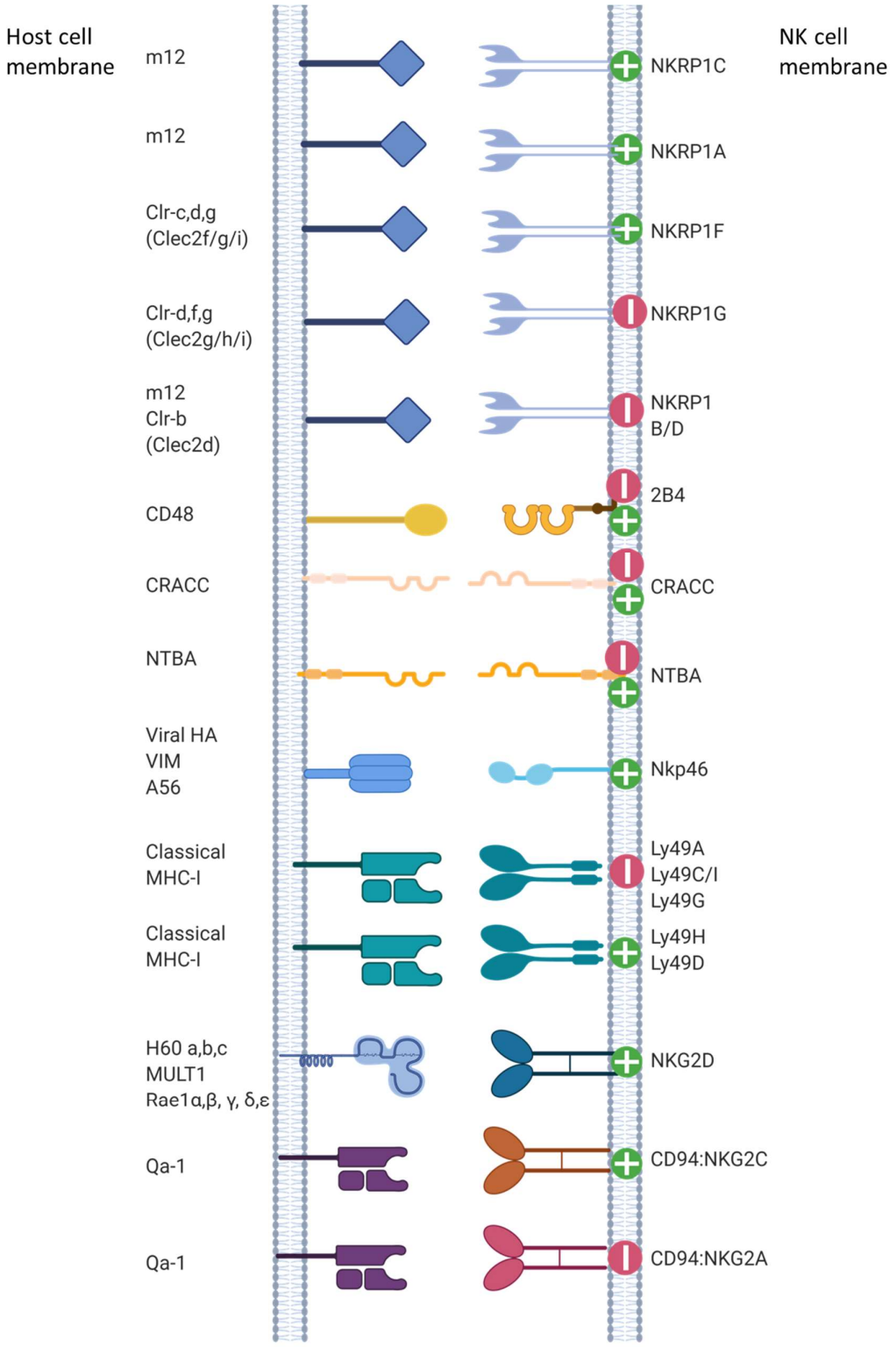

Figure 5 Murine NK cell receptor-ligands couples. The main receptors that regulate NK cells activation status are shown with their respective ligands. The signal they transmit upon engagement is indicated by a "+" for activating signals and "–" for inhibitory signals.

1.3.2.1 Receptors for MHC-I surveillance

One of the main family of receptors regulating NK cell activation, engages with major histocompatibility complex class I (MHC-I). MHC-I antigen presentation plays a major role in the detection of viral infection. MHC-I is a heterodimer made of β2-microglobulin in association with a type I integral membrane protein called heavy chain (Jones 1997). The MHC-I complex is also called human leukocyte antigen (HLA) system in humans and histocompatibility system 2 (H-2) in mice. In humans, there are six MHC-I heavy chains: HLA -A, -B, -C (classical HLA-I) and HLA -E, -F, G (non-classical HLA-I). The mouse H2 region also encodes classical and non-classical MHC-I, and these have homology with the human system. For example, the non-classical murine Qa-1, is the functional homologue of human HLA-E.

Classical MHC-I are polymorphic, ubiquitously and heavily expressed, and they can interact with T and NK cell surface receptors. Non-classical MHC-I are oligomorphic and their expression is usually low or restricted to certain tissues. HLA-E and -G are respectively expressed at low levels in most nucleated cells or limited to certain tissues such as the placenta (Alegre *et al.* 2014). HLA-E interacts with T and NK cells via NKG2A and NKG2C, whilst HLA-G can interact with the LILRB NKR but is mainly thought to have an important role in pregnancy. HLA-F is least studied, is mainly expressed intracellularly and is thought to mediate endocytosis of other HLA that have lost their peptide at the cell surface (Parham 2015).

In a healthy individual, MHC-I is expressed on the surface of all nucleated cells and presents intracellular peptides derived from self-molecules, therefore enabling "self-surveillance" by T and NK cells. In the context of viral infection, MHC-I can present peptides derived from viral proteins or host proteins that would normally not be presented, which alerts the immune system that the cell is infected. To avoid this, some viruses have evolved strategies to suppress MHC-I expression. This helps them to evade T cell-mediated recognition, but at the same time triggers the NK cell response by a phenomenon known as "missing self" (Ljunggren & Kärre 1990). The missing-self hypothesis suggests that NK cells become activated by recognising the absence of MHC-I (reviewed in (Kärre 2008)). In humans and mouse, there are two main NK cell receptor systems involved in the surveillance and detection of "missing-self".

Firstly, there is a highly conserved interaction between CD94/NKG2x (x being -A,-E,-C) with HLA-E, which presents peptides derived from the leader sequence of HLA-A,-B, -C and is conserved in mouse and humans. CD94 forms heterodimers at the cell surface with NKG2A and NKG2C. These transmit, respectively, inhibitory and activating signals (Houchins *et al.* 1997) upon recognition of HLA-E in human and Qa-1 in mouse (Borrego *et al.* 1998; Braud *et al.* 1998a; Lee *et al.* 1998). CD94 also forms

a heterodimer with NKG2E. In humans, this complex is found intracellularly whilst in mice, NKG2E is highly similar to NKG2C (91 % aa identity) and mediates the same function (Orbelyan *et al.* 2014; Vance *et al.* 1999). The expression of HLA-E and Qa-1 is dependent on the leader sequence of other HLA molecules (Aldrich *et al.* 1994; Houchins *et al.* 1997) and is expressed at a very low level in comparison to other classical HLA-I.

Secondly, there is the highly polymorphic interaction of KIRs in humans and Ly49 in mouse, with classical HLA-I (HLA-A, -B, -C) that present intracellular peptides. Human KIRs are immunoglobulin-like surface receptors and are highly polymorphic and owe their name to the fact that the first KIR to be discovered mediated inhibitory functions. However, KIRs can mediate both activating and inhibitory functions. Their nomenclature is based on the number of extracellular domains (D) and the length of their cytoplasmic tail, which is either short (S) or long (L) and mediate inhibitory or activating signals, respectively (Marsh *et al.* 2003). The interaction between KIRs and HLA-A,-B,-C is restricted to four epitopes, namely A11/3, Bw4, C1 and C2. Those four epitopes are mutually exclusive within each single HLA allotype. All HLA-C can interact with KIRs, whilst approximately 45 % of HLA-A and 36 % of HLA-B can interact with KIRs (Parham *et al.* 2012). Further, some KIRs are sensitive to the peptide presented by MHC-I complex (Malnati *et al.* 1995; Saunders *et al.* 2020); reviewed in (Cassidy *et al.* 2014)).

The Ly49 receptors are the murine functional homologues of human KIRs (Barten *et al.* 2001). In B6 mice, seven members of the Ly49 family can be expressed at the surface of mature NK cells (Moussa *et al.* 2013). Ly49H and D have activating functions (Mason *et al.* 1996), whilst Ly49A/F/G/C/I have inhibitory functions (Karlhofer *et al.* 1992). Interestingly, the binding of Ly49C and Ly49I receptors with H-2 is peptide sensitive (Franksson *et al.* 1999; Hanke *et al.* 1999; Wight *et al.* 2018).

1.3.2.2 NK cell activating receptors

Although detection of MHC-I downmodulation is a strong inducer of NK cell activation, the absence of MHC-I does not always result in NK cell killing. Indeed, NK cells can kill cells whose MHC-I expression is elevated, demonstrating that other NKRs are involved in the regulation of NK cell activation.

NKG2D (NK group 2, member D) is a well-described activating receptor conserved in mice and humans and is expressed as a heterodimer. In humans, NKG2D recognises MICA and MICB (MHC-I chain related) as well as ULBP1-6 (UL16 binding protein encoded by RAET1) (Bacon *et al.* 2004; Cosman *et al.* 2001; Kubin *et al.* 2001). In mice, NKG2D recognises the H-60 family (H60a, H60b, and H60c), the Rae family (retinoic acid early inducible gene 1) (Rae1α, Rae1β, Rae1γ, Rae1δ, Rae1ε), and MULT1 (murine ULBP-like transcript) (Carayannopoulos *et al.* 2002; Cerwenka *et al.* 2000; Diefenbach *et al.* 2000). Such ligands are often called “stress ligands” because they are expressed at low levels in healthy cells but upregulated following stress such as viral infection (Raulet *et al.* 2013).

Natural cytotoxicity receptors (NCRs) are Ig-like type I glycoproteins that transmit activating signals and are conserved in mice and humans. Human NK cells express three NCRs; NKp30 and NKp46, which are virtually expressed on all NK cells, and NKp44 that is expressed only upon activation (Pende *et al.* 1999; Sivori *et al.* 1997; Vitale *et al.* 1998). NKp46 is the only conserved NCR in mouse (Hollyoake 2005). These receptors recognise ligands expressed by cancer cells and multiple viral ligands as detailed in section (1.4.1.1), making receptors from this family good candidates to be studied in the context of viral infections.

The NKRP1 (NK cell receptor protein 1) receptors form another family of NKRs conserved between human and mice. In B6 mice, there are five functional NKRP1 receptors; NKRP1 -A, -C, -B/D, -F, -G, their main ligands are typically C-type lectin-related proteins (Clr) and are encoded in close proximity to their receptors (Iizuka *et al.* 2003). Three members of this family are activating (-A, -C, -F) and two inhibitory (-B/D,-G). NKRP1C is also known as NK1.1 and is a marker used to phenotype murine NK cells since it is expressed on all NK cells (Glimcher *et al.* 1977). NKRP1B/D recognises Clr-b (*clec2d*), NKRP1F recognises Clr-c/d/g (*clec2f/g/i*) (Aust *et al.* 2009; Rahim *et al.* 2015; Skálová *et al.* 2012), NKRP1G recognises Clr-d/f/g (*clec2g/h/i*) and NKRP1A and -C were recently found to recognise the mCMV m12 protein to mediate activating functions, whilst NKRP1B/D interacts with m12 to mediate inhibitory signals (Aguilar *et al.*, 2017; reviewed in Bartel *et al.*, 2013). In humans, NKRP1A engages with lectin-like transcript 1 (LLT1, *clec2d*) to transmit an inhibitory signal. The ligand pairs Nkp80: AICL (Activation-induced C-type lectin) (*clec2b*) (activating) and NKp65: KACL (Keratinocyte-associated C-type lectin) (*clec2a*) (activating) have been proposed to be homologues to NKRP1:clr murine system (Vogler & Steinle 2011).

1.3.2.3 NK cell receptors with dual functions

Receptors from the signalling lymphocytic activation molecule (SLAM) family are expressed in mice and human NK cells and can mediate both activating and inhibitory signals (reviewed in (Veillette 2010). The function of SLAM receptors is determined by the absence or presence of adaptors; SLAM associated protein (SAP) family, (SAP, *SH2D1A*), Ewing's sarcoma-associated transcript (EAT-2A/B, *SH2D1B1*) and EAT-2–related transducer (ERT, *SH2D1B2*). SLAM receptors mediate activating signals when these adaptors are co-expressed.

In the absence of those adaptors, the SLAM receptors can interact with SH2-containing inositol polyphosphate 5-phosphatase (SHIP-1, *INPP5D*), SH2 domain-containing protein-1 (shp1, *PTPN6*) and -2 (shp2, *PTPN11*) and mediate inhibitory signals. All SLAM receptors can associate with the three adaptors, except for CRACC (CD2-like receptor-activating cytotoxic cell) that does not associate with SAP but associates with EAT-2 and ERT reviewed in (Veillette 2010). Human and murine NK cells

express SLAMF4 (2B4), SLAMF6 (NTBA or Ly108) and SLAMF7 (CRACC or CD319). The former recognises CD48, whilst the two latter are engaged in homotypic interactions (Brown *et al.* 1998).

1.4 NK cells and diseases

NK cells are crucial components of the immune system and can either contribute to disease control or enhance it. Many association studies indicate a role between HLA and KIR combinations in the outcome of infectious diseases (reviewed in (Walter & Ansari 2015), autoimmune/inflammatory disorders (reviewed in (Agrawal & Prakash 2020)), cancer (reviewed in (Augusto 2016)) and reproduction (reviewed in (Colucci 2017). Their role in disease has been inferred from functional or correlation studies, and the study of patients with NK cell deficiency or dysfunction.

In individuals lacking NK cells, clinical signs are typically premature death, uncontrolled or recurrent viral infection, or enhanced susceptibility to cancer (Biron *et al.* 1989; Etzioni *et al.* 2005; Orange 2013). In some instances, NK cell absence does not result in clinical signs, suggesting that NK cells are redundant with other immune components (Parry *et al.* 2016; Vély *et al.* 2016). NK cell deficiency in humans is rare and refers to a condition where NK cell abnormality is the major factor contributing to the immunodeficiency. NK cell deficiency represents a small subset of a large group of primary deficiencies that include (~40) dysfunction/absence of NK cells which only have a minor contribution to the clinical immunodeficiency. Thus far, six genes (*GATA2, GINS1, IRF8, MCM4, RTEL1,* and *FCGR3A*) have been identified to cause NK cell deficiency in humans, although others are likely to exist but remain elusive/unpublished (reviewed in (Orange 2020)).

The role of NK cells in controlling tumour growth and metastasis is well established. It is known that NK cells typically recognise and attack cancer cells that downregulate surface expression of inhibitory ligands such as MHC-I or up-regulate activating stress ligands such as NKG2D ligands. Medium to high NK cell activity has been negatively correlated to the risk of developing cancer in an eleven year-long study (Imai *et al.* 2000). Cancer immunotherapy includes IL-2 administration to activate NK cells *in vivo* or adoptive transfer of NK cells activated *ex vivo* with IL-2 (Hayes *et al.* 1995; Miller *et al.* 2005; Rosenberg 1984). NK cells can also be modified to express a chimeric receptor that enhances their selectivity towards cancer cell (reviewed in (Wang *et al.* 2020)).

Further, the control of viral infection is another well-established role of NK cell. NK cells recognise and eliminate virus-infected cells (see section 1.4.1.1). Mice or humans with NK cell deficiency or dysfunction are more susceptible to viral infection, particularly herpesviruses and papillomavirus (Bukowski *et al.* 1984, 1983; Delano & Brownstein 1995b; Orange 2013). Many association studies link HLA/KIR combinations with the outcome of viral disease such as HIV (Mori *et al.* 2019), SIV (Walter & Ansari 2015), HCV (Gardiner 2015) as reviewed in (Blackwell *et al.* 2009; Rajagopalan & Long 2005).

Another evidence of the role of NK cells during viral infection is the myriad of mechanisms evolved by viruses to evade their response. CMV interplay with NK cells is the best-characterized model (Babić *et al.* 2011; Goodier *et al.* 2018; Lisnić *et al.* 2015) but other viruses such as HCV, influenza, HIV, KHSV and some orthopoxviruses have also evolved strategies to evade the NK cell response (reviewed in (Jonjić *et al.* 2008)). However, NK cells are not always beneficial during infectious disease as NK cell overproduction of cytokines can have a negative impact and contribute for example to liver damage during hepatitis infection or suppress T cell response (Fisicaro *et al.* 2019; Ghosh *et al.* 2016). Besides their role in viral infection, NK cells are also reported to contribute to fighting fungal (Ogbomo & Mody 2017; Vitenshtein *et al.* 2016), parasitic (Burrack *et al.* 2019) and bacterial infections(Crespo *et al.* 2020).

Additionally, multiple studies indicate that NK cells play a role in autoimmune disease. Certain HLA/KIRS combinations are associated with the risk of developing autoimmune diseases such as lupus, psoriasis, ankylosing spondylitis, multiple sclerosis, rheumatoid arthritis, type I diabetes (reviewed in (Agrawal & Prakash 2020)). Further, multiple studies have linked an NK deficit in peripheral blood with autoimmune diseases (reviewed in (Fogel *et al.* 2013b). However, it is unclear whether this reflects a true deficit or NK cell sequestration in other tissues since filtrating NK cells were observed to accumulate in pancreas islets of diabetes I patients, hair follicle of alopecia areata patients and muscle of juvenile dermatomyositis patients (reviewed in (Fogel *et al.* 2013b). Further, several studies have reported both a beneficial or detrimental correlation between NK cell activity and autoimmune disease. For example, in rheumatoid arthritis NK cells enhance the disease, whilst in a mouse model for multiple sclerosis, NK cell depletion leads to enhanced pathology (Morandi *et al.* 2008), as reviewed in (Mandal & Viswanathan 2015). Another controversial role of NK cell response is the case of graft-versus-host disease (reviewed in (Simonetta *et al.* 2017).

Together, these studies illustrate the importance of NK cells in various disease and the importance to understand their biology to exploit their functions to our advantage.

1.4.1 NK cells and viruses

Viruses can be defined as obligate intracellular parasites that infect all cellular forms of life. Whether viruses should be considered alive or not remains an opened question since viruses cannot survive outside of a host and typically require the cellular machinery to complete their infection cycle. Because viruses vary greatly in size, shape, structure, replication strategy, they can be classified in multiple ways. Despite this diversity, a common feature of all viruses is their ability to express genetic

information into mRNA. The Baltimore classification is based on this characteristic and allows to group all viruses into seven different groups based on the nature of their nucleic acids and their strategy to express genetic information into mRNA (Baltimore 1971).

1.4.1.1 NK cell recognition of virus-infected cells

Recognition of MHC-I downregulation during viral infection, known as the missing self-hypothesis, was thought to be the only mechanism by which NK cells recognise and eliminate virus-infected cells. However, NK cells can efficiently eliminate virus-infected cells whose MHC-I expression is maintained, indicating the relevance of other mechanisms involved in this recognition process (reviewed in (Addou-Klouche 2017; Khakoo & Carrington 2006)). Several studies have demonstrated the importance of activating receptors during viral infection and the recognition of virus-infected cells. Such receptors recognise multiple ligands, and in some instance, viral proteins.

The best-characterised example of NK recognition of a virus-infected cell is the case of mCMV infection in B6 mice. In this model, the mCMV m157 protein is expressed on the surface of infected cells and is recognised directly by the activating NKR Ly49H (Arase *et al.* 2002; Smith *et al.* 2002b). This interaction drives the preferential expansion of the Ly49H+ subset of NK cells, which subsequently form a pool of NK cells with memory qualities. Such cells display enhanced activity upon subsequent encounter with mCMV and mediate protection upon transfer in a naïve animal challenged with mCMV (Sun *et al.* 2009b, 2010).

Recently, the mCMV m12 protein was discovered to be a decoy ligand that engages with NKRP1-B/D to inhibit NK cell functions (Aguilar *et al.* 2017). Further, this study demonstrated that m12 is also recognised by two other members of the same receptor family, NKRP1-A and -C, which transmit activating signals (Aguilar *et al.* 2017). Together, this demonstrates the co-evolution between NK cell receptors and viral ligands and illustrates the importance of this family of receptors in the recognition of virus-infected cells.

Another viral ligand, the influenza haemagglutinin (HA) is recognised by NKp46 and NKp44. (Arnon *et al.* 2001; Mandelboim *et al.* 2001). Subsequently, it was shown that NKp46-deficient mice present a higher mortality to influenza virus than their wild-type (WT) counterparts (Gazit *et al.* 2006). Remarkably, other viral ligands are also recognised by NKp46, such as the HA of Sendai virus (Arnon *et al.* 2001), the HA of poxviruses (Jarahian *et al.* 2011), the reovirus sigma 1 protein (Bar-On *et al.* 2017) and the HA of Newcastle disease virus (Jarahian *et al.* 2009). Further, the human 2B4 (*slamf4*) and LY108 (*slamf6*) receptors bind influenza HA via N-glycosylation and lead to NK cell co-stimulation (Duev-cohen *et al.* 2015).

1.4.1.2 Viral evasion of the NK cell response

Given the importance of NK cells in viral infection, it is not surprising that viruses have evolved a myriad of strategies to evade the NK cell response (reviewed in (Jonjić *et al.* 2008; Jost & Altfeld 2013; Orange *et al.* 2002). Human cytomegalovirus (HCMV) is the best model for virus-NK cell interactions since many of the mechanisms it has evolved to evade the NK cell response are well described. Other viruses such as HSV, HCV, HIV, KHSV (Kaposi sarcoma-associated herpesvirus), DENV (Dengue virus) are also known to have developed strategies to prevent NK cell activation. Examples of such mechanisms are detailed below.

HCMV has evolved several proteins that downmodulate HLAs selectively. HCMV proteins US2 and US11 target HLA-A and HLA-B for degradation but spare HLA-E and HLA-C. This enables evasion of the T cell response but maintains NK cell inhibition via inhibitory receptors engaging with HLA-E and -C (Gewurz *et al.* 2001; Machold *et al.* 1997). HCMV UL40 has similarity with HLA-I sequence, and its leader peptide promotes HLA-E expression leading to NK cell inhibition via the engagement with NKG2A (Tomasec *et al.* 2000; Ulbrecht *et al.* 2000). HCMV UL18 is a MHC-I homologue and engages with LILRB1 to inhibit NK cell activation (Shiroishi *et al.* 2003, 2006). HCMV UL16 protein prevents expression of MICB and ULBP1-2, whilst UL142 prevents MICA expression, consequently preventing NKG2D-mediated NK cell activation (Cosman *et al.* 2001; Kubin *et al.* 2001).

HIV Nef protein leads to selective endocytosis of HLA-A, -B (Cohen *et al.* 1999) while HIV Vpu can mediate downregulation of HLA-C with a magnitude that varies amongst HIV strains (Bachtel *et al.* 2018). KSHV K5 protein leads to endocytosis of HLA-A and -B but also degradation of two activating NK ligands, ICAM-1 (intercellular adhesion molecule 1) and B7-2 (Ishido *et al.* 2000b, 2000a). HCV E2 protein binds CD81 directly on NK cells and prevents NK cell activation and cytotoxic functions (Crotta *et al.* 2002). A peptide derived from DENV NS1 protein binds to KIR3DL1 that transmits an inhibitory signal (Townsley *et al.*, 2016).

In the context of VACV infection, no such mechanisms of interference with the NK cell response have been described. Given the importance of the NK cell response during VACV infection, the large size of VACV genome and the many immune evasion strategies that VACV has evolved, it is reasonable to hypothesize that VACV might have developed a strategy to counteract the NK cell response.

1.5 Poxviruses

1.5.1 Poxviruses characteristics

Poxviridae is a family of large enveloped dsDNA viruses. Their genome is linear, has covalently closed termini, ranges from 130-300 kb, typically has more than 150 protein-coding genes and usually has a low G+C content (30-40 %) (Lefkowitz *et al.* 2006; Moss 2013). A distinctive feature is the presence of inverted terminal repeats at the genome extremities, which are tandem repeats necessary for concatemer resolution during genome replication (DeLange & McFadden 1987; Geshelin & Berns 1974). Typically, essential genes coding for DNA replication, transcription and virion assembly are located towards the centre of the genome while non-essential proteins with immunomodulatory functions cluster towards the extremities. Exclusive cytoplasmic replication is a unique characteristic of poxviruses as dsDNA viruses (Moss 2013). This feature has consequences on their biology: i) it prevents them from using the nuclear host machinery, leading to the necessity to encode their own DNA replication enzymes, transcription factors and accessory proteins ii) it makes them vulnerable to pathogen recognition receptors (PRRs) which are abundant in the cytoplasm and detect viral nucleic acids.

Poxviruses are divided in two sub-families; the *Entomopoxvirinae* and *Chordopoxcidinae,* that infect respectively insect and chordates. These subfamilies are further subdivided into genera based on criteria such as host range, morphology, antigenicity, and sequence similarity (Fauquet *et al.* 2005). Chordopoxviruses are subdivided into nine genera (Avipoxvirus, Capripoxvirus, Cervidpoxvirurs, Leporipoxvirus, Molluscipoxvirus, Orthopoxvirus, Parapoxvirus, Suipoxvirus, Yatapoxvirus) while the Entomopoxviruses is sub-divided into three genera (Alphaentomopoxvirus, Betaentomopoxvirus, Gammaentomopoxvirus) (Figure 6). Orthopoxvirus genus is the most extensively studied and includes ECTV, camelpox, VACV, CPXV and VARV. Following phylogenetic analysis, orthopoxviruses are thought to have evolved from a rodent-transmitted cowpox-like virus ancestor after loss, acquisition and modification of genes which led to the emergence of highly (Essbauer & Meyer 2007; McLysaght *et al.* 2003).

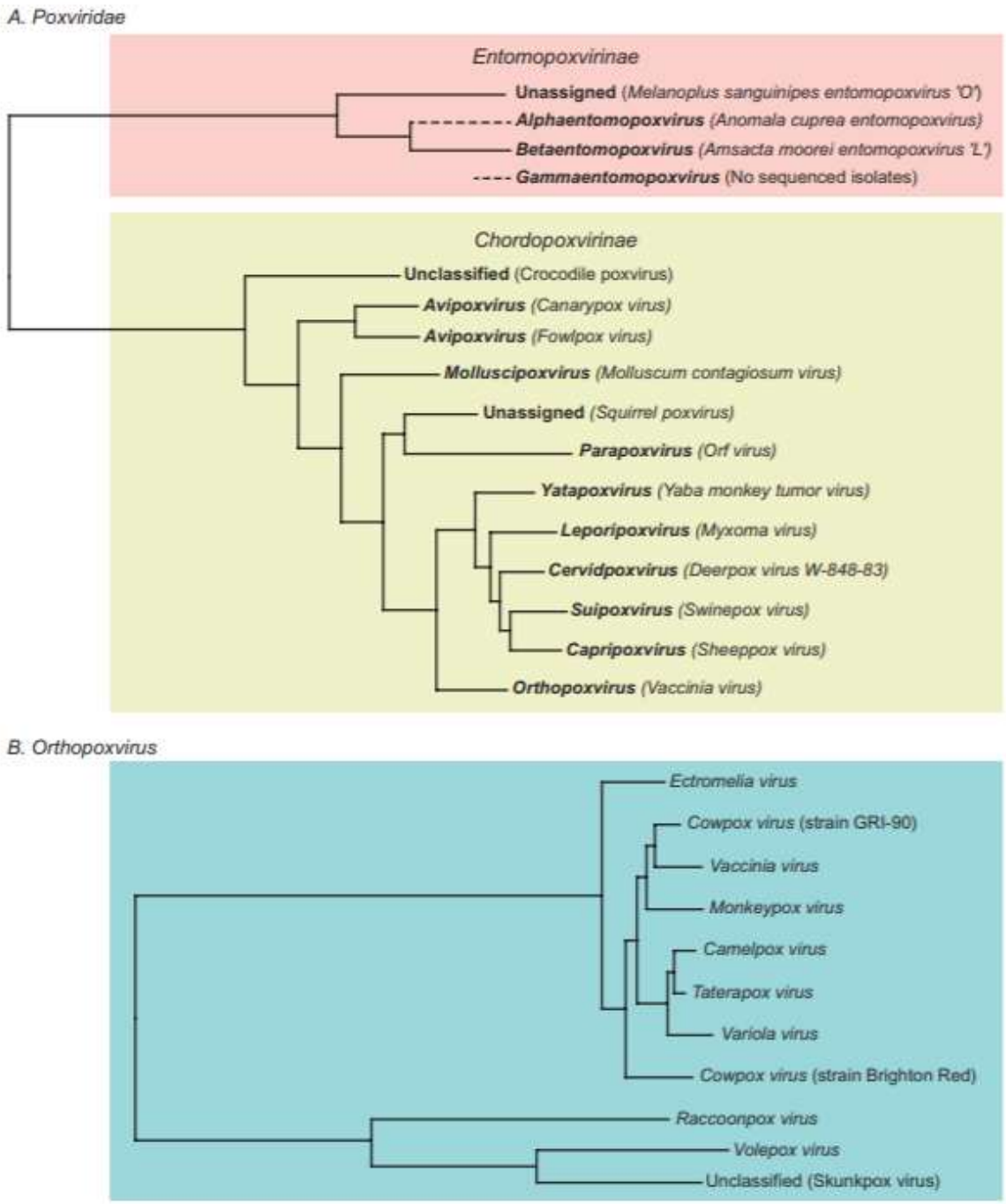

Figure 6 Phylogenetic tree representing the relationship among the Poxvirus family (A) and Orthopoxvirus genus (B). (Andrew M.Q. King 2012) Reused with licence permission, (licence number 4887630332811).

1.5.2 VACV life cycle

Poxvirus life cycle is complex and has the distinctive characteristic to occur exclusively in the cytoplasm. Most of the knowledge about poxvirus life cycle derives from VACV-based studies as reviewed in (Moss 2007). VACV life cycle can be divided in the following steps: virion attachment and entry, viral core release, establishment of viral factories, virion production and assembly, virion maturation and release.

1.5.2.1 VACV virions

VACV infectious life cycle produces two forms of morphologically and functionally distinct infectious particle: the intracellular mature virion (IMV), and the extracellular enveloped virion (EEV). The first virion produced is the IMV and it remains in the infected cell cytoplasm until cell lysis while EEV virion derives from the IMV and is transported to the cell surface, where it can remain attached and is then called a cell-associated enveloped virus (CEV). CEV/EEVs are prioritized since they exit the infected cell before its death. A characteristic that distinguishes IMV from CEV/EEV is their number of membranes, respectively one and three. Different viral proteins are expressed at these membranes, which makes IMVs and EEVs antigenically and functionally different.

The outer membrane of enveloped viruses makes them fragile, whilst IMV are more stable. CEVs are pushed by actin tails to neighbouring uninfected cells, contributing to cell-to-cell spread while EEVs are important for long-range spread within the host (Payne 1980), and IMVs which are most robust, are well-suited to mediate transmission between hosts (Payne 1980; Smith *et al.* 2002a). Moreover, poxviruses such as ectromelia (ECTV), canarypox, volepox, raccoonpox, CPXV can embed IMVs into structures called A-type inclusions (Ichihashi *et al.* 1971; Knight *et al.* 1992; Osterrieder *et al.* 1994; Sadasiv *et al.* 1985). These structures are thought to protect the virion from environmental stress and prolong their infectivity (Kastenmayer *et al.* 2014). Such features are advantageous for poxviruses which host are sparse, or which host-to-host transmission is poor or occurs through skin lesions (Kastenmayer *et al.* 2014). However, this feature might be disadvantageous for viruses such as VARV that transmit mainly via aerosol route in high-density populations. Poxviruses such as VACV, VARV, horsepox and MPXV do not produce ATI because of the truncation of A25 protein (Okeke *et al.* 2009; Patel *et al.* 1986). Deletion of A25 gene in CPXV led to higher virulence after respiratory tract infection, which supports the hypothesis that truncation of ATI gene reflects evolution for host-to-host spread via aerosol route (Kastenmayer *et al.* 2014).

Because IMVs remain in the host cell until cell lysis, they are less exposed to the immune system than the enveloped viruses. IMVs are vulnerable to host neutralising Abs and complement attack, whilst

EEVs display few antigens that are neutralizing Abs target (Law & Smith 2001), and express surface proteins derived from the host cell such as CD55 that protect them from complement attack (Pütz *et al.* 2006; Vanderplasschen *et al.* 1997, 1998). Only Abs against VACV B5 and A33 proteins neutralise EEVs (Bell *et al.* 2004; Benhnia *et al.* 2013; Pütz *et al.* 2006). EEVs neutralisation provides a greater benefit *in vivo* than IMVs neutralisation, suggesting that EEVs is the virion form involved in viral spread within the host (Boulter & Appleyard 1973).

1.5.2.2 Attachment, entry and viral core release

Attachment and entry of VACV IMVs and EEVs are different. IMVs attach to host cell surface GAGs thanks to viral membrane proteins: A27 and D8 bind to heparan sulfate (Chung *et al.* 1998; Hsiao *et al.* 1999), H3 to chondroitin sulfate, and A26 to laminin(Chiu *et al.* 2007; Lin *et al.* 2000). EEVs attachment remains elusive but F13 contributes to cell entry by enhancing the sensitivity of the membrane to dissolution (Bryk *et al.* 2018). Cellular receptors for VACV EEV and IMV are likely different but remain to be identified (Vanderplasschen & Smith 1997). VACV IMV enters the cell by three mechanisms: direct fusion with the PM (Armstrong *et al.* 1973; Carter *et al.* 2005), micropinocytosis (Mercer & Helenius 2008) or endocytosis followed by fusion with endocytic vesicle membrane to release free viral core in the cytoplasm (Townsley *et al.* 2006; Townsley & Moss 2007) (Figure 7). The fusion of the virion membrane with the endocytic vesicle is allowed by the entry fusion complex (EFC), a complex made of nine integral viral proteins, A16, A21, A28, G3, G9, H2, J5, L5, and O3, plus two EFC-associated proteins; L1 and F9 (reviewed in (Moss 2012)).

To enter the cell, VACV EEV sheds its additional membrane by disruption upon contact with the PM by a ligand-dependent non-fusogenic mechanism (Law *et al.* 2006), to release a free IMV that enters the cell as described above. Alternatively, VACV EEV enters the cell by endocytosis and subsequently loses its external membrane after acidification within intracellular vesicles to release an IMV that fuses with endocytic vesicle membrane via its EFC and release viral core within the cytoplasm (Figure 8) (Law *et al.* 2006; Schmidt *et al.* 2011).

1.5.2.3 Viral factories and genome replication

Once VACV viral core is free in the cytoplasm, it is transported further via microtubules (Figure 9) (Carter *et al.* 2003; Roberts & Smith 2008). Like other poxviruses, VACV replicates in the cytoplasm. To enable this, VACV encodes its own enzymes for transcription and DNA replication (Moss 2013). VACV gene expression occurs in three stages; early, intermediate and late, although there is evidence that the early class of genes is divided into two temporal groups (Assarsson *et al.* 2008; Moss 2013; Soday *et al.* 2019). Once the viral core is in the cytosol, early genes are transcribed, and mRNA exit the core via pores to be translated by host ribosomes in the cytoplasm. Subsequently, viral genome and

lateral bodies, which contain viral proteins, are released from the core. The viral genome then replicates in viral factories established in the perinuclear region (Cairns 1960). Late genes that are necessary to virus assembly are expressed and virion morphogenesis starts within the viral factories.

1.5.2.4 Virion assembly, maturation and exit

VACV morphogenesis is temporally regulated by intermediate and late promoters and transcription factors. Multiple viral proteins are required for virion morphogenesis and their expression is temporally regulated. The newly synthesised viral genome and viral proteins are encompassed by crescent-shaped lipid structures derived from the ER to form an immature virus (IV). The IV matures via proteolytic cleavage of capsid proteins and condensation of the core to form an IMV (Moss & Rosenblum 1973). It takes approximately 6 h for the first IMV to form (Tolonen *et al.* 2001). Newly formed IMVs are characterised by their single membrane, lateral bodies and are distinguished from IVs by the expression of additional membrane proteins. The vast majority of IMVs accumulate in the cytoplasm to be released upon cell lysis. Although, it has been observed that late in infection some IMV bud at the PM (Ichihashi *et al.* 1971; Tsutsui *et al.* 1983). IMVs accumulation correlates with A26 expression, which is anchored via A27, and is not expressed by EEVs (Howard *et al.* 2008). It is thought that A26 protein negatively regulates further wrapping of IMVs (McKelvey *et al.* 2002). A26 is expressed at late time pi, indicating that EEVs are prioritized and IMVs accumulation is temporally regulated to happen at late time pi.

The remaining of IMVs is transported on microtubules in an A27-dependent mechanism (Sanderson *et al.* 2000) and acquire a double membrane either derived from the trans-Golgi network (TGN) or early endosomes to form the intracellular enveloped virus (IEV) (Hiller & Weber 1985; Schmelz *et al.* 1994; Tooze *et al.* 1993). The IEVs are thus characterized by their double membrane. IEVs are transported on microtubules to the PM to externalise EEVs that can remain attached to the cell surface as a CEV and will be pushed away by actin tails, to be released as EEV (Hollinshead *et al.* 2001; Schmelz *et al.* 1994; Tooze *et al.* 1993). EEVs are characterized by their triple membrane.

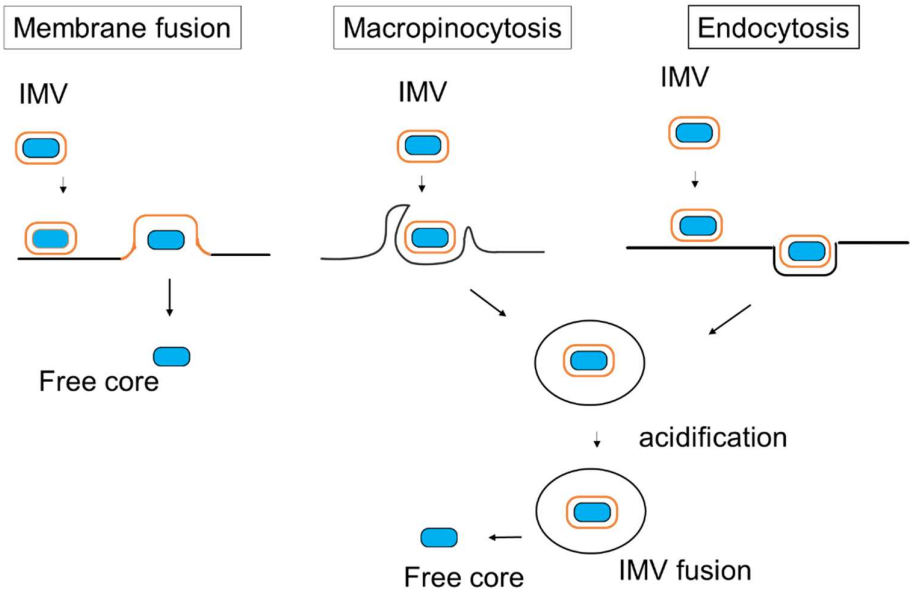

Figure 7 Diagram representing VACV IMV entry into the host cell. IMVs can enter the host cell by direct fusion of their external membrane with the PM leading to the release of a free core in the cytoplasm. Alternatively, IMVs can enter into the host cell by micropinocytosis or endocytosis, both mechanisms are followed by acidification of the endocytic vesicle and fusion of the IMV with the vesicle membrane releasing a free core in the cytoplasm. (Adapted from (Roberts & Smith 2008)*).*

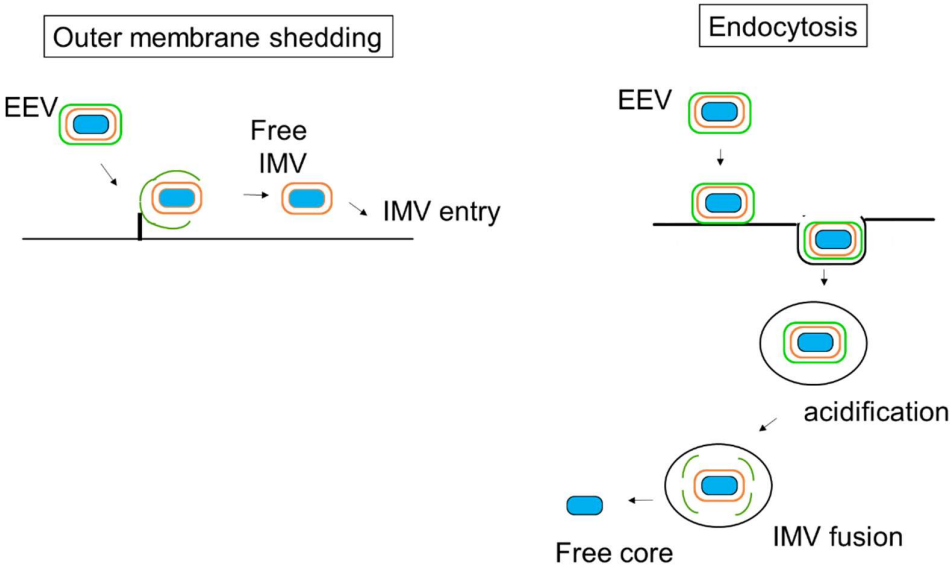

Figure 8 Schematic representing VACV EEV entry mechanism into the host cell. EEV can enter into the host cell by shedding its outer membrane via a ligand-induced, non-fusogenic mechanism to release a free IMV which then enter the cell as described in Figure 7. Alternatively, VACV EEV can enter into the host cell by endocytosis and then lose its outer membrane following acidification of the vesicle releasing an IMV which then fuses with the vesicle membrane releasing a free core in the cytoplasm. (Adapted from (Roberts & Smith 2008)*).*

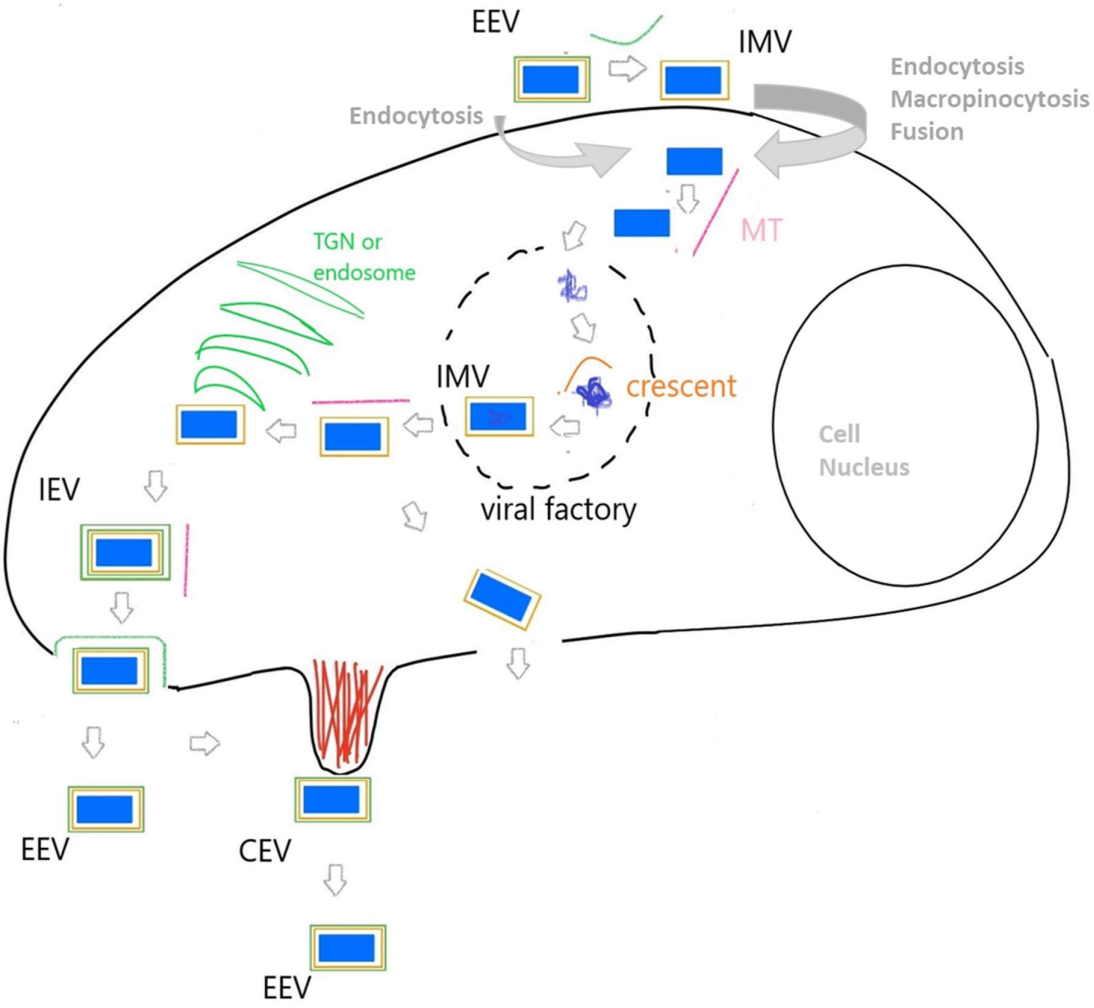

Figure 9 Schematic representing VACV life cycle. The two forms of infectious VACV particles, IMVs and EEVs enter into the host cell as described in Figure 7 and Figure 8, respectively. The viral core is released and transported on microtubules (pink) into the viral factory where VACV DNA genome is replicated and proteins synthesised. Crescents envelope the viral DNA and proteins to form IVs that mature in IMVs. Most of these IMVs will remain into the cytoplasm and will be released upon cell lysis, but a fraction of such IMVS is transported on microtubules to acquire an additional double external membrane derived from the TGN or early endosome and form IEVs. The IEVs are transported on microtubules to the PM to exit the cell by exocytosis and lose their outer membrane to release free EEVs. However, some EEVs can remain attached to the PM during this process (CEVs) and will be pushed away by actin tails (in red) to be released as free EEVs. Adapted from (Roberts & Smith 2008).

1.5.3 VACV surface glycoproteins

VACV infection leads to the expression of viral glycoproteins at the surface of the infected cell. Such proteins are exposed to the immune system and are therefore potential targets for immune cells. Moreover, such viral proteins often have a function related to immune evasion. So far, there have been 11 proteins described as expressed at the host PM during VACV infection. These proteins are discussed below.

One of the most abundant surface proteins is VACV HA, called A56 (Nagler 1942; Shida 1989). A56 is a heavily glycosylated surface protein (Blackman & Bubel 1972) that has an Ig-fold, a molecular mass of ~85 kDa and is expressed early and late p.i. (Shida & Dales 1982) (see section 1.6.2.3). A56 binds to two VACV proteins and anchors them at the cell surface: VACV protein K2, which is expressed early p.i. (serine proteinase inhibitor) (Turner & Moyer 2006), and the VACV complement control protein (VCP), which expressed late p.i. (DeHaven *et al.* 2010; Girgis *et al.* 2008). The A56-K2 complex prevents the fusion of infected cells and reduces the superinfection of infected cells by IMVs (Turner and Moyer, 2008; Wagenaar and Moss, 2009) through interaction with the IMV entry fusion complex (EFC) (Wagenaar *et al.* 2008; Wagenaar & Moss 2007). The A56-VCP complex protects infected cells against the complement (DeHaven *et al.* 2010; Girgis *et al.* 2008).

Another important VACV surface protein is B5 which is a 42-kDa (Engelstad *et al.* 1992; Isaacs *et al.* 1992) type I integral membrane glycoprotein whose extracellular domain comprises four short consensus repeats (SCR) that are characteristic of complement control protein and is expressed early and late p.i. (Takahashi-Nishimaki *et al.* 1991). B5 has been shown to interacts with A34 and A33 (Rottger *et al*., 1999) and is a major target for EEV neutralising Abs (Pütz *et al.* 2006). A33 is also a target for EEVs neutralising Abs (Benhnia *et al.* 2013) and is a 21-kDa type-II integral membrane glycoprotein expressed early and late p.i. (Roper *et al.* 1996) that forms a homodimer and is related to the C-type lectin family.

Besides its interaction with A34 and B5, A33 also forms a complex with the VACV protein A36, a 45 kDa type Ib membrane protein expressed early p.i. (Parkinson & Smith 1994; Snetkov *et al.* 2016; van Eijl *et al.* 2000). Importantly, A33, together with A36, is required for repulsion of super-infecting EEV (Doceul *et al.* 2010). When CEVs/EEVs are released from an infected cell, and encounter a VACV-infected cell, A33 and A36 lead to its repulsion via actin tails to the next neighbouring cell. This mechanism prevents super-infection and contributes to enhance VACV infection spread.

A34 is a type II transmembrane protein of 23 and 28 kDa according to its degree of glycosylation that is expressed late p.i. (Duncan & Smith 1992). Like A33, A34 is predicted to be a member of the C-type lectin-like family. A34 has a role in the formation of actin tails (Sanderson *et al.* 1998) and also affects the incorporation of other proteins into the surface of EEVs.

Most of the above-mentioned VACV proteins are also expressed on the outer membrane of EEVs, but there are additional VACV proteins that are expressed at the PM but not detected in viral particles. VACV encodes a growth factor called VGF (vaccinia growth factor) that is expressed early p.i. at the host cell PM under the form of a precursor (pro-VGF) before being cleaved and secreted (Chang *et al.* 1988). By interaction with EGFR, VGF induces cell proliferation in VACV-infected tissues, and this causes the surrounding cells to be metabolically active that supports viral replication (Buller *et al.* 1988).

A40 is a type II membrane glycoprotein with a single C-type lectin-like domain, its molecular mass ranges from 18 to 38 kDa according to the degree of glycosylation, and it is expressed early after infection at the PM but not found in virions (Wilcock et al., 1999). A40 has aa identity with other C-type lectins such as VACV A34, NKG2A and the rat CMV C-type lectin-like protein (Voigt *et al.* 2001).

A38 is a 33 kDa membrane glycoprotein, expressed at intermediate time p.i. at the PM but not found in virions, it has an Ig-fold and similarity to CD47 (ligand for SIRP- α) (Parkinson *et al.* 1995).

A43 is a type I transmembrane glycoprotein of ~23-30 kDa, it is not incorporated in virions but expressed at intermediate time p.i. at the PM, and it does not seem to have a known functional domain (Sood & Moss 2010).

This list of VACV proteins expressed on the cell surface is non-exhaustive and results from multiple independent studies that described individual VACV proteins. Thus far, there is no comprehensive study that has attempted to discover all VACV proteins expressed at the cell surface. Given that VACV encodes many proteins (~200), there might be additional unknown VACV surface proteins. Such putative surface proteins might play an important role in the immune response to VACV and the interplay between VACV-infected cell and NK cells.

1.5.4 Poxviruses medical importance

Poxviruses that can infect humans include the human-specific molluscum contagiosum virus (MOCV) and variola virus (VARV), as well as zoonotic viruses such as cowpox virus (CPXV), monkeypox virus (MPXV) and VACV. The main reservoir of many orthopoxviruses is rodents. Transmission typically occurs via mechanisms such as aerosol, direct contact or contaminated object (Andrew M.Q. King 2012). The severity of infection varies from mild for MOCV and VACV (Hanson & Diven 2003), to potentially serious for zoonotic poxviruses such as CPXV (Bera *et al.* 2011; Maksyutov *et al.* 2015) and particularly severe for central African strains of MPXV and VARV (McCollum & Damon 2014).

The orthopoxvirus that has impacted human being the most is VARV, the causative agent of smallpox. There are two forms of VARV, minor and major, which led to 20-50% and 1 % mortality rate in humans, respectively (Seitz 2010). Smallpox transmission occurs between humans, mostly via aerosol and droplets, leading first to infection of respiratory tract cells. The virus spreads asymptomatically to the lymph nodes, lymphoid organs and is then transported to the peripheric blood vessels by infected lymphocytes. A rash develops first in the mouth and pharynx and then spreads on the face, lower arms, trunk and legs. After 8-9 days the lesions transform into vesicles and pustules that will eventually resolve leaving the individual with important scars, often disfiguring. By day 10-12th after infection, high fever, headache, backache, and exhaustion occur (Seitz 2010). Smallpox epidemics had a major impact on humans for centuries until its eradication in 1977 (Fenner *et al.* 1988).

Since variola extinction, MXPV is the next most significant orthopoxvirus that threatens humans. There are two genetic clades of MPXV; West African and Central African, which result respectively in 1 and 11 % mortality (Jezek *et al.* 1988; Sklenovská & Van Ranst 2018). The illness can be mild or severe and the clinical signs and incubation period are similar to VARV at the exception that lymphadenopathy (enlarged lymph nodes) is observed in most cases. Complications include secondary bacterial infections, bronchopneumonia, sepsis, encephalitis, and corneal infection with concomitant loss of vision (Sklenovská & Van Ranst 2018). Cases of MXPV used to be rare, perhaps confounded with VARV, but epidemics have occurred more frequently in recent years, particularly in remote populations in Central and West Africa (reviewed in (Beer & Rao 2019)). MPXV can infect a wide range of mammals but the natural host remains unknown. Transmission is typically related to bushmeat consumption but Central African MPXV transmission has been reported to occur from human-to-human (Arita *et al.* 1985; Jezek *et al.* 1988).

A few cases of CPXV infection have been reported in humans in Europe. The natural reservoir and primary host of CPXV is thought to be wild rodents. Human infection occurs upon contact with infected animals such as pet rats or cats that became infected after preying rodents (Campe *et al.* 2009; Ninove *et al.* 2009). The clinical signs are typically influenza-like symptoms and skin lesions limited to the site of infection (BAXBY *et al.* 1994; Seitz 2010). However, in immunocompromised individuals, CPXV infection can be systemic, resembling VARV and become lethal (Czerny *et al.* 1991).

VACV is best-known for its use as a vaccine against smallpox (see section 1.5.5.1). Post-vaccination it can lead to systemic infection in immunocompromised individuals and adverse effects such as eczema vaccinatum, progressive vaccinia, myocarditis and postvaccinal encephalitis (Belongia & Naleway 2003). However, natural infections also occur and have been reported in Brazil in individuals having direct contact with infected cattle (Abrahão *et al.* 2015). VACV infection in immunocompetent

individuals is characterised by skin lesions at the site of infection, typically the hands and forearms for farmers infected by dairy cattle, and can be accompanied by fever, myalgia, headache and lymphadenopathy (de Souza Trindade *et al.* 2007).

1.5.5 Poxviruses-based therapeutics

VACV is the most studied poxvirus and is used broadly for investigating virus-host interactions, studying the immune response to infection, and for the development of recombinant vaccines against infectious diseases and cancers. There are many different strains of VACV, of which the most widely used laboratory strain is Western Reserve (WR). VACV WR is virulent in inbred laboratory mice (Parker *et al.* 1941) and was used in this thesis.

1.5.5.1 VACV as a vaccine against orthopoxviruses

Thanks to its antigenic similarity with VARV, which is the causative agent of smallpox, VACV was used as a vaccine in humans. Edward Jenner made a major contribution to VARV eradication by discovering vaccination against smallpox in 1976 and promoting it widely (Riedel 2005). It is traditionally believed that Jenner used CPXV, however this is not certain and how VACV then replace CPXV for vaccination against smallpox remains unknown (Baxby 1981). Later, a World Health Organisation (WHO) VACV-based vaccination campaign led to smallpox eradication in May 1980. This remains the only human disease to be eradicated by vaccination (Fenner *et al.* 1988) and has saved an estimated 200 million lives over the past 40 years (Hinman 1998).

However, this success was achieved without fully understanding the host immune response to VACV immunisation and the vaccine itself carried risks that would not meet the safety standards required nowadays. The risks associated with the inoculation of a live replicating virus led to the use of attenuated VACV strains (reviewed in (Jacobs *et al.* 2009). Nowadays, to protect against re-emergence of smallpox and monkeypox, VACV is available as a vaccine under the name of ACAM2000 in the USA, and Modified Vaccinia Ankara (MVA) is commercialised under the name of Jynneos in the US and Imnavex in the EU (Meyer *et al.* 2020). ACAM2000 is an attenuated VACV whose modifications include truncated version for TNF receptor (A53R), type I IFN receptor (B18R) and thymidylate kinase (Osborne *et al.* 2007). MVA is attenuated and non-replicative in most mammalian cells that underwent large genomic deletions after multiple passages in chicken embryo fibroblasts(Mayr *et al.* 1975).

1.5.5.2 VACV as a vaccine vector

VACV is a good vaccine vector candidate because of its ability to accommodate large insertion of DNA (Smith & Moss 1983) that encodes foreign antigens against which a humoral and T cell memory response can be generated (Smith *et al.* 1983b, 1983a). Additionally, because of its broad infection spectrum and the ease to modify its genome, there has been much interest in developing VACV as a vaccine vector for various infectious diseases and cancers. VACV encoding rabies glycoprotein has

been used as an oral vaccine in wild animals (Pastoret *et al.* 1988) (reviewed in (Maki *et al.* 2017)). However, due to safety concern in humans arising from complication related to VACV replication potential after vaccination (Perkus *et al.* 1995), research has focused on attenuated, non-replicative VACV-based vectors (reviewed in (Gomez *et al.* 2008)). Studies showed that these attenuated VACV can induce protective immunity against foreign pathogens but that long term protection and efficacy are lost at the benefits of higher safety (reviewed in (Jacobs *et al.* 2009)). Alternative strategies to improve the safety of replicative VACV and increase its immunogenicity include the deletion of immunomodulatory genes, combine use with co-stimulatory molecules or adjuvants, and optimisation of foreign antigen expression. These studies have showed promising results (reviewed in (Jacobs *et al.* 2009; Mayrink de Oliveira *et al.* 2019)) and such modified VACV-based live vaccine vectors hold promises as safe effective vaccine vectors. Recent encouraging clinical trials include an MVA-based vaccine that expresses the Middle East Respiratory Syndrome (MERS) spike glycoprotein (Koch *et al.* 2020).

1.5.5.3 VACV as an oncolytic virus

Oncolytic viral therapy holds great promises for the treatment of cancer. It relies on the use of viruses that preferentially replicate and propagate in cancer cells, causing their death mostly via lysis, while leaving healthy cells unharmed, and leading to the development of antitumoral immunity. The success of oncolytic viral therapy depends on the balance between induction of antiviral immunity, which leads to clearance of oncolytic virus, and the development of antitumoral immunity, which leads to clearance of the tumour and long-term anti-tumoral response. Multiple poxviruses have been studied as oncolytic vectors candidates including rabbitpox, myxoma virus, cowpox, VACV, racoonpox, squirrelpox (Ricordel *et al.* 2018). For conciseness, the subsequent section focuses on VACV which is the best characterised poxvirus-based oncolytic vector.

VACV is a good candidate for oncolytic virus therapies because i) it has a tropism for cancer cells, ii) it is highly cytolytic for many tumour cells, iii) it has a fast replication cycle and spreads rapidly from cell-to-cell, iv) it carries little risks for mutagenesis since its replication cycle occurs in the cytoplasm, v) it does not integrate in the host genome, vi) it has a large genome that can accommodate foreign DNA such as therapeutics transgenes, vii) it is easily genetically modified, viii) it has been clinically well characterised, ix) drugs exist to treat potential uncontrolled infection (reviewed in (Haddad 2017; Minev *et al.* 2019; Pelin *et al.* 2020)). Moreover, VACV-based oncolytic viruses have a well-established safety profile in patients with advanced cancer, persist in the tumour environment and can be administered systematically via intravenous or directly in the tumour (Pelin *et al.* 2020). Moreover, VACV produces two forms of infectious virions (see section 1.5.2) one of which, the EEV, displays few antigens, making it ideal for systemic administration (Hill & Carlisle 2019).

A limitation VACV-based oncolytic viruses is that VACV encodes genes whose function are incompletely or not at all understood, therefore carrying a risk for unpredictable outcomes. There has been several studies aimed at improving safety and anti-tumoral immunity of VACV-based oncolytic vectors. Such strategies include i) deletion mutants for virally encoded immunomodulatory genes, ii) insertion of genes encoding cytokines such as GM-CSF, IL-2, IL-24 (Deng *et al.* 2020; Mastrangelo *et al.* 1999; Quoix *et al.* 2016; Umer *et al.* 2020), iii) insertion of genes coding for tumour-associated antigens, iv) insertion of immuno-stimulatory molecules, v) combined use with CART-T cells or inhibitory checkpoints inhibitors (reviewed in (Guo *et al.* 2019; Pelin *et al.* 2020)).

Several WT and modified VACV have been tested in preclinical and clinical studies and have shown encouraging results (reviewed in (Lundstrom 2018; Pelin *et al.* 2020; Torres-Domínguez & McFadden 2019). Furthermore, novel VACV-based oncolytic viruses have been modified to express reporter genes that allow non-invasive tracking and imaging and thus monitoring for the presence of metastasis and assessing the progress of cancer therapy (Haddad 2017). Further studies are required to unlock VACV full potential in the context of oncolytic viral therapy as it currently holds great promises.

1.5.5.4 VACV as a model for vaccine research

Thanks to its ability to encode foreign antigens and high immunogenicity, VACV is a great tool for vaccine research. It is a useful vector to express gene products from various pathogens and leads to the expression of proteins with conserved structure and epitopes (VanSlyke & Hruby 1990). Recombinant VACVs allow to determine which proteins are the target of humoral and cellular immunity and which factors are required for the development of a protective immune response. Moreover, because of its broad host range, VACV can be used to infect various animal cells *in vitro* and *in vivo.* For example, mice can be infected with “pathogen x” and primed CD8+ T cells can be tested in a functional assay against cell lines infected with a set of recombinant VACVs encoding each a single gene from “pathogen x”. Alternatively, mice can be infected with recombinant VACV and cell line with “pathogen x.” VACV recombinant based studies allowed to identify MHC-I and MHC-II restricted CTL, to identify CTL epitopes and to confirm the target of neutralizing antibodies for viruses such as influenza A, respiratory syncytial virus, rabies, herpes simplex, Epstein Barr (reviewed in (Moss *et al.* 1988)).

1.6 NK cells and poxviruses

1.6.1 Immune response to poxviruses

Defences against viruses involve a coordinated response of the innate and adaptive immune system. Innate immunity is the first defence against infection and helps shape the adaptive immune response that produces pathogen-specific memory and protection during secondary exposure. The immune response to VACV has been well studied in humans and murine infection models. Of particular relevance to this thesis, the intradermal and intranasal (i.n.) murine infection models, which resemble vaccination and systemic viral infection, respectively.

The i.n. infection model is a systemic infection model in which VACV replicates primarily in the lungs, infecting epithelial cells, alveolar macrophages and DCs, before entering the bloodstream (viremia) and disseminating to secondary organs such as the lymph nodes, liver, spleen and ovaries (Alcami & Smith 1992; Bonduelle *et al.* 2012; Chapman *et al.* 2010; Rivera *et al.* 2007; Turner 1967; Williamson *et al.* 1990).

This infection model causes a strong inflammatory response leading to hypertrophy and hyperplasia of epithelial cells and damage to alveolar cells (Chapman *et al.* 2010), general signs of illness such as reduced mobility and arched back, and leads to weight loss from which animals typically recover within two weeks (Chapman *et al.* 2010; Nelson 1938; Turner 1967).

Control of VACV i.n. infection requires the engagement of both the innate and adaptive immune response. Independent studies have reported that toll-like receptors (TLRs) (Hutchens *et al.* 2008b, 2008a; Martinez *et al.* 2010b; Zhu *et al.* 2007), macrophages (Rivera *et al.* 2007), DCs (Beauchamp *et al.* 2010; Bonduelle *et al.* 2012; Yammani *et al.* 2008), NK cells (Abboud *et al.* 2016) and CD8+ T cells (Goulding *et al.* 2012) are all involved in the control of VACV infection and recovery from i.n. infection. This infection model is well suited to study the virulence of mutant viruses and also mimics natural infection with VARV or MPXV via the respiratory tract (Williamson *et al.*, 1990; Parker *et al.*, 2007; Cann *et al.*, 2013).

I.d. infection provides an alternative model that allows the study of cutaneous infection and more closely mimics dermal vaccination (Tscharke & Smith 1999).

In the i.d. model, VACV is injected in the ear pinnae and leads to the development of skin lesion after 5-6 days that resolves by 22 d.p.i. (Tscharke & Smith 1999). The infection is local, and the virus does not spread except at low levels to draining lymph nodes, and leads to ear tissue thickening due to inflammation, oedema and recruitment of immune cells (Tscharke & Smith 1999). Macrophages are

recruited rapidly and their number peaks at 4 d.p.i., NK cells reach a maximum at 7 d.p.i., whilst CD4+ and CD8+ T cells peak at 10 d.p.i. (Jacobs *et al.* 2006). This infection model reveals differences between WT and single deletion VACV mutants that are sometimes not seen during i.n. infection model and is well-suited to mimic vaccination (Tscharke *et al.* 2002).

During a second exposure to VACV, both antibodies (Abs) and CD8+ T cells are important for protection. Remarkably, in humans vaccinated against smallpox with VACV, both the humoral and cellular adaptive immune memory are long-lasting, with anti-poxvirus B cells being described as stable for >50 years by one study (Crotty *et al.* 2003) and anti-poxvirus serum Abs titres being stable for 75 years as described by another study (Hammarlund *et al.* 2003).
In contrast, T-cell immunity decreases gradually with a half-life of 8-15 years (Hammarlund *et al.* 2003). Recently, NK cells were shown to display memory qualities following VACV infection. Upon adoptive transfer in a naïve mice lacking T and B cells, VACV-primed NK cells conferred protection to recipient mice against VACV challenge (Gillard *et al.* 2011).

1.6.1.1 NK cells are involved in the immune response to poxviruses

Early evidence that NK cells are involved in the immune response to poxviruses was provided by Bukowski and colleagues. They reported that B6 mice controlled VACV replication better than other inbred laboratory mice strains and showed that NK cell depletion led to an increase in VACV viral titres (Bukowski *et al.* 1987, 1983). Later, this observation was confirmed by several independent groups (Abboud *et al.* 2016; Martinez *et al.* 2008, 2010a).

Further, B6 mice were shown to be resistant to ectromelia virus (ECTV, the causative agent of mousepox) whilst other mice strains such as Balb/C or DBA2 could not control infection (Bhatt & Jacoby 1987). B6 mice had a significantly lower viral load than susceptible mice strains, and their innate resistance was abrogated by depletion of NK cells (Jacoby *et al.* 1989). Delano and colleagues mapped the innate resistance of B6 mice to ECTV to a region of chromosome 6 that encodes NK cell–activating and inhibitory receptors (Delano & Brownstein 1995a). Further depletion studies confirmed that the NK cell response is required for the resistance to mousepox (Parker *et al.*, 2007).
More recently, the activating NKR NKG2D was shown to be a co-stimulator that optimise NK cell-mediated resistance to ECTV (Fang *et al.* 2008b). Its blockade in B6 mice led to decreased NK cell cytotoxicity (but not abrogation), increased viral titres and increased lethality (Fang *et al.* 2008b). It is believed that ECTV might lead to a shift in the peptides presented by Qa-1 that favours engagement with the activating receptor CD94/NKG2E rather than the inhibitory receptor NKG2A/CD94 (Fang *et*

al. 2011). Strikingly, this interaction requires the presence of NKG2D, presumably as a supporting receptor, but its exact role remains unresolved (Fang *et al.* 2008b).

1.6.1.2 NK cells migrate to the site of infection and expand in response to VACV

Early studies reported that after intraperitoneal (i.p.) injection with VACV WR, NK cell number increased at the site of infection due to recruitment and proliferation (Dokun *et al.* 2001; Natuk & Welsh 1986; Prlic *et al.* 2005). Further, using BrdU incorporation, Prlic and colleagues showed that NK cells proliferate at the primary site of infection and at higher levels in other organs such as the spleen, lungs and liver (Prlic *et al.* 2005). Later, other independent research groups reported NK cell amplification during VACV infection (Jacobs *et al.* 2006; Martinez *et al.* 2008, 2010a).

Another marker used to study cellular proliferation is the intracellular staining for Ki67, a nuclear protein whose expression is restricted to cells undergoing proliferation. Using this marker, Abboud and colleagues showed that NK cells proliferate in the lungs and other organs, such as the spleen and bone marrow, and that NK cell numbers increase is at least partially due to active proliferation (Abboud *et al.* 2016). This groups also showed that NK cells in the lungs increased dramatically between 1-4 d.p.i. and reached a peak at 7 d.p.i. (Abboud *et al.* 2016). Similarly, using the i.d. infection model, it was reported that NK cell numbers also increased in the spleen and the ear, reaching a maximum at 7 d.p.i. (Jacobs *et al.* 2006). This observation was also confirmed recently by Evgeniya Schmeleva in our laboratory (unpublished data).

1.6.1.3 NK cells display signs of activation during VACV infection

Multiple markers can be used to determine the activation state of NK cells. Common NK cell activation markers are, for example, the upregulation of intracellular IFNγ, GzmB (Granzyme B), perforin and the upregulation of cell surface CD107a, which is expressed transiently at the PM after degranulation. Besides, other surface markers can be used such as CD69 (Cibrián & Sánchez-Madrid 2017), Killer cell lectin-like receptor G1 (KLRG1) (Ito *et al.* 2006; Tessmer *et al.* 2007), stem cell antigen 1 (Sca1) (Fogel *et al.* 2013a; Yutoku *et al.* 1974) and gp49A/B (Gu *et al.* 2003), which are lymphocyte activation markers.

In the context of VACV infection, *in vivo*, several independent groups have reported the increased expression of activation markers on NK cells such as Sca1 (Fogel *et al.* 2013a), CD69 (Abboud *et al.* 2016; Gillard *et al.* 2011; Gu *et al.* 2003; Notario *et al.* 2016), CD107a (Abboud *et al.* 2016; Gillard *et al.* 2011; Hatfield *et al.* 2018), gp49A/B (Gu *et al.* 2003) and KLRG1 (Fogel *et al.* 2013a; Gillard *et al.* 2011). Higher levels of intracellular GzmB, IFNγ and perforin, were also reported by independent groups (Abboud *et al.* 2016; Brandstadter & Yang 2011; Hatfield *et al.* 2018; Martinez *et al.* 2008, 2010b; Prlic *et al.* 2005).

Another method for studying NK cell activity is to test the cytotoxic capacity of NK cells towards YAC-1 target cells that are MHC-I negative cells. Multiple independent studies have reported that NK cells taken from mice infected with VACV had higher activity against YAC-1 cells *ex vivo*, than NK cells derived from mock-infected mice (Bukowski *et al.*, 1983; Martinez, Huang and Yang, 2008; Benfield *et al.*, 2013; Brandstadter, Huang and Yang, 2014; Hatfield *et al.*, 2018). Martinez and colleagues also reported the same phenotype when L929 cells (murine fibroblasts) were used as target cells (Martinez *et al.* 2010a).

Further, a study by Costanzo and colleagues analysed the transcripts of human NK cells before and 7 d after vaccination with VACV strain MVA. This group compared the differential expression of 96 NK cell transcripts after stimulation by direct recognition, cytokines or ADCC. They showed that NK cells displayed a general activation signature and that their transcriptomic signature showed upregulation of genes primarily associated with direct cell recognition (Costanzo *et al.* 2018).

1.6.1.4 NK cells have higher cytotoxicity towards VACV-infected cells

NK cell cytotoxic activity can be studied by a functional assay such as the ^{51}Cr release assay. In this assay, target cells are infected or not and then labelled with ^{51}Cr before co-incubation with NK cells. Upon NK-mediated killing, target cells release ^{51}Cr in the culture medium that can be measured to calculate the cytotoxic activity of NK cells.

Several independent groups have reported that VACV infection leads to enhanced cytotoxicity using such assays with human (Baraz *et al.* 1999; Brooks *et al.* 2006; Chisholm & Reyburn 2006; Kirwan *et al.* 2006) and murine NK cells (Baraz *et al.* 1999; Brutkiewicz *et al.* 1992; Tanaka-Kataoka *et al.* 1999). Multiple independent studies reported that NK cells have enhanced cytotoxicity towards cells that are infected with VACV, suggesting that NK cells can recognise VACV-infected cells directly as a target (Baraz *et al.* 1999; Brooks *et al.* 2006; Chisholm & Reyburn 2006). Other studies reported similar results based on the detection of CD107a during VACV infection in a mouse model (Abboud *et al*., 2016; Hatfield *et al.*, 2018).

Of note, a lower NK cell cytotoxicity was observed in experimental settings using target cells, such as HeLa (Henrietta Lacks) cells, that present a high NK mediated killing background (Jarahian *et al.* 2011). The use of cancer cell lines as target cells that are known to express NK ligands should be considered with caution because viral infection may interfere with the expression of such proteins. Similarly,

interpretation of data obtained with the NK-92 MI cell line as effector NK cells needs to be interpreted cautiously because the NK response is known to be clonally distributed because different NK cells express different subsets of receptors.

1.6.1.5 Cytokines that regulate NK cell activation during VACV infection

Along with activating and inhibitory signals emanating from the engagement of cell surface receptors, cytokines such as IL-12, IL-15, IL-18 and type I IFN play an important role in the regulation of NK cell activation. In the context of VACV infection *in vivo*, multiple groups observed that NK cells require the presence of IL-12 and IL-18 (Brandstadter *et al.* 2014; Gherardi 2003) and type I IFN to control VACV infection (Martinez *et al.* 2008, 2010a; Zhu *et al.* 2007).

Administration of IL-18 during VACV intravenous (i.v.) infection leads to better infection control. This was associated with enhanced NK cells and CTL (Cytotoxic T lymphocyte) activity (Tanaka-Kataoka *et al.* 1999). In mice infected with a recombinant VACV encoding IL-12 and IL-18, a significant enhancement in virus clearance was observed and was attributed to NK and T cells because mice depleted for NK cells presented higher viral titres (Gherardi 2003).

Further, in mice i.n. infected with a VACV mutant that does not express C12 (an IL-18-binding protein), enhanced NK cell cytotoxicity towards YAC1 cells was observed *ex vivo*, and lower weight loss and signs of illness were observed in comparison to WT VACV (Reading & Smith 2003; Symons *et al.* 2002).

In mice carrying a deletion for the IL-18 receptor, i.p. infection with VACV led to lower NK activation (assessed in a Cr^{51} release towards target cells), higher viral titres in ovaries, lower production of IFNγ and GzmB by NK cells when compared to WT mice (Brandstadter *et al.* 2014).

IFNs have potent antiviral activity, and VACV has evolved many strategies to impair their production or signalling functions (Smith *et al.* 2018). Using IFNα/β receptor-deficient mice, Martinez and colleagues showed that following VACV infection, there was no NK cell expansion, that NK cells did not produce effector molecules such as perforin, GzmB or IFNγ and that NK cells did not display enhanced cytolytic capacity in comparison to WT mice (Martinez *et al.* 2008).

Further, this group reported that IFNα/β receptor-deficient mice and WT mice depleted for NK cells presented a similar increase in viral titres during VACV infection in comparison to WT B6 mice. This group also showed that transfer of WT NK cells into IFNα/β receptor-deficient mice was sufficient to restore VACV clearance (Martinez *et al.* 2008).

However, these data contrast with a previous study reporting that the lower viral load associated with IFN-β injection before VACV i.p. infection was NK independent (shown by NK depletion) (Bukowski *et al.* 1987). This group itself described this finding as surprising and suggested that: i) activation of NK

cells by exogenous IFN-β may be redundant with the IFN-β-mediated activity generated by natural viral infection; or ii) injection of exogenous IFN leads to systemic NK activation, which might disrupt the capacity of NK cells to migrate to the site of infection.

A more physiologically relevant study of the role of IFN on NK cells in the context of VACV was performed by Hatfield and colleagues. This group reported an increased frequency of IFNAR+ NK cells and IFN regulatory factor 4+ (IRF4) NK cells, *in vivo* at 3 d.p.i. with VACV. Since IRF4 expression is triggered by type I IFN, these observations suggest that NK cells sense type I IFN and respond to it in the context of VACV infection *in vivo* (Hatfield *et al.* 2018). Moreover, an independent study reported that VACV-mediated NK cell activation required type I IFN signalling through MyD88 and TLR2, suggesting the importance of IFN for NK cell response during VACV infection *in vivo* (Martinez *et al.* 2008, 2010a; Zhu *et al.* 2007).

These studies taken together emphasise the necessity of working in physiologically relevant conditions and suggest that IL-12, IL-18 and IFNs play a role in the activation of NK cells during VACV infection.

1.6.1.6 MHC-I surface expression during VACV infection

A major determinant of NK cell activation is the detection of a diminution of host cell surface MHC-I. The impact of VACV infection on MHC-I surface expression has been incompletely studied. There are a few reports about the level of host MHC-I surface expression during VACV infection, but they are difficult to interpret collectively because of the different cell lines, reagents, multiplicity of infection (MOI), duration of infection used across these multiple studies. These studies are summarised below.

Studies performed in the human system by several independent groups reported that VACV infection leads to either no change or a mild downregulation of total MHC-I. This was observed in human foreskin fibroblast cells (HFFF) (Chisholm & Reyburn 2006), in B-lymphoblastoid cells (BLCL) (Brooks *et al.* 2006), in Jurkat T cells (Kirwan *et al.* 2006), in HeLa cells (Jarahian *et al.* 2011) and DT-76 cells (Baraz *et al.* 1999). In contrast, a pronounced downregulation of total MHC-I was observed in HEK293T cells and T cells at late time p.i. (Baraz *et al.* 1999; Kirwan *et al.* 2006). Studies in the murine system reported a very mild downregulation of total MHC-I in C1498 cells (murine myeloid leukaemia cell line) (Williams *et al.* 2012) but a marked downregulation of class I antigens in L929 cells (Brutkiewicz *et al.* 1992).

Besides, VACV has been widely used to characterize the presentation of foreign antigens inserted in its genome to murine and human CD8+ T cells, indicating that MHC-I complex is expressed after VACV infection (Yewdell *et al.* 1985). Other studies have shown that MHC-I presents peptides derived from VACV intracellular proteins, indicating that VACV infection does not abolish MHC-I surface expression (reviewed in (Kennedy & Poland 2007)).

Due to the lack of specific Abs, the study of individual HLA-I expression during VACV infection has been difficult. In the human system, Brooks and colleagues used the MEME/08 monoclonal antibody (mAb) to report the selective downregulation of HLA-E whilst MHC-I expression (studied with pan MHC-I Ab) remained intact during VACV infection (Brooks *et al.* 2006). Kirwan and colleagues used the MHC-I deficient 721.221 stably expressing a single HLA-I and observed a selective downregulation of HLA-C (Kirwan *et al.* 2006).

Some of these studies went a step further and investigated whether MHC-I contributes to the NK-cell mediated killing of VACV-infected cells. In the human model, Chisholm and colleagues showed that blocking MHC-I does not influence the NK cell-mediated cytolytic activity suggesting that MHC-I is not involved in triggering NK cell cytotoxicity during VACV infection. This group attributed enhanced NK cell killing to NCR (natural cytotoxicity receptor) activation (Chisholm & Reyburn 2006). Jarahian and colleagues made similar observations regarding the role of MHC-I (Jarahian *et al.* 2011).
Baraz and colleagues reported that upon infection, DT-76 cells have enhanced susceptibility to NK-cell-mediated killing but showed no MHC-I downregulation. This suggests that other factors are responsible for triggering NK cell activation (Baraz *et al.* 1999). This group also reported enhanced killing of VACV-infected colo-205 cells (MHC-I negative cells) in comparison to mock-infected cells, suggesting that other factors are involved in NK cell activation (Baraz *et al.* 1999).
Brooks and colleagues reported that MHC-I levels remain sufficient to maintain KIR-mediated inhibition. However, HLA-E selective downregulation seemed to be sufficient to trigger NK activation from certain NK clones, presumably by loss of inhibitory signals from CD94/NKG2A (Brooks *et al.* 2006). Finally, Kirwan and colleagues reported that HLA-C downregulation is sufficient to trigger KIR2DL1+ or KIR2DL3+ NK cells (Kirwan *et al.* 2006).

In the murine model, Brutkiewicz reported that enhanced killing by NK cells of VACV-infected cells correlates with H2K decrease, but did not show a direct involvement of MHC-I (Brutkiewicz *et al.* 1992). Still in a mouse model, Williams and colleagues attributed enhanced NK-cell-mediated killing of VACV-infected cells to loss of Clr-b and not to MHC-I alteration (Williams *et al.* 2012).

Overall, it seems unlikely that VACV completely prevents MHC-I expression *in vivo*, since VACV infection leads to a strong and specific T cell response in humans and mice (review in (Kennedy & Poland 2007). However, VACV might selectively affects the expression of individual HLA-I subtypes. Whether VACV prevents MHC-I expression significantly and/or with a certain degree of selectively remains to be clarified.

1.6.1.7 Contribution of NKRs to the immune response to VACV infection

The literature indicates that the NK cell response to poxvirus-infected cells is clonally distributed, suggesting that a subset of receptors is involved. It is currently unknown which receptors contribute to NK cell activation during VACV infection. Despite MHC-I receptors being considered as major regulators of NK cell activation, other receptors can be involved. A few studies partially address this question and are summarised below.

In the murine system, Dokun and colleagues showed that there was no preferential proliferation of Ly49H+ NK cells in the spleen and the liver early after i.p. infection with VACV (Dokun *et al.,* 2001). Similarly, another group showed that the frequencies of Ly49G2+ and Ly49C/I+ liver NK cells were stable before and after VACV infection in B6 mice (Daniels *et al*., 2001). Orr and colleagues used a CD94 deficient mice strain (*kldr 1*-/-) to show that CD94 is not required in B6 mice to control VACV infection (Fang *et al.* 2011). Further, it was shown that the inhibitory ligand Clr-1b expression is rapidly lost after VACV infection in murine cell lines, suggesting that its receptor NKR-P1B/D, in B6 mice, might be involved in the recognition of VACV-infected cells (Williams *et al.,* 2012).

In humans, Chisholm and colleagues report that NKp30, NKp44, and NKp46, are involved in the recognition of VACV-infected cells, whilst NKG2D is not (Chisholm *et al*., 2006). Further, human and murine NCRs were shown to interact with VACV HA (Jarahian *et al.* 2009). Besides, a correlation between HLA-E downregulation and the enhanced cytotoxicity of NKG2A+ NK cells was reported (Brooks *et al.* 2006). Similarly, KIR2DL3+ and KIR2DL1+ NK cells were seen to display enhanced cytotoxicity correlating with HLA-C downregulation (Kirwan *et al.* 2006).

Of note, some of these studies should be interpreted with caution because they were performed *ex vivo* and might not represent physiological conditions. Nonetheless, taken together, these studies help narrow down the number of potential NKRs involved in the recognition of VACV-infected cells.

Which NKR(s) is/are determinant in the NK cell response to VACV and whether a receptor-ligand couple drives the NK cell response to VACV in a similar fashion to Ly49H and m157 does in the context to mCMV remains to be determined.

1.6.1.8 VACV-induced memory NK cells

Despite their fixed repertoire of germ-line encoded receptors, NK cells can recognise virus-infected cells to mount a pathogen-specific response (section 1.4.1.1) and can develop memory qualities (section 1.2.3). Importantly, NK memory cells have been reported in the context of VACV infection (Gillard *et al*., 2011). This group identified a subset of hepatic NK cells expressing Thy1 that protects

against VACV challenge upon adoptive transfer in *Rag*-/- mice (Gillard *et al.,* 2011). This study is summarised below.

First, this group demonstrated that 6 months after primary i.p. infection with VACV, B cell-deficient mice in which T cells were also depleted right before challenge with VACV could resolve VACV infection. In contrast, mice that were mock-infected and subsequently challenged did not. This indicated that a non-B non-T cell population could mediate a recall response and protection.
Gillard and colleagues further showed that Thy1+ cell depletion abrogated the protection described above during secondary challenge, indicating that a non-T non-B Thy1+ population was mediating the recall response.

To rule out the possibility that mAb depletion of T cells might not be complete, Gillard and colleagues performed an adoptive transfer of VACV-primed Thy1+ and Thy1- NK cells, and peripheral blood mononuclear cells (PBMCs) depleted for NK cells (6 months pi) into naïve Rag1-/- recipient mice. Simultaneously to the cell transfer, mice receiving NK cells were given a T cell depleting mAb to eliminate putative contaminating T cells. Five days post-transfer, mice were challenged with VACV. Mice that had received VACV-primed Thy1+ NK cells cleared VACV infection a week faster than mice receiving PBMCS depleted for NK cells. Mice receiving VACV-primed Thy1- NK cells could not clear VACV infection.
These observations indicate that VACV infection induces the development of memory NK cells with protective capabilities. Important questions remain unresolved such as the mechanism at the basis of memory acquisition, how primed NK cells mediate protective recall response, and what primed NK cells recognise on VACV-infected cells. The identification of the ligand(s) and NKR(s) engaged during the primary response, and the recall response to VACV, is crucial to better understand VACV-induced NK cell biology.

1.6.2 Poxvirus evasion strategies to evade NK cell response

Viruses and the immune system have co-evolved, and consequently, both virus and host have evolved a myriad of strategies against each other. Viruses with a large DNA genome, such as VACV, encode many proteins that are non-essential for virus replication, but interfere with the host immune system. It is estimated that 30 to 50 % of VACV proteins are dedicated to immune evasion (Smith *et al.* 2013). VACV targets many extracellular mediators of the innate immune response such as IFNs, complement, chemokines and cytokines, but also targets many intracellular pathways triggering apoptosis, establishing an antiviral state or leading to a pro-inflammatory state (reviewed in (Albarnaz *et al.* 2018; Stephensen 2001)).

Strategies evolved by poxviruses include, i) secretion of cytokines and chemokines receptors that compete with host-encoded receptors, ii) secretion of cytokine analogues, that act as decoys, iii) production of inhibitors and antagonists of intracellular signalling pathways, iv) prevention of the host protein translation. Some of these strategies interfere with the NK cell response directly or indirectly and are described in the subsequent sections.

1.6.2.1 Manipulation of cell surface MHC-I by poxvirus proteins

Despite the important role that MHC-I expression modulation has during viral immune response, there are only a few poxviruses for which an MHC-I downmodulation strategy has been described: CPXV, MOCV and myxoma virus (MYXV).

CPXV has evolved two independent mechanisms to downregulate host cell surface MHC-I levels. The first relies on CPXV203 that exploits the KDEL receptor rescue pathway (whose normal function is to retrieve proteins from the Golgi to the endoplasmic reticulum (ER)) to retain host MHC-I in the ER and prevents its trafficking to the cell surface (Byun *et al.* 2007; McCoy *et al.* 2012). The second mechanism relies on CPXV12 that prevents MHC-I peptide loading by interaction with transporter associated with antigen (TAP) and as a consequence prevents MHC-I assembly (Alzhanova *et al.* 2009; Byun *et al.* 2009). Besides, MOCV encodes MC80 wich was initially described as associated with β2m (Senkevich & Moss 1998). Recently, MC80 was shown to disrupt MHC-I by targeting tapasin (peptide loading chaperone) for ubiquitylation, which leads to its degradation and subsequent loss of TAP (peptide transporter), therefore disrupting peptide loading on MHC-I (Harvey *et al.* 2019). Further, MYXV, which causes myxomatosis in the European rabbit, relies on the MYXV leukaemia-associated protein (MV-LAP) to downregulates MHC-I surface expression (Guerin *et al.* 2002). This protein possesses an atypical zing-finger domain and resides in the ER, where it retains MHC-I (Guerin *et al.* 2002). In contrast, VACV does not encode a protein that resembles any of the viral proteins described above. It is not clear whether VACV has evolved a strategy to downmodulate MHC-I surface expression or interfere with the engagement of MHC-I -NKRs.

1.6.2.2 Poxvirus mechanisms to antagonise NKG2D signalling

NKG2D is an activating receptor that binds stress ligands (see section1.3.2.2). Its expression is targeted by multiple viruses, including poxviruses.

CPXV encodes a protein that resembles host MHC-I and is called orthopoxvirus MHC-I like protein (OMCP) (Campbell *et al.* 2007). OMCP is a secreted protein that binds the human and murine NKG2D receptor and prevents engagement with its host ligands. OMCP also blocks NKG2D-mediated killing

by competition binding (Campbell *et al.* 2007; Lazear *et al.* 2013). Most orthopoxvirus do not encode an orthologue of CPXV OMCP, except for MPXV. Another strategy used to antagonise NKG2D-mediated killing is to prevent the expression of its host ligands. NKG2DL ligands (NKG2DL) are typically upregulated during stress conditions such as viral infection. Recently, it was reported that VACV E3, a dsRNA binding protein, prevents the expression of NKG2DL (Esteso *et al.* 2017). By binding and masking dsRNA produced during viral replication, VACV E3 prevents the sensing of the viral dsRNA and the upregulation of NKG2DL (Esteso *et al.* 2017).

1.6.2.3 NCR function modulation by poxvirus HA

It is known that some viral proteins engage with NKRs and antagonise their functions. The study of such interactions in the context of VACV is limited by the absence of a comprehensive list of VACV surface proteins. Only a few studies have characterised individual VACV surface proteins (see section 1.5.3). Given the many proteins encoded by VACV, it is possible that some VACV proteins are expressed at the PM but have not been described as such. Thus far, VACV A56 is the only VACV surface protein known to directly interact with NKRs. VACV A56 characteristics and functions are described below.

VACV protein A56, also called VACV HA (Nagler 1942; Shida 1986), is abundantly expressed and heavily glycosylated (Ichihashi & Dales 1971; Shida & Dales 1981, 1982). A56 is a membrane protein that is expressed on the surface of VACV-infected cells (Blackman & Bubel 1972) and EEV but is absent from the IMV (Payne & Norrby 1976). The primary translation product has a predicted molecular mass of 35 kDa, but the mature protein is heavily glycosylated with both N-linked and O-linked carbohydrate and has a molecular mass of 85 kDa. The A56 N-terminal region has an Ig fold, followed by a stalk region containing repeats, a transmembrane domain and a C-terminal 13 aa within the cytosol (Figure 10). Its deletion leads to the formation of syncytia resulting from the fusion of infected cells (Ichihashi & Dales 1971; Seki *et al.* 1990).

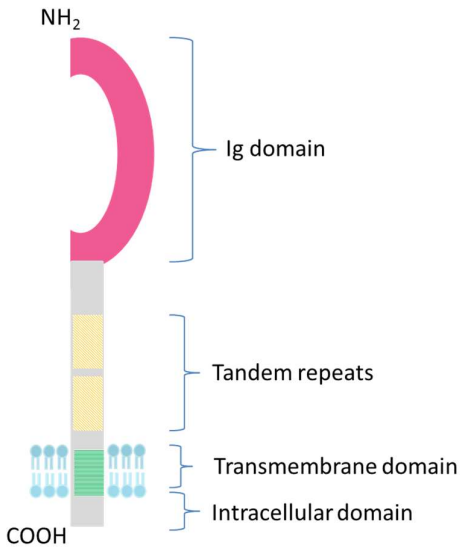

Figure 10 Representation of VACV A56 protein structure. The extracellular Ig domain is separated from the intracellular domain by a stalk region containing two tandem repeats. The Ig domain is thought to be involved in binding VACV K2, and the VCP binds to the stalk region (Adapted from DeHaven et al., 2011).

Further, A56 interacts with VACV protein K2 (a serine protease inhibitor) and VACV VCP to retains these proteins on the cell surface (DeHaven *et al.* 2010; Girgis *et al.* 2008). The A56-K2 complex prevents syncytium formation and superinfection by binding to the fusion machinery on the IMV surface (Turner & Moyer 2006, 2008; Wagenaar & Moss 2009). The A56-VCP complex prevents the destruction of infected cells by complement (DeHaven *et al.* 2010). Moreover, protein A56 is non-essential for viral replication and has sometimes been removed from candidate vaccines (Jacobs *et al.* 2009).

The VACV and ECTV HA are ligands for all murine and human NCRs (Jarahian *et al.* 2011). VACV and ECTV HA expression was associated with increased binding of soluble NKp30, human and murine NKp46, and a weak increased binding for NKp44 (Jarahian *et al.* 2011). This binding was abrogated when cells were infected with a virus lacking gene *A56R* or when a mAb blocking A56 was used (Jarahian *et al.* 2011). Ectopic expression of A56 led to increased binding of soluble NKp46 and NKp30 (but negligible binding for NKp44), but to a lower extent than during infection with VACV. This is probably due to a lower expression level of A56 after transfection. Further, using an ELISA, soluble NKp30 and NKp46 (NKp44 binding negligible) were shown to bind to recombinant VACV and ECTV A56 proteins, VACV WT IMVs particles but not to VACV ΔHA IMVs (Jarahian *et al.* 2011).

Using viruses that lacked K2, or A56 and K2, it was shown that K2 does not affect NCR binding (Jarahian *et al.* 2011). However, the effect of VCP, the second binding partner of A56 was not tested in their

studies. Using deglycosylating enzymes, it was shown that glycan interactions were involved in the interaction between A56 and NKp30 as well as NKp46. The exact residues remain to be identified as well as the putative contribution of other host proteins to this interaction.

To assess the impact of A56 on NK cell functions, Jarahian and colleagues compared the NK cell response to HeLa cells infected with WT VACV and ΔA56 in a ^{51}Cr release cytotoxic assay. They reported a surprising diminution of NK-mediated lysis late after VACV WT infection in comparison to mock and ΔA56 infection, suggesting that A56 mediates inhibition.
Besides, they showed that ectopic expression of VACV or ECTV A56 in tumour cells, such as HeLa and MaMel-8A cells, correlated with reduced killing by NK92 and primary human NK cells. Addition of soluble A56 during co-incubation of NK cells with HeLa cells led to the diminution of NK-mediated killing, indicating that A56 has an inhibitory effect on NK cells. Finally, this group showed that A56 limits NKp30 function, but weakly enhance NKp46 signalling. To show this, they used the human NK-92 cell line with selectively silenced NCR expression and LacZ-inducible, NCR-reporter cells. They concluded that VACV and ECTV A56 inhibit NKp30 signalling but enhance NKp46 signalling.
These last results require cautious interpretation because HeLa cells are cancer cells that express NK ligands whose surface expression may be affected by VACV infection, thereby impacting the binding of NCRs and/or their susceptibility to NK cell killing.

The effect of A56 on the expression of other NK ligands and other VACV proteins remains to be determined to clarify whether A56 itself is responsible for the phenotypes described. Moreover, the biological relevance of their findings remains to be addressed in physiologically relevant conditions, since chimeric receptors may not behave like the native receptor, and NK92 cells are derived from a single NK clone whereas the NK response is polyclonal.

1.6.2.4 Interference with apoptosis mediators

It is common for viruses to evolve strategies to interfere with apoptosis. In the poxvirus family, a few viral proteins have been reported to mediate such functions.

MYXV MV-LAP interferes with Fas-mediated apoptosis by downregulating Fas surface expression via its ER retention (Guerin *et al.* 2002). MV-LAP was reported to alter T-cell cytotoxicity but was not tested on NK cells (Guerin *et al.* 2002).
ECTV encodes a serpin called SPI-2, whose deletion leads to increased numbers and enhanced activation of NK cells, higher IFNγ and IL-18 concentration in the serum, reduced viral load and a better control of ECTV infection (Melo-Silva *et al.* 2011). The depletion of NK cells abrogates the favourable

outcome observed in the absence of ECTV SPI-2, suggesting that NK cell functions are impaired by ECTV SPI-2 (Melo-Silva *et al.* 2011).

VACV proteins that interfere with apoptosis are VACV SPI-2 (also called B13 and cytokine response modifier (CrmA), in CPXV) (Kettle *et al.* 1997; Tewari & Dixit 1995; Wasilenko *et al.* 2001), VACV CrmC and CrmE (that inhibit Fas and TNF-mediated apoptosis) (Alcami *et al.* 1999; Graham *et al.* 2007), VACV Golgi anti-apoptotic protein (vGAAP) (only expressed in Lister, USRR and Evans VACV strain) (Carrara *et al.* 2015; Gubser *et al.* 2007; Gubser & Smith 2002; Veyer *et al.* 2017), or the Bcl2-like (B-cell lymphoma-2 like)proteins F1 (Aoyagi *et al.* 2006; Cooray *et al.* 2007; Kvansakul *et al.* 2008; Wasilenko *et al.* 2003). These proteins might all interfere with NK cell functions, but this has not been tested.

1.6.2.5 Indirect interference with NK cell functions

Poxviruses encode many proteins that prevent the action of cytokines and chemokines. Some of these proteins might therefore interfere with NK cell activation. This is the case of VACV proteins, N1, K7 and C12 which have been described to alter NK cell response *in vivo*, in murine infection models as described below.

Infection of mice with VACV ΔK7, in comparison to WT VACV, led to enhanced NK-mediated lysis against YAC-1 cells, suggesting that K7 interferes with NK cell activation (Benfield *et al.*, 2013). Similar results were reported for mice infected with VACV ΔN1 (Jacobs *et al.* 2008). N1 and K7 inhibit IFN induction and activation of NF-κB (Nuclear factor-kappa B, a transcription factor that regulates the expression of genes critical for the immune response) and therefore are likely to interfere with NK cell function indirectly. Additionally, VACV protein C12 is an IL-18 binding protein and reduces IFNγ production and NK cell cytolytic activity following i.n. infection, presumably by depriving NK cells of IL-18 (Reading & Smith 2003).

Other VACV proteins might also interfere indirectly with NK cell functions but have not been tested as such so far. Unravelling the stimuli that trigger NK cell activation during VACV infection will allow to predict which VACV immune-modulatory proteins might also interfere with NK cell functions.

1.7 Thesis aims

As outlined in the introduction of this thesis, the literature shows that NK cells respond to VACV infection; they are recruited to the site of infection, proliferate, display signs of activation, upregulate proteins that mediate their cytotoxic functions, can kill VACV-infected cells and they can mount a recall response to VACV. However, the factors that rule the interplay between NK cells and VACV are unknown. Importantly, the NK cell receptor(s) engaged in the recognition of VACV-infected cells is/are unknown, and the ligand(s) that trigger NK cell activation remain elusive. The literature indicates that A56 and NKp46 could be a receptor-ligand complex involved in this interaction rather like Ly49H:mCMV m157 is for mCMV.

Given that VACV is used as i) a vaccine-vector for foreign antigens, ii) as an oncolytic virus in cancer therapy, and iii) as a vaccine for antigenically related orthopoxviruses, it is crucial to understand better the molecular basis of the interaction between NK cells and VACV-infected cells. Beyond advancing our current understanding of NK cell biology in the context of viral infection, such knowledge could facilitate the exploitation of the NK cell response in these therapeutic settings. Hence, the research performed in this thesis is intended to better understand the interplay between NK cells and VACV-infected cells.

The main questions asked in this thesis are:

1) Which NK cell receptor(s) is/are involved in the recognition of VACV-infected cells?

2) Which ligand(s) trigger NK cell response during VACV infection?

3) What is the role of VACV A56 and NKp46 in the outcome and control of VACV infection?

2 Chapter 2: Methods

2.1 Cell maintenance

BSC-1, HeLa, MEFS, A549 and HEK293 (Human embryonic kidney) cell lines were grown in Dulbecco's modified Eagle's medium (DMEM) (Invitrogen) supplemented with 1 % (volume/volume) (v/v) penicillin/streptomycin (P/S) (PAA Laboratories) and 10 % (v/v) heat-treated (56 ˚C, 1 hour (h)) foetal bovine serum (FBS) (Seralab). RK13 cells (Rabbit kidney cells) were grown in (minimum essential medium (MEM, Gibco) supplemented as for DMEM. Suspension cells P815, RMA-S and YAC-1 cells were grown in RPMI (Roswell Park Memorial Institute) supplemented as for DMEM. HFFF-TERT (primary human foetal foreskin fibroblast, telomerase reverse transcriptase- immortalised) were grown in DMEM supplemented with 10 % foetal calf serum (v/v) and 1 % P/S (v/v). All cell lines were maintained at 37 ˚C in 5 % CO_2 and were verified to be mycoplasma negative every two months. Upon reaching sub-confluence (80-90 %), adherent cells were washed with phosphate-buffered saline (PBS) and detached with trypsin-EDTA (Ethylenediaminetetra-acetic acid) (Gibco). The trypsin was inactivated by addition of DMEM supplemented with 10 % FBS, and the desired number of cells were reseeded in fresh culture medium. When suspension cells had reached an appropriate cell density, cells clumps were shaken to be broken, and a fraction of them resuspended in fresh culture medium.

Table 1: Cell lines used in this study and their origin

Name	**Origin**
A549	Human lung carcinoma, epithelial
BSC-1	African green monkey kidney, epithelial
HEK293T	Human embryonic kidney, epithelial
HeLa	Human cervix adenocarcinoma, epithelial
RK-13	Rabbit kidney, epithelial
HFFF-TERT	Human foetal foreskin telomerase reverse transcriptase-immortalized, fibroblast
P815	Murine, mastocytoma
RMA-S	Murine, Rauscher virus-transformed lymphoma
YAC-1	Murine, Moloney leukaemia virus-induced lymphoma

2.2 Virus work

2.2.1 Virus strain and mutants

Unless otherwise stated, VACV strain Western Reserve (WR) strain was used for all experimental procedures, WT (Smith *et al.* 1991) and single mutants vΔA56 (Smith *et al.* 2002a), ΔA40 (Wilcock *et al.* 1999), ΔA38 (Falkner & Moss 1988; Parkinson *et al.* 1995) and their revertant (Rev) were all described previously.

2.2.2 Virus titration by plaque assay

Samples were thawed, sonicated for 20 sec (seconds) at 120 W, vortexed and diluted from 10^{-2} to 10^{-9} in DMEM supplemented with 2 % (v/v) FBS and 1 % (v/v) P/S. Confluent BSC-1 cells were infected with 500 µl of the appropriate dilutions for 90 min at 37 °C before incubation under 1 ml of semi-liquid overlay (1:1 (v/v) mixture of 3 % weight/volume (w/v) carboxymethyl cellulose (CMC) and 2x MEM supplemented with 5 % (v/v) FBS and 1 % (v/v) P/S) for 2-3 d. Cells were washed and then stained for 1 h with 1 ml of crystal violet solution (5 % (w/v) crystal violet (Sigma), 25 % (v/v) ethanol) prior to counting plaques.

2.2.3 Virus stock production

RK13 cell monolayers were infected at an MOI of 0.1 until full cytopathic effect (CPE) appeared, typically 2-3 d. Infected cells were harvested and resuspended into 10 mM Tris pH 9.0. Cell-associated virus was released from cells by freeze-thaw and two rounds of Dounce homogenisation (20 strokes each). The supernatant (containing free virus) was harvested and centrifuged at 600 *g* for 30 min to sediment cell debris. The supernatant was layered over a 36 % (w/v) sucrose cushion and centrifuged for 80 min at 32,900 *g* at 4 °C (Optima L-100 XP, Beckman Coulter). After centrifugation, the pellet was resuspended in 1 ml 10 mM Tris pH 9.0 by sonicating for 10 sec three times and then layered again over a 36 % (w/v) sucrose cushion and centrifuged for 80 min at 32,900 *g* at 4 °C. The pellet was resuspended in 36 ml 10 mM Tris pH 9.0 and centrifuged at 26,000 *g* for 50 min at 4 °C. After centrifugation, pellets containing purified virus were resuspended in PBS, aliquoted, and titrated as described in section 2.2.2.

2.2.4 Virus genotyping by polymerase chain reaction

2.2.4.1 Amplicon size-based discriminative PCR

A well of sub-confluent BSC-1 cells in a 96-well plate was infected with 1 µl of the sucrose purified viruses to be genotyped until sufficient CPE formation. The inoculum was removed, the cells washed with 150 µl PBS and 50 µl proteinase K (Sigma) was added per wells (8.5 µg PK, 200 µl water, 20 µl 10x High fidelity PCR buffer (Invitrogen)) before freezing the plate - 80 °C. Cells were thawed and scraped in the proteinase K mix and transferred in PCR tubes to be incubated in a thermocycler (Applied

Biosystems) at 56 °C for 20 min to degrade proteins followed by 80 °C for 10 min to inactivate the proteinase K. The lysates were frozen at - 20 °C until PCR reaction was performed. Polymerase chain reaction (PCR) was carried out to genotype recombinant viruses based on amplicon size discrimination. The reactions contained reagents described in Table 2 and the sequence of the primers used were in the forward direction TGATGTTCGAACTAATACATCTG, and in the reverse direction TCCTAAAAACTCAGTATGTTCT. Reactions were run in a thermocycler (Applied Biosystems) with the parameters specified in Table 3. PCR products were analysed by agarose gel electrophoresis.

Table 2: Reagents used per PCR reaction

Nuclease free water	Make up to 25 µl
5x green Gotaq flexi buffer	5 µl
$MgCl_2$ 25mM	1.65 µl
Nucleotide Mix 10 mM each	0.5 µl
Forward primer 10 µM	1 µl
Reverse primer 10 µM	1 µl
Template DNA (lysate)	3 µl
GoTaq DNA polymerase (Promega)	0.125 µl

Table 3 Thermocycler parameters for PCR

Cycles	x1		x35		x1	x1
Temperature (°C)	95	95	48	72	72	4
Time (min:sec)	2:00	1:00	1:00	1:00 per 1kb	5:00	∞

2.2.4.2 Agarose gel electrophoresis

PCR product samples were mixed with 6 x Gel Loading Dye (NEB) and then loaded on 1 % (w/v) agarose (Invitrogen) gel, made in Tris-acetate-EDTA buffer (40 mM Tris-acetate, 1 mM ethylenediaminetetraacetic acid (EDTA)), supplemented with SYBRSafe (Invitrogen) diluted at 1: 5000 ratio. HyperLadder 1 kb DNA ladder was also run to allow for amplicon size estimation. The samples were run at 90 V for 1 h and DNA was visualised using Gel Doc XR+ imaging system (Bio-Rad).

2.2.5 Virus comet formation assay

To assess the degree of release of progeny extracellular enveloped virus (EEV) from the cell surface, the formation of comets, which results from the unidirectional spreading of EEV in the culture

medium, was analysed. Monolayers of BSC-1 cells in 6-well tissue culture plates were infected with the indicated viruses for 1 h at 37 C° and rocked occasionally. The inoculum was replaced by liquid cell culture medium (DMEM supplemented with 2 % FBS and 1 % P/S). The plates were incubated at 37 ˚C, 5 % CO_2 until sufficient plaque development. Cells were stained with crystal violet as described in section 2.2.2, and the stained monolayers were imaged.

2.2.6 Virus plaque morphology and size measurement

Monolayers of BSC-1 cells in 6-well plates were infected with the indicated viruses for 1 h and rocked occasionally. The inoculum was replaced by a semi-liquid overlay containing 1.5 % CMC and the plates were incubated at 37 ˚C in 5 % CO_2 until sufficient plaque development. Plaques were imaged using phase-contrast on an Axio Observer.Z1 inverted microscope. After being imaged, cells were stained with crystal violet (CV) and the area of 30 plaques per virus was measured at least twice, using the spline selection tool in AxioVision.

2.2.7 Virus infection of cells

2.2.7.1 With VACV

To perform viral infection of suspension or adherent cells, cells were seeded to be at sub-confluence and in the exponential phase of replication at the time of infection. Cells were enumerated with a Chemometec automated cell counter (NC-250) and viral stocks of known titre were used to infect cells at the indicated MOI. MOI is obtained by dividing the number of infectious virions by the number of cells to be infected and enables the percentage of cells to be infected to be calculated using the Poisson distribution (Fields et al., 2007). Viral stocks were thawed, sonicated and diluted to give the desired MOI, in a volume that is the minimum required to cover the cell monolayer. Infections were carried out at 37 ˚C, in 5 % CO_2, for 90 min with gentle agitation every 15 min.

2.2.7.2 With Influenza

Infection was carried as for VACV with the exception that viral stocks were not sonicated, but were treated with trypsin with N-tosyl-L-phenylalanine chloromethyl ketone (TPCK trypsin, Sigma) was added to the medium at a final concentration of 2 µg/ml to enable virions to detach from the cell surface and infect another cell.

2.2.8 Flow cytometry to monitor infection level

To monitor infection levels with VACV and influenza, cells were harvested with Accutase (Innovative Technology) or EDTA 5 mM and stained with the indicated Zombie viability dye (Biolegend) for 15 min as per manufacturer's instruction. Cells were washed with PBS, collected by centrifugation at 300 *g* for 5 min and incubated with mouse monoclonal antibody (mAb) against A/PR/8/34 influenza HA

(clone 9B3.2, MS x influenza A MAB8261, Merck Millipore) or VACV protein A56 WR181 (Immune Technology clone LC10 IT-012-006M1). All mAbs were used at a dilution of 1:100 (v/v).

Where intracellular staining for VACV protein D8 (Parkinson and Smith, 1994; mAb AB1.1) was performed, cells were permeabilised and fixed directly after viability and surface staining using the Fixation/Permeabilization solution from BD kit cytofix/cytoperm (#554714) following the manufacturer's instruction. Cells were washed in Perm/Wash™ Buffer (BD kit cytofix/cytoperm, #554714), centrifuged at 300 *g* for 5 min at 4 °C and mAb AB1.1 against VACV D8 (Parkinson & Smith 1994) was added at a dilution of 1:500 (v/v) for 30 min at 4 °C. For surface and intracellular staining, cells were incubated with 1:200 (v/v) of anti-mouse phycoerythrin (PE)-conjugated secondary Ab at 1:200 dilution (v/v) for 30 min at 4 ˚C in the dark. Cells were washed in PBS and collected by centrifugation at 300 *g* for 5 min, twice, resuspended in PBS and analysed on an LSR Fortessa (BD), Attunes NxT (Thermo Fisher) or a Cytek Aurora.

2.2.9 Microscopy to monitor cell infectivity

P815, RMA-S and YAC-1 target cells were infected or not with vA5GFP (VACV expressing green fluorescence protein (GFP) under late promoter (as described in (Carter *et al.* 2003)) at the indicated MOI and time according to section 2.2.7.1. Cells were fixed in paraformaldehyde (PFA) 4 % for 30 min, washed with PBS and mixed with mowiol containing 4',6-diamidino-2-phenylindole (DAPI) at a ratio 1:1. Approximately 40 µl of this cellular suspension was transferred onto microscopes slides (Menzel-Glaser) and round glass coverslip and left to dry in the dark at 4 °C. Cells were visualised with the help of Mike Hollinshead on a Zeiss LSM 700 inverted confocal microscope and imaged with Zeiss Zen software.

2.3 Animal work

2.3.1 Mice maintenance and origin

All animal experiments and procedures were performed in compliance with Animals (Scientific Procedures) Act 1986 as regulated by the UK Home Office and with the approval of the University of Cambridge Animal Welfare Ethical Review Body. Unless otherwise stated, all *in vivo* experiments were performed with six-to eight-week-old female B6 (Envigo). Mice were maintained under specific pathogen-free conditions. NKp46$^{GFP/GFP}$ mice on the B6 background (Gazit *et al.*, 2006) were generously provided by Dr Francesco Colucci and were bred in house. Age and sex-matched WT B6 animals were used as controls.

2.3.2 Mice intradermal and intranasal viral infection

For both procedures, mice were anesthetised by inhalation of isoflurane, superficially for i.d. infection and more deeply for i.n. infection to prevent the sneezing reflex. For i.d. injection, 10 µl of the indicated virus suspension or vehicle control (0.01 % bovine serum albumin (BSA) in PBS) was injected in the dorsal surface of each ear pinna using a 27-gauge needle and 100 µl glass syringe (Hamilton Company). Mice were examined daily under brief isoflurane-induced anaesthesia and the diameter of lesions developing at the inoculation site were measured using a micrometre as described in (Tscharke *et al.* 2002). For i.n. infection, 10 µl of the indicated virus suspension or vehicle control (0.01 % BSA in PBS) were administered with a 10 µl pipet in each nostril. Animals were weighed before injection to determine their initial weight and then monitored daily for weight change and signs of illness - hair ruffling, back-arching and decreased mobility as described (Alcami & Smith 1992; Williamson *et al.* 1990). Animals that lost greater than or equal to 25 % of their initial weight or showed signs of illness with a score > 4 were culled immediately. The virus dose administered was always verified by plaque assay (section 2.2.2) of the inoculum on the day of infection.

2.3.3 Murine sample collection and preparation

2.3.3.1 Murine serum collection

Blood was collected into microvette tubes (Sarstedt, Cat # 16.440.100) and left at room temperature (RT) to clot. After centrifugation at 10,000 *g* for 5 min, the serum was carefully collected from the upper phase and stored at -80 C° until processing.

2.3.3.2 Murine tissues homogenisation

Murine tissues were harvested in sterile conditions and stored at – 80 °C until processing. Tissues were homogenised in 400 µl PBS supplemented with 0.5 % BSA using an OMNI tissue homogeniser with plastic hard tissue probes (OMNI International). For Luminex sample preparation, homogenates were centrifugated at 10,000 *g* for 20 min at 4 ˚C° and supernatants were isolated and stored at -80 C° until use. For viral load calculation, homogenates underwent 3 cycles of freezing-thawing and were sonicated for 20 sec at 120 W to release the cell-associated viruses. Homogenates were then centrifuged at 300 *g* for 5 min to sediment cellular debris. Subsequently, the supernatant was diluted by 10-fold with nuclease-free water (Cat. # AM9930, Ambion) until use for plaque assay or real-time quantitative PCR (RT qPCR).

2.3.4 VACV neutralising Ab titration

Serum was collected as described in section 2.3.4. Subsequently, it was incubated at 56 °C for 30 min to inactivate the complement that would otherwise interfere with the test. Two-fold serial dilutions of the serum samples were prepared, ranging from 1:50 to 1:1600 using DMEM supplemented with

2.5 % FBS and 1 % PenStrep. A solution containing ~120 pfu of WT VACV that had been purified by sedimentation through a sucrose cushion was prepared and added to all samples in a ratio of 1:1 (v/v). A reference sample (medium without serum mixed 1:1 with viral solution) was included to determine the number of plaque-forming units (pfu) obtained in the absence of serum. After 1 h incubation at 37 ˚C, samples were titrated by plaque assay (section 2.2.2) and the half neutralising dose (ND50) (corresponding to the minimal serum dilution necessary to lead to a plaque number reduction of 50 %) was calculated.

2.3.5 Cytokine and chemokine concentration measurement in murine tissues

Mice serum and tissues were harvested and prepared as described in section 2.3.3.2. The concentration of the indicated analytes was determined using a magnetic Luminex mouse premixed multi-analyte kits (R&D Systems #LXSAMSM-17), and a Luminex analyser (Luminex Corporation) as per the manufacturer's instructions.

2.3.6 Viral load measurement in murine tissues

The VACV load in murine tissues and blood were measured by plaque assay (section 2.2.2) for infectious particles or by RT-qPCR for virus genome copy number as described (Baker & Ward 2014). Murine serum and organs were collected and prepared as described above (section 2.3.3). The reaction mix for RT qPCR was made of 2 µl of template (here tissue homogenate), 10 µl of 2x qPCRBIO Probe Mix (Cat. # PB20.21-5, PCR Biosystems), 0.8 µl of 10 µM VACV gene *E9L* forward primer (CGGCTAAGAGTTGCACATCCA), 0.8 µl of 10 µM gene *E9L* reverse primer (CTCTGCTCCATTTAGTACCGATTCT), 0.4 µl of 10 µM gene *E9L* probe (TaqMan MGB Probe – AGGACGTAGAATGATCTTGTA, Applied Biosystems). The total reaction volume was brought up to 20 µl with nuclease-free water. A plasmid containing the VACV *E9L* gene was used as a standard and was kindly gifted by Brian M Ward, University of Rochester Medical Center, USA. The qPCRs were run on a ViiA 7 Real-Time PCR System (Applied Biosystems) with the following parameters: initial denaturation at 95 °C for 3 min, followed by 40 cycles of denaturation at 95 C° for 5 sec and annealing and extension at 60 °C for 30 sec. Each sample was run in duplicate, standards in triplicate and water was used as a negative control.

2.3.7 Flow cytometry of murine lymphocytes

2.3.7.1 Single-cell suspension preparation from murine tissues

Murine spleens or liver were mechanically disrupted through a 0.70 µm cell strainer (Falcon, BD) to obtain a single-cell suspension. The liver samples were processed with an extra Percoll centrifugation step to remove hepatocytes. Liver cells were resuspended in 10 ml RPMI supplemented with 35 % (v/v) Percoll (Sigma, #1644) and spun for 30 min at 800 *g* with deceleration without use of break.

Erythrocytes from splenic and hepatic cell suspensions were lysed with 2 ml of 1X lysis buffer (BD Pharmlyse, # 555899) following the manufacturer's instructions. PBS was added to quench the lysis reaction, and samples were centrifuged at 500 *g* for 5 min. Cells were then enumerated using a Chemometec (NC-250). Subsequently, single-cell suspensions were labelled for phenotype analysis or sorting.

2.3.7.2 Labelling for fluorescence-activated cell sorting (FACS) phenotyping

Lymphocyte single-cell suspensions were pre-incubated with CD16/32 to block the Fc (Fragment, crystallisable) receptors for 5 min at 4 ˚C. Cells were labelled with Zombie viability dye (Biolegend) for 15 min at 4 ˚C as per the manufacturer's instructions. Where MHC dextramer H-2Kb/TSYKFESV (Immunodex, PE-conjugated) was used, it was added at a 1:20 dilution (v/v) 15 min before any other mAbs for surface markers to prevent steric encumberment and facilitate its binding. A cocktail of the indicated Abs for surface markers were added for another 30 min at 4 °C in the dark. Cells were washed with PBS twice and collected by centrifugation at 300 *g* for 5 min at 4 °C. Where intracellular staining was required, cells were fixed and permeabilised using 100 µl cytofix/cytoperm buffer (Cytofix/Cytoperm kit, BD) following the manufacturer's instructions. Cells were washed in 1 X permwash buffer (Cytofix/Cytoperm kit, BD), collected by centrifugation at 300 *g*, 4 °C for 5 min and the indicated mAbs for intracellular markers were added in permwash buffer for 30 min at 4 °C in the dark. Cells were washed in permwash buffer 1 X twice, collected by centrifugation at 300 *g* and 4 °C for 5 min before being resuspended in PBS. The relevant fluorescence-minus-one (FMO) and isotype mAb labelling conditions were included as controls. All samples were fixed with 4 % paraformaldehyde (PFA) before acquisition by flow cytometry on an LSR Fortessa (BD) or Aurora Cytex flow cytometer. Cells were gated as indicated in Figure 11 for the analysis of VACV-specific dextramer and as indicated in the relevant sections for other surface markers.

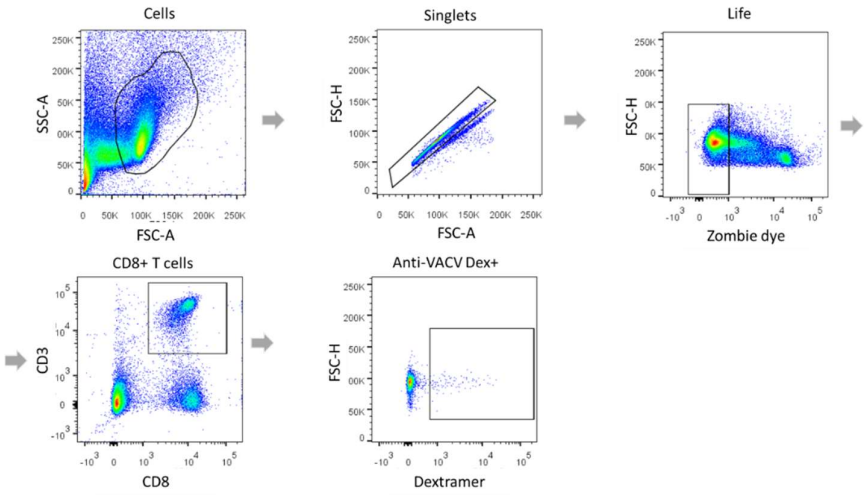

Figure 11 Representative gating strategy for the analysis of anti-VACV specific CD8+ T cells by FACS surface staining. Debris were gated out, singlets and then life cells were selected, CD8+ T cells were isolated and analysed for expression of cell surface VACV-specific dextramer.

2.3.8 Murine lymphocyte isolation by FACS

Splenic single suspension cells were resuspended in 600 µl PBS, and Fc receptors were blocked with 10 µg/ml anti-mouse CD16/CD32 (clone 2.4G2, BD #553142). Cells were incubated with the viability dye Zombie Violet Fixable Viability kit (Biolegend, #423113, 1:120 (v/v)) for 15 min in the dark. Cells were washed twice in PBS and a cocktail of 10 µg anti-CD3 APC (Allophycocyanin antigen) (145-2C11, BD), 10 µg anti-NK1.1 PE (PK136, Biolegend) and 50 µg anti-CD45 FITC (Fluorescein isothiocyanate) (3F11) mAbs was added to each sample. After 20 min of incubation in the dark, cells were washed twice in PBS, collected by centrifugation, and resuspended in 1.5 ml PBS.

Viable NK cells ($CD45^+CD3^-NK1.1^+$, Figure 12A) from spleens of mock and VACV-infected mice were sorted by FACS in sterile PBS using an 86-µm nozzle on a FACS Aria or a BD Influx instrument. Half a million NK cells were harvested per sample, with a purity >96 %, as analysed by running a sample of the sorted cells (Figure 12B). Directly after cell sorting, the samples were spun at 7500 *g* for 7 min. The pellets were resuspended in 350 µl of RLT buffer (Qiagen kit, #74104) supplemented with β-mercaptoethanol (10 µl/ml). Samples were snap-frozen and stored at -80 °C before RNA extraction.

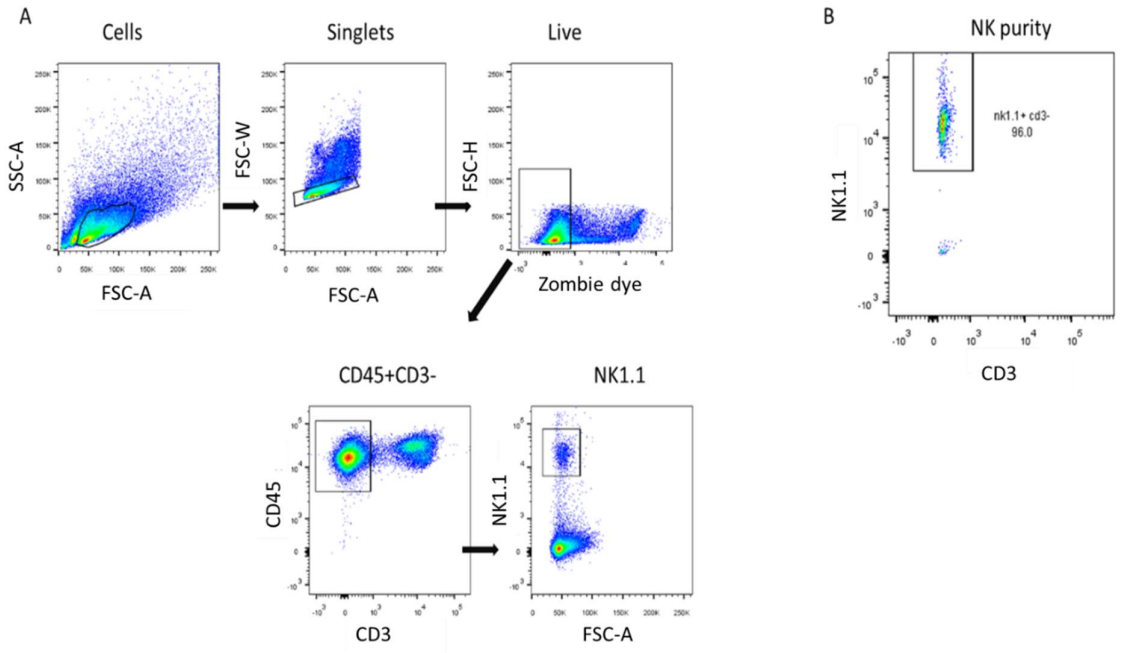

Figure 12. Gating strategy for NK cell isolation by FACS and purity check. A) Debris were gated out and viable singlet cells that were negative for CD3, and positive for CD45 and NK1.1, were isolated by FACS in sterile PBS. B) The purity of the NK cells was checked by running a sample of the sorted cells on the flow cytometer.

2.3.9 Murine NK cells cytotoxic assays

2.3.9.1 ^{51}Cr release cytotoxic assay

The cytotoxicity of NK cells was measured by ^{51}Cr release assay (all radioactive work was performed by Dr Hongwei Ren) as described (Clark *et al.*, 2006). Briefly, P815 cells were infected with the indicated virus at an MOI of 10 for 8 h before incubation with ^{51}Cr for 2 h. In parallel, single-cell suspensions were prepared from the spleen or liver of mice infected 28 d earlier with VACV, or mock-infected with PBS, as described in section 2.3.7.1. NK cells were isolated with a Miltenyi magnetic antibody cell sorting (MACS, NK Cell Isolation Kit II mouse, cat #130-096-892) according to the manufacturer's instructions. NK cells and VACV-infected P815 cells were co-incubated in 100 µl in 96-well plate for 4 h following successive double dilutions of effector: target cells ratios, ranging from 1:50 to 1:1.56. Groups of 5 mice were used per experiment and measurements of ^{51}Cr release were done in duplicate to minimise experimental errors. A student's t-test (two-tailed), was performed to assess statistical significance. Specific release was calculated as:

$$\%\ Specific\ release\ = \frac{experimental\ release - spontaneous\ release}{total\ detergent\ release - spontaneous\ release} \times 100$$

2.3.9.2 Degranulation assay

The indicated VACV-infected target cells and NK effector cells were prepared as described in section 2.3.9.1 with the exception that cells were not incubated with ^{51}Cr. Effector and target cells were incubated at 37 ˚C, with 5 % CO_2 in a 96-well plate in 200 µl complete DMEM at ratios ranging from 10:1 to 1:1. Anti-CD107-α (1D4B), Cat# 121611, BioLegend, 5 µl per 1 million cells) was added at the beginning of the incubation and protein transport inhibitor cocktail 1X, (eBioscience) was added 1 h after the co-incubation started to retain cytokines intracellularly. Cell stimulation cocktail 1X, (eBioscience) was used as a positive control stimulus according to the manufacturer's protocol.

After incubation, cells were washed with PBS and collected by centrifugation at 300 *g* for 5 min at 4 ˚C and resuspended in 100 µl of PBS. Fc receptors were blocked, and cells were stained (as described in section 2.3.7.2) with Zombie violet dye (BioLegend) at a dilution of 1:400 (v/v), anti-NK1.1-BV650 (clone PK136, BioLegend, 2.5 µl per million cells), anti-CD3-APC (clone 145-2C11, BioLegend, 2.5 µl per million cells). Where indicated, intracellular staining was performed as described in section 2.3.7.2 with anti-IFNγ PE-conjugated (clone XMG1.2, BioLegend 1 µl per million cells), anti-GzmB AF647 conjugated (clone GB11, BioLegend; 5 µl per million cells) or isotype controls (Alexa Fluor 647 Mouse IgG1, κ Isotype Ctrl (# 400155, BioLegend), PE Rat IgG1, κ Isotype Ctrl Ab, κ Isotype Ctrl (# 400408, BioLegend)). Finally, samples were resuspended in PBS, and the $NK1.1^{+}$, $CD3^{-}$ population (NK cells) were analysed using a BD LSR Fortessa, or an Aurora Cytek.

2.3.9.3 Splenocytes co-incubation assay

Single cells suspension from murine spleens were prepared as described in section 2.3.7.1. Cells were enumerated, and half the cells were infected with the indicated virus using the MOI described in section 2.2.7. The other half of cells were incubated in RPMI supplemented with 2 % FBS, 1 % P/S at 37 ˚C. After the infection period, cells were washed in RPMI, collected by centrifugation at 300 *g* for 5 min at RT and resuspended in fresh RMPI supplemented as above. Control and infected cells were enumerated, and the indicated number of cells were co-incubated in 96-well round-bottom plates for 4 h at 37 °C in 5 % Co_2. After incubation, cells were washed in PBS, collected by centrifugation as above and kept at 4 ˚C for all the subsequent steps. Cells were stained for flow cytometry as indicated in section 2.3.7.2 with the following reagents: viability dye (Zombie NIR, Biolegend, 1:500 (v/v)), CD8-PE/Cy7 conjugated (1:100 (v/v)), CD3-BUV395 (1:50), CD4-BV510 (clone, 1:100), NKp46-FITC (1:100),

CD107a-BV421 (1:20) and intracellular staining with IFNγ-PE 1:100 (v/v). Samples were run on a Fortessa LSR or Aurora Cytek and analysed following the gating strategy in Figure 13.

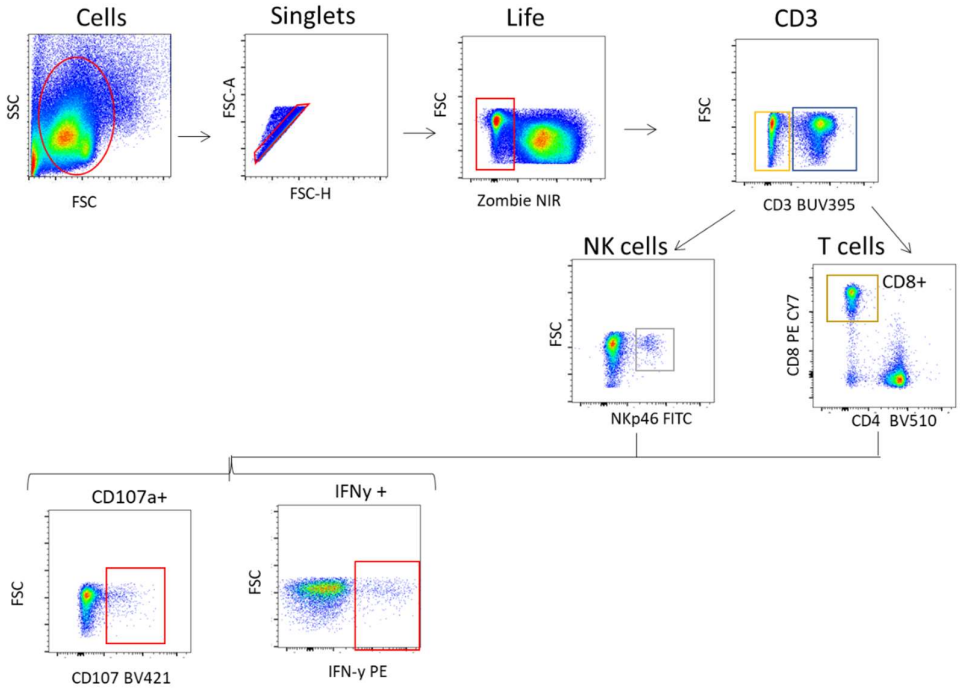

Figure 13. Gating strategy for co-incubation assay of splenocytes. Debris were gated out, and viable singlet cells were separated according to their expression of surface CD3. Positive cells for CD3 that were also positive for CD8 were selected for the study of surface CD107a and intracellular IFNγ. Cells negative for surface CD3 and positive for surface NKp46 were selected for the study of surface CD107a and intracellular IFNγ.

2.3.9.4 Lactate dehydrogenase (LDH) assay

The range of target cells to be used in the linear range of the LDH signal was determined before experiment for the target cell lines as per manufacturer's instruction (CytoTox 96, Nonradioactive cytotoxicity assay, Promega). VACV-infected target and murine NK cells were prepared as described above for Cr^{51} cytotoxicity assay (2.3.9.1) with the exception that cells were not incubated with Cr^{51}. Target cells and NK cells were incubated in 96-well plates, and LDH release was detected by colourimetric reaction calculated as per manufacturer's instruction. An optical photo luminometer was used to measure OD_{490} of experimental wells, which is proportional to the amount of LDH released and therefore the number of lysed cells. The culture medium background was subtracted from all values of experimental wells, and specific release was calculated as:

$$\%\ Cytotoxicity\ = \frac{Experimental - Effector\ Spontaneous - Target\ Spontaneous}{Target\ Maximum - Target\ Spontaneous} x100$$

2.4 Molecular biology

2.4.1 Protein immunoblotting

2.4.1.1 Sample preparation

Cells were lysed with 100 µl of phosphate-buffered saline (PBS) with 1 % (v/v) Nonidet-P40 (NP-40) for 45 min on ice, the cell lysate was centrifuged at 1000 *g* for 15 min, and the supernatant was collected. This clarified cell lysate was mixed with 5x loading buffer (5x solution consisting of 250 mM Tris pH 6.8, 10 % (w/v) sodium dodecyl sulphate (SDS), 0.5 % (w/v) bromophenol blue, 50 % (v/v) glycerol, 250 mM DTT (Dithiothreitol) and the samples were heated for 10 min at 95 °C.

2.4.1.2 Sodium dodecyl sulphate – polyacrylamide gel electrophoresis (SDS-PAGE)

The clarified cell lysate was loaded onto an SDS-polyacrylamide gel (12 % gel) (made of components described in Table 4. The protein marker ladder (Prestained Blue protein ladder, GeneFlow, 5 µl) was loaded on the gel for molecular size reference. Proteins were separated by electrophoresis using Tris-glycine running buffer (250 mM glycine, 25 mM Tris-HCL and 0.1 % (w/v) SDS) at 75 V for 20 min and then at 135 V for 1 h.

Table 4: Composition of the running and the stacking gel of an SDS-polyacrylamide gel (12 % gel)

Components	**Running gel 12 %**	**Stacking gel 5 %**
H_2O	3.3 ml	2.7 ml
1.5 M Tris (pH 8.8)	2.5 ml	/
1 M Tris (pH 6.8)	/	0.5 ml
10 % (w/v) SDS	0.1 ml	0.04 ml
30 % (v/v) acrylamide mix	4.0 ml	0.67 ml
10 % (w/v) ammonium persulfate	0.1 ml	0.04 ml
TEMED	0.004 ml	0.004 ml

2.4.1.3 Transfer and immunoblotting

After electrophoresis, proteins were transferred onto a nitrocellulose membrane (Ge Healthcare Life Science, # 10600004) using a semi-dry transfer in transfer buffer (50 mM glycine, 25 mM Tris-HCL and 20 % (v/v) methanol). Membranes were blocked in 5 % (w/v) milk powder with PBS Tween (PBS-T) (PBS with 0.01 % (v/v) Tween-20) for 1 h at RT. Membranes were incubated with their relevant primary Ab (Table 5) diluted in 5 % (w/v) milk overnight at 4 °C with agitation. The membranes were washed three times for 10 min in PBS-T, then incubated for 1 h with agitation with the appropriate secondary Ab (Table 5) diluted in 5 % (w/v) milk PBS-T. Membranes were washed three times again in PBS-T. Proteins visualised using an Odyssey infrared imaging system (Li-COR biosciences).

Table 5: Primary and secondary Abs used for immunoblotting.

Ab (host specie, target, use)	Source	Concentration
Mouse, α-tubulin, primary	Sigma	1:5000
Mouse, anti-VACV protein D8, primary	MAb AB1.1 (Parkinson & Smith 1994)	1:3000
Goat, anti-mouse, secondary	Li-COR #C60107-06	1:10 000
Mouse, anti-VACV A56, primary	Shida anti-HA anti-sera (Shida & Dales 1982)	1:200

2.4.2 Binding assay with NCR-Fc fusion proteins

2.4.2.1 Production of NCR-Fc fusion proteins

NCR-Fc fusion proteins were produced by Dr Kafai Leung as described (Jarahian *et al.* 2011; Mandelboim *et al.* 1999). Briefly, HEK293T cells stably expressing receptor globulins NKG2D-Ig, NKp30-Ig, NKp44-Ig, h-NKp46 and m-NKp46 (kindly provided by Dr Ofer Mandelboim) were seeded at 70-80% confluency and grown in DMEM supplemented with 2 % FBS and 1 % P/S. NCR-Fc fusion proteins were collected from the supernatant of those cells and incubated with protein G beads overnight under agitation at 4 ˚C to isolate the NCR-Fc fusion proteins. Beads were transferred in Bio-Spin chromatography columns (Bio-Rad 732-6008), centrifuged at 1000 x *g* for 1 min at 4 °C and washed 6 times with 1 column volume (CV) (1 ml) of PBS at 1000 x *g* for 1 min at 4 °C. Proteins were eluted with 1 CV (1 ml) of 0.1 M glycine pH 2.7. The elution buffer was neutralised with 200 µl of 1 M Tris pH 9.0 in collection tubes. Eluted fractions were stored at 4 °C for short term use, or -80 °C for long term storage. The purity and integrity of the receptor globulins was assessed by Coomassie blue staining and immunoblotting.

2.4.2.2 NCR-Fc fusion protein binding assessment by flow cytometry

Cells were infected with the indicated virus at an MOI of 5 for 14 to 16 h as described in section 2.2.7. Cells were detached with Accutase (Innovative Cell Technologies, # AT104-500) or 5 mM EDTA, enumerated, resuspended in PBS and 2×10^5 cells were stained with viability dye (Zombie NIR or Zombie violet 1:500 (v/v) for 15 min as per manufacturer's instructions. Cells were washed with PBS and collected by centrifugation at 300 *g* for 5 min at 4 ˚C and subsequently incubated with 5 µg of soluble NCR-Fc fusion protein, or 5 µg human IgG Fc fragment protein as an isotype control (Abcam, #ab90285) for 1 h incubation at 4 ˚C. Cells were washed with PBS, collected by centrifugation at 300 *g* for 5 min, and incubated for 30 min at 4 ˚C in the dark with secondary Ab, anti-human IgG at a

dilution of 1:100 (anti-human IgG Fc PE-conjugated BioLegend, clone HP6017). Cells were washed with PBS, collected by centrifugation as above and fixed for 30 min with 4 % PFA, and then washed and resuspended in PBS. Data were acquired on Attunes flow cytometer or BD LSR Fortessa or Aurora cytek and gated as shown on Figure 14.

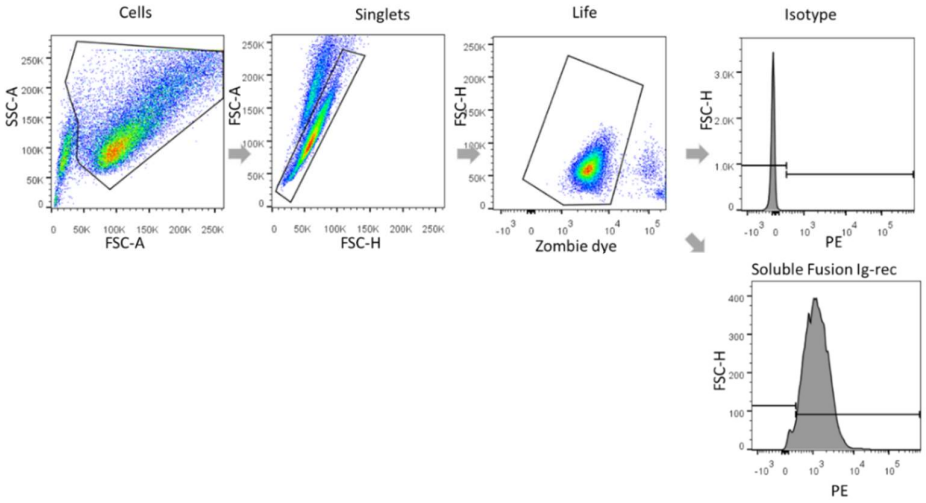

Figure 14 Representative gating strategy used for the analysis of the soluble chimeric NCR-Ig binding assay. Debris were gated out, then single and viable cells were gated for analysis of surface-bound soluble Ig-receptor, isotype control was used to set the gate for analysis of the NCR binding.

2.5 Transcriptomic study of murine NK cells

2.5.1 Mice infection and sample collection

Female B6 mice (6-8 weeks old) were i.n. infected as described in section 2.3.2 with 1.5×10^3 pfu of WT VACV or with vehicle control. Mice were monitored daily for signs of illness and weight change. At 1.5 and 6.5 d.p.i., mice were sacrificed by cervical dislocation and organs were taken for RNA-sequencing (RNA-seq) and FACS analysis as described in Figure 22.

The study was performed as follows: in a first experiment, two groups of 12 mice were infected i.n. at d 0 either with VACV or with vehicle control. At 1.5 and 6.5 d.p.i., 6 mice of each group were sacrificed, livers were used for NK cells surface phenotyping by FACS, whilst the spleens were processed to isolate NK cells (NK1.1+CD3-) by FACS for subsequent analysis by RNA-seq. In a second experiment, two groups of 10 mice were infected i.n. at d 0 either with VACV or with vehicle control. At 1.5 and 6.5 d.p.i., 5 mice of each group were sacrificed, spleens and livers were used for NK cell surface phenotyping by FACS.

2.5.2 Sample preparation and RNA extraction from NK cells

From this step onwards, all subsequent procedures were done on ice under sterile conditions using RNAse-free materials and reagents. NK cells were extracted from spleens and livers by FACS (as described in section 2.3.8) and stored at -80 C° until RNA extraction was performed. To minimise experimental variation, all samples for RNA-seq were processed simultaneously in the subsequent steps. Total RNA was extracted using the RNeasy Mini Kit (Qiagen, #74104) and an additional DNAse (Deoxyribonuclease) treatment was performed using the Qiagen RNase-Free DNase Set (Qiagen, #79254). Both kits were used according to the manufacturer's instructions.

2.5.2.1 Library preparation

From this step onwards, samples were handed to the Cambridge Genomic Service (CGS) sequencing facility who prepared the libraries, carried out the sequencing and generated differential gene expression data files. First, RNA concentration, purity and integrity were checked using a SpectroStar FLUOstar OMEGA (BMG LabTech) and an Agilent 2100 Expert bioanalyser (Agilent Technologies). The SMART-Seq v4 Ultra Low Input RNA Kit for Sequencing (Takara Bio, USA) was used to generate cDNAs from an input of 5 ng RNA. The cDNAs quality was assessed using the Agilent 2100 bioanalyser and a high sensitivity DNA chip. cDNAs were then quantified by Qubit and normalised to 25 pg/µl. The Nextera XT DNA Library Prep Kit (Illumina) was used to generate libraries from 125 pg of input cDNAs. Library quality was checked with a tapestation (HS D1000) and a Qbit with dsDNA high sensitivity. Libraries were normalised to the lowest concentration and pooled together to be run on the NextSeq500 (Illumina) for single-end sequencing on 75 cycles. Samples were normalised to the lowest concentration amongst all samples.

2.5.2.2 RNA-seq data processing and analysis

The quality of the sequencing reads was assessed using FastQC v0.11.4. The quality scores per base and the average quality score per sequence given by the sequencer were analysed. A score of 10 corresponds to 1 error in 10, a score of 20 corresponds to 1 error in 100, and so on. It is expected that reads have a mean quality score of 30 or greater. As shown in Figure 15, the 16 samples performed well and have a mean quality score above 30. Further, the sequence GC content was checked. Non-biased libraries should have a normal distribution of GC content. Figure 15 shows that the 16 samples follow a normal distribution as expected. Next, the sequence read length distribution was examined and is anticipated to match the sequence length of the protocol. Figure 15 shows that the 16 samples clustered well together around 75, which corresponds to the sequencing read length used in this study.

After the quality control was completed, the low-quality base calls (quality score <30) and the adapter at the 3' end of the sequencing reads were removed using TrimGalore v0.4.1. Reads inferior to 20 bases long were discarded from the dataset. The percentage of reads removed and left after trimming is shown in Table 6. Trimmed reads were mapped to the Ensembl Mus musculus GRCm38 (release 95) using STAR v2.5.2.a. The number of reads that mapped to genomic features was calculated using HTSeq v0.6.0 and is represented in Figure 16.

For differential expression analysis, the threshold was set to include genes with at least 5 cpm, detected in at least 4 samples to allow for an on/off situation to be included in the analysis. Normalisation factors were calculated by considering the sequencing depth and RNA composition. A correction was applied for GC content and gene length bias by using CQN Bioconductor package v.1.24.0 that allows removal of a systematic GC content and gene length bias by a smoothing function. Pairwise comparisons between groups were performed using the counted reads and the R package edgeR version 3.16.5 (R version 3.4.1). The resulting p-value was then corrected for multiple hypothesis testing using the Benjamini-Hochberg method.

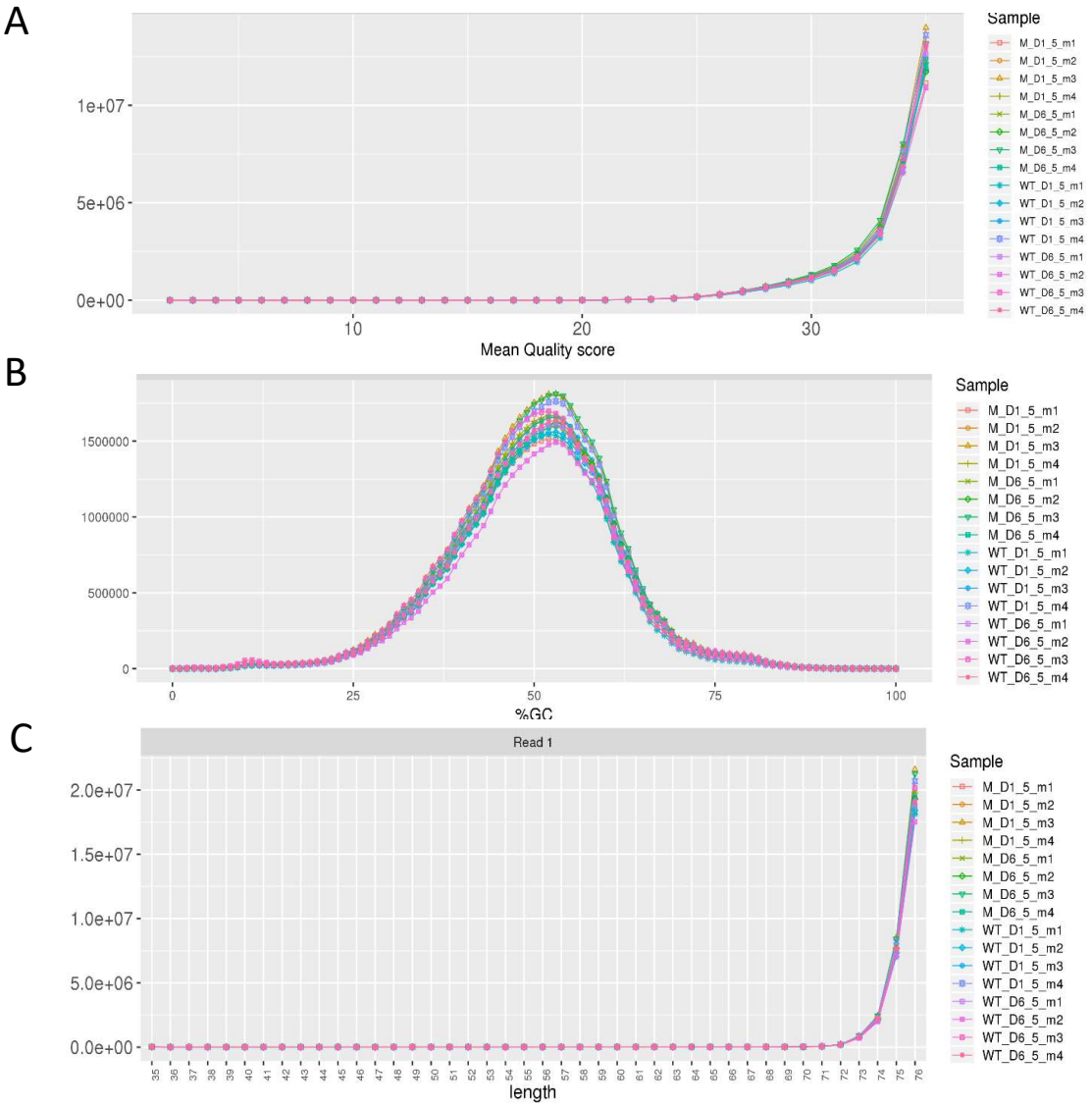

Figure 15. Quality control for the 16 samples of the RNA-seq experiment. A) The average quality score given by the sequencer (Fred score) for each sample, as expected was above 30. B) Average GC content expressed in percentage, follows a normal distribution. C) Read length distribution of the 16 samples, shows that they cluster together and peak around 75 as expected. These graphs were generated by CGS.

Table 6. The number of reads before and after trimming the low-quality bases and adapters for each sample of the RNA-seq experiment. This table was generated by CGS.

Sample name	Raw reads	After trimming	% removed
M_D1_5_m1	28,749,774	28,746,108	0.0128
M_D1_5_m2	30,041,926	30,038,087	0.0128
M_D1_5_m3	34,212,393	34,207,784	0.0135
M_D1_5_m4	31,280,601	31,276,697	0.0125
M_D6_5_m1	31,289,817	31,285,960	0.0123
M_D6_5_m2	30,635,478	30,631,807	0.012
M_D6_5_m3	33,849,447	33,845,404	0.0119
M_D6_5_m4	29,905,412	29,901,619	0.0127
WT_D1_5_m1	28,621,125	28,617,668	0.0121
WT_D1_5_m2	29,250,886	29,247,091	0.013
WT_D1_5_m3	30,961,475	30,957,841	0.0117
WT_D1_5_m4	32,822,780	32,818,726	0.0124
WT_D6_5_m1	30,260,477	30,256,438	0.0133
WT_D6_5_m2	27,951,165	27,947,514	0.0131
WT_D6_5_m3	31,805,393	31,801,369	0.0127
WT_D6_5_m4	30,422,873	30,418,979	0.0128

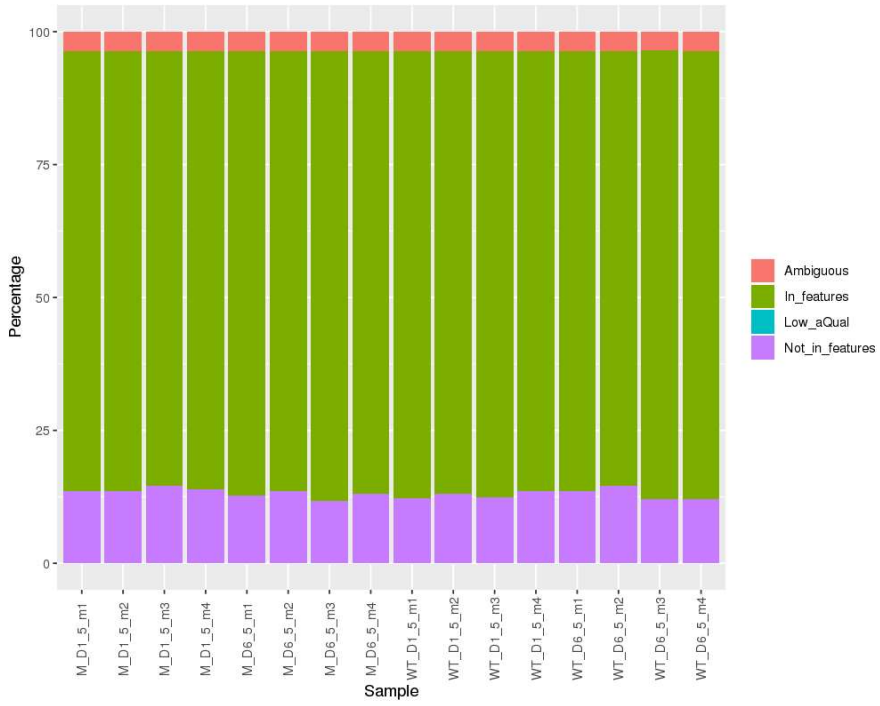

Figure 16. The proportions of reads mapped in features to the murine genome. In green is the percentage of reads that mapped to genes (in features), in purple the reads that mapped to other genomic regions (not in features) and in red the reads that mapped to ambiguous locations. There were no low quality (blue) reads and the majority of reads mapped to genes. This graph was generated by CGS.

2.5.3 Validation of NK cell phenotyping by FACS

NK cells were prepared and labelled for phenotyping as described in section 2.3.7.2. Samples were labelled with a common cocktail of Abs for the identification of NK cells (Zombie, NK1.1, CD45, CD3 - ,Table 7) and then with combinations of mAbs for the markers of interest (Table 7). NK cells were gated as represented in Figure 17, and the indicated markers of interest were gated as represented in Figure 17. Single stains for each marker were used to set up the compensation, and relevant FMO was used to set up the gates.

Table 7. Abs used for NK surface phenotyping by FACS.

Antigen	Fluorochrome	Clone	Company cat. number	Abs vol in 50 µl
Fixable Viability Dye	Zombie violet	/	Biolegend #423113	0.12 µl
CD3	BV421	145-2C11	Biolegend #100341	1 µl
CD45	BV650	30-F11	Biolegend #103151	1.5 µl
NK1.1	APC-Cy7	PK136	Biolegend # 108724	2 µl
CD27	APC	LG.3A10	Biolegend # 124211	1 µl
CD11b	FITC	M1/70	Biolegend #101205	2 µl
KLRG1	BV510	2F1	BD #740156	5 µl
Thy-1.2	PerCP	30-H12	Biolegend #105321	1 µl
CD69	PE	H1.2F3	Biolegend #104507	2 µl
Ly49C/I	FITC	5E6	BD # 553276	5 µl
Ly49H	AF647	3D10	BD #62207	1 µl
CD107a	PE	1D4B	Biolegend # 121611	2 µl
Ly49A	FITC	YE1/48.10.6	Biolegend 116805	2 µl
Ly49F	APC	HBF-719	Miltenyi Biotech 130-104-293	1 µl
CD319	PE	4G2	Biolegend#152005	2µl
Ly49D	FITC	4E5	BD #555313	1µl
Ly49G2	APC	4D11	BD #555316	1µl
DNAM-1	PE	Tx4.1	Biolegend #133603	2.5µl
NKG2D	PE	A10	Biolegend #115605	1µl
CD94	FITC	18D3	eBioscience #11-0941-81	2µl
NKp46	AF647	29A1.4	BD #560755	2µl
LY108	PE	330-AJ	Biolegend #134605	3µl
CD49b	FITC	HMα2	Biolegend 103503	3µl
gp49B	PE	H1.1	Biolegend 144904	3µl
CXCR6	APC	SA051D1	Biolegend #151104	3µl

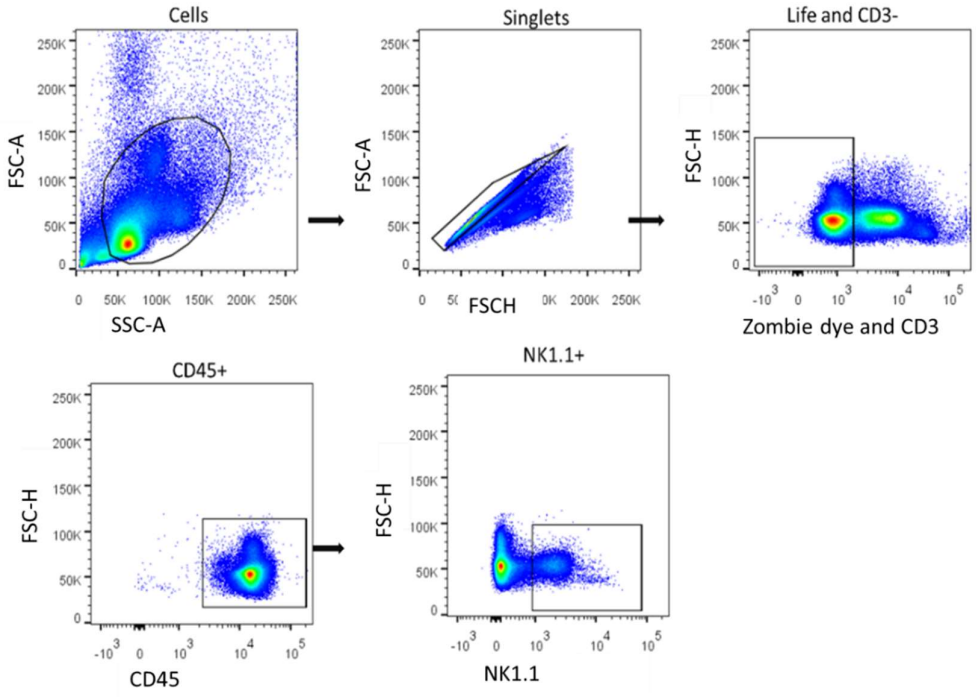

Figure 17. Common gating strategy used for NK phenotyping by FACS. Debris were gated out, then viable single cells negative for CD3, and positive for CD45 and NK1.1 were gated. Further, NK cells were analysed for multiple markers as described in Figure 18.

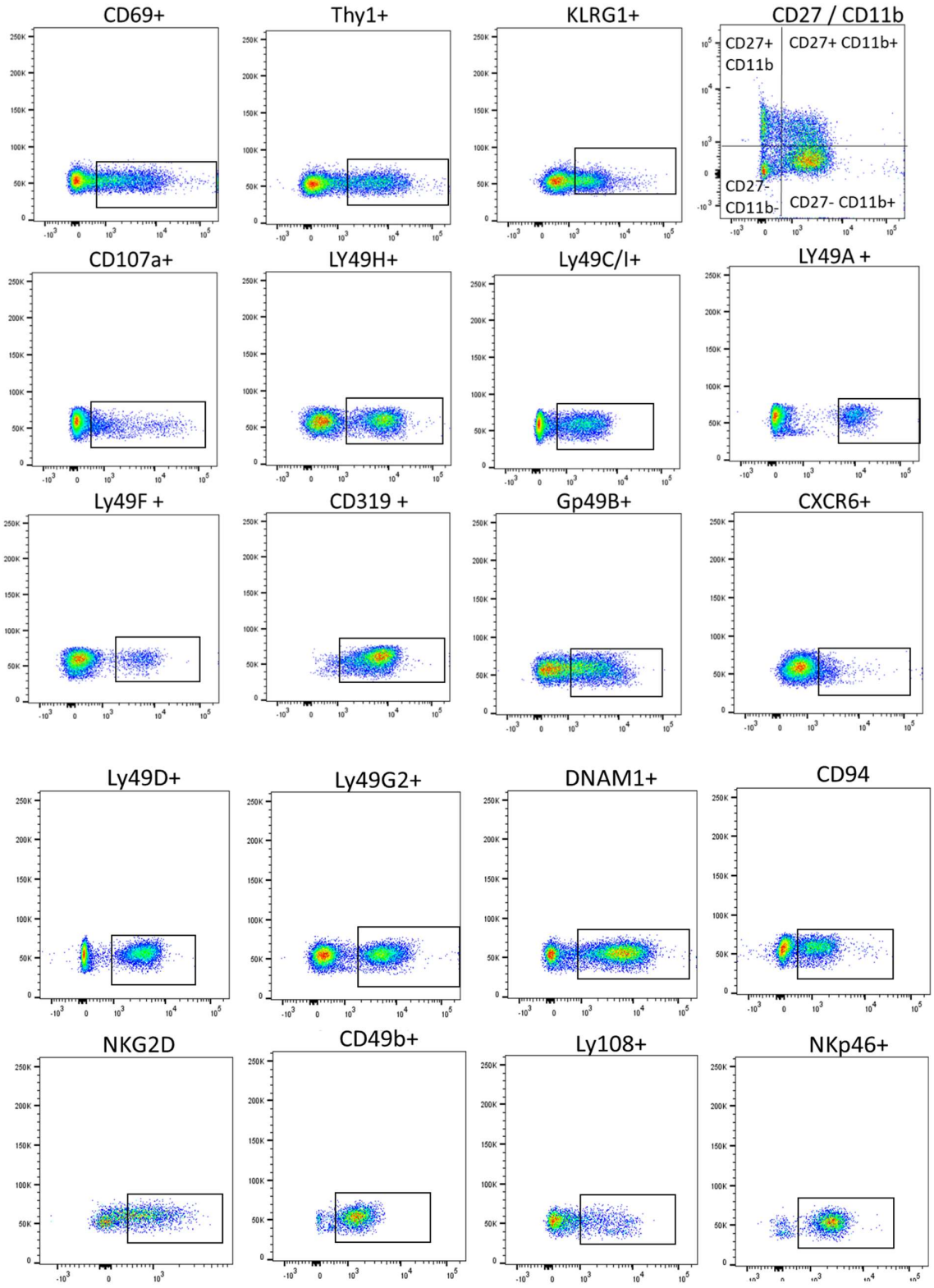

Figure 18. Gating strategy for NK cell surface markers studied during FACS-based validation of RNA-seq data. A representative plot and the gate applied to study each marker of interest is represented.

2.6 Proteomic study of the PM proteome

This work is the result of a collaborative effort. The conception and experimental design were outlined by me, cell infection and labelling by myself and Arwen Altenburg, TMT labelling and fractionation by M. Weekes lab, mass spectrometry by CIMR Proteomics Facility (Robin Antrobus), mass spectrometry data processing by M. Weekes lab. All subsequent bioinformatic analyses, graphs, interpretation and FACS-based validation of the data presented in this thesis were made by me.

2.6.1 VACV infection of HFFF-TERTS

HFFF-TERTs were seeded in 155cm^2 circular flasks to reach ~90 % confluence at the time of infection. Immediately before infection, the medium of all flasks was replaced with fresh DMEM supplemented with 2 % FCS and 1 % P/S. Infections were staggered so that all flasks were harvested simultaneously. The indicated VACV that had all been purified by sedimentation through a sucrose cushion (WT, ΔA56, ΔA38 and ΔA40) were diluted in DMEM 2 % FCS, 1 % P/S and used to infect cells at MOI 5 in a volume of 6 ml. Flasks were incubated at 4 ˚C where indicated and otherwise at 37 ˚C, with 5 % CO_2 for 90 min and were rocked every 15 min to ensure equal dispersion of the inoculum. Flasks were then topped up with 15 ml DMEM supplemented as above and incubated at 37 ˚C with 5 % CO_2 until harvesting.

For samples treated with the proteasome inhibitor MG132, 0.5 µl/ml medium (v/v) (Merck Cat#474787) of 20 mM MG132 was added per flask 2 h pi. This timing allows the proteasomal-dependent uncoating of VACV to occur before inhibition of the proteasome. Infection levels of the indicated viruses were checked at 15 h.p.i. as described in section 2.2.8 (Figure 19) and were always > 96.6 % for all infected samples.

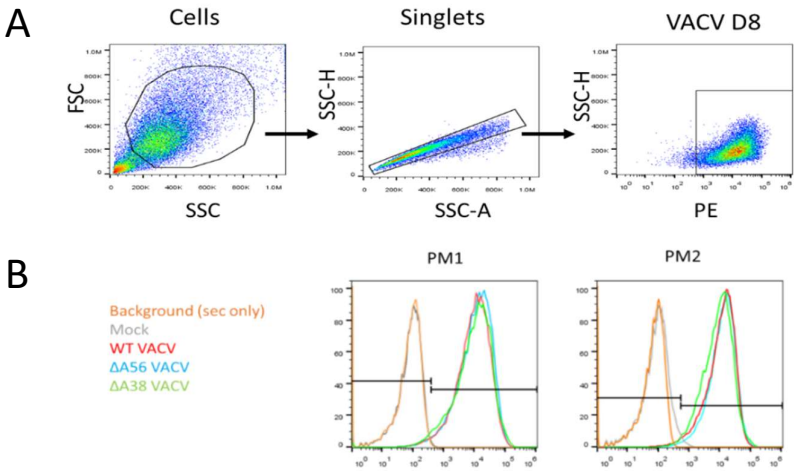

Figure 19 Infection level was controlled by flow cytometry. HFFF-TERTs cells infected with the indicated virus were stained with anti-VACV D8 at 15 h.p.i., a mock and a background staining (secondary mAb only) samples were also included. A) Gating strategy B) Overlay of histograms for anti-VACV D8 staining in both PMP experiments

2.6.2 Plasma membrane protein biotinylation

Plasma membrane protein labelling was performed as described (Weekes *et al.* 2010, 2014), and all steps were performed on ice. Briefly, the medium of each flask (155 cm^2) was discarded and cells were washed twice in PBS pH 7.4 with $CaCl_2$ and $MgCl_2$ (Sigma, D8662-6x). A biotinylation/oxidation mix was made up of 1 mM sodium periodate (prepared in PBS pH 6.7) (Thermo 20504), 100 mM aminooxy-biotin (prepared from 5mg aminooxybotin dissolved in 100 µl dry DMSO (Dimethyl sulfoxide) (Biotium Inc, 90113) and 10 mM aniline (Sigma, 242284) in PBS pH 6.7 (Sigma, D8662). Addition of 8 ml of the mix per flask led to the oxidisation and then biotinylation of surface sialic acids. After 30 min incubation at 4 °C under agitation, the reaction was stopped by addition of glycerol to a final concentration of 1 mM, for 5 min. The reaction mixture was discarded, and cells washed twice in PBS pH 7.4 with $CaCl_2$ and $MgCl_2$. A lysis buffer was made of 1.6 % Triton X-100 (Thermo 28314), 150 mM NaCl (Sigma, S6546), 1 x protease inhibitor per 10 ml lysis buffer (Roche, 11 836 153 001) and 5 mM iodoacetamide (Sigma, I1149), and 10 mM Tris-HCl pH 7.6 (Sigma, 93313). Cells were scrapped in 1 ml of the lysis buffer and transferred to an Eppendorf tube on ice where lysis occurred for 30 min. Cells were spun for 5 min at 13,000 *g* 4 ˚C three times to remove nuclei. Samples were snap-frozen in liquid nitrogen and stored at – 80 °C until the subsequent use. From this stage, the samples were handed to our collaborator in the Weekes lab.

2.6.3 Biotinylated proteins isolation and TMT labelling

Samples were processed as described (Weekes *et al.* 2014). Briefly, biotinylated glycoproteins were enriched with high-affinity streptavidin agarose beads (Pierce) and washed extensively. Captured protein were denatured with SDS and urea, reduced with DTT, alkylated with iodoacetamide (IAA, Sigma) and digested on-bead with trypsin (Promega) in 200 mM HEPES (4-(2-hydroxyethyl)-1-piperazineethanesulfonic acid) pH 8.5 for 3 h. The digested peptides were eluted, and each sample labelled with 56 µg of a different tandem mass tag (TMT) reagent (Thermofischer) in a final acetonitrile concentration of 30 % (v/v) for 1 h at room temperature. Tandem mass tags are chemical structures made of a reactive amine-group, a spacer and a mass reporter that is different for each of the 11 TMT used and allows to multiplex samples. Samples were labelled as follows: TMT 126 (WT VACV 90 min), TMT 127N (WT VACV 6 h), TMT 127C (WT VACV 12 h), TMT 128N (WT VACV 18 h), TMT 128C (Mock 18 h), TMT 129N (ΔA38 VACV 18 h), TMT 129C (ΔA56 VACV 18 h), TMT 130N (WT VACV + MG132 18 h), TMT 130C (Mock + MG132 18 h), TMT 131 (WT VACV 4 °C 90 min), TMT11-131C (Mock 90 min). The reaction was then quenched with hydroxylamine to a final concentration of 0.5 % (v/v). TMT-labelled samples were combined at equal ratio (1:1 for each of the 11 samples), and the samples were vacuum-centrifuged and subjected to C18 solid-phase extraction (Sep-Pak, Waters).

2.6.4 Liquid chromatography-mass spectrometry 3 (LC-MS3)

LC-MS3 was performed at CIMR proteomic facility by Robin Antrobus as described in Nightingale et al., 2018 using an Orbitrap Lumos (Thermo Fisher Scientific, San Jose, CA) for acquisition and a MultiNotch MS3-based TMT method (McAlister *et al.* 2012, 2014). First, an unfractionated single-shot was analysed to ensure similar peptide loading across each of the 11 samples. The remaining TMT-labelled tryptic peptide samples were subjected to High pH reversed-phase chromatography (HpRP) fractionation, as described in Nightingale et al. (Nightingale *et al.* 2018), at the difference that samples were yielded as a single-set of 6 fractions. These fractions were dried and resuspended in 10 µl MS solvent (4 % MeCN/5 % formic acid) before LC-MS3. Subsequently, data from the single-shot experiment was analysed with data from the corresponding fractions to increase the overall number of peptides quantified. Data processing was performed by M. Weekes laboratory members as described in Soday et al., 2019) using MAssPike (collaboration with Pr. Steven Gygi's laboratory).

2.6.5 FACS validation of temporal profiles

HeLa or HFFF-TERT cells were infected as described in section 2.6.1 for 16h at MOI 5 with WT VACV. Cells were detached wit accutase solution (Sigma, cat #A6964) following the manufacturer's instructions. Cells were enumerated, and 2*10^5 cells were used per samples in a v-shaped 96 well plate. Cells were stained for viability as per manufacturer's instruction (Zombie NIR Fixable Viability Kit, Biolegend), primary mAb was added in 50 µl PBS for 30 min, in the dark, at 4 °C (Table 8). Cells were washed in PBS twice, spun at 300 *g* for 5 min, and secondary mAb (PE-conjugated Goat anti-mouse IgG, BioLegend) was added (dilution 1:100 (v/v) in 100 µl of PBS for 30 min in the dark, at 4 °C. Cells were washed twice with PBS, spun at 300 *g* for 5 min, fixed with PFA 4 % for 30 min at RT and resuspended in PBS to be acquired on the Attune NxT 290 FACS. Cells were gated as indicated on Figure 20. Isotype controls were always included, and infection controls were performed in parallel as described in section 2.2.8 with anti-VACV D8 intracellular staining and with anti-VACV A56 surface staining (Figure 21).

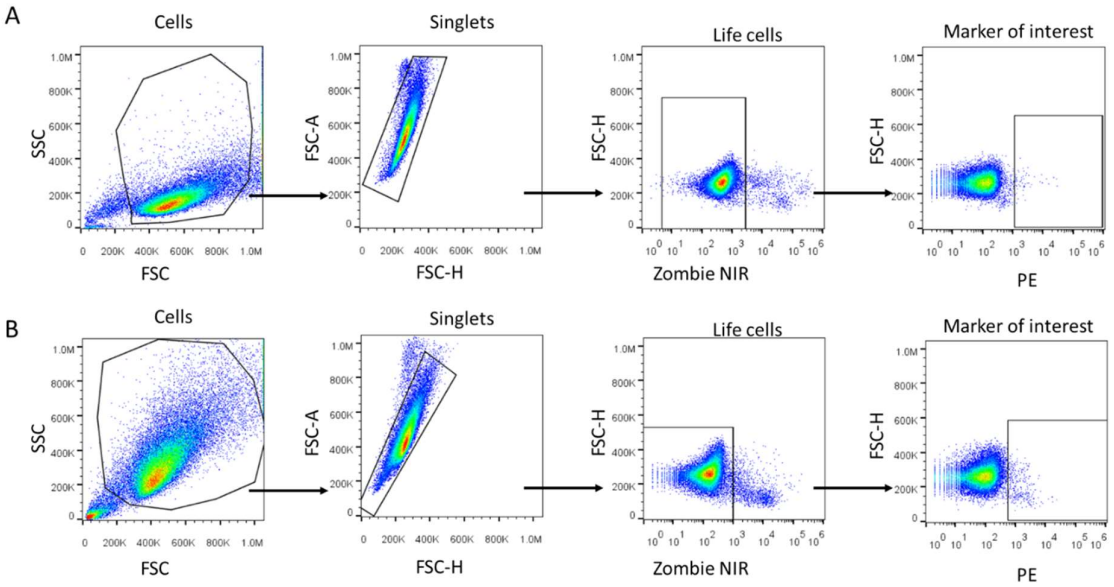

Figure 20 Gating strategy for validation by FACS of surface protein temporal profile during VACV infection. HeLa cells (A) or HFFF-TERT cells (B) were mock-treated or infected with WT VACV for 15 h at MOI 5. Debris were gated out, then single and viable cells were gated and studied for surface expression of a marker of interest on the PE channel. Cells were acquired on an Attune NxT 290.

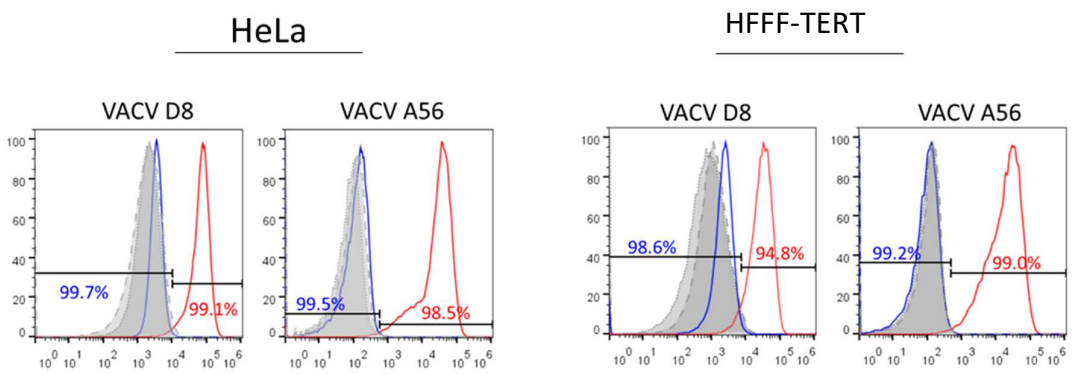

Figure 21 Infection level control in HeLa and HFFF-TERTs for temporal profile FACS validation. HeLa and HFFF-TERTS cells were mock (blue line) or infected (red line) with WT VACV at MOI 5 for 16 h. Cells were harvested and stained for cell viability and surface expression of VACV A56 or intracellular expression of VACV D8. Isotype control was used for both infected (grey dotted line) and non-infected cells (grey dashed line). Cells were analysed on Attunes Nxt FACS.

Table 8 Abs used for FACS validation of surface protein temporal profiled during VACV infection.

Target	**Clone**	**Reference**	**Origin**	**Type**
MICA	2C10	sc-23870	Santa Cruz	IgG1
Anti-EPHB4-PE	rea923	130-115-596	Miltenyi Biotech	IgG1
CD95 (Fas)-PE	dx2	130-099-094	Miltenyi Biotech	IgG1
EGFR	528	sc-120	Santa Cruz	IgG2a
HLA-B/C	4E	(Yang *et al.* 1984)	L. Boyle lab	IgG2a
HLA-C/E	DT9	(Braud *et al.* 1998b)	L. Boyle lab	IgG2b
MHC-I	W6/32	(Parham *et al.* 1979)	L. Boyle lab	IgG2a
Human ULBP-3	166510	MAB1517	R&D systems	IgG2a
Human B7-H6	875001	MAB7144	R&D systems	IgG1
Human ULBP-2/5/6	165903	MAB1298	R&D systems	IgG2a
Anti-Plexin-B1-PE	rea728	130-111-480	Miltenyi Biotech	IgG1
VACV-A56	WR181	IT-012-006M1	Immune tech	IgG1
Anti-human MICB	236511	MAB1599	R&D systems	IgG2b
Anti-human trail-R4	104918	MAB633	R&D systems	IgG1
Isotype mouse Igg2b	NA	sc3879	Santa Cruz	IgG2b
Isotype mouse IgG2a	NA	sc3878	Santa Cruz	IgG2a
Isotype mouse IgG1	NA	sc3877	Santa Cruz	IgG1

2.7 Software and bioinformatic analyses

2.7.1 Sequence similarity

Amino acids sequence similarities were searched for using the protein Blast software with default parameters.

2.7.2 Flow cytometry analysis

Samples acquired by flow cytometer were analysed with FlowJo version 10.15 (TreeStar, Oregon USA).

2.7.3 Statistical analyses

Unless otherwise stated, all statistical analyses were carried out using Prism 5.0 (GraphPad, CA San Diego).

2.7.4 Transcriptomic dataset analysis

2.7.4.1 Pathway and biological process enrichment

To assess the pathways and the biological processes affected during VACV infection in NK cells, transcripts that were differentially-expressed between mock and VACV-infected samples ($p < 0.05$) were used as input in the Reactome database. Those genes were tested for GO (Gene Ontology) enrichment against a background made of the union of all the genes detected in the mock and WT-infected samples. Enrichment scores (p-values) for GO annotations were corrected for multiple hypothesis testing using the Holm-Bonferroni method. Data which met the significance threshold of 0.05 were plotted as -log10 of the p-value using Prism 5.0 (GraphPad, CA San Diego).

2.7.4.2 Comparison of NK cell transcriptomic signatures

2.7.4.2.1 With activation transcriptomic signature

Expression patterns corresponding to the unique NK cell transcriptomic signature associated with i) direct cell recognition, ii) cytokine stimulation, iii) ADCC, iv) and with a general activation pattern induced by all such three stimuli, were identified in our RNA-seq dataset by comparison with the study of Costanzo and colleagues (Costanzo et al., 2018). The supplementary data from this study (data reference GSE110446) was used to generate four lists of transcripts differentially expressed for each of these four conditions (further divided in upregulated and downregulated). These four lists were used to search for the expression of such transcripts in our RNA-seq dataset using the unique gene IDs corresponding to each transcript. Human gene IDs were converted in murine gene IDs using DAVID software. All the transcripts detected in our RNA-seq study were found for hits that were among the upregulated genes lists from Costanzo et al. study - no genes amongst the downregulated hits lists

were detected in our dataset. Hence, the identification of common and unique activation pattern in our dataset concerns transcripts that are expected to be upregulated during NK cell activation.

2.7.4.2.2 With MVA-associated transcriptomic signature

Overlap between VACV-induced transcriptomic signature in murine NK cells and MVA-induced transcriptomic signature in human NK cells was determined by comparison of our RNA-seq data with a study published by Costanzo and colleagues (Costanzo et al., 2018) (data reference GSE110446). Transcripts with a FC >1.5 or <-1.5 (regardless of the statistical value associated with their differential expression) were isolated in the study of Costanzo and colleagues to generate a list. The expression for such transcripts was searched in our RNA-seq dataset. The unique gene IDs corresponding to each transcript were used to make comparisons. All the transcripts from the list isolated in Costanzo et al. study that were detected in our RNA-seq data, were reported as upregulated in Costanzo study. Hence, the identification of common and unique activation pattern in our dataset concerns transcripts that are expected to be upregulated during NK cell activation.

2.7.4.2.3 With MCMV-associated transcriptomic signature

To identify NK cell transcripts whose expression is affected by both VACV and mCMV or solely by one of the two viruses, our RNA-seq data was compared to the GSE15907 data set from the Immunogen project (Bezman *et al.* 2012). In this study, the differential expression of B6 splenic NK transcripts at d 1 and d 7 post mCMV infection was studied in comparison to mock samples. The Intermine software was used to handle the datasets. To minimise the temporal variation resulting from the infection dose and route of each study and the different virus replication kinetic, data from the two time points in each study were analysed together. To ensure that transcripts found to be uniquely affected by one of the two viruses did not result from the absence of detection in one of the datasets, only the genes detected in both studies were retained for further analysis. Transcripts whose expression was up/downregulated with statistical significance (FDR <0.05) within each dataset, were compared for the two viruses using the union and asymmetric exclusion function on Intermine. Further, to identify NKRs whose genes expression was affected by both or only one of the two viruses, a gene list for NKRs was curated manually. This list was used against the common and unique transcriptomic signatures of each virus to isolate transcripts of NKRs that were differentially expressed in both conditions.

2.7.5 Proteomic dataset analysis

2.7.5.1 Data handling

The GO annotations were searched for all proteins detected in the proteomic screens. Proteins that have GO annotation for “PM”, “cell surface”, “extracellular” or “short GO” were defined as GO PM-annotated in this thesis. FC were calculated within each PMP screen between the two samples of interest, and then the FC were averaged for the two PMP screens. When a FC was expressed in

comparison to mock, the nearest relevant mock was always used (Mock 1.5h was used for VACV 1.5 and 6 h.p.i. , Mock 18h was used for VACV 12 and 18 h.p.i.). All data was handled using Microsoft Excel, unless otherwise stated.

2.7.5.2 Scatter plots

For proteins quantified in both PMP screens, the average FC was calculated for the indicated samples. FC and intensity (protein quantitation also called signal: noise ratio) for each protein were used as input in Perseus 3.0. to calculate significance A and estimate p values which were then corrected for multiple hypothesis testing with Benjamin-Hochberg (Cox and Mann, 2008). P values, FC and intensity for each protein were then inputted in Excel to generate the volcano plots using a macro as described in Soday *et al*., 2019.

2.7.5.3 Functional GO and pathways enrichment

To assess whether proteins affected during VACV infection are associated with a biological pathway or a biological function, all GO PM-annotated proteins from VACV WT infection time course (1.5, 6,12,18 h.p.i.) which FC was greater than ± 2 (in comparison to their relevant mock samples) were used as input in DAVID (Database for Annotation, Visualization and Integrated Discovery) software. These proteins were tested for enrichment against a background made of all the proteins detected in the PMP screens. Default settings in DAVID software were used to search for functional cluster and pathway enrichment. Enrichment scores (p-value) were corrected for multiple hypothesis testing using the Holm-Bonferroni method. Data which met the significance threshold of 0.05 were plotted using Prism 5.0 (GraphPad, CA San Diego).

2.7.5.4 Hierarchical clustering

All PM-annotated and viral proteins in each of the 11 samples per PMP screen were compared to their relevant mock to calculate FC. FC for each of the 11 samples were averaged between the two PMP repeats, proteins whose FC exceeded 50 in either direction were discarded to avoid skewing of the data. Hierarchical clustering of these 11 samples, based on uncentered Pearson correlation was performed with Cluster 3.0. and a heatmap was generated in Java TreeView 3.0.

2.7.5.5 HLA clean-up

Raw peptide sequences initially assigned to HLAs heavy chains in the PMP screen were checked manually against the reference sequences of all HLA class I expressed by HFFF cells (-A11:01, -A24:02, -B35:02, -B40:02, -C02:02, and -C04:01, -E, -F, -G) (van der Ploeg *et al.* 2017). Reference sequences were obtained from the IPD-IMGT/HLA Database (Immuno polymorphism database-international ImMunoGeneTics project/HLA) (Table 9). Only peptides matching uniquely to the reference sequence

of a chain type (-A, -B, -C, -E, -F, -G) were kept to calculate the relative abundance of the HLA-I heavy chain they correspond to amongst the 11 samples in each of the PMP screens.

Table 9 Reference sequences for all HLA class I expressed by HFFF cells.

HLA class I heavy chain	IEDB accession number
A11:01	HLA00043
A24:02	HLA00050
B35:02	HLA00238
B40:02	HLA00293
C02:02	HLA00404
C04:01	HLA00420
E	HLA00934
F	HLA01096
G	HLA00939

2.7.5.6 Data mining for putative NK ligands

For the mining of human proteins, the InterPro database (Hunter *et al.* 2012) was downloaded, and InterPro annotations domain were added to proteins whose FC had an associated FDR (False discovery rate) <0.05 using the VLOOKUP function in Excel (Microsoft Office). For the mining of viral proteins, the VACV reference proteome (UP000000344) was downloaded from the Uniprot database, and protein domains of viral proteins detected in the PMP screens were searched in Uniprot, InterPro and the literature. The functional domains typically found in NK and T cells ligands (cadherin, collagen, MHC, C-type lectin, immunoglobulin, Ig, TNF, butyrophylin) were searched with the conditional formatting function in Excel. Proteins that had at least one of these domains were isolated for further analysis.

2.7.5.7 MG132 rescue ratio

A rescue ratio was calculated for the NK ligands that were downregulated during VACV infection in the PMP screens. For this, the normalised intensity of such proteins in samples treated with MG132 or not were used to calculate a rescue ratio as follows:

$$\frac{(\text{Norm intensity MG132 VACV 18h}/\text{Norm intensity VACV 18h})}{(\text{Norm intensity MG132 Mock 18h}/\text{Norm intensity Mock 18h})} = \text{MG132 rescue ratio}$$

The denominator was set to a minimum of 1 to avoid artificial inflation. Proteins whose rescue ratio was superior to 1.5 were considered as rescued by the addition of MG132.

3 Chapter 3: Investigation of the NK cell response to VACV at a transcriptomic-wide level

NK cells contribute to the immune response to VACV. Several studies report that NK cells are activated, proliferate, migrate to the site of infection, limit viral replication and develop memory qualities during VACV infection. However, little is known about how NK cells become activated, which of their receptors are engaged and which transcriptional or proteomic changes NK cells undergo in response to VACV.

To understand how NK cells respond to VACV infection *in vivo*, the transcriptional profile of NK cells isolated from VACV-infected mice was studied by RNA-seq. Differential gene expression between mock and VACV-infected mice was analysed to reveal the transcriptional changes occurring in response to VACV. Further, the expression of multiple NK cells surface proteins was analysed by FACS. A particular focus on NK cell receptors (NKRs) was pursued to identify putative NKRs specifically involved in the immune response to VACV. The RNA-seq data were then compared with published transcriptomic studies investigating: i) the murine NK cell response to mCMV; ii) the human NK cell response to MVA vaccination; and iii) the NK cell response to a single stimulus such as ADCC, direct target cell recognition or cytokines. The results of these analyses are discussed sequentially below.

3.1 Experimental design

To study the NK cell response to VACV infection, we aimed to get a broad overview by using a genome-wide and unbiased assay. Proteomic approaches such as TMT based spectrometry or stable isotope labelling of aa (SILAC) were impractical because of the high amount of starting material required, which directed our choice towards transcriptomic techniques. Amongst the transcriptomic techniques available to us, single-cell sequencing was ruled out because of the limited detection of lowly expressed genes such as receptors, which are one of the focus of this study. RNA-seq was chosen over micro-array because it is more accurate when sufficient sequencing depth is achieved (Zhou *et al.* 2017). RNA-seq was combined with a FACS-based approach for surface proteins of interest, to study how transcriptomic changes correlate with surface expression of proteins.

We sought to work in physiologically relevant conditions and therefore chose an *in vivo* model. B6 mice were i.n. infected with VACV WR, which mimics a systemic infection. The response of conventional NK cells (cNK) to VACV rather than resident NK cells was studied to avoid the bias of a specific subset of specialised NK cells. The spleen was chosen as the source of cNK cells for RNA-seq and flow cytometric analysis because the spleen contains enough cNK cells for our experimental

requirements and is easily and reproducibly isolated. Livers were also used for flow cytometric analysis to study whether hepatic NK cells that are enriched in resident NK cells respond differently to VACV infection than cNK cells.

We reasoned that changes specific to VACV infection were more likely to be detected at a time when a putative NK cell subset has specifically expanded in response to VACV and is at the maximum of its expansion before the contraction phase. This NK cell expansion peak is around seven days after VACV infection. Two time points were chosen that represent a very early response (1.5 d.p.i.) and the peak of NK cell amplification (6.5 d.p.i.).We reasoned that a comparison of the differential gene expression at such time points would allow us to unravel the kinetics of the NK cell response to VACV, and to discriminate the VACV-specific NK cell transcriptomic signature from an unspecific early response. The experiment was performed as outlined in Figure 22.

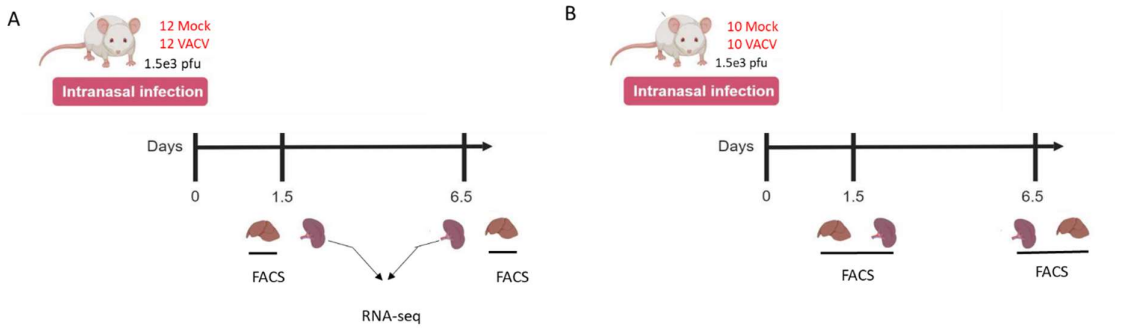

Figure 22. Experimental design to study the NK cell response to VACV infection by RNA-seq and FACS. A) In a first experiment, two groups of 12 mice were infected i.n. with VACV or vehicle control at d 0. At 1.5 and 6.5 d.p.i., 6 mice of each group were sacrificed, spleens were processed for analysis of NK cells (NK1.1.+ CD3-) by RNA-seq whilst livers were used for NK surface phenotyping by FACS. B) In a second experiment, two groups of 10 mice were either mock or VACV-infected i.n. at d 0. At 1.5 and 6.5 d.p.i., 5 mice of each group were sacrificed, and spleens and livers were used for NK cell surface phenotyping by FACS.

Samples were collected as outlined in methods section 2.5 (NK cells defined as live, singlets, CD45+, CD3-, NK1.1+ and gated as shown on Figure 12). Quality controls were performed at multiple stages of the RNA-seq procedure. RNA concentration, purity, and integrity as well as cDNAs and libraries quality were assessed, and all met the necessary requirements. The quality of the raw sequencing reads was assessed, the GC content and the sequence read length distribution were examined, and all performed extremely well as outlined in the methods section 2.5.2.1 and 2.5.2.2. Since the quality controls all indicated that the dataset was of high quality and robust, an analysis of the differential gene expression was undertaken.

3.2 Overview of NK cell transcriptomic profile

Firstly, the number of transcripts in each experimental group and their relative expression was analysed. Four pairwise comparisons were performed to compare the two experimental conditions (mock and VACV-infected) at both time points (1.5 and 6.5 d.p.i.), against each other. Differential gene expression analysis between VACV-infected and their respective mock samples, at 1.5 and 6.5 d.p.i. revealed, respectively, 70 and 3280 transcripts significantly modulated (FDR<0.05). Pairwise comparisons of the two VACV-infected samples with each other revealed 4045 significantly modulated transcripts. Comparison between the two mock samples, revealed 140 transcripts significantly modulated (FDR<0.05) (Table 10).

The technical variation between the two time points is likely to increase the number of transcripts reaching statistical significance when datasets from different time points are compared together. Interestingly, the pairwise comparison of the two mock samples showed greater variation than the pairwise comparison of VACV-infected and mock samples at 1.5 d.p.i. (140 vs70), suggesting that the biological relevance of the latter is probably low and that those hits represent background noise. Therefore, all further analysis focussed on the pairwise comparison of VACV-infected and mock samples at 6.5 d.p.i. unless otherwise stated.

Further, hierarchical clustering of the 16 RNA-seq samples showed that the 4 VACV-infected mice samples at 6.5 d.p.i (WT-D6.5-m) clustered together, apart from the other 12 samples (Figure 23). The 4 VACV-infected mice samples at 1.5 d.p.i (WT-D1.5-m) did not cluster apart from the eight mock samples. This is consistent with the number of genes that are differentially expressed, as described in Table 10. This suggests that the genes that are differentially expressed in WT infected mice at 1.5 d.p.i are background noise whilst the ones detected in WT infected mice at 6.5 d.p.i are biologically relevant and were induced in response to VACV infection.

Table 10 Number of genes differentially expressed for the indicated pairwise comparisons during RNA-seq study of murine NK cells. Groups of B6 mice (n=4) were i.n. infected with WT VACV or vehicle control for 1.5 or 6.5 d. The transcriptional activity of splenic NK cells was compared by RNA-seq. Differential expression of transcripts was analysed following 4 pairwise comparisons, as indicated in the first column. The number of transcripts differentially expressed in a statistically significant manner is indicated in the second column (FDR<0.01) and in the third column (FDR<0.0.5). The total number of genes detected is indicated in the last column.

Comparison	FDR < 0.01 genes	FDR < 0.05 genes	Total genes
Mock_D6.5__VS__WT_D6.5	2314	3280	9647
Mock_D1.5__VS__WT_D1.5	16	70	9646
Mock_D1.5__VS__Mock_D6.5	55	140	9664
WT_D1.5__VS__WT_D6.5	2977	4045	9645

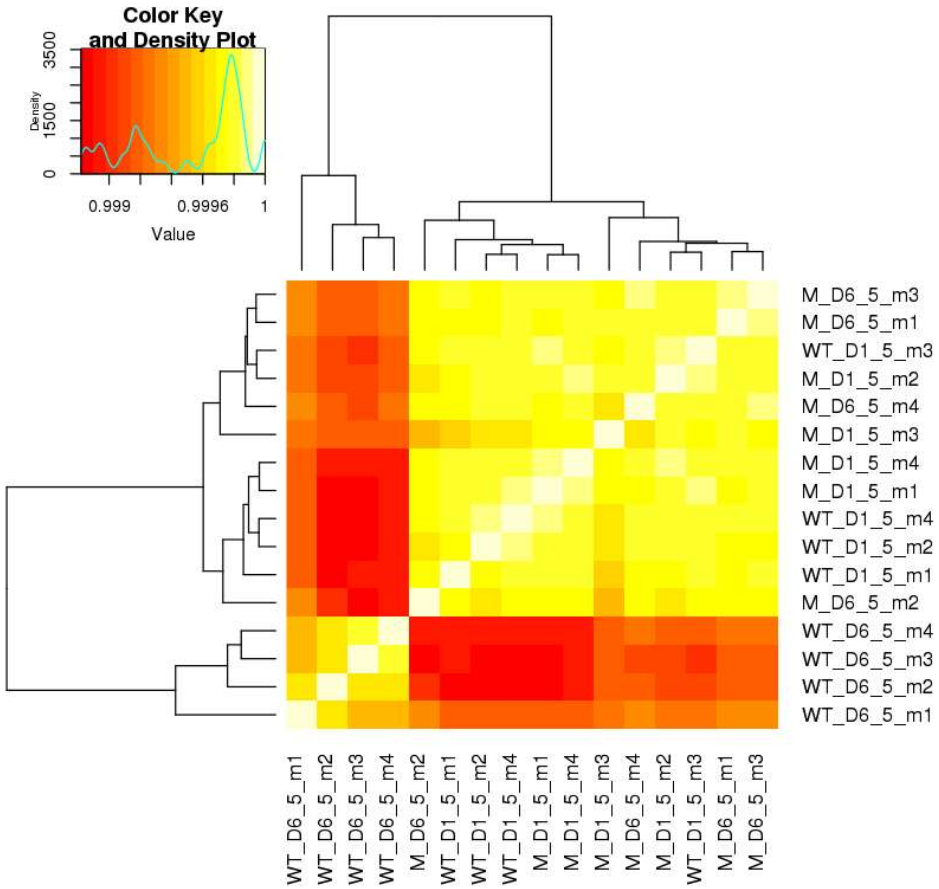

Figure 23. Hierarchical clustering heatmap of the full transcriptomic dataset. Groups of B6 mice (n=4) were i.n. infected with WT VACV or vehicle control for 1.5 or 6.5 d. The transcriptional activity of splenic NK cells was compared by RNA-seq. The heatmap represents correlations among the 16 RNA-seq samples, compared by euclidian distance. The intensity of the cell colour corresponds to the degree of correlation between the compared groups. As shown by the colour key, a darker colour corresponds to more variation whilst a lighter colour corresponds to a closer identity between groups. "WT" represents infected mice, "M" the mock-infected mice, D1.5 and D6.5 is the number of dpi at which NK cells were isolated. This figure was created by CGS.

Analysis of the differentially expressed genes between VACV-infected and mock-infected mice showed that the most significantly differentially-expressed genes included multiple NKRs (*gp49A/B, TIGIT (T cell immunoreceptor with Ig and ITIM domains)*), effector molecules (*serpinb9b, gzmk, serpin3af)*, ISGs (*gbp6, Ifi44, gbp10, stat1*) and cell cycle regulators (*cables1*) (Figure 24). Some of these transcripts will be discussed in greater detail in further sections.

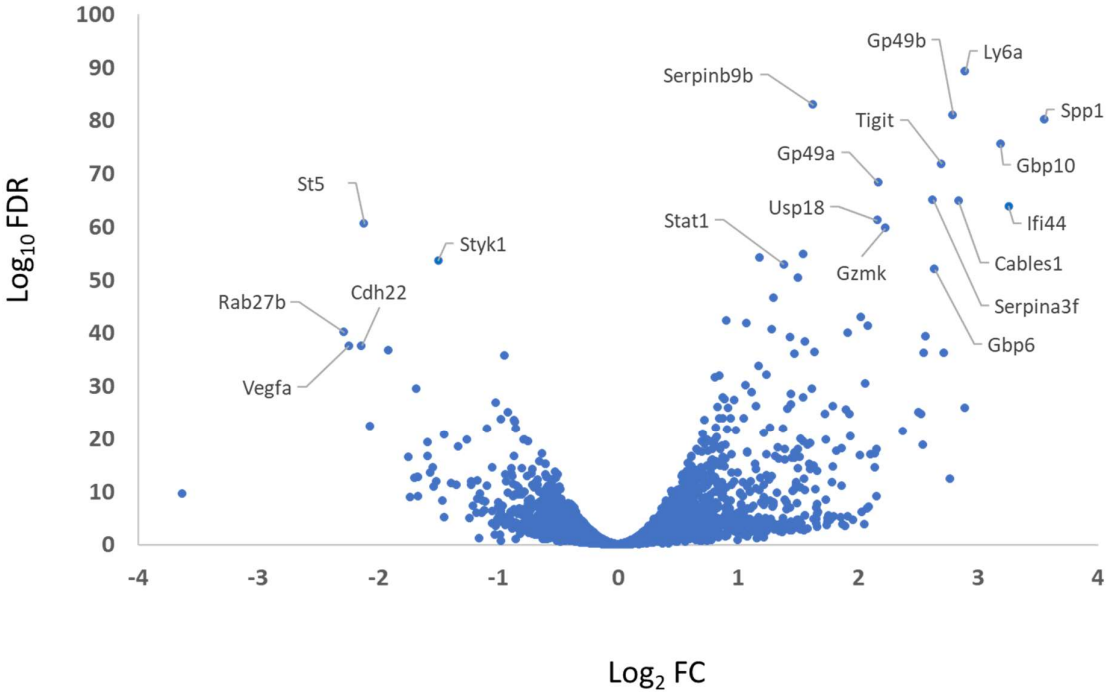

Figure 24. Volcano plot of NK cell transcripts differentially expressed at 6.5 d.p.i. in VACV-infected mice compared to mock. B6 mice (n=4) were infected i.n. with WT VACV or vehicle control. At 6.5 d.p.i. splenic NK cells were isolated and transcriptional activity analysed by RNA-seq. Each differentially expressed transcripts (FDR<0.05) (WT vs mock) is represented by a blue dot, the X-axis represents the FC expressed as log_2, and the Y-axis represents the FDR associated with the FC and is expressed as log_{10}.

To assess whether NK cell transcripts affected during VACV infection are associated with a biological function and/or a pathway, the differentially-expressed genes (FDR<0.05) were annotated using GO (gene ontology). At 6.5 d.p.i., 26 pathways were found to be enriched amongst the transcripts upregulated in infected mice compared to mock, and no pathway enrichment was found for downregulated transcripts. The pathways that were enriched suggest active transcription, the production and secretion of granules, immune response and cell division (Figure 25).

Analysis of biological processes showed that 207 biological processes were significantly enriched between mock and VACV-infected NK cell transcripts at 6.5 d.p.i. (FDR<0.05). The 20 most significantly enriched hits are shown and suggest that NK cells display an active defence phenotype and engage effector mechanisms in response to VACV infection (Figure 26).

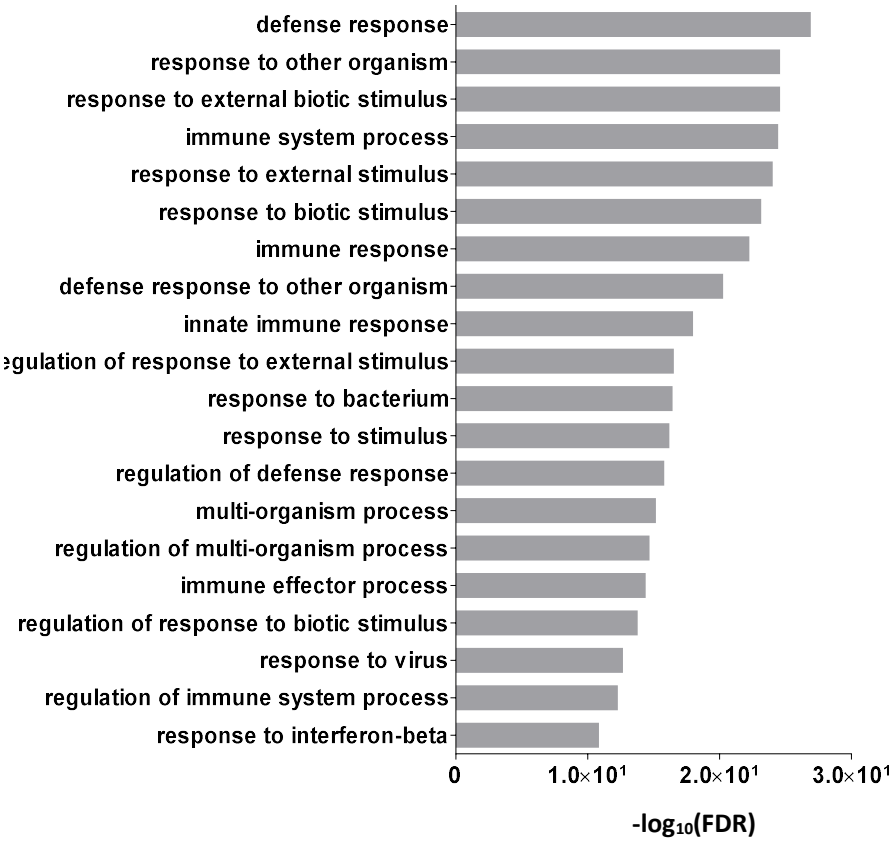

Figure 25. Pathways enrichment amongst murine NK cell transcripts upregulated during systemic WT VACV infection. Groups of B6 mice (n=4) were mock or WT VACV i.n. infected. At 6.5 d.p.i, NK cell transcripts were analysed by RNA-seq, and differential expression was calculated (VACV vs mock). The transcripts upregulated (FDR<0.05) were inputted in the Reactome database to search for pathway enrichment by GO. A term representative of the pathway is indicated on the left of the bar graph, and the significance of this enrichment is represented on the X-axis and expressed as log_{10}. The Holm-Bonferroni method was used to correct for multiple hypothesis testing.

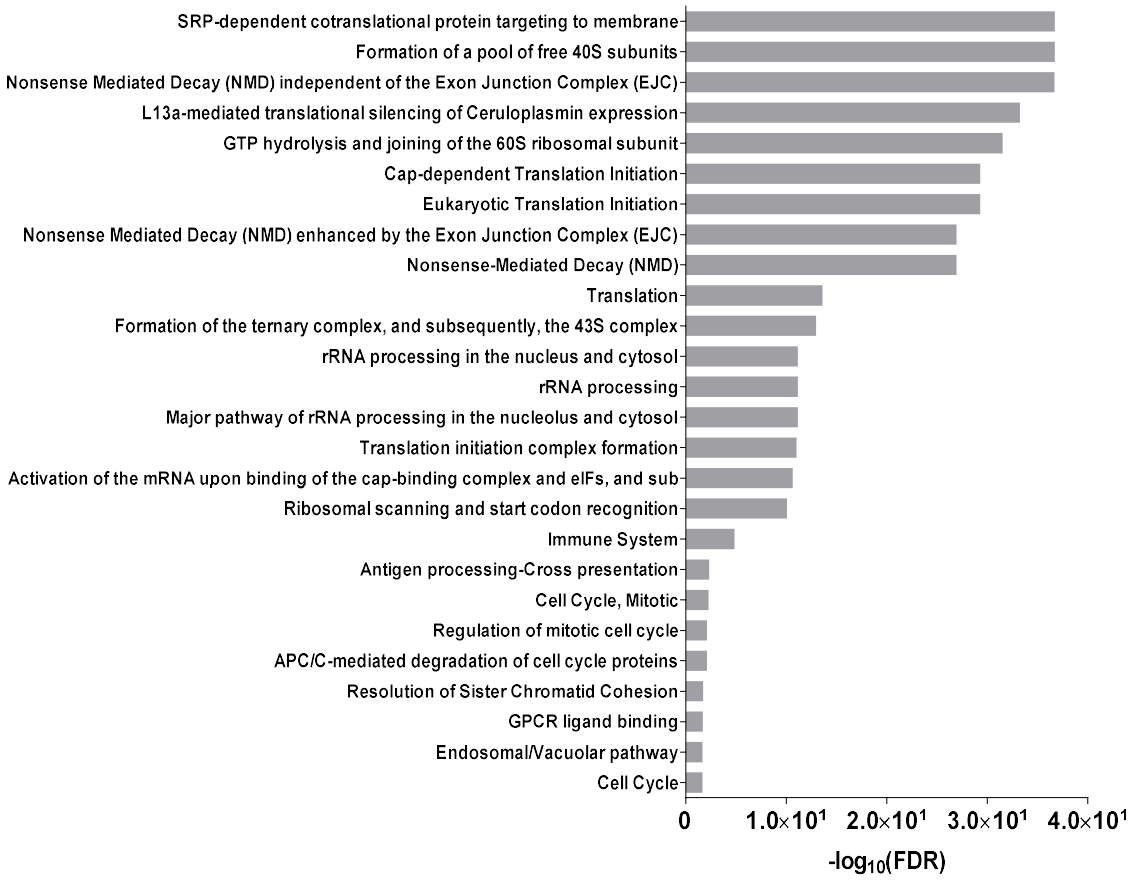

Figure 26. Biological processes enriched amongst murine NK cell transcripts upregulated during systemic WT VACV infection. Groups of B6 mice (n=4) were mock or VACV-infected, at 6.5 d.p.i, NK cell transcripts were analysed by RNA-seq and differential expression calculated (VACV vs mock). The transcripts upregulated (FDR<0.05) were inputted in the Reactome database to search for biological process enrichment by GO. The top 20 biological processes enriched by GO in such transcripts is shown. A term representative of the biological process is indicated on the left of the bar graph, and the significance of the enrichment is represented on the X-axis, expressed as log10. The Holm-Bonferroni method was used to correct for multiple hypothesis testing.

3.3 NK cells number and maturation subsets analysis

NK cell numbers were monitored along with their maturation stage, proliferation and effector markers to investigate the function and nature of the NK cell population expanding in response to VACV infection. The absolute number of NK cells in the spleen and the liver were significantly upregulated at 6.5 d.p.i. compared to mock (Figure 27A). The transcription of two proliferation markers, Ki67 (*MKI67*) and CD25 *(Il2ra*), were substantially upregulated, suggesting the proliferation of NK cells in response to VACV (Figure 27B).

Murine NK cell maturation can be modelled in a four-stages programme based on the surface density of CD27 and CD11b. This program presents the following intermediates: $CD27^{-}CD11b^{-}$ referred to as double-negative (DN), $CD27^{+}CD11b^{-}$ referred as $CD11b^{low}$, $CD27^{+}CD11b^{+}$ referred as double-positive (DP) and $CD27^{-}CD11b^{+}$ referred to as $CD27^{low}$ (Chiossone *et al.* 2010). The DN are the most proliferative NK cells and are considered as immature with poor effector functions. The more differentiated DP and $CD11b^{low}$ NK cell subsets are also capable of proliferating. They contribute to NK cell expansion during inflammation (Chiossone *et al.* 2010) and have a high capability to secrete cytokines (Fu *et al.* 2011). The final maturation stage of NK cells is the $CD27^{low}$ subset, which is sometimes considered as senescent because of their susceptibility to spontaneous apoptosis (Robbins *et al.* 2004). This subset also has a high threshold to stimulation (Hayakawa & Smyth 2006) and a high capacity to mediate cytotoxicity (Fu *et al.* 2011).

Here, FACS analysis of splenic NK cells at 6.5 d.p.i. showed that the DP and $CD27^{low}$ subsets accounted for the majority of NK cells present in the spleen, followed by the $CD11b^{low}$ and the DN (Figure 28A). Analysis of the absolute numbers of each maturation subset showed that the DP and the $CD11b^{low}$ NK cells subsets expanded the most (Figure 28B).

Analysis of RNA-seq data for splenic NK cells at 6.5 d.p.i. showed that multiple effector protein transcripts were upregulated (Figure 28C). Amongst them were GzmB (*gzmb*), GzmK (g*zmk*) and IFNγ (*ifng*), which directly mediate NK cell effector functions. Other upregulated transcripts were cathepsin B (*ctsb*), serpin B6 (*serpinb6b*) and serpinB9 (*serpinb9b*), which protect NK cells from damage by their own granules by cleaving perforin (Balaji *et al.* 2002), GzmB (Hirst *et al.* 2003) and GzmA (Kaiserman *et al.* 2014), respectively.

Together, the FACS data showed that the NK cell subsets that expanded the most present a maturation phenotype associated with effector functions. The transcriptomic data support this by showing upregulation of genes transcripts for effector proteins involved directly in NK cells effector functions.

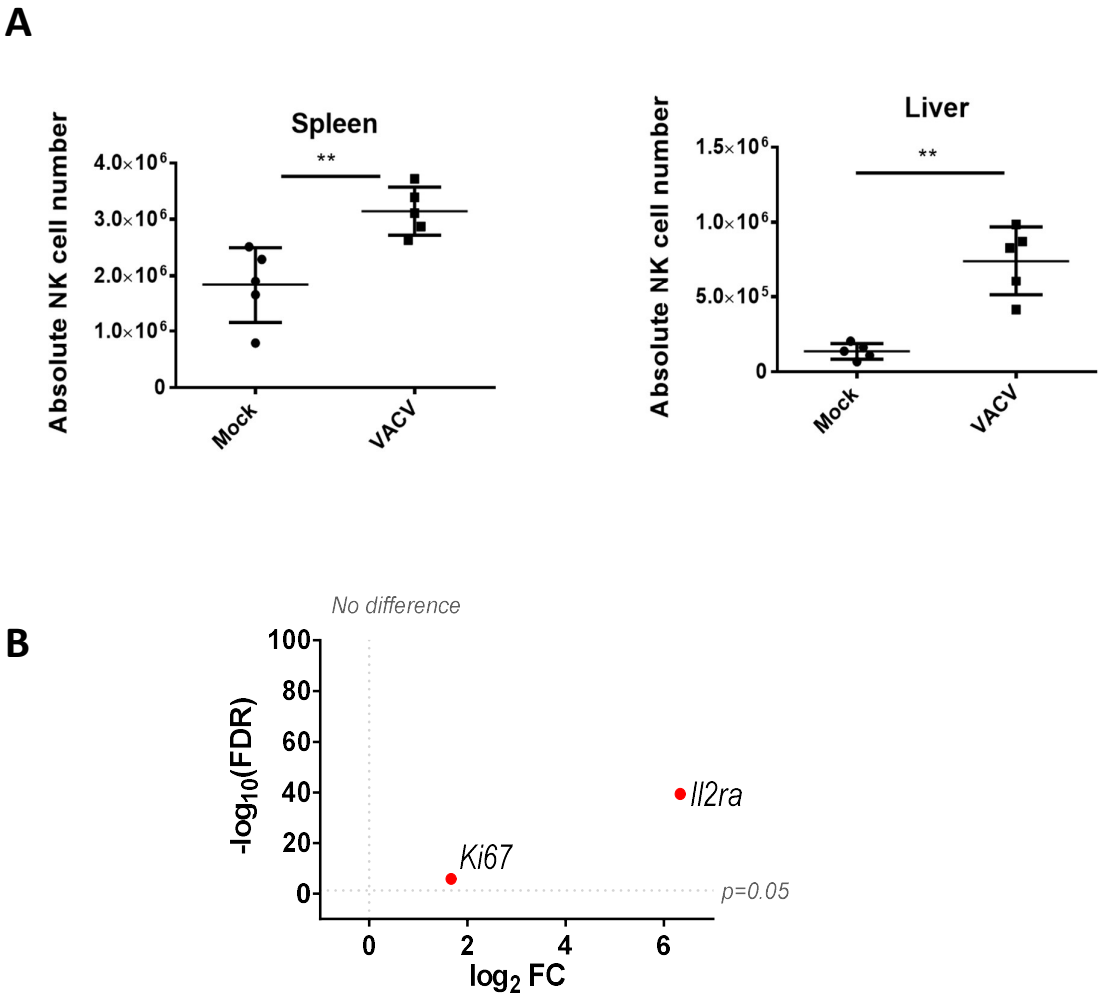

Figure 27. Measurement of murine NK cell absolute numbers and transcriptomic analysis of proliferation markers in murine NK cells during VACV infection. B6 mice were i.n. infected with VACV or vehicle control, at 6.5 d.p.i., NK cells were enumerated, and their transcriptomic activity analysed by RNA-seq (n=4).

*A) The absolute number of NK cells in the spleen and liver is represented for each group. Error bars represent ± SD. Statistical significance was calculated using a Mann-Whitney test (*p<0.05, ** p<0.01, ***p<0.001).*

B) Differential expression (WT vs mock) of proliferation markers transcripts by RNA-seq analysis. Each dot represents a transcript, the FC is shown on the X-axis, expressed as log_2, the statistical significance of the FC (FDR) is shown on the Y-axis, expressed as log_{10}. Red indicates statistical significance(FDR<0.05).

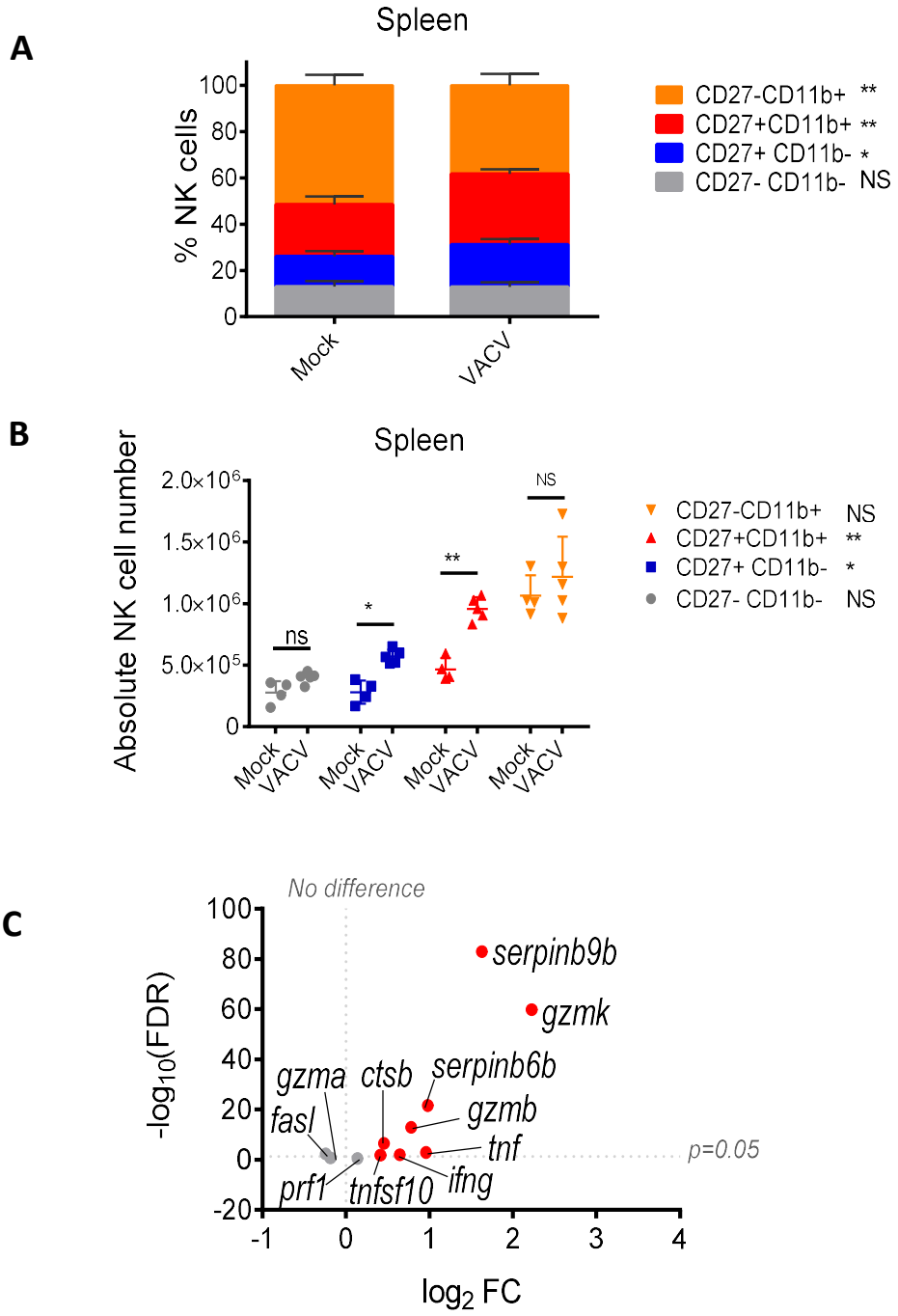

Figure 28. Frequency of four NK cell maturation subsets and differential expression of effector protein transcripts in murine NK cells during VACV i.n infection. B6 mice were i.n. infected with VACV or vehicle control, at 6.5 d.p.i, NK cells were isolated for RNA-seq (n=4) and FACS-based study (n=5).

*The percentage (A) and absolute number (B) of splenic NK cells expressing the indicated combinations of CD27 and CD11b in mock-infected or VACV-infected mice was analysed by FACS surface staining. Statistical significance was calculated using a Mann-Whitney test,*p<0.05, ** p<0.01, ***p<0.001.*

C) The differential expression of effector proteins transcripts (VACV vs mock) by RNA-seq. Each dot represents a transcript, the X-axis value is the FC expressed as log_2, and the Y-axis value is the FDR (statistical significance) of this FC expressed as log_{10}. Red indicates statistical significance (FDR<0.05).

3.4 NK cells display an active phenotype

Next, the NK cell activation status during VACV infection was investigated by analysing the protein surface expression and transcript levels of known activation markers, such as CD69, Sca1, KLRG1, CD107a, and gp49A/B.

The C-type lectin-like cell receptor CD69 (*cd69*) is also called 'very early antigen' because of its upregulation on activated lymphocytes (Cibrián & Sánchez-Madrid 2017). Here, both FACS and transcriptomic analyses showed considerable upregulation of CD69 after VACV infection (Figure 29).
Gp49A *(gp49a/ Lilr4b*) and gp49B (*gp49B/lilrb4a)* share 88 % aa identity, and mediate inhibitory and activating functions, respectively (Lee *et al.* 2000). Both gp49a and B are induced in NK cells during mCMV infection (Wang *et al.* 2000), and gp49B expression is induced on activated T and NK cells during the immune response to virus, bacteria or tumour challenge (Gu *et al.* 2003) and also persists in the memory phase (Gu *et al.* 2003). Here, FACS analysis showed that the expression of gp49A/B (the mAb employed recognises both proteins) is induced on NK cells during VACV infection with a prevalence shifting from 6 to 41 % and an expression level (median fluorescence intensity (MFI) increasing by 7.3 fold. RNA-seq data also showed that gp49A and B are upregulated at the transcriptomic level with a 4.49 fold and 6.92 fold increase for gp49A and gp49B, respectively (Figure 29).
CD107a (*lamp1*) is a degranulation marker that is expressed temporarily at the surface of activated NK cells during infection, and functions as a shield to protect NK cells from damages by their own cytotoxic granules (Cohnen *et al.* 2013). Data showed that after VACV infection, CD107a was upregulated at the protein level but not at the transcriptomic level. The discrepancy between the transcriptomic and surface protein level can be explained by the transient nature of CD107a expression at the PM, which results from protein relocalisation but does not rely on transcriptomic activity. These data suggest that NK cells are activated in response to VACV and degranulate.in
Stem cell antigen (Sca1, Ly6a) is an early activation marker, initially described as upregulated on activated lymphocytes (Yutoku et al. 1974). Here, the RNA-seq data showed a remarkable upregulation of Sca1 transcripts with a FC of 7.4 (Figure 29).
The killer cell lectin-like receptor G1 (KLRG1, klrg1) is a lymphocytes activation marker and binds to E- N- and R-cadherins (Ito et al. 2006; Tessmer et al. 2007). KLRG1 is also considered to be a specific marker for activation because its expression is particularly high in LY49H+ NK cells during mCMV infection at 6-10 d.p.i. (Fogel et al. 2013). Our FACS data showed upregulation of KLRG1 on NK cells during VACV infection at the transcriptomic and protein level (Figure 29).

Together, these data demonstrate that during VACV infection, NK cells express markers of an active phenotype (CD69, KLRG1, gp49A/B, Sca1, CD107a) both at the proteomic and the transcriptomic level.

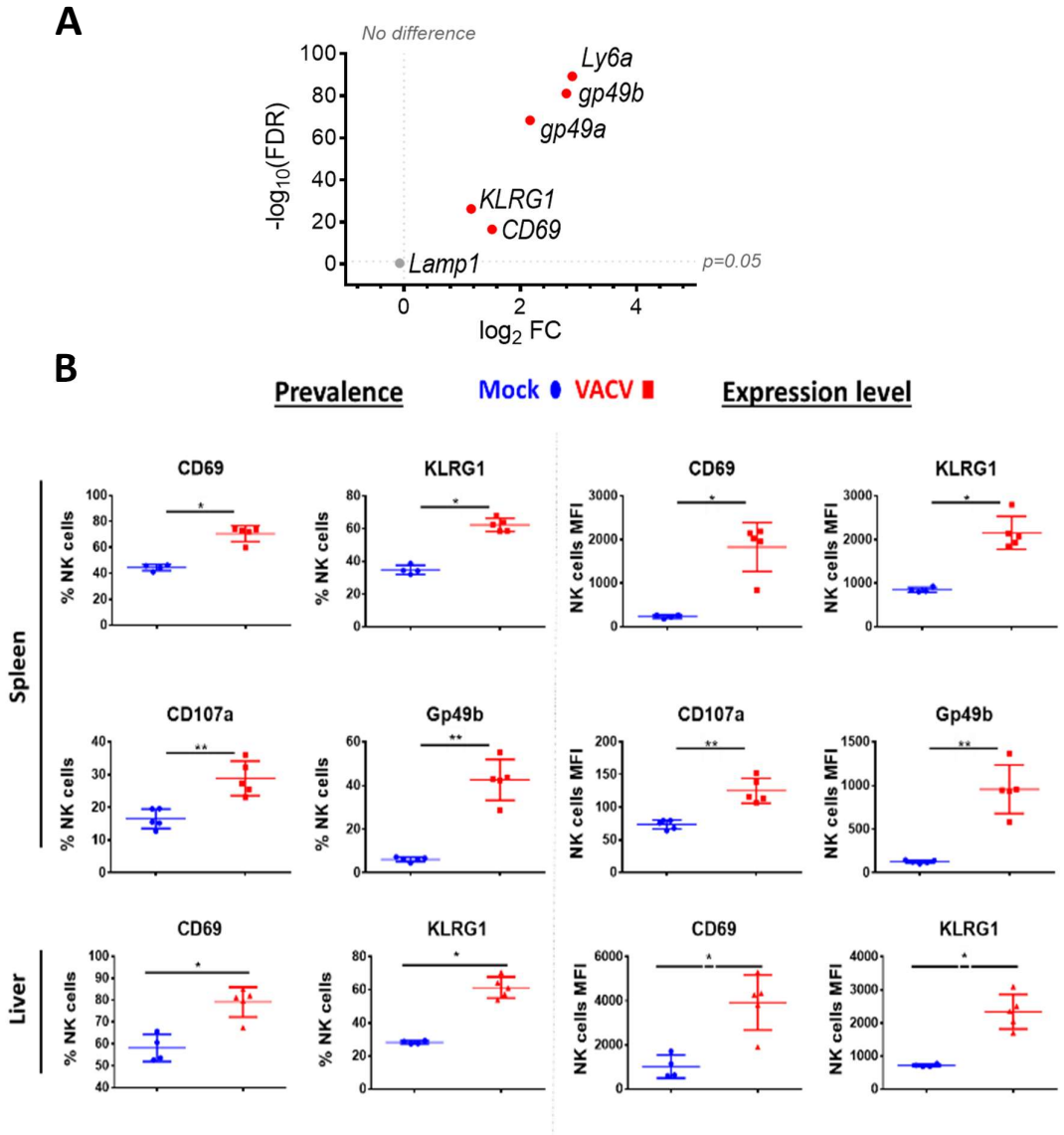

Figure 29. Study of activation markers at the protein and transcript level in murine NK cells during systemic VACV infection. B6 mice were i.n. infected with VACV or vehicle control for 6.5 d., NK cells were isolated for RNA-seq (n=4) and FACS-based (n=5) studies.

A) Differential expression of activation markers transcripts (VACV vs mock). Each dot represents a transcript, the X-axis shows the FC expressed as log_2, and the Y-axis value shows the FDR (statistical significance) of this FC expressed as log_{10}. Red indicates statistical significance (FDR<0.05).

*B) FACS analysis for surface activation markers of splenic and hepatic NK cells in mock (blue) and VACV-infected mice (red). Percentage of NK cells expressing the indicated marker (prevalence) and MFI (expression level) are shown. Error bars represent ± SD. Statistical significance was calculated using a Mann-Whitney test (*p<0.05, ** p<0.01, ***p<0.001).*

3.5 NK cells transcriptomic signature correlates primarily with direct target recognition

NK cell activation can be triggered by the direct recognition of surface ligand(s), the presence of stimulatory cytokines and chemokines, or the recognition of Abs bound to the target cell surface. In the context of VACV, multiple studies have reported the direct recognition of VACV-infected cells by NK cells via *ex vivo* Cr^{51} release assays (Baraz *et al.* 1999; Brooks *et al.* 2006; Chisholm & Reyburn 2006). Additionally, several studies have indicated that type I IFN and IL-18 are necessary for NK cell activation during VACV infection (Brandstadter *et al.* 2014; Martinez *et al.* 2008). However, some of these studies were performed in non-physiological conditions and the relative contribution of each stimulus to NK cell activation is unknown.

To discover which of these stimuli contribute to NK cell activation during VACV infection *in vivo*, our RNA-seq data were compared with a published study describing the unique transcriptomic fingerprint of NK cells activated by independent stimuli.

Costanzo and colleagues analysed the transcriptomic signature of NK cells following three activation models; direct cell recognition, ADCC, and cytokine activation (data reference GSE110446) (Costanzo et al., 2018). They then assembled lists of transcripts that i) were uniquely up- or downregulated for each of those three activation mechanisms, which they defined as a specific unique transcriptomic signature (Figure 31A), and ii) were commonly modified by all three activation mechanisms, which they defined as a general activation transcriptomic signature Figure 30A).

The list of transcripts involved in the general activation transcriptomic signature in Costanzo et al., 2018 study was used to identify an activation transcriptomic signature in our RNA-seq data. Seventeen transcripts from this list were detected in our dataset. These 17 transcripts were all upregulated in the study of Costanzo et al., 2018.

Thus, the transcripts (amongst these 17) that were detected in our RNA-seq data, and which are upregulated, indicate a general activation pattern. Figure 30B shows that in our RNA-seq data, 11 of such transcripts were upregulated in a statistically significant manner (FDR<0.05) and six were not statistically affected. These data indicate that during VACV infection, murine NK cells display a transcriptomic signature that overlaps with a general activation transcriptomic activity as defined by Costanzo and colleagues (Costanzo et al., 2018).

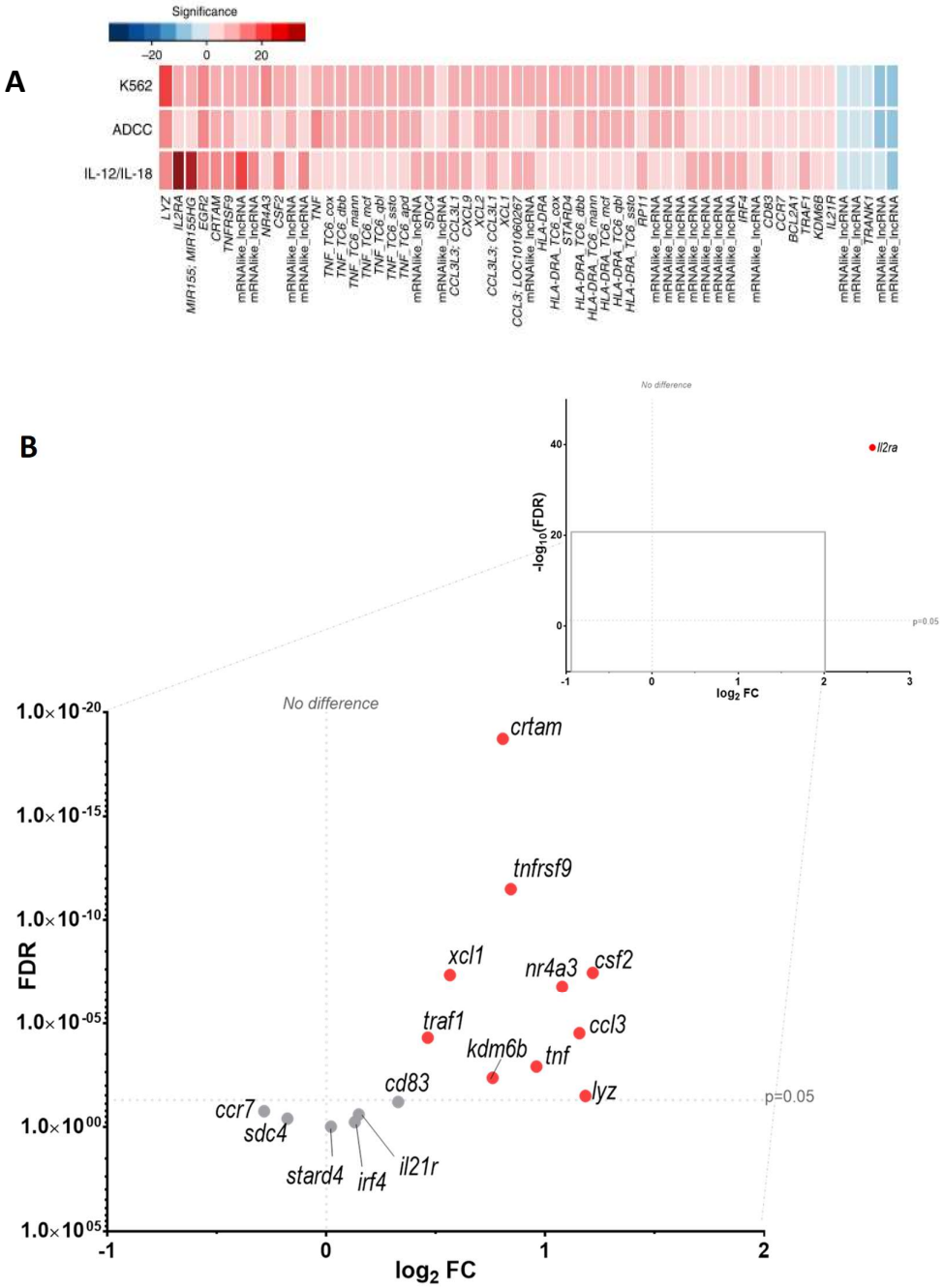

Figure 30 Identification of a general activation pattern (as defined by Costanzo et al., 2018) in murine NK cells during VACV systemic infection.

A) List of NK cell transcripts commonly modulated by three independent stimulation mechanisms (direct recognition(k562), cytokine stimulation (Il-12/-18), ADCC), and defining a general activation signature in NK cells. The transcripts downregulated (blue) and upregulated (red) similarly by these three stimuli are shown. Statistical significance of the differential expression is indicated by the intensity of the colour. (Adapted from (Costanzo et al., 2018) following open access guidelines http://creativecommons.org/ licenses/by/4.0/ s.)

B) Differential expression of transcripts defined in A and detected in our RNA-seq dataset. Seventeen transcripts from list A were detected in our RNA-seq experiment (all of which were upregulated in Costanzo et al., 2018 study). The graph shows the differential expression of such transcripts in our dataset, their FC (WT vs mock) is expressed as log_2 (X-axis), and the statistical significance of this FC is expressed as FDR (Y-axis). Each dot represents a transcript, and red indicates statistical significance (FDR<0.05).

Next, we analysed whether our transcriptomic data was overlapping with any of the unique transcriptomic signature corresponding to the three activation mechanisms described by Costanzo and colleagues. For this purpose, we isolated transcripts genes from such lists in the Costanzo study and searched for them in our RNA-seq dataset. All the transcripts from these lists that were detected in our RNA-seq study were reported as upregulated in the Costanzo et al., study. Thus, upregulation of such transcripts in our dataset indicates a correlation with the transcriptomic fingerprint defined in Costanzo et al. study.

Figure 31A shows how many transcripts constitute the unique transcriptomic signature for each activation mechanism (K562 for direct cell recognition, IL-12/IL-18 for cytokine activation, cells coated with Abs for ADCC) as described in the Costanzo study (number circled in the Venn diagrams). The number of transcripts detected in our RNA-seq study for these three transcriptomic signatures are shown (number after the arrow) on Figure 31A. This figure shows that none of the transcripts downregulated in Costanzo study were detected in our RNA-seq data. Among the upregulated transcripts, 48 (direct recognition), 42 (cytokine stimulation), and six (ADCC) transcripts were detected in our RNA-seq data.

Of note, the difference in the number of transcripts detected in Costanzo and colleagues in comparison with our study results from the use of microarray versus RNA-seq. The main difference between these techniques resides in the data clean-up. The numbers of transcripts are inflated in the microarray study because transcripts for non-coding RNA, ambiguous sequences, miRNA and mRNA-like transcripts were kept. Such transcripts were not included in our RNA-seq study, to reflect transcriptomic changes corresponding to protein coding genes.

Figure 31B, C, D shows the differential expression in our RNA-seq data, for transcripts corresponding to the three unique activation transcriptomic signature. For the direct recognition stimulation signature (NK cells incubated with K562 target cells), 48 transcripts were detected in our dataset. Of these, 34 were significantly upregulated, one significantly downregulated and 14 statistically indistinguishable (Figure 31B). For the cytokine-induced stimulation signature (NK cells incubated with IL-12 and IL-18), 42 transcripts were detected in our RNA-seq data. Of these, 18 were significantly upregulated, five were significantly downregulated, and the others were statistically unchanged (Figure 31C). For ADCC-induced activation signature (NK resistant cell line coated with antigen and incubated with IgG against those antigens), six transcripts were detected in our RNA-seq study. Three of these were significantly downregulated, two of them upregulated and one not modulated (FDR<0.05) (Figure 31D).

Side by side comparison of the expression pattern of such transcripts showed that our RNA-seq data matches primarily with the unique transcriptomic signature corresponding to direct recognition. Transcripts for this category presented the highest upregulation in our dataset (Figure 31B), whereas genes involved in response to cytokines were less modulated Figure 31C), and genes involved in the ADCC response showed slight upregulation (Figure 31D).

This analysis suggests that NK cells may recognise ligands on target cells during VACV infection *in vivo*, but also that cytokines are involved in the activation of NK cells *in vivo*.

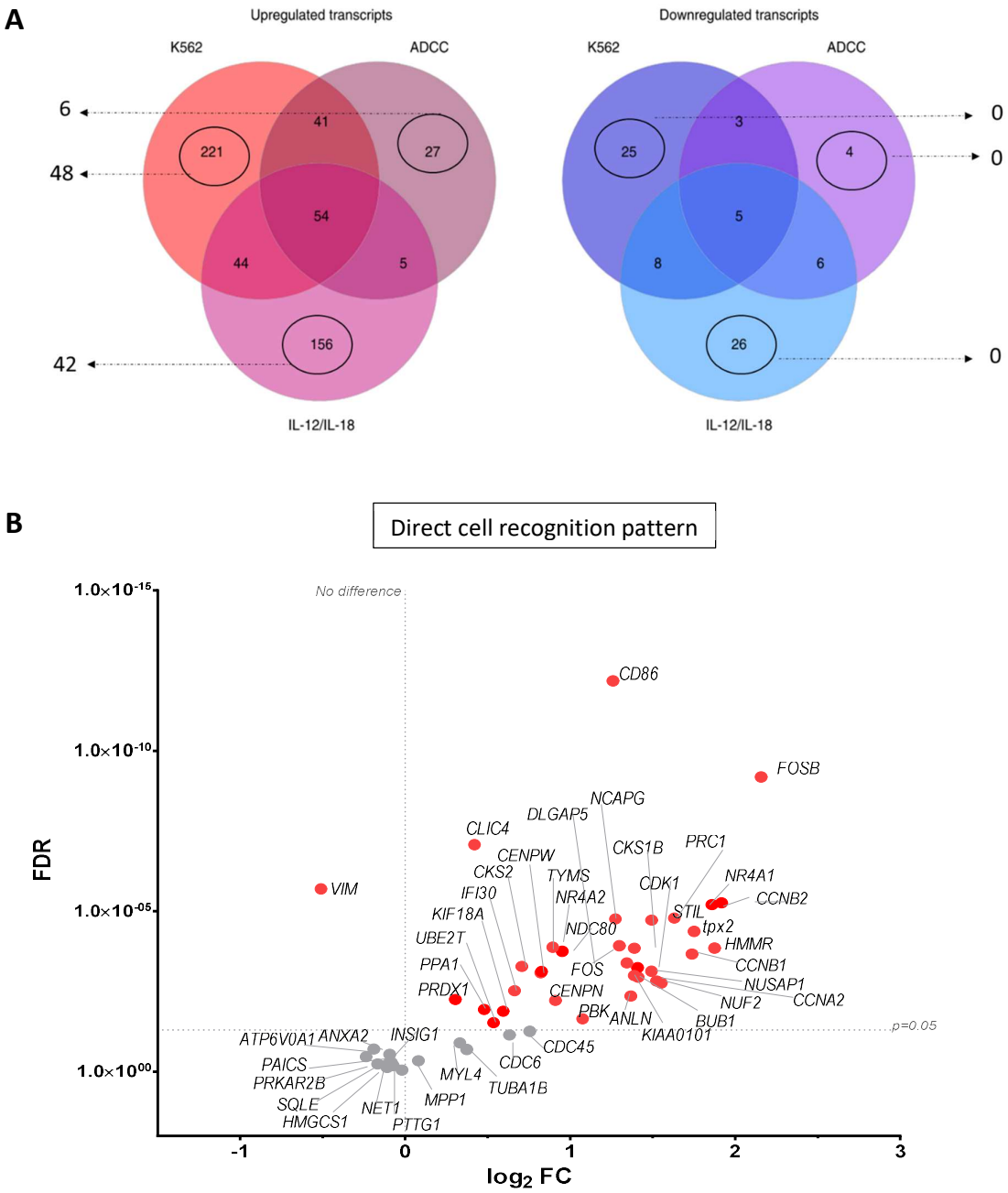

Figure 31. Identification of patterns corresponding to the unique transcriptomic signature for three distinct NK cell activation mechanism (ADCC, direct recognition and cytokine stimulation) in murine NK cells during VACV systemic infection. Groups of B6 mice (n=4) were infected with WT VACV or mock for 6.5 d. NK cells were isolated, and the differential expression of their transcripts was analysed by RNA-seq. The unique transcriptomic signature for NK cell activation by ADCC, direct recognition or cytokine stimulation was extracted from Costanzo et al., 2018 and used to search for patterns corresponding to each of these activation mechanisms in our RNA-seq data.

A) Venn diagram showing the number of transcripts modulated during NK cell activation by direct recognition (k562), cytokines (IL-12/-18), or ADCC, as described in Costanzo et al., 2018. The number of transcripts corresponding to the three unique transcriptomic signature is indicated within the black circles. Expression of such transcripts were searched in our RNA-seq data, and the number of them that were detected in our RNA-seq indicated by the number after the arrow. This figure was adapted from (Costanzo et al., 2018) following open access guidelines http://creativecommons.org/ licenses/by/4.0/ s

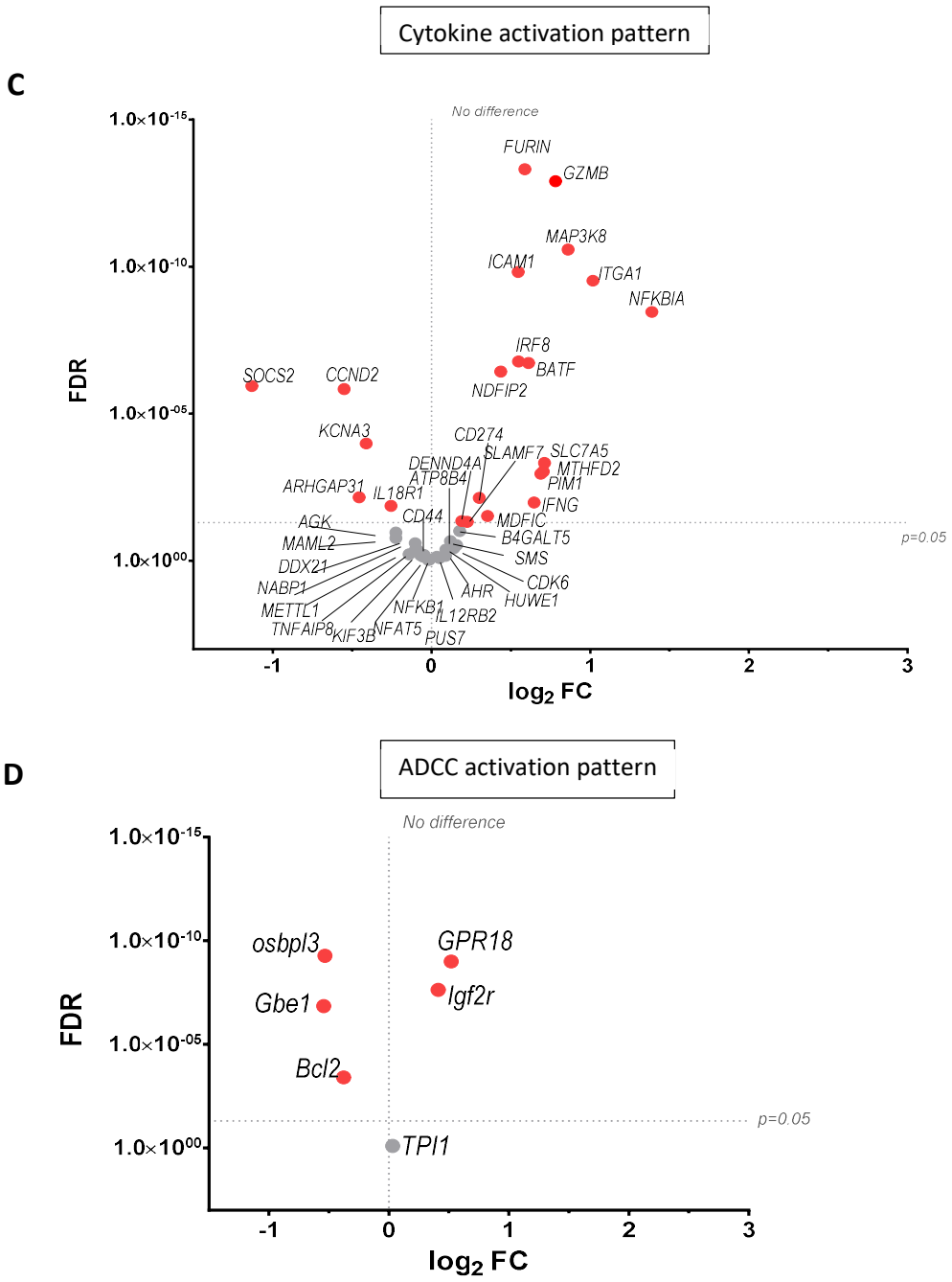

(Figure 31 following previous page)

B, C, D) The differential expression profile (VACV vs mock) of transcripts defined in A and detected in our RNA-seq (48 for direct recognition, 42 for cytokine stimulation and 6 for ADCC) is shown for each three individual stimuli: B) represents direct cell recognition, C) cytokine stimulation, and D) ADCC. Each transcript is represented by a dot, its FC (W vs mock) is shown on the Y-axis, and statistical significance of the FC (FDR) is shown on the X-axis. Red indicates statistical significance (FDR<0.05).

3.6 NK cells express IFN-stimulated genes

The analysis described in the previous section, based on a published study (Costanzo et al., 2018), indicated that during VACV infection in mice, NK cells are activated via direct recognition of VACV-infected cells and cytokines. However, the study of Costanzo and colleagues did not investigate the role of IFNs. Since IFNs are potent activator of NK cells (Paolini *et al.* 2015) and VACV is known to interfere with the IFN response (Smith *et al.* 2018), we analysed the expression of ISGs transcripts to determine if IFNs are being sensed by NK cells during VACV infection.

Because of the high number of ISGs that exist and the absence of a comprehensive list, it was not possible to screen our whole RNA-seq dataset for ISGs. Consequently, the 100 most significantly modulated genes of our dataset were manually checked for ISGs. The aim was to identify whether NK cells display signs of IFN response rather than making a comparison with the transcriptomic activation signature defined in the previous section.

The differential expression of such genes is shown in Figure 32. RNA-seq data showed that multiple ISGs were upregulated during VACV infection, including IFN induced protein 44 (*IFI44*), IFNγ inducible protein 211 (IFI211), IRF2, IRF7, IFN-induced protein with tetratricopeptide repeats -1 and -3 (IFIT1, IFIT3), Gbp10 and -6, Oas1, CXCL10 (C-X-C motif chemokine) and ligp1 (Figure 32). Together, these data suggest that in VACV-infected mice, NK cells are exposed to IFNs and in turn, activate the expression of ISGs.

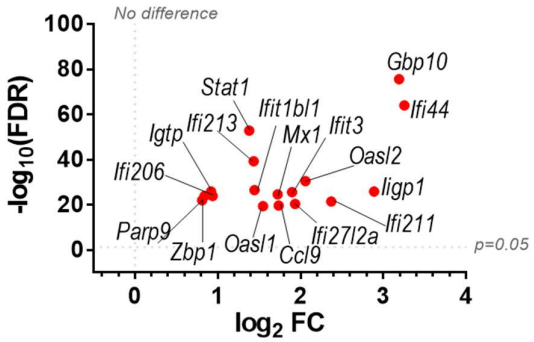

Figure 32. Differential expression of ISGs transcripts in NK cells from VACV-infected mice compared to mock. Group of B6 mice (n=4) were infected with VACV WT or mock, at 6.5 d.p.i, NK cell transcriptomic activity was studied by RNA-seq, and differential expression (VACV vs mock) was calculated. ISGs were searched among the 100 most significantly modulated transcripts (VACV vs mock (FDR<0.05)). Each dot represents the differential expression of an ISG transcript (WT vs mock). The X-axis represents the FC expressed as log2, and the Y-axis represents the statistic value associated with the FC (FDR). Red indicates statistical significance (FDR<0.05).

3.7 NKRs expression is altered during VACV infection

NK cells modulate the expression of their surface proteins during viral infection, and some NK cell subsets can expand preferentially during viral infection (Brooks *et al.*, 2006; Gumá *et al.*, 2006; Fang *et al.*, 2011; Lopez-Vergès *et al.*, 2011; Hendricks *et al.*, 2014; Hammer *et al.*, 2018). Recognition of a ligand by a matching receptor can drive the clonal expansion of a subset of NK cells. Some of these ligand:receptor interaction are well described: the murine LY49 receptor with mCMV m157 (Arase *et al.* 2002; Smith *et al.* 2002b), the human NKG2C receptor with HCMV peptides presented by HLA-E (Hammer *et al.* 2018) and the human KIR2DS2 receptor engages with HCV NS3 protein-peptide presented by HLA-C*0102 (Naiyer *et al.* 2017). We hypothesised that such receptor-ligand couple may exist in the context of VACV infection. To investigate this, we analysed how NKR expression is modulated during VACV infection and searched for putative NKRs that recognise VACV-infected cells and lead to the expansion of an NK subset bearing this receptor.

A manually curated list of NKRs known to influence the activation status of NK cells was generated, based on literature (Lanier, 1998; Lanier, 2008; Ravetch, 2000; Kelley, Walter and Trowsdale, 2005; Vivier *et al.*, 2008). The expression profile for such NKRs was analysed in our RNA-seq data (Figure 33). This showed that several transcripts were significantly upregulated ($-\log_2FC>0.5$) (*tigit, gbp49a/b, klrg1, cd69, crtam, lag3 (Lymphocyte-activation gene 3), thy1, klrb1b, cd160, lair1 (*Leukocyte-associated immunoglobulin-like receptor) or downregulated ($\log_2FC<-0.5$) (*klra9, klrc2*), whilst other were less substantially modulated or not statistically differentially expressed. To unravel whether the protein level of NKRs followed the same trend as the transcripts, several NKRs were studied by FACS and are discussed in subsequent paragraphs of this chapter.

Since NK cells do not rearrange their receptors like T cells to adapt and match specifically to pathogens, and since viral infection affects the pool of peptides presented by MHC-I, we reasoned that receptors engaging with MHC-I are more likely than other receptors to specifically recognise VACV-infected cells and lead to the preferential expansion of a specific subset of NK cells. The expression of LY49 and NKG2 receptors families, two murine NKR families known to engage with MHC-I ligands, was therefore analysed.

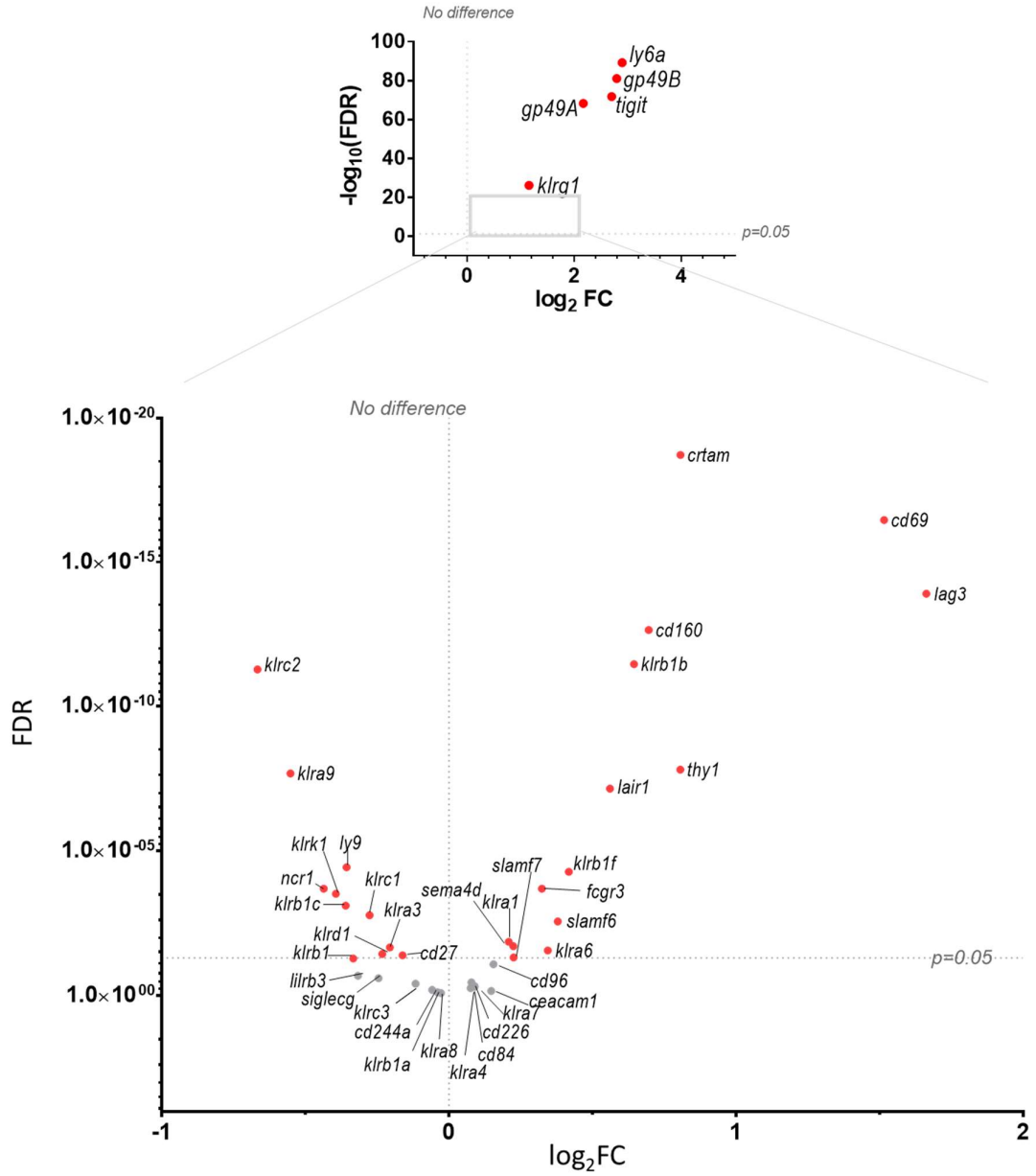

Figure 33. Differential expression of NKR transcripts during VACV systemic infection. Group of B6 mice were infected with VACV WT or mock, at 6.5 d.p.i, NK cell transcriptomic activity was studied by RNA-seq (n=4), and differential expression of transcripts (VACV vs mock) was calculated. A manually curated list of 43 genes coding for NKRs was used to search for NKRs in the RNA-seq dataset. Each dot represents the differential expression profile of an NKR transcript (WT vs mock). The X-axis represent the FC expressed as log2, and the Y-axis represents the statistic value of the FC (FDR). Transcripts whose values were out of axis on the bottom graph are shown on the top graph where the FDR is expressed as log_{10}. Red indicates statistical significance (FDR<0.05).

3.8 Expression of Ly49 receptor family is mildly affected

The Ly49 receptor family is an interesting family to study in the context of viral infection because Ly49 receptors interact with MHC-I. During viral infection, NK cells can detect changes in the self-peptide pool normally displayed by MHC-I. This alters the balance of inhibitory and activating signals, and consequently NK cell activity. Moreover, Ly49 receptors have been reported to recognise viral ligands in multiple studies (Arase *et al.* 2002; Kielczewska *et al.* 2009; Pyzik *et al.* 2011; Smith *et al.* 2002b) and to be involved in the development of memory NK cells (O'Leary *et al.* 2006; Paust *et al.* 2010; Sun *et al.* 2009b; Wight *et al.* 2018).

In B6 mice, seven members of the Ly49 family can be expressed at the surface of mature NK cells (Moussa *et al.* 2013); Ly49H and D have activating functions, whilst LY49A/F/G/C and I have inhibitory functions (see fuller description 1.3.2.1). We analysed the expression of such receptors at the transcript and protein level in NK cells during VACV infection.

Data showed that LY49H, Ly49D and LY49G2 expression in NK cells was not altered at the protein or transcript level during VACV infection in mice (Figure 34). Ly49C and Ly49I were downregulated (mAb recognises both) at the protein level and the transcriptomic level, and this, with a greater FC for Ly49I (Figure 34). Further, our FACS data showed significant upregulation for LY49A both on splenic and hepatic NK cells and our RNA-seq data showed upregulation of Ly49A transcripts (Figure 34). However, the frequency of NK cells expressing Ly49A is small (10-15 % here), suggesting that NK cells expressing Ly49A do not dominate the NK cell response to VACV. Finally, our data showed that Ly49F transcripts and surface protein expression were upregulated in splenic NK cells (Figure 34). However, surface expression of Ly49F was not seen to be upregulated in the liver, and overall, the population expressing LY49F is minor (5-7 % here) suggesting that this receptor does not define a subset of NK cells dominating the response to VACV.

To summarise, our FACS and RNA-seq data showed that in the context of VACV infection, no members of the Ly49 family receptors underwent extensive expression level modification. No NK cells bearing a particular LY49 receptor were seen to dominate the NK cell response during VACV infection, such as it is the case for the Ly49H+ NK cells during mCMV infection.

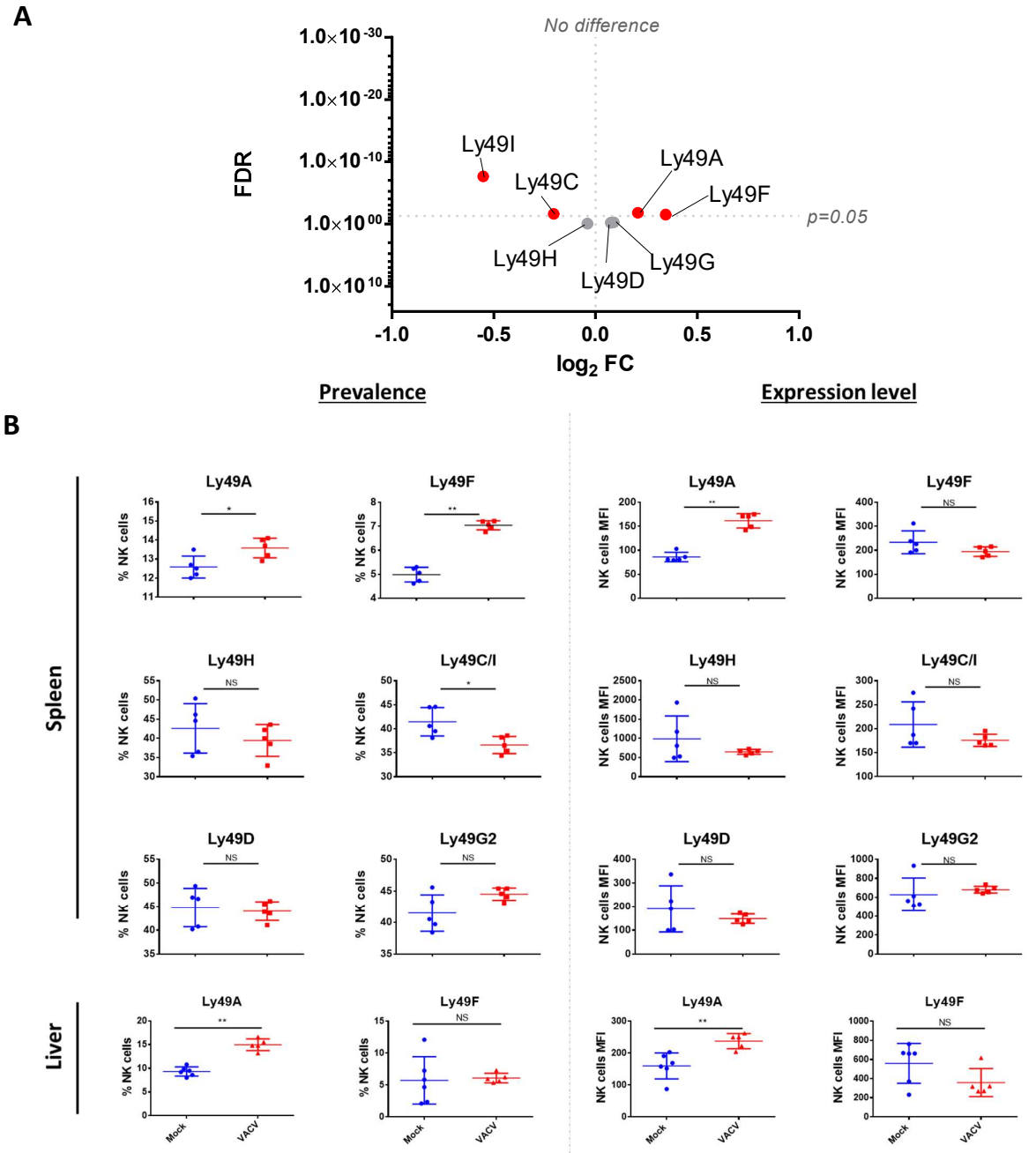

Figure 34 Differential expression of Ly49 family receptors at the transcriptomic and proteomic level during VACV systemic infection. Group of B6 mice were infected with VACV WT or mock, at 6.5 d.p.i, NK cell transcriptomic activity was studied by RNA-seq (n=4), and differential expression (VACV vs mock) was calculated. In parallel, NK cell surface protein expression was analysed by FACS (n=5).

A) Each dot represents the differential expression profile of LY49 transcript (WT vs mock). The X-axis represent the FC expressed as log_2, and the Y-axis represents the statistic value associated with the FC (FDR). Red indicates statistical significance (FDR<0.05). For clarity, protein name is indicated rather than gene name.

*B) Protein expression assessed by FACS analysis for LY49 receptors in splenic and hepatic NK cells from mock (blue) and VACV-infected mice (red). The percentage of NK cells expressing the receptor (prevalence) and MFI (expression level) for the indicated receptor is shown. Error bars represent ± SD, statistical significance was assessed with a Mann-Whitney test (*p<0.05, ** p<0.01, ***p<0.001).*

3.9 Expression of NKG2/CD94 receptors is mildly affected

Next, we studied the NKG2/CD94 family, the second NKR family that recognises MHC-I-ligands and is conserved in mice and humans (see section 1.3.2.1). This family of receptor is of particular interest since several studies have reported that NKG2 family members are involved in the control of viral infections in humans and mice (Fang *et al.* 2008a, 2011; Hammer *et al.* 2018). B6 mice express five receptors of the NKG2 family, NKG2A/C/E heterodimerise with CD94 and NKG2D is expressed at the PM on its own. The expression of CD94 was studied by FACS as a proxy for other NKG2x receptors along with NKG2D because of the limited number of NK cells available for FACS analysis.

RNA-seq data showed that transcripts for NKG2A/D/C and CD94 were slightly downregulated whilst NKG2E expression was not statistically affected (Figure 35). FACS data showed that NKG2D expression levels were not affected and a slight increase of CD94 MFI was observed at the cell surface of splenic NK cells Given that the FCs are relatively minor, these data suggest that VACV infection does not lead to a substantial transcriptomic alteration of NKG2 family members and does not preferentially drive the expansion of an NK cell population expressing NKG2 receptor.

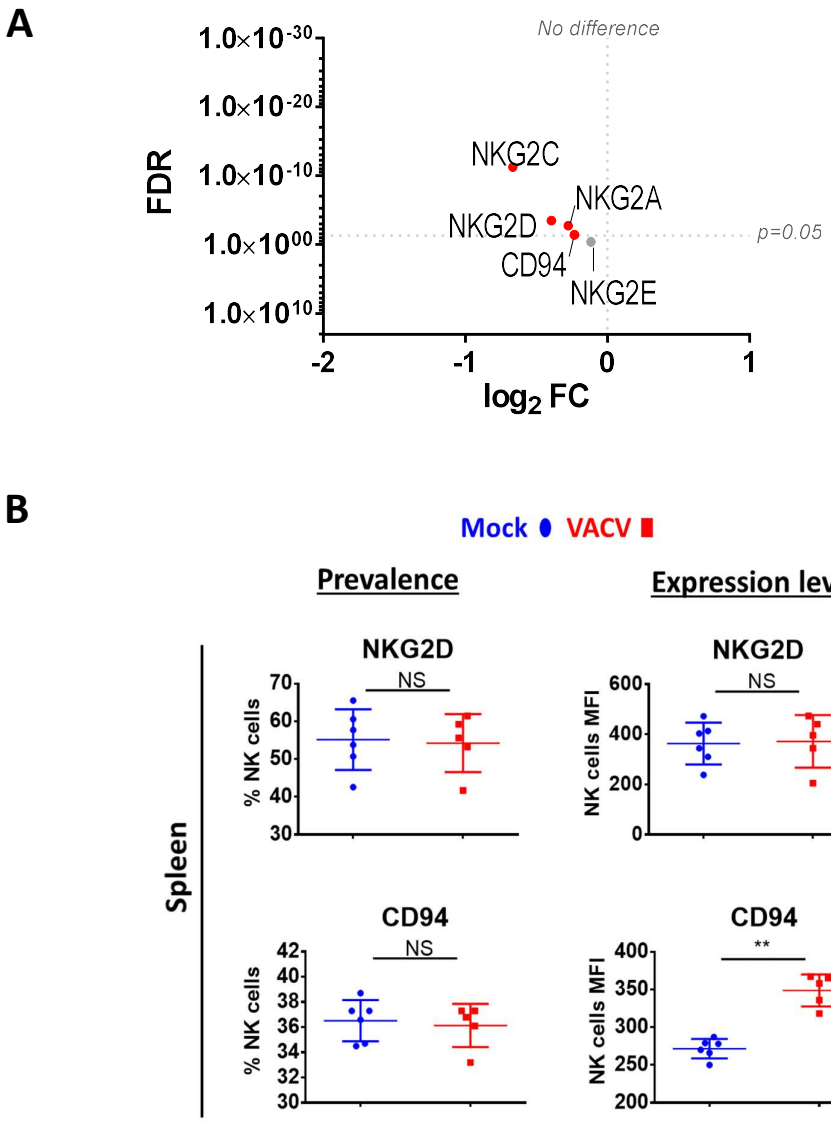

Figure 35. Differential expression of NKG2 family receptors at the transcriptomic and proteomic level during VACV infection. Group of B6 mice were infected with VACV WT or mock, at 6.5 d.p.i, NK cell transcriptomic activity was studied by RNA-seq (n=4), and differential expression (VACV vs mock) was calculated. In parallel, surface proteins expression was analysed by FACS (n=6).

A) Each dot represents the differential expression profile of NKG2 family transcripts (WT vs mock). The X-axis represents the FC expressed as log_2, and the Y-axis represents the statistical significance of the FC (FDR). Red indicates statistical significance (FDR<0.05). For clarity, the protein name is indicated rather than the gene name.

*B) FACS analysis for LY49 family surface receptors on splenic and hepatic NK cells in mock (blue) and VACV-infected mice (red). The percentage of NK cells expressing the receptor (prevalence) and MFI (expression level) for each receptor is shown. Error bars represent ± SD, statistical significance was assessed with a Mann-Whitney test (*p<0.05, ** p<0.01, ***p<0.001).*

3.10 Members of the SLAM receptors family are upregulated

Next, the signalling lymphocytic activation molecule (SLAM) receptor family, which is conserved in mice and humans, was studied. Receptors of this family can be both activating or inhibitory depending on their interactions with intracellular adaptors (see fuller description 1.3.2.3).

In the context of VACV infection, our FACS data showed that SLAM receptors CD319 (*slamf7*) and Ly108 (*slamf6*) were both upregulated in splenic and hepatic NK cells (Figure 36). Our transcriptomic data also showed upregulation of those two receptors suggesting that the higher protein expression is at least partially due to a higher transcriptomic activity (Figure 36).

Transcripts for the activating adaptors EAT2A/B, SAP, and ERT were upregulated whilst transcripts of inhibitory mediators were downregulated or unchanged, suggesting an activating function for SLAM receptors. Besides, the transcriptomic data showed that the expression of other SLAM receptors transcripts for 2B4 (*slamf4*), CD48 (*slamf2*) and CD229 (*slamf3*) was downregulated or unaffected (Figure 36).

Taken together, these data suggest that CD319 and LY108 are the two members of the SLAM family whose expression is upregulated in NK cells, in the context of VACV infection. These receptors are likely to mediate activating functions via their co-expression with activating adaptors.

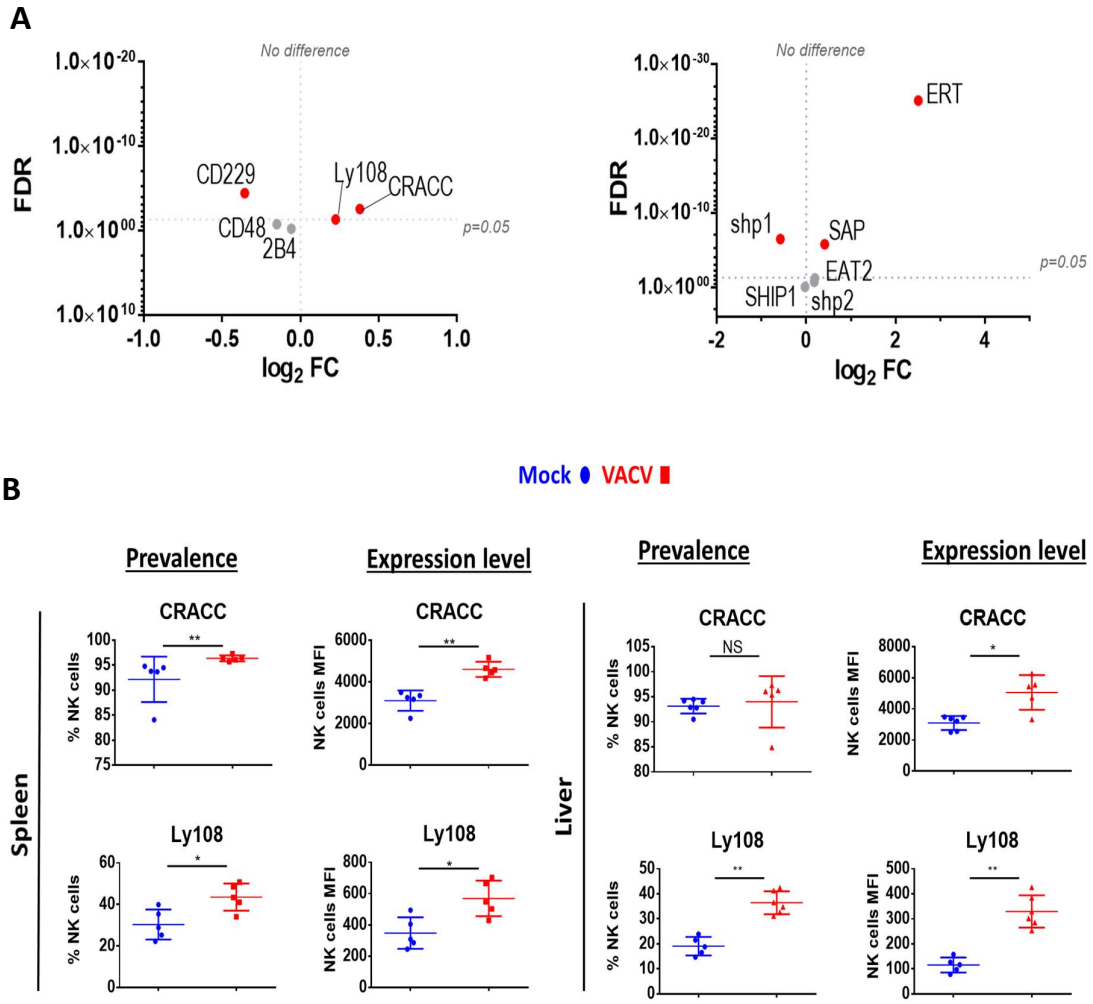

Figure 36 Differential expression of SLAM family receptors at the transcriptomic and proteomic levels in NK cells during systemic VACV infection. Group of B6 mice were infected with VACV WT or mock, at 6.5 d.p.i, NK cell transcriptomic activity was studied by RNA-seq (n=4), and differential expression (VACV vs mock) was calculated. In parallel, surface protein expression was analysed by FACS (n=5).

A) Each dot represents the differential expression profile of a SLAM family receptor or adaptor transcript (WT vs mock). The X-axis represent the FC expressed as log_2, and the Y-axis represents the statistic value expressed associated with the FC (FDR). Red indicates statistical significance (FDR<0.05). For clarity, the protein name is indicated rather than the gene name.

*B) FACS analysis for SLAM family surface receptors on splenic and hepatic NK cells in mock (blue) and VACV-infected mice (red). Percentage of NK cells expressing the receptor (prevalence) and MFI (expression level) for each receptor is shown. Error bars represent ±SD, statistical significance was assessed with a Mann-Whitney test (*p<0.05, ** p<0.01, ***p<0.001).*

3.11 Modulation of other activating receptors

Next, the expression of three other NKRs with activating functions, NKp46, DNAM-1 (DNAX accessory molecule-1) and CD49b, was analysed.

NKp46 (*Ncr1*), is an activating receptor, and is the only NCR conserved in mice and humans. It is involved in the recognition of cells infected with viruses such as Sendai, influenza, Newcastle disease, and VACV (Jarahian *et al.* 2009; Mandelboim *et al.* 2001), and is involved in the clearance of *Streptococcus pneumoniae* in B6 mice (Elhaik-Goldman *et al.* 2011), HCV in humans (Golden-Mason *et al.* 2012) and influenza in B6 mice (Gazit *et al.*, 2006). Here, FACS analysis showed that NKp46 was stably expressed in hepatic and splenic NK cells during VACV infection (Figure 37B). RNA-seq data showed a slight downregulation of NKp46 transcript expression in splenic NK cells (Figure 37A), but this is unlikely to have a functional impact given the high expression level of NKp46 in all NK cells.

DNAM-1, is a co-stimulatory receptor that does not contain ITAMS and competes with the NKRs TIGIT and TACTILE (T cell–activated increased late expression) to bind to nectin 2 (CD122) and nectin-like protein/poliovirus receptor (CD155), which are upregulated during stress response (reviewed in (de Andrade *et al.* 2014). DNAM-1 is involved in the response to mCMV (Lenac Rovis *et al.* 2016) and HCV (Stegmann *et al.* 2012) and is necessary for the development of mCMV-induced memory NK cells (Nabekura *et al.* 2014). Here, data showed that DNAM-1 protein and transcript levels in splenic and hepatic NK cells were stable during VACV infection (Figure 37).

CD49b (*Itga2*), is an integrin that binds to collagens, laminins and E-cadherins and enhances lymphocytes adhesion to target cells. It is also a maturation marker and its relative expression with CD49a defines two subsets of hepatic NK cells: CD49a+CD49b- are resident, and CD49a-CD49b+ are conventional. FACS data showed that during VACV infection, NK cell CD49b expression level was higher in the liver and the spleen whilst CD49b prevalence was higher in the liver but stable in the spleen (this is because the percentage of splenic CD49b+ before infection averaged 100 %) (Figure 37B). RNA-seq data from splenic NK cells showed that CD49b transcripts were downregulated (Figure 37A). Those data suggest that the higher MFI results from a mechanism other than higher transcriptional activity.

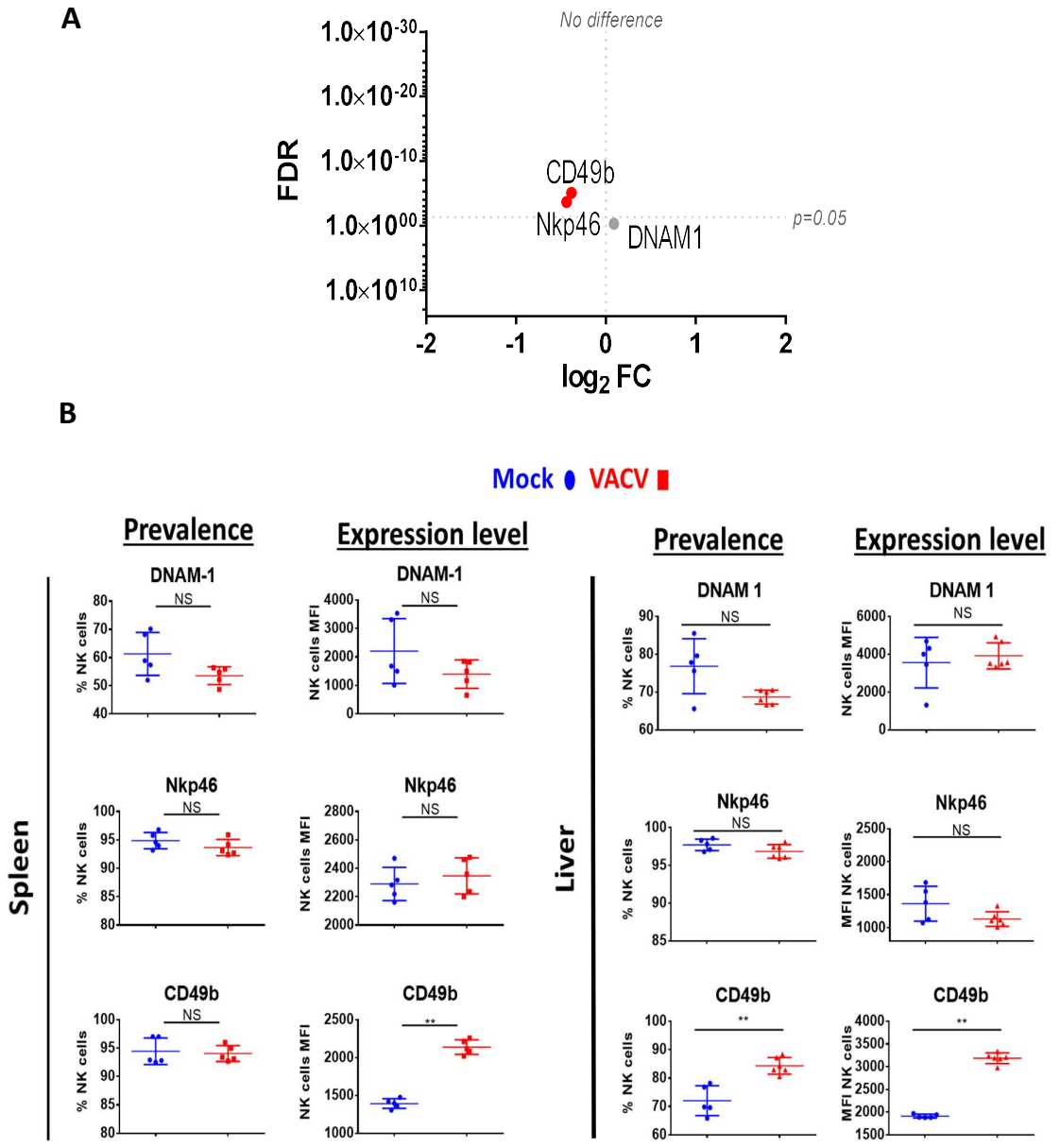

Figure 37 Differential expression of NKp46, DNAM-1 and CD49b in NK cells, at the transcriptomic and proteomic level during VACV infection. Group of B6 mice were infected with VACV WT or mock, at 6.5 d.p.i, NK cell transcriptomic activity was studied by RNA-seq (n=4), and differential expression (VACV vs mock) was calculated. In parallel, NK cell surface proteins expression was analysed by FACS (n=5).

A) Each dot represents the differential expression profile of the indicated transcript (WT vs mock). The X-axis represent the FC expressed as log_2, and the Y-axis represents the statistic value associated with the FC (FDR). Red indicates statistical significance (FDR<0.05). For clarity, the protein name is indicated rather than the gene name.

*B) FACS analysis for NKp46, DNAM-1, CD49b surface receptors on splenic and hepatic NK cells from mock (blue) and VACV-infected mice (red). The percentage of NK cells expressing the receptor (prevalence) and MFI (expression level) for each receptor is shown. Error bars represent ±SD, statistical significance was assessed with a Mann-Whitney test (*p<0.05, ** p<0.01, ***p<0.001).*

3.12 NK cell memory-associated markers are upregulated

Gillard and colleagues showed that hepatic NK cells primed with VACV mediate protection after adoptive transfer in $Rag^{-/-}$ mice upon subsequent VACV infection (Gillard *et al.* 2011). Interestingly, these cells presented a higher expression of Thy1 and CXCR6 (Gillard *et al.* 2011). Thy1 contributes to T cell expansion and is involved in T cell co-stimulation (reviewed in (Haeryfar & Hoskin 2004)). Thy1 expression is associated with NK cells mediating the recall response in the CHS model (O'Leary *et al.* 2006). However, Thy1 (*CD90*) function is poorly understood and its ligand remains unidentified. CXCR6 (C-X-C motif chemokine receptor 6) is a chemokine receptor that binds CXCL16 (CXC chemokine 16) and is mostly expressed by hepatic sinusoids endothelial cells. CXCR6 expression is also associated with hepatic NK cells mediating a memory response to CHS or VLPs (Paust *et al.* 2010).

FACS analysis showed that, during VACV systemic infection, both Thy1 and CXCR6 proteins were upregulated in splenic NK cells. Thy1 protein level was also upregulated on hepatic NK cells (no data was obtained for CXCR6 in hepatic NK cells) (Figure 38B). RNA-seq data also showed a substantial upregulation for those two markers (Figure 38A).

Other NK cell memory-associated makers include CD49a (*Itga1*) and homeobox only protein (*hopx).* Bezman et al. (2012) described these two markers as initially expressed in effector cells and maintained in mCMV-induced memory NK cells (Bezman *et al.* 2012). Here, in the context of VACV infection, *Itga1* and *hopx* were transcripts levels were upregulated in NK cells (Figure 38A).

Together, these data suggest that splenic and hepatic NK cells, in the acute stage of VACV systemic infection, substantially upregulate markers that are typically associated with memory NK cells.

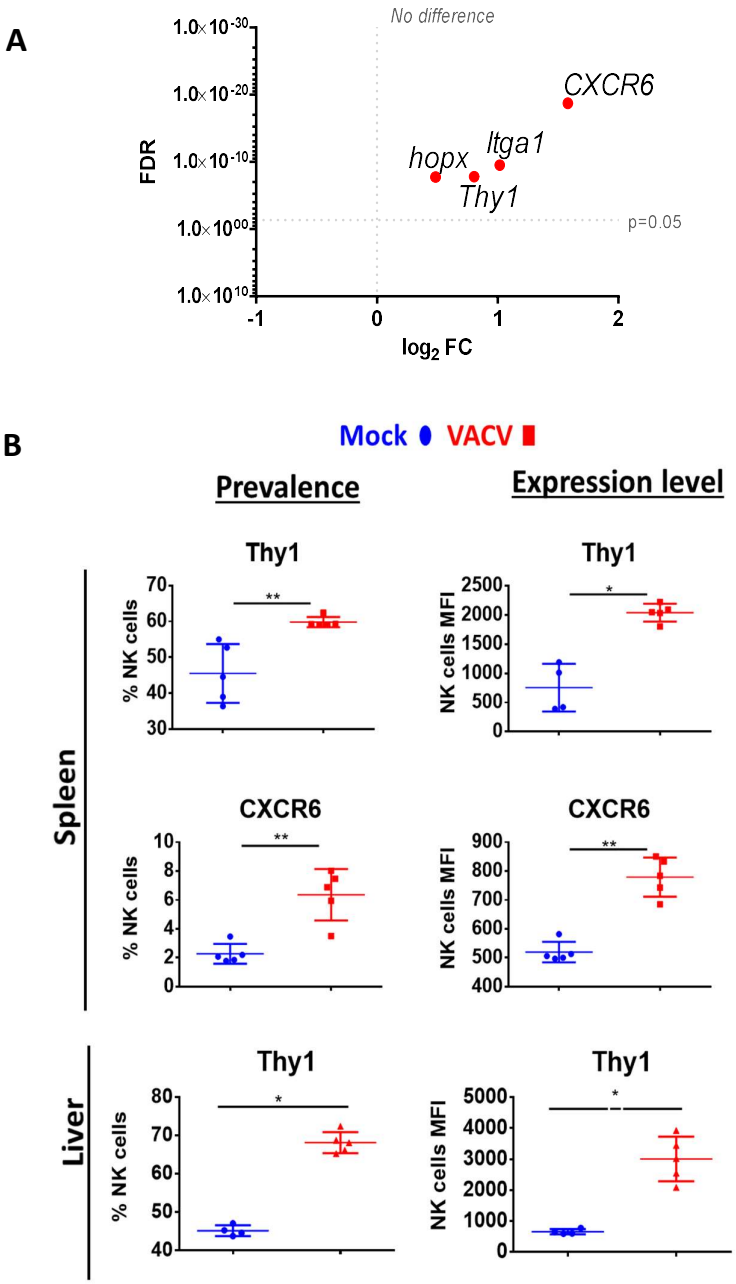

Figure 38 Differential expression of markers associated with memory NK cells, at the transcriptomic and proteomic level, during VACV infection. Group of B6 mice were infected with VACV WT or mock, at 6.5 d.p.i, NK cell transcriptomic activity was studied by RNA-seq (n=4), and differential expression (VACV vs mock) was calculated. In parallel, surface proteins expression was analysed by FACS (n=5).

A) Each dot represents the differential expression profile of a transcript of interest (WT vs mock). The X-axis represent the FC expressed as log_2, and the Y-axis represents the statistic value associated with the FC (FDR). Red indicates statistical significance (FDR<0.05). For clarity, the protein name is indicated rather than the gene name.

*B) FACS analysis for markers associated with memory NK cells in splenic and hepatic NK cells from mock (blue) and VACV-infected mice (red). The percentage of NK cells expressing the receptor (prevalence) and MFI (expression level) for each receptor is shown. Error bars represent ±SD, statistical significance was assessed with a Mann-Whitney test (*p<0.05, ** p<0.01, ***p<0.001).*

3.13 VACV and mCMV lead to unique and common NKRs transcriptomic modulation

To identify pathogen-induced modulation of NKRs, the transcriptomic signature of splenic NK cells during mCMV infection at 1 and 7 d.p.i. (Immunological Genome Project (ImmGen), GSE15907) were compared with our RNA-seq dataset. Using a manually curated list of 43 murine NKRs (as described in Figure 39), unique and common expression modulation between the two viruses was analysed. Eleven NKRs transcripts (*ly49f, ly49a, lair1, lag3, klrg1, cd319, Tigit, CD69, Thy1, Gp49A* and *Gp49B*) were upregulated, and four (*NKRP1C, Ly49I, NKG2C* and *CD27*) were downregulated by both viruses and are therefore not pathogen-specific. mCMV infection only led to the upregulation 4 NKRs transcripts (*Klra3, Klra8, Cd244a* and *Klrc1*) (Figure 39). As expected, Ly49H (*klra3*) which engages specifically with mCMV m157 protein and whose expression is not altered during VACV infection, was only modulated in the mCMV dataset. The NKRs whose expression was upregulated solely during VACV infection and not mCMV are particularly relevant since they might represent NKRs specifically engaged during VACV response. Those receptors included NKRP1b (*klrb1b*), SEMA4D (*sema4d*), CRTAM (*crtam*), CD160 (*cd160*) and NKRP1F (*klrb1f*).

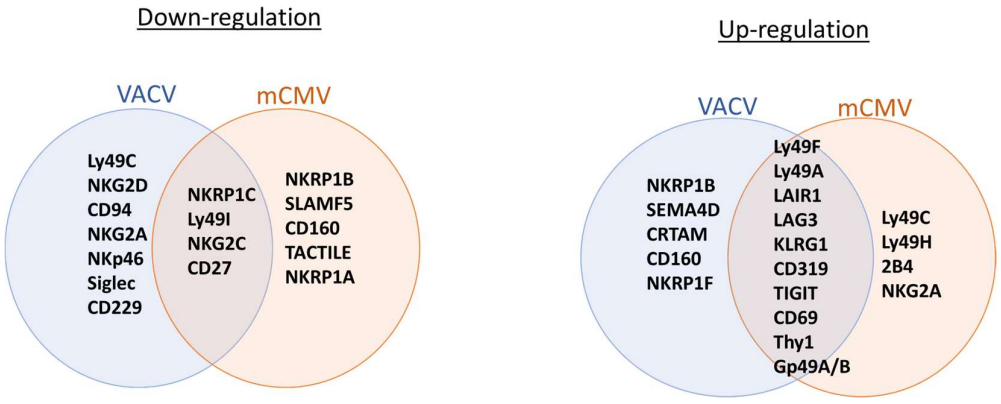

Figure 39. Comparative analysis of the NK cell transcriptomic signature during VACV and mCMV infection, focused on NKRS. Group of B6 mice (n=4) were infected with VACV WT or mock. NK cell transcriptomic activity was studied by RNA-seq and differential expression (VACV vs mock) was calculated at 1.5. and 6.5 d.p.i.. This dataset was compared with a similar study in NK cells from B6 mice during mCMV infection at 1 and 7 d.p.i. (dataset GSE15907, Bezman et al., 2012). Transcripts detected in both datasets were isolated and NKRs transcripts significantly up/downregulated (FDR <0.05) were extracted for comparison. The Venn diagrams represent the NKR transcripts found to be differentially expressed in NK cells following murine infection by both viruses (intersection) or only one (sides). For clarity, the protein name is shown rather than the gene name.

3.14 NK cell transcriptomic signature in murine NK cells post VACV-infection and human NK cells post MVA-vaccination display similarities

Costanzo and colleagues analysed human circulating NK cells before and 7 d post-vaccination with MVA, an attenuated VACV strain that is mostly non-replicating in human cells and which is commonly used as a vaccine vector. In this paper, the transcripts of 96 pre-selected genes were studied at both time points by qPCR and their FC analysed. Seven transcripts were significantly (FDR<0.05) upregulated at 7 d.p.i. with MVA in humans and were also significantly upregulated following VACV infection in mice (indicated by a circle in Figure 40).

Additionally, we reasoned that, since MVA is highly attenuated and non-replicative, it is likely to lead to less pronounced changes in the transcriptome of NK cells. Moreover, statistical analysis of FC by qPCR is less powerful than the statistical analysis of FC by RNA-seq. Consequently, the statistical values of the FC are likely to be smaller in Costanzo et al. study and might not reflect the biological relevance. Therefore, the transcripts with the highest FC in their datasets were selected (FC >1.5 or <-1.5) regardless of their statistic values. With this threshold, 47 transcripts were isolated from Costanzo et al. study and the expression profile of such genes were analysed in our dataset.

Thirty-six of such transcripts were detected in our dataset, all of which were described as upregulated in Costanzo et al. study. Hence, upregulation of these transcripts in our dataset indicates overlap with the transcriptomic signature of NK cells post MVA-vaccination. The differential expression of these 36 transcripts in our dataset is displayed in Figure 40. Somewhat surprisingly, 88 % of these transcripts were upregulated in our dataset, 64 % reaching statistical significance.

Further, Costanzo and colleagues described that the transcriptomic changes occurring in NK cells post MVA-vaccination match closely the transcriptomic signature of NK cells activated by direct recognition. These data are consistent with the observation we made earlier (see section 3.5) and support the view that NK cells from humans and mice share a transcriptomic signature in response to poxviruses.

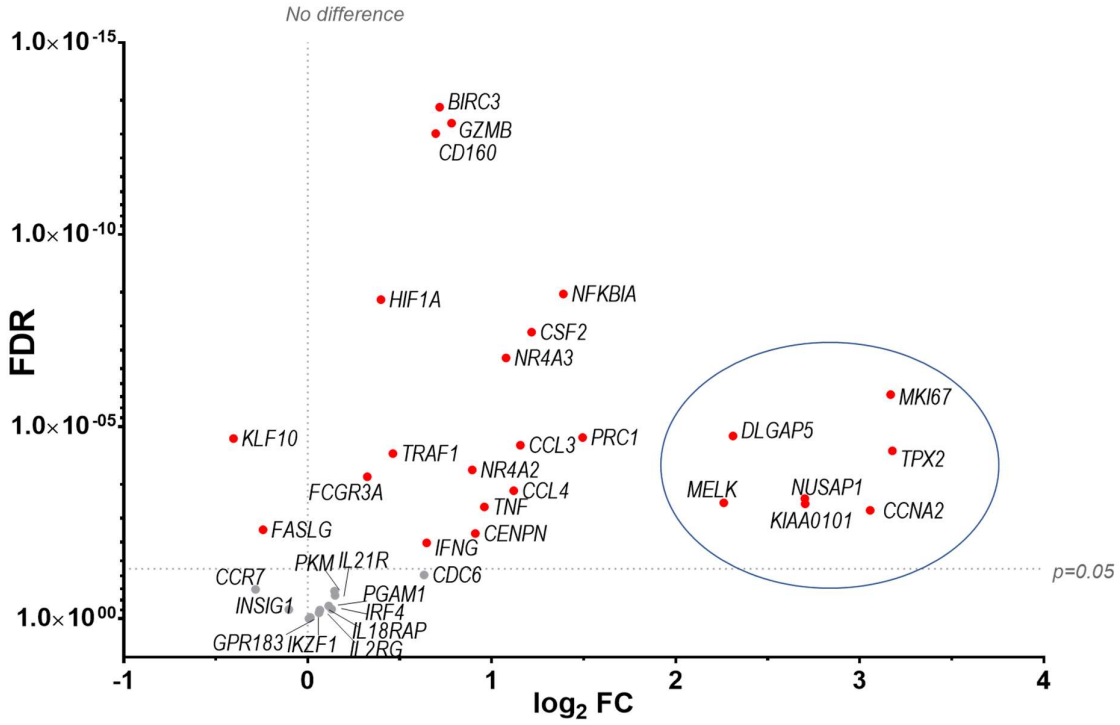

Figure 40. Identification of a transcriptomic signature common to human NK cells post MVA-vaccination and murine NK cells post VACV-infection. Groups of B6 mice (n=4) were mock or VACV infected. At 6.5 d.p.i, NK cell transcriptomic activity was studied by RNA-seq and differential expression of transcripts was calculated (WT vs mock). The transcriptomic data (qPCR) from a study looking at human NK cells (n=11) before and at 7 d post MVA vaccination (Costanzo *et al.* 2018) *was compared to our RNA-seq data. Transcripts whose expression post MVA-vaccination was differentially expressed with a FC >±1.5 were isolated. The expression of such transcripts was searched in our RNA-seq data. All such transcripts that were detected in our dataset were described as upregulated in Costanzo et al., 2018. Their differential expression in our dataset is represented on the graph. Each dot represents a transcript, the FC (VACV vs mock) is expressed on the X-axis as log_2, and the FC statistic value (FDR) is expressed on the Y-axis. Red indicates statistical significance (FDR<0.05). Circled are the transcripts that were most significantly (FDR<0.05) upregulated at 7 d.p.i. with MVA.*

3.15 Discussion: investigation of the NK cell response to VACV at a transcriptome-wide level

Little is known about how NK cells detect VACV-infected cells, which stimuli trigger their activation, and which NKRs are involved in the immune response to VACV. Such questions were addressed by studying VACV-infected mice NK cells by a combination of RNA-seq, FACS and comparative bioinformatic analyses. The results of these studies and their implications are discussed sequentially below.

3.15.1 NK cells activation status

Our RNA-seq data indicated that NK cells underwent broad transcriptional changes in response to VACV infection. The function of modulated genes related in part to immune defence and response to external stimuli, suggesting that NK cells respond actively to fight VACV infection. Further, NK cell numbers in VACV-infected mice increased, and transcripts for proliferation markers were substantially upregulated, which is consistent with the literature (see section 1.6.1.2) (Abboud *et al.* 2016; Dokun *et al.* 2001; Jacobs *et al.* 2006; Natuk & Welsh 1986; Prlic *et al.* 2005). Besides, the NK cell subsets that expanded the most during VACV infection had cytotoxic and cytolytic capabilities, which is also in line with the literature (Abboud *et al*., 2016). Additionally, transcripts for mediators of cytotoxic functions (GzmB and GzmK, IFNγ, TNF-α, TRAIL) and protection against cytolytic granules damages (serpins and cathepsins) were upregulated, indicating that NK cells were armed to mediate a cytotoxic and cytolytic response. Further, activation markers (CD69, Sca1, KLRG1, CD107a and gp49A/B) were significantly upregulated at the protein (where tested) and the transcript level, which, is consistent with the literature (see section 1.6.1.3). Finally, the transcriptional changes in VACV-infected mice NK cells, correlated with the NK cell general activation transcriptomic signature defined by Costanzo and colleagues (Costanzo *et al.* 2018), further indicating NK cell activation status in response to VACV.

Interestingly, some activation markers were studied in mutant mouse models in the context of VACV infection and provide additional information regarding their function. In a mouse model deficient for CD69, infection with VACV was better controlled (reduced weight loss and viral titres) in comparison to WT mice (Notario et al., 2016). This phenotype was attributed to a higher number of NK cells in $CD69^{-/-}$ mice that resulted from a lower spontaneous cell death rate of activated NK cells. This study suggests that CD69 upregulation during VACV infection is involved in NK cell homeostasis (Notario et al., 2016). Further, VACV infection in a $gp49B^{-/-}$ mouse model in comparison to its WT counterpart, showed an enhanced IFNγ production by NK cells, but no alteration of the cytotoxic response (Gu *et al.* 2003), suggesting that gp49B regulates NK cell IFNγ production (Gu *et al.* 2003).

The comparative analysis of the NK cell transcriptomic signature in VACV-infected mice suggested that NK cells are activated by a combination of IFNs, direct cell recognition, and IL-12 and IL-18. The VACV-induced transcriptomic signature correlated primarily with direct cell recognition as defined by Costanzo et al. 2018. This suggests that direct cell recognition might be the main driver of the NK cell response during VACV infection *in vivo* and supports the hypothesis that a VACV-specific NK receptor: ligand couple could exist. This is also in line with the literature since multiple independent studies report that NK cells recognise and kill VACV-infected cells (see section 1.6.1.4). Of note, a lower killing capacity of NK cells in the context of VACV infection has been reported in experimental settings where target cells present a high lysis background or when the NK92-MI cell line was used as effector cells. This discrepancy can be explained by multiple factors. Cell lines that present a high level of background lysis are not representative of physiological conditions where little or no lysis background is expected. VACV infection might reduce the expression of activating surface proteins, therefore resulting in a lower percentage of lysis when compared to non-infected cells. Moreover, the NK92-MI cell line is derived from a single human clone and has been stably transfected with IL-2, thus, it is poorly representative of the polyclonal NK cell response found in individuals. Together, those observations emphasise the importance of using physiologically relevant conditions to study the interplay of NK cells with virus-infected cells.

Besides, the correlation of our dataset with an IL-12/-18- induced transcriptomic signature is also in line with the literature since IL-18 and -12 are reported as involved in NK cell activation during VACV infection*, in vivo* (see section 1.6.1.5) (Brandstadter *et al.* 2014; Gherardi 2003). Similarly, the upregulation of ISGs in VACV-infected mice NK cells could have been somewhat expected since IFNs are potent antiviral and published studies report that VACV-mediated NK cell activation requires IFN-I signalling (Martinez *et al.* 2008, 2010a; Zhu *et al.* 2007) (see section 1.6.1.5). Interestingly, VACV expresses soluble binding proteins for IFNα/β, IFNγ and IL-18 (encoded by genes *B18R*, *B8R* and *C12L*, respectively) (Alcamí & Smith 1995; Born *et al.* 2000; Colamonici *et al.* 1995; Reading & Smith 2003; Symons *et al.* 1995; Waibler *et al.* 2007) and has evolved many strategies to impair IFNs expression and signalling (Smith *et al.* 2018). The fact that VACV has developed strategies to interfere with these cytokines indicates their biological relevance. However, our transcriptomic data suggests that VACV is only able to partially prevent the signalling of such cytokines.

Further, our data did not show correlation with ADCC-induced transcriptomic signature, which is consistent with the late onset of ADCC that requires the pre-existence or the generation of VACV-specific Abs, which are produced at later time p.i. Nevertheless, it would be interesting to study NK cell-mediated ADCC in the memory phase of VACV infection to assess its contribution to the recall

response since recent studies describe the important role of NK-mediated ADCC in the protection against viruses such as Ebola (Gunn *et al.* 2018; Saphire *et al.* 2018a, 2018b).

Together, these data indicate that during VACV systemic infection, NK cells proliferate, undergo broad transcriptomic changes and become activated. NK cell activation is a controlled process since NK cells express markers that contribute to limiting their response (CD69, gp49A/B), presumably to avoid uncontrolled activity that would be detrimental to the host. Stimuli that contribute to NK activation during VACV infection are direct recognition, IFNs and cytokines mediated. These data confirm previously known aspect of VACV NK cell response and further our understanding of host-pathogen interactions.

3.15.2 Surface NKRs are modulated during systemic VACV infection

The second part of this first result chapter provides information regarding NKRs and investigated the hypothesis that a dominating NK receptor: ligand couple may exist in the context of VACV infection and would lead to the preferential expansion of an NK subset bearing this receptor. To study this hypothesis, the expression of NKRs during VACV infection *in vivo* was studied at the transcriptomic and protein level at the peak of the NK response (7 d.p.i.), with a focus on NKRs that engage with cell surface proteins and influence NK cell activation status.

3.15.2.1 LY49 family

Our results showed stable expression of LY49H, -D and -G2 at the transcript and protein level, suggesting that these receptors are not likely to define an NK cell subset expanding preferentially during VACV infection. The stable expression of LY49H is consistent with the literature (Dokun *et al.* 2001; Gillard *et al.* 2011), indicating that LY49H$^+$ NK cell expansion during mCMV is specific to this virus. Further, the diminution of Ly49C/I$^+$ NK cells during VACV infection might reflect the internalisation of Ly49C/I after NK cell activation (Shi *et al.* 2018), or the preferential expansion of NK cells that do not express these receptors, similarly to the preferential expansion of Ly49H$^+$ NK cells, lacking Ly49C/I during mCMV infection in B6 mice (Orr *et al.*, 2010). Next, the inhibitory receptors LY49A and LY49F were significantly upregulated at the mRNA and protein level, but were present on a low percentage of NK cells, 10-15 % and 5-7 % respectively. This suggests that they are unlikely to define an NK cell subset that dominate VACV infection response in a similar way to mCMV-induced expansion of LY49H$^+$ NK cells from 55 % to 90 % at 7 d.p.i. (Fogel 2016). Besides, Ly49A and LY49F transcripts were also upregulated in NK cells during mCMV infection, suggesting that their upregulation is not specific to VACV infection. A hypothesis to explain Ly49A and F upregulation is that viral infection leads to the preferential amplification of NK cell subsets expressing MHC-I-specific inhibitory receptors to raise activation threshold and tightly control NK cell response to prevent

inappropriate cytotoxic response. In other words, higher MHC-I-specific inhibitory receptors maintain NK cell responsiveness (reviewed in (Kumar 2018)).

3.15.2.2 NKG2/ CD94 family

Study of the NKG2 receptor family showed no differences other than a slight increase of CD94 MFI, which is likely due to protein stabilisation since no change at the transcript levels were observed. These results are to a certain extent in line with the literature reporting that VACV does not alter NKG2D ligands expression (Chisholm & Reyburn 2006), which under stress conditions, such as viral infection, are expected to be upregulated. This was also confirmed in chapter two of this thesis by studying the surface proteome of VACV-infected HFFF-TERTs. Interestingly, other poxviruses such as CPXV and MPXV encode decoy ligands for NKG2D (1.6.2.2)(Campbell *et al.* 2007), and NKG2D was shown to be required for NK cell activation during ECTV infection (see section 1.6.1.1, (Fang *et al.* 2008a)). Hence, our results may indicate that VACV has evolved a strategy to prevent NKG2D-mediated activation, which seems to be important for the NK cell response to other orthopoxviruses. Understanding how VACV might interfere with NKG2D mediated activation could have implications for the optimisation of NK cell response in VACV-based oncolytic vectors.

3.15.2.3 SLAM family

The study of the SLAM receptor family during VACV infection showed that Ly108 (or NK-T-B-antigen (NTB-A)) and CD319 (or CRACC) were substantially upregulated at the protein and transcript level whilst other SLAM receptors were not substantially modulated. Additionally, the adaptors required for SLAM activating functions were upregulated (ERT and SAP), suggesting that SLAM receptors were more likely to mediate activating functions. These results would deserve further investigation since other SLAM receptors are involved in the NK cell response to various viral infection. For example, human 2B4 and LY108 bind influenza HA via N-linked glycosylation and lead to NK cell co-stimulation (Duev-cohen *et al.* 2015). Blocking 2B4 or Ly108 inhibit NK cell-mediated lysis of influenza virus-infected cells (Duev-cohen *et al.* 2015). Further, soluble decoy for SLAM receptors are found in multiple viruses including MOCV and squirrel poxvirus, which encode homologues for SLAMF1 and SLAMF2, respectively (Farré *et al.* 2017). These data raise the hypothesis that a VACV-induced ligand might lead to the preferential expansion of an NK cell subset expressing CD319 and Ly108 receptors and/or that VACV encodes a decoy for such receptors

3.15.2.4 NKp46, DNAM-1, CD49b receptors

Furthermore, results showed that neither DNAM-1, nor Nkp46 were substantially modulated following VACV infection, suggesting that they do not define a NK cell subset that preferentially amplifies during VACV infection. However, this does not preclude that NKp46 might be involved in the immune response to VACV because NKp46 is expressed by almost all NK cells. The fact that DNAM-1

was not upregulated on NK cells during VACV infection contrasts with its important role during mCMV infection (Nabekura *et al.* 2014) and suggests this might be specific to mCMV.

Further, the study of CD49b receptor showed that its transcriptomic level was mildly downregulated whilst its surface protein expression level was upregulated. A possible explanation is that integrins (such as CD49b) are known to be constantly recycled, hence, their expression level does not necessarily correlate with protein expression (Adorno-Cruz & Liu 2019). Besides, the prevalence of $CD49b^+$ NK cells in the liver showed a significant increase during VACV infection which was not observed in the spleen. This can be explained by the fact that almost all splenic NK cells are $CD49b^+$ (therefore not allowing a further percentage increase) and that the liver contains a resident NK cell subset, which does not express CD49b. Interestingly, CD49b is the only marker whose expression was altered differently in splenic and hepatic NK cells during VACV infection. Despite the limited number of markers studied by FACS in both NK cell subsets, these data suggest that there might only be minor differences in the way these two NK cell subsets respond to VACV infection. This is particularly relevant in the context of memory NK cell development that is often described as restricted to NK cell resident subsets. Further work is necessary to clarify how different NK cell subsets respond to VACV infection. Nevertheless, the mild alteration in CD49b expression suggests that this receptor is unlikely to represent an NK subset that is specifically engaged in response to VACV infection.

3.15.3 Comparison of mCMV- and VACV-induced transcriptomic changes in NK cells highlights NKR candidates preferentially involved in VACV response

To narrow down further the search for a candidate NKR preferentially involved during VACV infection, NKR transcripts modulation in our RNA-seq dataset was compared with a similar study during mCMV infection. This showed that five receptors were substantially upregulated during systemic infection with VACV but not with mCMV: NKRP1F, NKRP1B, CRTAM, CD160 and Sema4D.

Sema4D and CRTAM are not the strongest candidate for further studies given that Sema4D was only modestly upregulated after VACV infection and that CRTAM is known to be expressed at the surface of activated NK cells (Arase *et al.* 2005). The absence of CRTAM upregulation in the mCMV dataset could be due to the transient nature of its upregulation. In contrast, the NKRP1 receptor family and their ligands (CLEC2 subfamily) are of great interest because they are conserved in human and mouse and can mediate surveillance of missing-self (reviewed in (Bartel *et al.* 2013). Interestingly, the murine NKRP1B/D ligand, Clr-b, which is ubiquitously expressed, is downregulated by VACV and ECTV, which renders target cells more susceptible to lysis by NKRP1B+ NK cells (Williams *et al.* 2012). Additionally, LLT1 (*clec2d*), the human ligand for human NKRP1A (*klrb1*, inhibitory), which is typically expressed following infection, is downregulated at the mRNA and protein level during VACV infection (Williams

et al., 2016). Moreover, another unidentified protein is upregulated during VACV WR infection, cross-links with the 4C7 mAb (raised against clec2d), and has an expression kinetic that is inversely correlated with the degradation of clec2d mRNA (Williams *et al.*, 2016). These data suggest that during VACV infection, a decoy ligand might be expressed to replace loss of clec2d. Candidate decoys could be VACV C-type lectin surface proteins such as A40, A33 or A34 (see chapter 2). Taken together, these data suggest that NKRP1: CLEC2 system could play an important role during VACV infection and may illustrate a co-evolution process between host and pathogen. Further, CD160 in human and mice binds classical and non-classical MHC-I (Barakonyi *et al.* 2004; Maeda *et al.* 2005) but also HVEM (herpesvirus entry mediator) and enhances NK cell lytic activity and cytokine secretions (Le Bouteiller *et al.* 2011; Liu *et al.* 2019; Šedý *et al.* 2013; Tu *et al.* 2015). Interestingly, CD160 upregulation was also observed in human NK cells post MVA vaccination (Costanzo *et al.* 2018), suggesting that CD160 might be involved in the recognition of poxvirus-infected cells, and that it could be conserved in mouse and humans. Hence, CD160 is a very good candidate receptor to investigate further in the context of VACV infection.

In summary, FACS study of NKR expression during VACV infection did not highlight a dominating NKR similarly to what is observed during mCMV infection, but in combination with transcriptomic and bioinformatic studies allowed the identification of a few candidate NKRs (Ly108, CD319, NKRP1B, NKRP1F, CD160) that may be involved in VACV immune response. Several hypotheses could explain why no receptors were seen to dominate the NK cell response to VACV infection in B6 mice among the one that were tested by FACS. First, B6 mice are not the natural host of VACV (which is unknown), and a receptor-ligand couple such as Ly49H and mCMV m157 is likely the result of a co-evolution process, and might be more likely to occur during persistent infection (such as CMV), thus might not exist in the context of acute VACV infection in B6 mice. In that regards, the study of ECTV (mousepox) in B6 mice might be more likely to reveal the existence of such ligand-receptor couples. This hypothesis is supported by the fact that B6 mice are resistant to ECTV, which is linked to the NKC gene complex that encodes NKR (Delano & Brownstein 1995a). Although ECTV-based studies can lead to a better understanding of host-pathogen interactions and NK cell biology, their applications are less likely to be transferable to the development of poxvirus-based therapeutics since these rely on VACV/ MVA. A second hypothesis to explain the absence of a dominating NKR, is that the NK cell response to VACV might be distributed among several NK cell subsets rather than being limited to a subset defined by one receptor. Several VACV-induced ligands might be recognised by various NKRs. Alternatively, VACV-induced NK cell response might rely on an NKR that is ubiquitously expressed on NK cells such as NKp46 that is required for influenza clearance (Gazit *et al.* 2006). A third hypothesis is that NK cell response to VACV might rely on a receptor that remains unknown.

Overall, these data constitute the foundation for further studies. For example, functional assays where candidates NKR are blocked with a specific mAb or with NKR reporter cells, could inform us on their contribution to VACV-infected cells lysis. Binding studies with soluble receptors incubated with VACV recombinant proteins or cells infected with WT VACV or mutants lacking individual genes could determine whether a specific VACV protein is recognised by such candidate receptors. Further, studying the expression kinetics of candidates NKRs defined in this thesis, in human and mice during VACV/MVA infection could provide valuable information regarding their functions. Additionally, animal models carrying deletion for such receptors could be used to clarify their contribution to the primary and recall response to VACV infection. Besides, following the hypothesis that the NK cell response might be redundant with other immune cells, using animals lacking other immune cells could lead to an enhanced NK cell response that might reveal a stronger phenotype. Further, if technical advances were to allow single-cell surface proteomic study of NK cells during VACV infection, this would be valuable to study simultaneously multiple surface proteins expression and overcome the limitations of NK cell numbers and specific Abs.

Taken together, our data highlight similarities and discrepancies between VACV and mCMV NK cell response and thus contribute to a better understanding of NK cell biology and host-pathogen interactions. Our RNA-seq dataset is a useful resource that could be used for future comparative studies of the NK cell response to various pathogens. Our work also has applications in oncolytic viral therapy; where knowing the NKR(s) involved in VACV-infected cell recognition could be exploited to enhance or optimise NK cell response, for example by activating NK subset bearing this receptor *ex vivo*, prior to adoptive transfer or by engineering CAR NK cells expressing such receptor.

3.15.4 Expression of memory NK cell-associated markers during VACV acute infection

Since VACV infection leads to the development of memory NK cells (see section 1.6.1.8.) (Gillard *et al.* 2011), we investigated whether NK cell memory-associated markers could already be detected in the acute stage of infection. Our dataset revealed that such markers were upregulated both at the transcriptomic (CXCR6, Thy1, CD49a and hopx) and protein level (CXCR6 and Thy1 tested). Additionally, Sca1 and KLRG1 which are also thought to be memory-associated markers because their expression is particularly high in LY49H^{+} NK cells at 6-10 d.p.i. with mCMV (Fogel *et al.* 2013a), were substantially upregulated following VACV infection. These results suggest that memory-associated markers might already be expressed in the acute stage of infection. This is consistent with the literature since CD49a and Hopx are known to be upregulated on conventional and resident NK cell subsets during the acute and memory stage of mCMV infection and maintained in the memory stage (Bezman *et al.* 2012).

Whether the upregulation of such markers is sufficient to define which NK cells will become memory cells is unclear. Our data raise the hypothesis that the liver might represent a favourable environment for the long survival of memory NK cells whilst the priming/development of NK cells into memory cells could occur in different organs during the acute infection stage. Further investigations in the memory stage of VACV infection will be necessary to clarify this. Besides, other NK cell resident subsets such as the ones found in the lungs or the skin would be interesting to study since they are directly present at the site of infection and might respond differently. Whether VACV-induced memory NK cells are limited to a subset of NK cells defined by a receptor engaging with a VACV-induced ligand remains elusive. This first results chapter provides a list of candidates NKRs that could define such subset and deserve further investigations.

3.15.5 Comparison with the human NK cell response to infection with MVA

Lastly, comparative analysis showed that transcriptomic changes in human NK cells post MVA vaccination correlated significantly with our RNA-seq dataset, suggesting that VACV MVA and WR induce similar changes in the transcriptional activity of NK cells, and that there are similarities in the human and mice NK cell response to poxviruses. Moreover, the transcriptomic changes in both datasets correlated best with direct cell recognition transcriptomic signature, which supports the hypothesis that a receptor: ligand couple might be involved in VACV-infected cell recognition. Interestingly, CD160 was substantially upregulated both in NK cells post-VACV infection and post-MVA vaccination, suggesting that CD160 might be a NKR that recognises poxvirus-infected cells, in mice and humans. Our data support the validity of a mouse model to study the NK cell response to poxvirus to translate findings to the human system. This has implications for the development of VACV-based therapeutics such as VACV oncolytic vectors which typically rely on studies performed in mouse models during early stages.

Collectively, the first results chapter of this thesis provides a global context for known and previously unknown molecular aspects of NK cell functions and homeostasis during VACV infection. It is the first transcriptomic study of NK cells in response to VACV infection, *in vivo*. Our work has implication for the design of poxvirus-based vaccines for heterologous pathogens and VACV-based oncolytic therapy and further our understanding of NK cell biology and host-pathogen interactions.

4 Chapter 4: Study of the host cell surface proteome during VACV infection

Several independent studies report that human and murine NK cells play an active role in the immune response to VACV *in vivo*. Our transcriptomic data also shows that NK cells respond to VACV infection *in vivo* and suggests that NK cells can recognise VACV-infected cells directly. Further, the discovery of VACV-induced memory NK cells (Gillard *et al.* 2011) raises the possibility that a cell surface ligand expressed during VACV infection can be recognised by murine NK cells.

However, it is not known how VACV affects the expression of host surface proteins. There is also an incomplete understanding of which VACV proteins are expressed at the PM during infection. It is unclear which ligands trigger the NK cell response to VACV infection and whether VACV has strategies to prevent NK cell activation. To address these questions, it is necessary to unravel how the host cell surface proteome is altered during VACV infection and to establish which VACV proteins are expressed at the surface of the infected cell. This led us to study the host cell surface proteome during VACV infection with a focus on NK cell ligands.

4.1 Experimental design

An unbiased, multiplexed proteomic screen utilising a technique called PM profiling (PMP) (Weekes *et al.* 2012, 2014) was performed to obtain a comprehensive view of the host cell PM proteome during VACV infection. The use of isobaric chemical tags called tandem mass tags (TMT) enabled the quantification of the relative abundance of proteins in eleven different samples simultaneously. An infection time course with WT VACV and mock samples was designed (Figure 41).

In addition, a special interest in VACV A56 and A38 proteins as potential NK ligands led us to investigate how the absence of those proteins impact the surface proteome in comparison to WT VACV. Additionally, a VACV-infected and a mock-sample were treated with the proteasome inhibitor MG132 to determine if any alteration in protein abundance involved proteasomal degradation. Finally, to distinguish VACV proteins expressed at the PM from putative contaminants non-specifically bound to the host cell surface, a sample was infected with WT VACV and incubated at 4 °C to prevent virus penetration.

Importantly, to interpret our data further, the parameters such as the cell type, infection time points, and MOI were chosen to match those of a recently published proteomic study at the whole-cell level (WCL, whole-cell lysate) with VACV (from our group in collaboration with the Weekes lab (Soday *et al.*

2019)). These parameters also allow for comparison with another PMP and WCL study with HCMV (Weekes *et al.* 2014).

The results obtained with WT VACV are presented in this chapter and data resulting from the mutant viruses lacking genes *A56R* and *A38L* will be presented and discussed in Chapter 5 of this thesis.

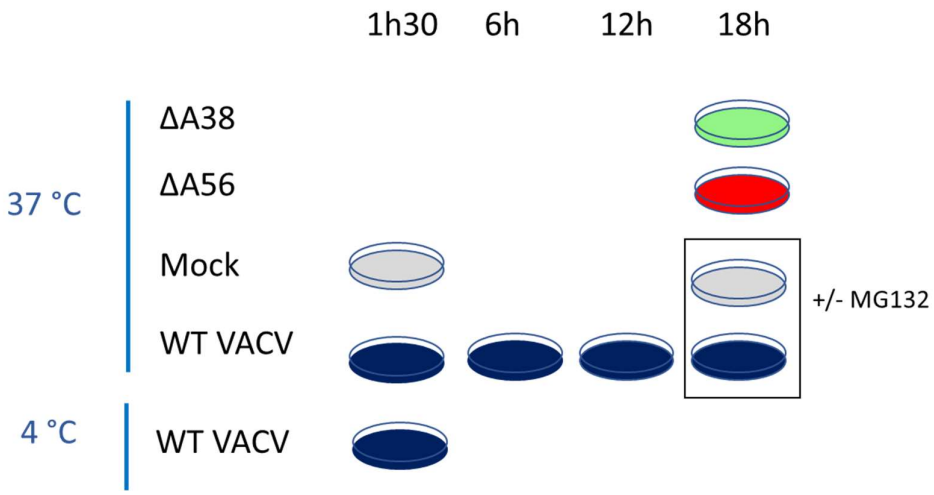

Figure 41 Experimental design for the PMP study of VACV-infected cells. HFFF-TERT cells were infected with the indicated virus at MOI 5 for the indicated time and temperature. Additionally, a mock and a WT infected samples were treated with the proteasome inhibitor MG132 for 18 h. The experiment was performed twice and independently.

4.2 Analysis of the proteins at the host cell surface during WT VACV infection

A total of 1099 proteins (PM-annotated and viral) were quantified in both PMP experiments, of which 266 were downregulated and 282 were upregulated by more than 1.5-fold during VACV infection. A heatmap of the fold change (FC) of all proteins quantified in the eleven samples (Figure 42) showed that the 3 mock samples clustered with the very early time points of VACV infection (1.5 and 6 h), whilst the late time point (12 and 18 h) clustered together as a distinct group and showed the most substantial changes. Enlarged sub-clusters of the heat map showed that the upregulated proteins (red area) include mostly viral proteins whilst the downregulated clusters (green areas) include host proteins downregulated by viral infection.

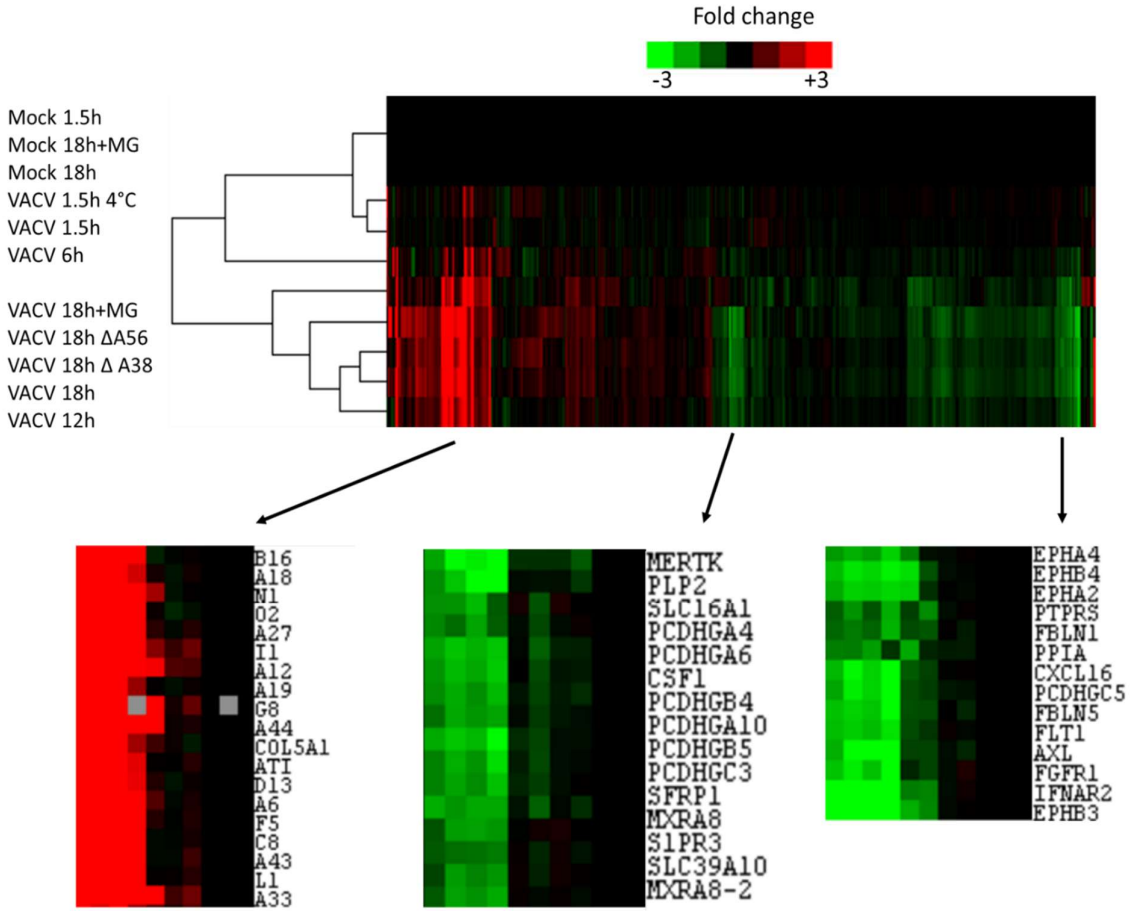

Figure 42 Hierarchical cluster analysis of all PM-annotated and viral proteins quantified in both PMP screens. HFFF-TERT cells were mock or VACV-infected with the indicated time and virus at MOI 5. The cell surface proteins abundance was quantified by PMP screen in two independent experiments. The average FC for each protein was calculated for each 11 samples, in comparison to their relevant mock. Hierarchical clustering of these 11 samples, based on uncentered Pearson correlation was performed with Cluster 3.0. and the heatmap created with JavaTreeview. The intensity of the colour indicates the FC as shown by the colour scale, and grey colour represents proteins that were not quantified in a sample. An enlargement of three sub-clusters is shown for proteins that were substantially upregulated (red) or downregulated (green).

Analysis of the functional gene ontology (GO) of the host PM proteins that were substantially modulated by VACV showed that these were enriched in glycoproteins, ephrins, cadherins, and proteins with tyrosine kinase activity (Figure 43). Pathway enrichment analysis suggested that the proteins downregulated by VACV were enriched in proteins with tyrosine kinase activity and ephrin signalling (Figure 44). Examples of proteins from the enriched clusters are shown in Figure 45, and FACS-based validation for a subset of such proteins is shown in Figure 46.

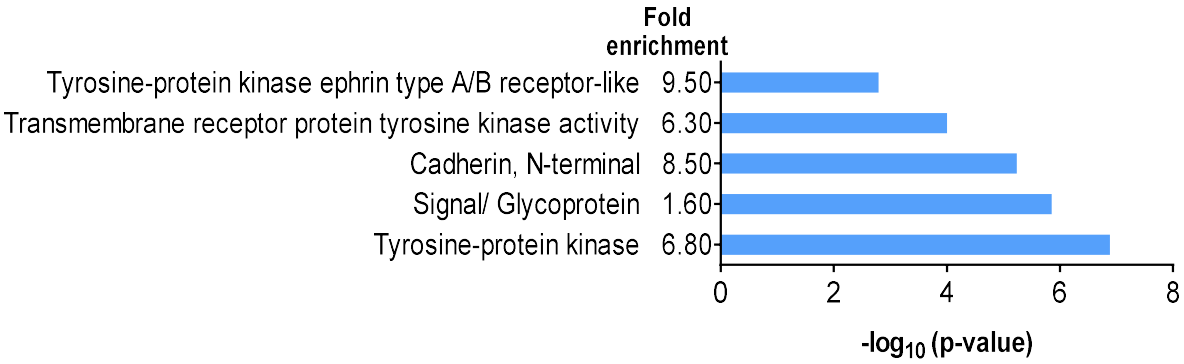

Figure 43 Functional cluster enrichment among host PM proteins downregulated after infection with WT VACV. HFFF-TERT cells were mock or VACV-infected with WT VACV at MOI 5, as described in Figure 42. Cell surface protein abundance was quantified by PMP screen, twice and independently. The average FC for each protein was calculated for each sample, in comparison to the mock. Host PM proteins downregulated > 2-fold ($p<0.05$) at any time after WT VACV infection, were analysed for functional enrichment against all proteins detected in the PMP screens, using DAVID software. A term representative of each cluster is shown alongside its fold enrichment, and the p-value corrected for multiple hypothesis testing with the Benjamini method is shown on the X-axis.

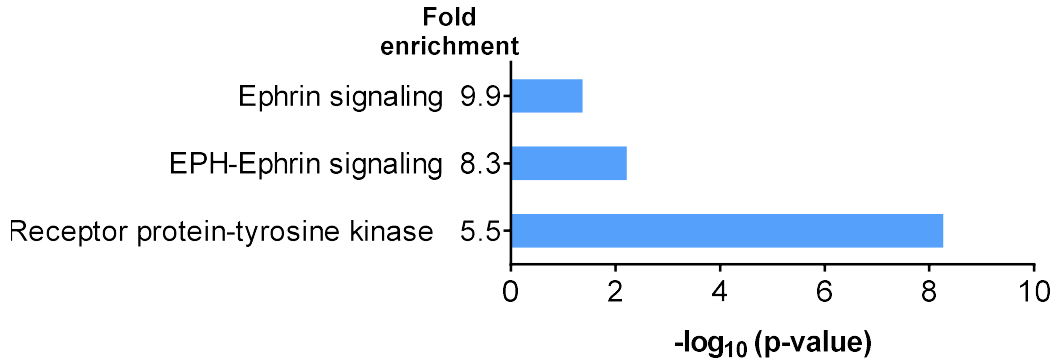

Figure 44 Pathway enrichment among host PM proteins downregulated after infection with WT VACV. HFFF-TERT cells were mock or VACV-infected with WT VACV at MOI 5, as described in Figure 42. The cell surface proteins abundance was quantified by PMP screen in two independent experiments. The average FC for each protein was calculated for each 11 samples, in comparison to their relevant mock. Host PM proteins downregulated > 2-fold ($p<0.05$) at any time after infection with WT VACV, were analysed for pathway enrichment against background of all proteins detected in the PMP screens using DAVID software. A term defining the pathway is shown alongside the fold enrichment, and the p-value corrected for multiple hypothesis testing with the Benjamini method is shown on the X-axis.

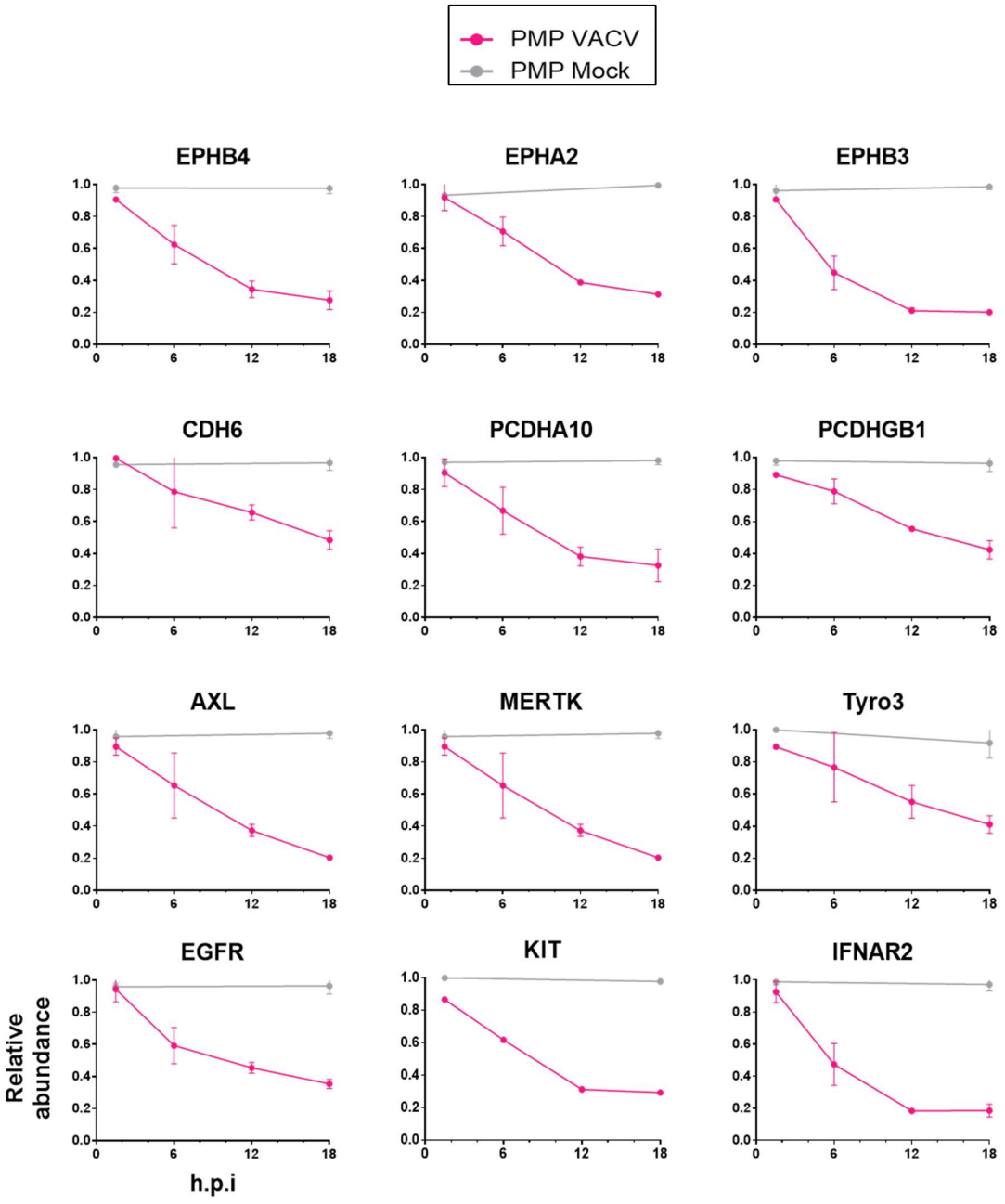

Figure 45 Examples of ephrins, cadherins, surface glycoproteins, and tyrosine kinase proteins downregulated by WT VACV at the PM. HFFF-TERT cells were mock or VACV-infected at MOI 5 for the indicated time course. PM protein abundance was quantified by PMP screen in 2 independent experiments. The temporal profile of the relative abundance for the indicated proteins is shown for mock samples (grey) and WT VACV infected samples (pink). Error bars represent the ± standard deviation (SD).

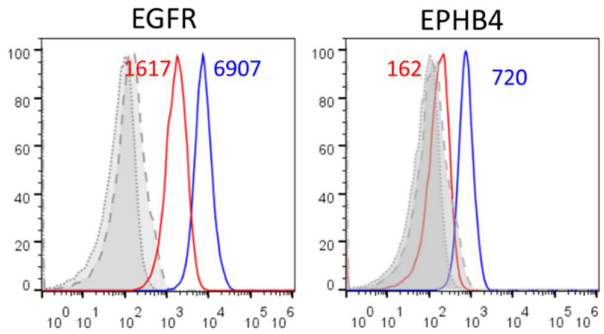

Figure 46 Expression profiles of surface host proteins during VACV infection determined by FACS surface staining. HFFF-TERTs cells were mock or infected with WT VACV at MOI 5 for 15 h. Cells were stained for surface expression of the indicated protein and the MFI corresponding to this marker is indicated next to the histogram curves, VACV-infected cells (red), mock cells (blue). Matching isotype controls were used for mock (dotted line) and infected cells (dashed line). Data is representative of at least two independent experiments.

4.3 Study of the expression of NK ligands at the PM during VACV infection

The study of host proteins modulated by VACV presented in this thesis was focused on NK ligands. Those results are presented in the subsequent sections.

4.3.1 Manually curated NK ligands list

The NK field is expanding, and new NK ligands are being reported frequently. However, there is no recent and comprehensive review of NK ligand-receptor complexes and GO databases rely on manual entry and are usually poorly annotated for NK ligands. Consequently, it was necessary to assemble a list of known NK ligands-receptors pairs by thoroughly reviewing the literature (Table 11). This list was limited to host surface proteins that engage with NK cell surface proteins and whose interaction has been shown to influence the susceptibility of the target cells to NK cells. This list was used to search for NK ligands in the proteomic datasets presented in this thesis.

Table 11 Host cell surface proteins known to engage with NK surface proteins and that influence the susceptibility of the host cell to NK cells.

Host protein Uniprot ID	Host protein symbol	Host protein name	NK cell receptor/protein	Reference	Effect on NK cell upon engagement
Q5ZPR3	B7-H3 (CD276)	CD276 antigen	unknown	(Castriconi *et al.* 2004)	Inhibition
Q68D85	B7-H6 (NCR3LG1)	Natural cytotoxicity triggering receptor 3 ligand 1	NKp30	(Brandt *et al.* 2009; Matta *et al.* 2013)	Activation
P46379	BAT3 (BAG6)	HLA-B-associated transcript 3	NKp30	(Pogge von Strandmann *et al.* 2007)	Activation
Q9BY67	CADM1 (necl-2)	Cell adhesion molecule 1	CRTAM	(Arase *et al.* 2005; Boles 2005; Tahara-Hanaoka 2004)	Activation, adhesion
Q92692	CD112 (nectin 2)	Nectin 2	TIGIT, DNAM-1, CD96 (TACTILE), PVRIG	(Bottino *et al.* 2003; Chan *et al.* 2014; Stanietsky *et al.* 2009; Tahara-Hanaoka 2004; Xu *et al.* 2017; Zhu *et al.* 2016)	Activation via DNAM1, inhibition via CD96, TIGIT and PVRIG
Q9NQS3	CD113 (nectin3)	Nectin 3	TIGIT	(Yu *et al.* 2009b)	Inhibition
P16284	CD31/PECAM-1	Platelet endothelial cell adhesion molecule	CD31/CD3	(Bianchi *et al.* 1993; Muller *et al.* 1993)	Adhesion and migration
P25942	CD40	Tumour necrosis factor receptor superfamily member 5	CD40L	(Carbone *et al.* 1997)	Activation
Q08722	CD47	Leukocyte surface antigen CD47	SIRPα	(Kim *et al.* 2008)	Inhibition
P09326	CD48	CD48 antigen	2B4, CD2 (low affinity)	(Brown *et al.* 1998; Latchman *et al.* 1998; Tangye, *et al.*	Activation and inhibition

				2000; Tangye *et al.* 2000)	
P32970	CD70 (CD27L)	CD70 antigen	CD27	(Takeda *et al.* 2000)	Activation
P21854	CD72	B-cell differentiation antigen CD72	Semaphorin 4D(CD100)	(Mizrahi *et al.* 2007)	Adhesion
P33681	CD80 (B7-1)	T-lymphocyte activation antigen CD80	CD28, CTLA-4, unknown receptor and CD82	(Azuma *et al.* 1992; Chambers *et al.* 1996; Luque *et al.* 2000; Montel *et al.* 1995b)	Activation
P42081	CD86 (B7-2)	T-lymphocyte activation antigen CD86	CD28	(Azuma *et al.* 1992; Luque *et al.* 2000)	Activation
P06731	CEACAM_5	Carcinoembryonic antigen-related cell adhesion molecule 5	CEACAM-1	(Stern *et al.* 2005; Watt *et al.* 1994)	
P13688	CEACAM-1	Carcinoembryonic antigen-related cell adhesion molecule 1	CEACAM-1	(Hosomi *et al.* 2013; Markel *et al.* 2002)	Inhibition
Q92478	clec2b (AICL)	C-type lectin domain family 2 member B	Nkp80	(Spreu *et al.* 2010)	Activation
Q5TAT6	COL13A1	Collagen α-1(XIII) chain	LAIR-1	(Lebbink *et al.* 2006)	Inhibition
H0Y420	COL17A1	Collagen α-1(XVII) chain	LAIR-1	(Lebbink *et al.* 2006)	Inhibition
Q86Y22	COL23A1	Collagen α-1(XXIII) chain	LAIR-1	(Lebbink *et al.* 2006)	Inhibition
Q5KU26	COLEC12	Collectin-12	PILR-α	(Sun *et al.* 2012)	Non tested
Q9NQ25	CRACC (slamf7)	SLAM family member 7	CRACC (slamf7)	(Boles *et al.* 1999; Kumaresan *et al.* 2002)	Activation and inhibition
P16410	CTLA4	Cytotoxic T-lymphocyte protein 4	CD86	(Peng *et al.* 2013)	Activation
P12830	E-cadherin (CDH1)	Cadherin-1	KLRG1	(Ito *et al.* 2006; Tessmer *et al.* 2007)	Inhibition
P25445	Fas	Tumour necrosis factor receptor superfamily member 6	FasL	(Montel *et al.* 1995a)	Apoptosis of target

Q14517	FAT1	Protocadherin Fat 1	unknown	(Weekes *et al.* 2014)	Activation
Q08830	FGL1	Fibrinogen like protein 1	Lag3	(Wang *et al.* 2019)	Inhibition
NA	GAGs	Glycosaminoglycan	NKp46, NKp44, NKp30	(Hecht *et al.* 2009)	Unclear
P05362	ICAM-1 (CD54)	Intercellular adhesion molecule 1	LFA-1 (CD11a)	(Barber *et al.* 2004; Barber & Long 2003; Chong *et al.* 1994)	Adhesion and activation
P13598	ICAM-2	Intercellular adhesion molecule 2	LFA1	(Barber *et al.* 2004)	Adhesion and activation
O75144	ICOSL	ICOS ligand	ICOS	(Ogasawara *et al.* 2002)	Activation
NA	IgG (secreted, surface-bound)	Immunoglobulin G	CD16	(Titus *et al.* 1987)	Activation
P05556	ITGB1	Integrin β-1	Semaphorin 7A (CD108)	(Ghofrani *et al.* 2019)	Promotes cytokine-induced NK cells differentiation and functionality,
Q6UVW9	KACL (clec 2A)	C-type lectin domain family 2 member A	NKp65	(Spreu *et al.* 2010; Welte *et al.* 2006)	Activation
P19256	LFA-3 (CD58)	Lymphocyte function-associated antigen 3	CD2	(Dustin 1987; Rabin *et al.* 1993; Selvaraj *et al.* 1987)	Adhesion, co-stimulation
Q9UHP7	LLT-1 (clec2d)	C-type lectin domain family 2 member D	NKRP1-a (CD161)	(Aldemir *et al.* 2005; Rosen *et al.* 2005)	Inhibition
P14151	L-selectin (CD62L)	L-selectin	PSGL-1	(Andre *et al.* 2000)	Homing/ trafficking
P36941	LTBR (TNFSFR3)	Lymphotoxin-β receptor	Lymphotoxin α1β2, TNSF14 (LIGHT)	(Maeda *et al.* 2018; Rooney *et al.* 2000)	Apoptosis of target
NA	MHC-I	Major histocompatibility complex	KIRs, PIR-A, PIR-B, LILRs, CD160	reviewed in (Carrillo-Bustamante *et al.* 2016; Gwozdowicz *et al.* 2019; Kuroki *et al.* 2012; Lanier 1998; Nowak	Inhibition and Activation depending on receptor

				et al. 2017; Tomasec *et al.* 2000)	
Q29983	MICA	MHC class I polypeptide-related sequence A	NKG2D	(Bauer 1999)	Activation
Q29980	MICB	MHC class I polypeptide-related sequence B	NKG2D	(Steinle *et al.* 2001; Wu *et al.* 1999)	Activation
Q8IZD2	MLL5 (KMT2E)	Inactive histone-lysine N-methyltransferase 2E	NKp44	(Rajagopalan & Long 2013)	Activation
NA	NA	α 2,6, α 2,8 and α2,3 saccharides	Siglec7	(Falco *et al.* 1999; Nicoll *et al.* 1999)	Inhibition
P19022	N-cadherin (CDH2)	Cadherin-2	KLRG1	(Ito *et al.* 2006; Tessmer *et al.* 2007)	Inhibition
Q15223	Nectin1 (CD111)	Nectin-1	CD96	(Holmes *et al.* 2019)	Activation
P14543	NID1	Nidogen 1	NKP44	(Gaggero *et al.* 2018)	Inhibition
Q9NQX5	NPDC1	Neural proliferation differentiation and control protein 1	PILRα	(Sun *et al.* 2012)	Activatory rec but physiology unknown
P12004	PCNA	Proliferating cell nuclear antigen	NKp44	(Horton *et al.* 2013; Kundu *et al.* 2019; Rosental *et al.* 2011)	Inhibition
Q9NZQ7	PD1-L1 (CD274)	Programmed cell death 1 ligand 1	PD1,	(Benson *et al.* 2010)	Inhibition
Q9BQ51	PD1-L2 (CD273)	Programmed cell death 1 ligand 2	PD1	(Ghiotto *et al.* 2010)	Inhibition
Q9GZP0	PDGF-DD	Platelet-derived growth factor D	NKp44	(Cox *et al.* 2017)	Activation
Q6P1B3	PANP	PILR-alpha associating neural protein	PILRα	(Kogure *et al.* 2011)	unclear
O43157	Plexin B1	Plexin-B1	Semaphorin 4D (CD100)	(He *et al.* 2017)	Activation
O15031	Plexin B2	Plexin B 2	Semaphorin 4D (CD100)	(He *et al.* 2017; Mizrahi *et al.* 2007)	Activation

P15151	PVR (CD155)	Poliovirus receptor	DNAM-1, TIGIT, CD96	(Bottino *et al.* 2003; Fuchs *et al.* 2004; Joller *et al.* 2011; Li *et al.* 2014; Tahara-Hanaoka 2004; Tahara-Hanaoka *et al.* 2005)	Activation via DNAM1, inhibition via CD96 and TIGIT
P55283	R-cadherin (cdh4)	Cadherin-4	KLRG1, other cadherins	(Ito *et al.* 2006)	Inhibition via KLRG1, adhesion via homotypic interaction with cadherins
O15041	Sema3E	Semaphorin-3E	Plexin D1	(Alamri *et al.* 2017)	Inhibition of migration
Q96DU3	SLAMF6 (NTBA)	SLAM family member 6	SLAMF6 (NTBA)	(Griewank *et al.* 2007)	Activation or inhibition depending on adaptors present
O00220	TNFRSF10A/TRAIL-R1/DR4	Tumour necrosis factor receptor superfamily member 10A, /death receptor 4	TRAIL	(Pan *et al.* 1997)	Apoptosis of target
O14763	TNFRSF10B/ TRAILR2/DR5/	Tumour necrosis factor receptor superfamily member 10B	TRAIL	(Sheridan J P *et al.* 1997; Walczak *et al.* 1997)	Apoptosis of target
O14798	TNFRSF10C/ TRAIL-R3/DcR1	Decoy receptor 1, Tumour necrosis factor receptor superfamily member 10C	TRAIL	(Degli-Esposti *et al.* 1997b; Sheridan J P *et al.* 1997)	Decoy for TRAIL, prevents apoptosis
Q9UBN6	TNFRSF10D/ TRAILR4/DcR2	Decoy receptor 2, Tumour necrosis factor receptor superfamily member 10D	TRAIL	(Meng *et al.* 2000)	Decoy for TRAIL, prevents apoptosis
P19438	TNFRSF1A/ TNFR1	Tumour necrosis factor receptor superfamily member 1A	TNFα (TNFSF1) and LT-α (TNSF2)	(Grell *et al.* 1998)	Apoptosis of target and NF-κB activation

P20333	TNFRSF1B/ TNFR2	Tumour necrosis factor receptor superfamily member 1B	TNF-α, LT-α	reviewed in (Yang *et al.* 2018)	Promotes cell proliferation strongly, can induce NF-κB but slow, can only induce apoptosis in very limited conditions
Q9NP84	TNFSFR12A	TWEAK receptor (Fn14, fibroblast growth factor-inducible molecule 14)	TWEAK (secreted)	(Chicheportiche *et al.* 1997; Winkles 2008)	Very weak apoptosis inducer on target cells, strong inflammation inducer via NF-κB
Q9BZM6	ULBP1	UL16 binding protein 1	NKG2D	(Cosman *et al.* 2001)	Activation
Q9BZM5	ULBP2	UL16 binding protein 2	NKG2D	(Cosman *et al.* 2001)	Activation
Q9BZM4	ULBP3	UL16 binding protein 3	NKG2D	(Cosman *et al.* 2001)	Activation
Q8TD07	ULBP4	UL16 binding protein 4	NKG2D	(Bacon *et al.* 2004; Jan Chalupny *et al.* 2003)	Activation
Q6H3X3	ULBP5	UL16 binding protein 5	NKG2D	(Bacon *et al.* 2004)	Activation
Q5VY80	ULBP6	UL16 binding protein 6	NKG2D	(Eagle *et al.* 2009)	Activation
P19320	VCAM-1	Vascular cell adhesion protein 1	Integrin α4 and β1/7; LFA1 (ITGB2)	(Chan *et al.* 2000; Perez-Villar *et al.* 1996)	Adhesion, activation for LFA1
P08670	VIM	Vimentin	NKp46	(Garg *et al.* 2006)	Activation

4.4 Modulation of known NK ligands during VACV infection

Forty surface proteins that are known to interact with NK cell surface proteins (as defined in Table 11) were detected in the PMP screens. Their expression profile during VACV infection time is shown hereafter. Data from the PMP study is shown alongside data obtained during a previous WCL study of VACV-infected cells (Soday *et al.* 2019). These data are presented in groups defined by their characteristics and/or the NK cell proteins with which they interact. In addition, FACS-based validation for the surface expression of a subset of those proteins during VACV infection is shown.

NK cells rely on adhesion molecules to enter in physical contact with surrounding cells and determine whether they are to be eliminated. Six such molecules were quantified in the PMP (Figure 47A). LFA3 (Lymphocyte function-associated antigen leukocyte 3), VCAM1 (Vascular cell adhesion molecule-1), ICAM1 and ITGB1 expression at the cell surface (PMP dataset) and the whole-cell (WCL dataset) was stable during VACV infection while CDH4 and CDH2 were moderately downregulated in both datasets, suggesting selective downregulation.

Upon contact with target cells, NKRs can engage with inhibitory or activating checkpoint molecules that regulate lymphocytes activation status. Our data showed that inhibitory checkpoint molecules such as programmed cell death ligand 1 and 2 (PD-L1, PD-L2), and B7-H3 were stably expressed during VACV infection (Figure 47B). The temporal profile of CD40 was stable, whilst ICOSLG was substantially downregulated (Figure 47C).

Further, our data showed that “stress NK ligands” that are typically upregulated following cellular stress, such as viral infection, and lead to NK activation, were not upregulated during VACV infection. Instead, stress ligands were downregulated at the surface and total cell level (Figure 48A). This was further validated by FACS (Figure 49), and suggests that VACV has a mechanism to prevent the synthesis of those proteins and/ or induce their degradation as a strategy to evade NK cell recognition.

NCRs can trigger NK cell activation on their own and host cells can express activating or inhibitory ligands for such receptors. Our data showed that inhibitory NCR ligands PCNA (proliferating cell nuclear antigen) and NID1 were, respectively, stable and downregulated (Figure 48B), suggesting that NID1 modulation may contribute to NK cell recognition of VACV-infected cells. Activating NCRs ligands MLL5 and B7-H6 were downregulated while VIM showed a substantial upregulation at the PM but not the whole-cell level. This suggests that VIM could play a role in the recognition of VACV-infected cells by NK cells.

Host cells express surface receptors that are involved in the regulation of apoptosis and interact with ligands expressed by lymphocytes such as NK cells. Here, our data showed that TRAIL receptor

(TRAILR) 1 and 2 were, respectively, mildly upregulated and downregulated. The surface expression of decoy receptors for TRAIL, TRAILR3 and 4, was respectively, stable or upregulated (Figure 50). The upregulation of TRAIL-R4 during VACV infection was further validated by FACS (Figure 51) and suggests a strategy to evade TRAIL-mediated apoptosis. Furthermore, Fas receptor, which triggers apoptosis upon interaction with FasL, was slightly downregulated following VACV infection (Figure 50). This was further validated by FACS (Figure 51). Additionally, TNFR2 and lymphotoxin b receptor (LTBR), which trigger apoptosis upon engagement with secreted TNF-α and LTα/β, were substantially downregulated (Figure 50). Finally, TWEAK receptor, which is a mild inducer of apoptosis but a strong inducer of NF-κB, was substantially upregulated at the PM (Figure 50).

Further data showed that surface proteins that compete for the activating receptor DNAM-1, and inhibitory receptors TIGIT, PVR-related Ig domain (PVRIG) and CD96, were all mildly downregulated except for Nectin-1Nectin-1 which was substantially downregulated (Figure 52A). The host protein CD47, which is a ligand for SIRP-α, was stably expressed during VACV infection (Figure 52B). Lastly, plexins, which are ligands for semaphorins, showed a mild downregulation at the cell surface during VACV infection (Figure 52C and Figure 53).

Overall, data showed that VACV infection leads to the selective modulation of NK ligands at the cell surface. Some of these are likely to promote NK cell activation, whilst others may contribute to the evasion of the NK cell response. Together, these data illustrate the complexity of interactions between NK cells and VACV-infected cells and constitute a valuable dataset for the study of host-pathogen interaction.

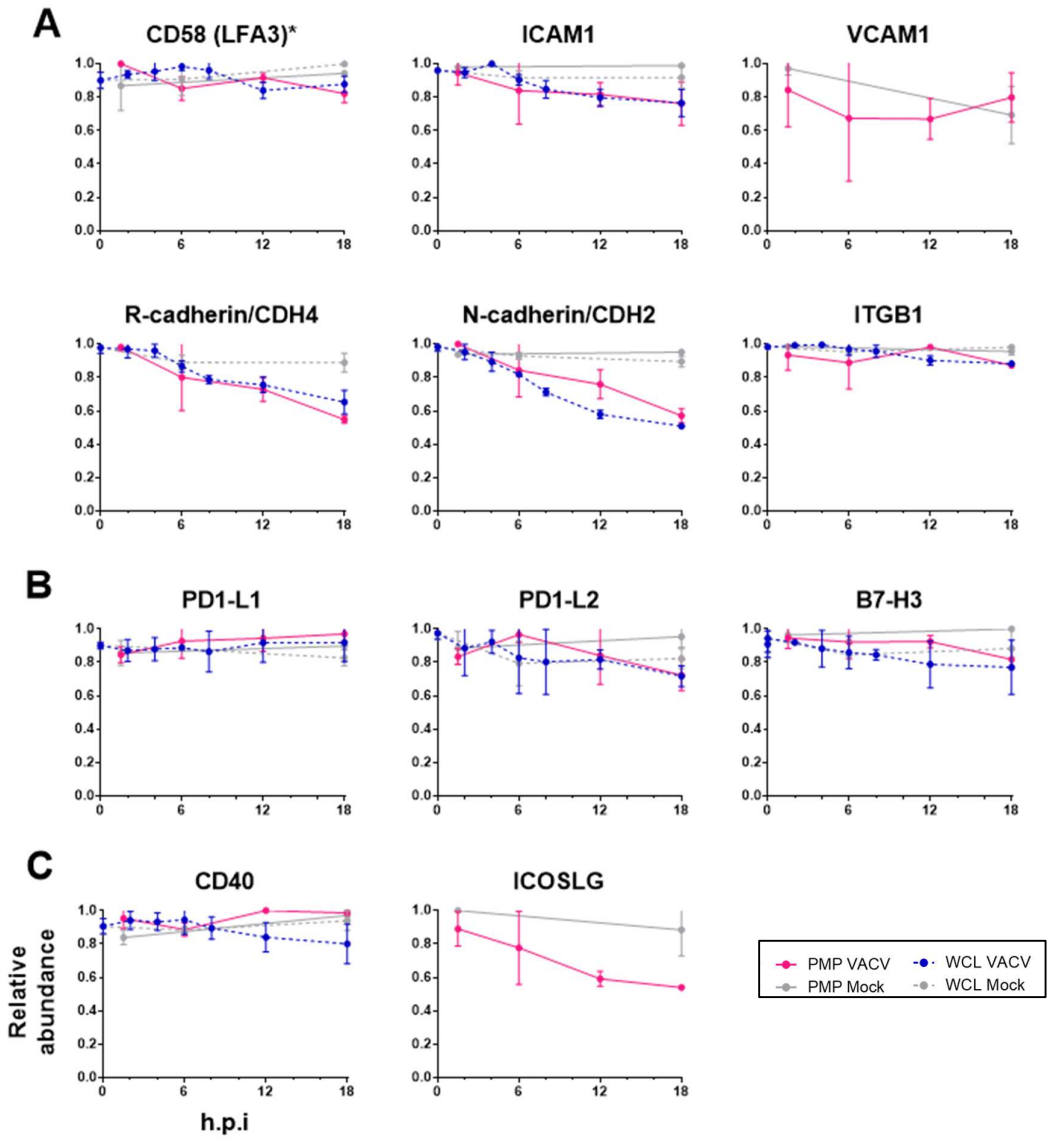

Figure 47 Temporal expression profile of NK ligands during VACV infection at the cell surface (PMP) and whole-cell (WCL). HFFF-TERT cells were mock or VACV-infected at MOI 5 for the indicated time course. PM protein abundance was quantified by PMP screen. Whole-cell protein expression (WCL) data were extracted from (Soday et al., 2019). The temporal expression profile of the indicated proteins within each screen is shown. Data from the PMP (full line) and WCL (dotted line) for mock samples (grey), and VACV-infected sample (pink for PMP and blue for WCL) is shown. Error bars represent ± SD for the two independent PMP screens, and 3 independent WCL screens. A) Surface proteins that mediate adhesion of lymphocytes such as NK cells. . an outlier has been removed from the WCL data for CD58. B) Immune inhibitory checkpoint proteins, C) Immune activating checkpoints proteins.*

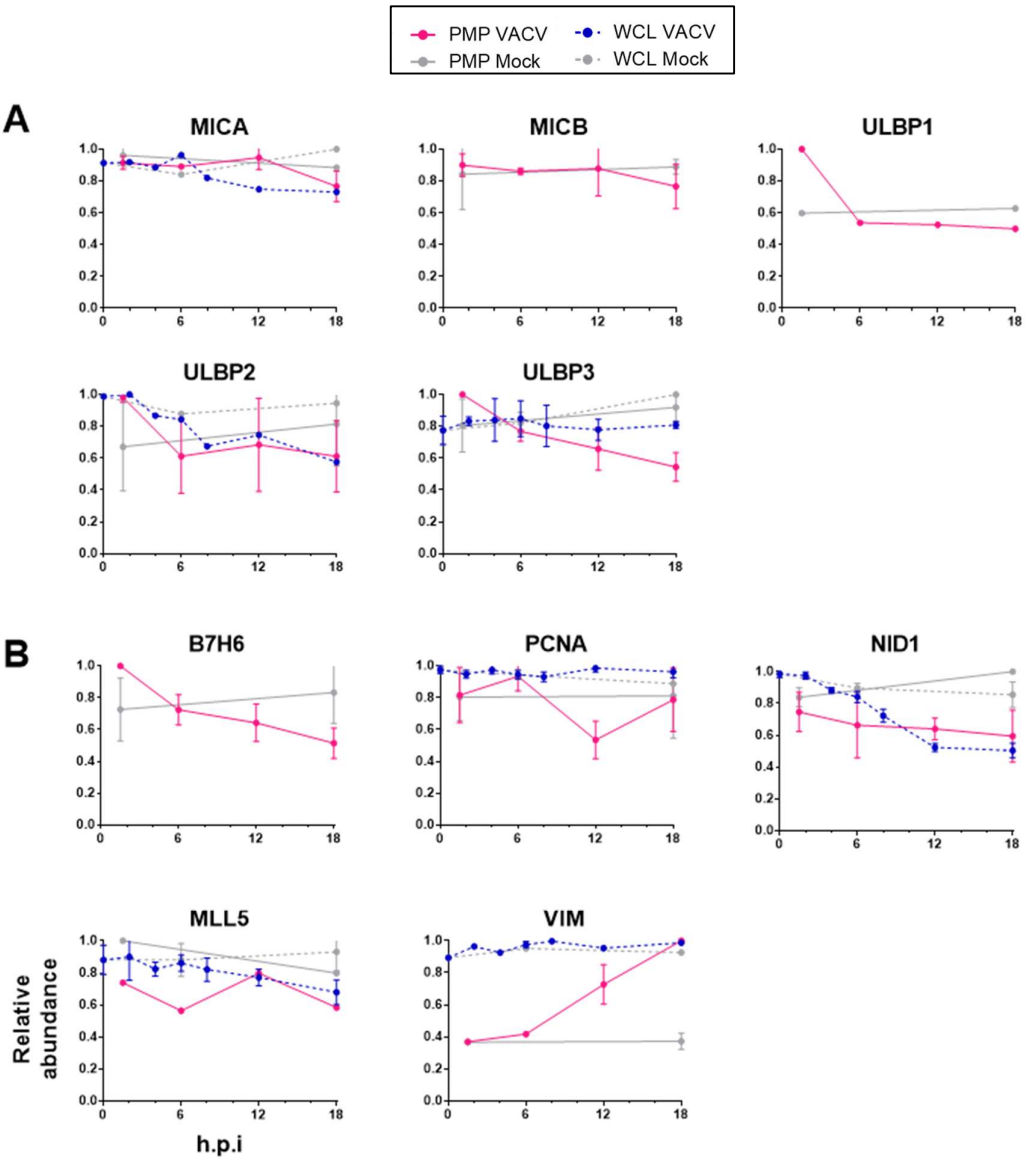

Figure 48 Temporal expression profile of NK ligands during VACV infection at the cell surface (PMP) and whole-cell (WCL). HFFF-TERT cells were mock or VACV-infected at MOI 5 for the indicated time course. PM protein abundance was quantified by PMP screen. Whole-cell protein expression (WCL) data were extracted from (Soday et al., 2019). The temporal expression profile of the indicated proteins within each screen is shown. Data from the PMP (full line) and WCL (dotted line) for mock samples (grey), and VACV-infected sample (pink for PMP and blue for WCL) is shown. Error bars represent ± SD for the two independent PMP screens, and three independent WCL screens. A) NK Stress NK ligands for NKG2D receptor, B) NCR ligands.

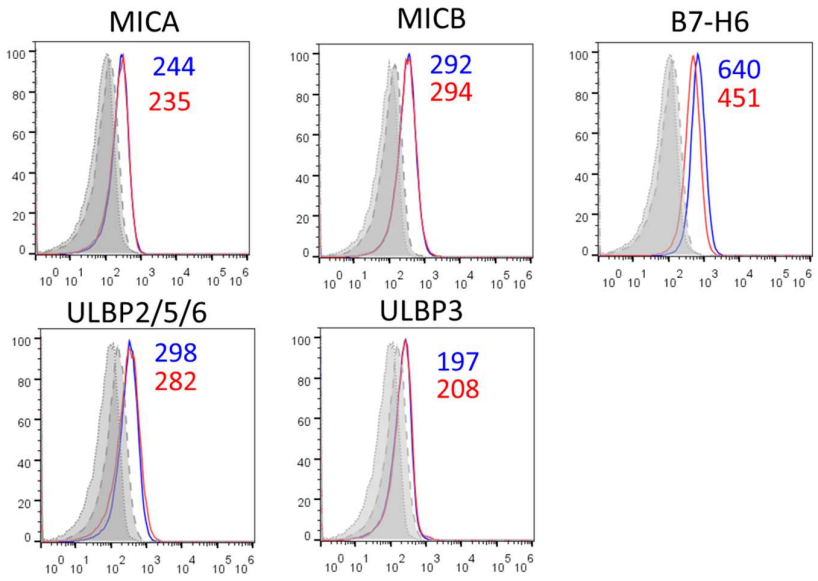

Figure 49 Expression profiles of surface host proteins during VACV infection determined by FACS. HeLa cells were mock or infected with WT VACV at MOI 5 for 15 h. Cells were stained for surface expression of the indicated protein and the corresponding MFI is indicated next to the histogram curves, VACV-infected cells (red), mock cells (blue). Matching isotype Igg controls were used for mock (dotted line) and infected cells (dashed line). This data is representative of at least two independent experiments.

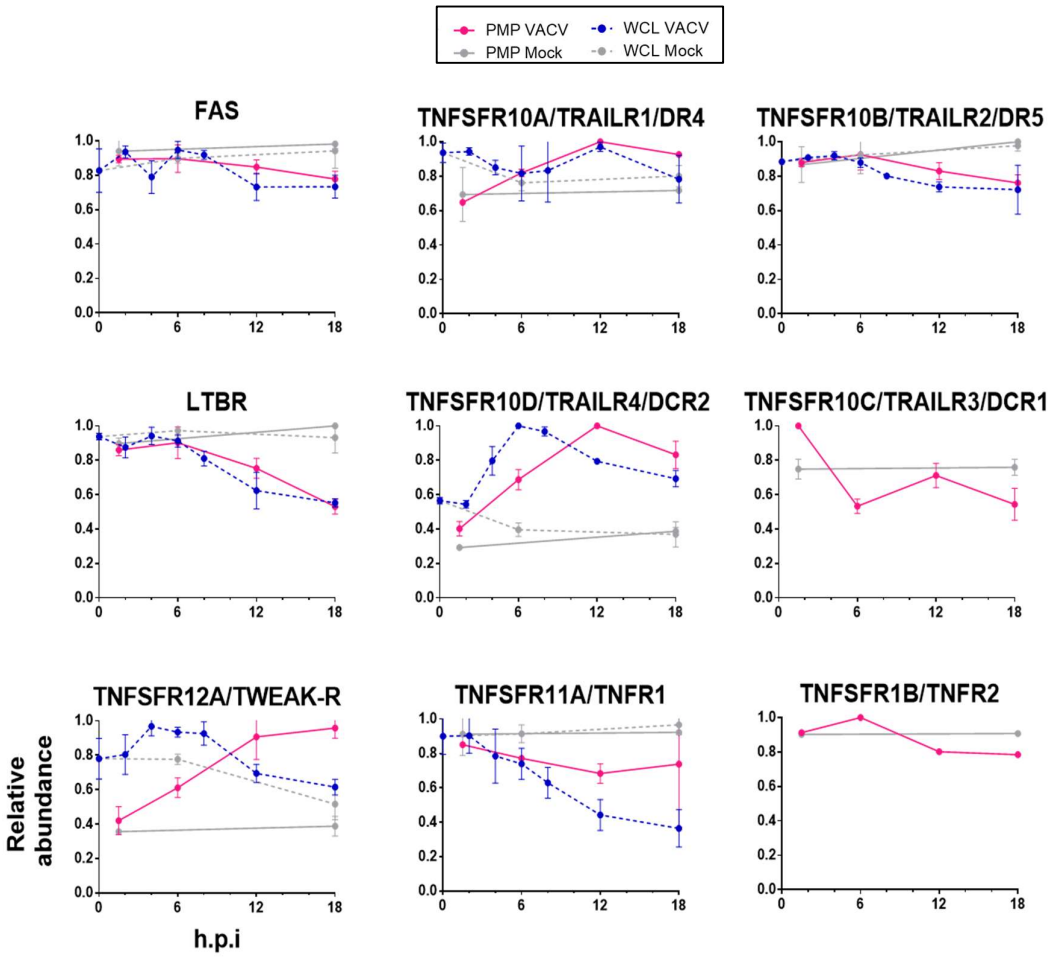

Figure 50 Temporal expression profile of apoptosis regulators, during VACV infection at the cell surface (PMP) and whole-cell (WCL). HFFF-TERT cells were mock or VACV-infected at MOI 5 for the indicated time course. PM protein abundance was quantified by PMP screen. Whole-cell protein expression (WCL) data were extracted from (Soday et al., 2019). The temporal expression profile of the indicated proteins within each screen is shown. Data from the PMP (full line) and WCL (dotted line) for mock samples (grey), and VACV-infected sample (pink for PMP and blue for WCL) is shown. Error bars represent ± SD within triplicates (WCL) and duplicate screens (PMP).

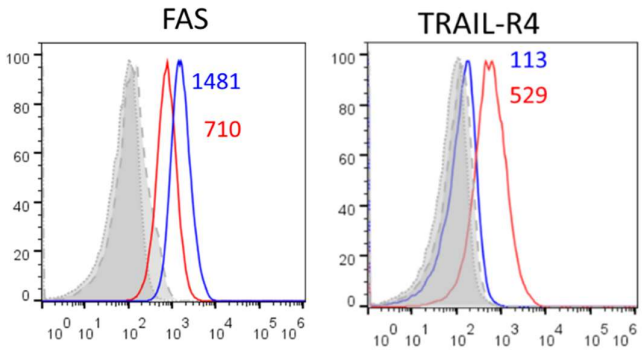

Figure 51 Validation of the temporal expression of apoptosis regulators during VACV infection by FACS surface staining. HFFF-TERTS (left panel) or HeLa cells (right panel) were mock or infected with WT VACV at MOI 5 for 15 h. Cells were stained for surface expression of the indicated protein and the corresponding MFI is indicated next to the histogram curves, VACV-infected cells (red), mock cells (blue). Matching isotype Igg controls were used for mock (dotted line) and infected cells (dashed line). This data is representative of at least two independent experiments.

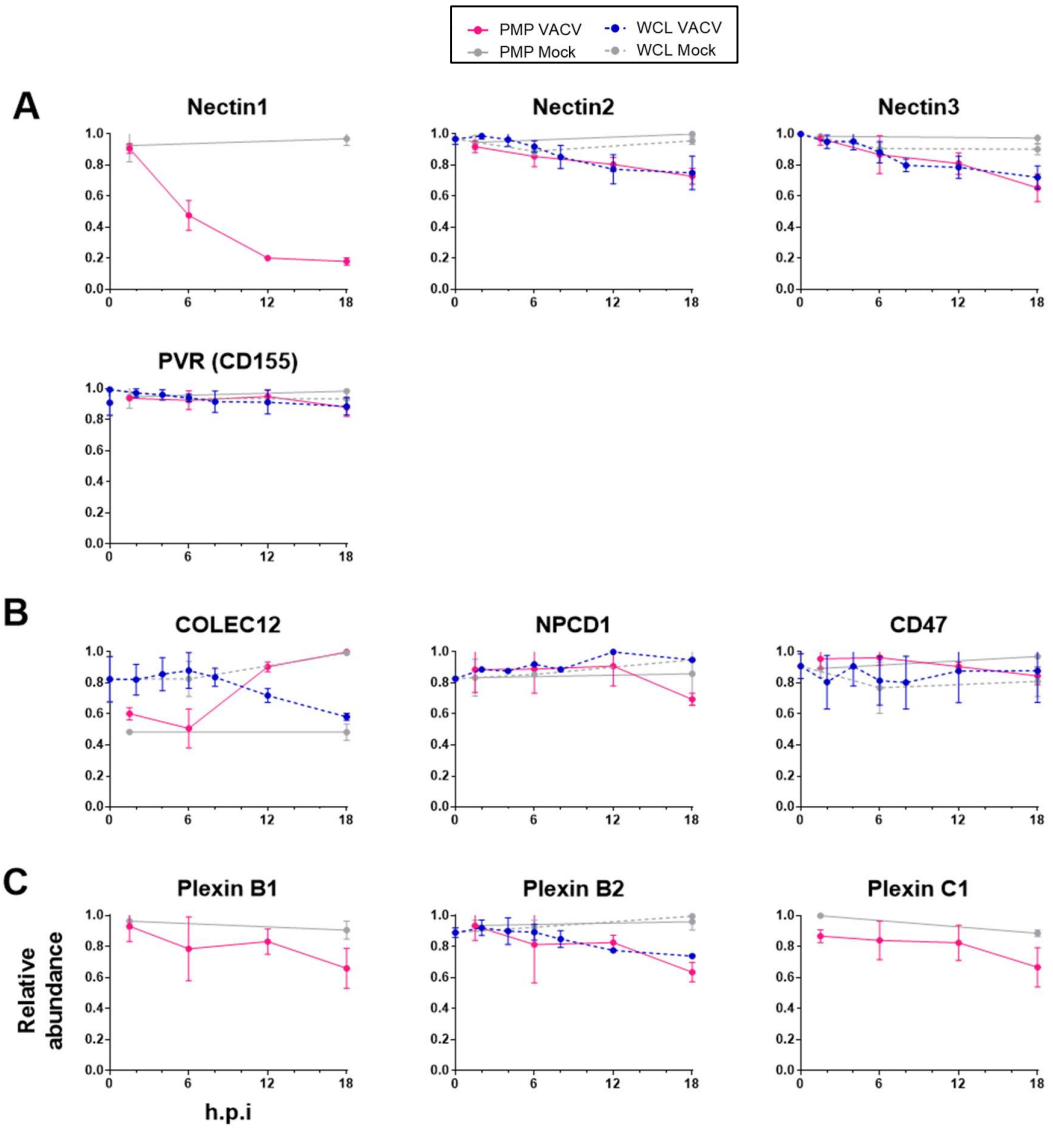

Figure 52 Temporal expression profile of NK ligands, during VACV infection at the cell surface (PMP) and whole-cell (WCL). HFFF-TERT cells were mock or VACV-infected at MOI 5 for the indicated time course. PM protein abundance was quantified by PMP screen. Whole-cell protein expression (WCL) data were extracted from (Soday et al., 2019). The temporal expression profile of the indicated proteins within each is shown. Data from the PMP (full line) and WCL (dotted line) for mock samples (grey), and VACV-infected sample (pink for PMP and blue for WCL) is shown. Error bars represent ± SD for the two independent PMP screens, and three independent WCL screens. A) Ligands for DNAM-1, TIGIT, PVRIG and CD96 receptors B) Ligands for SIRP-a and CD47 C) Ligands for semaphorins.

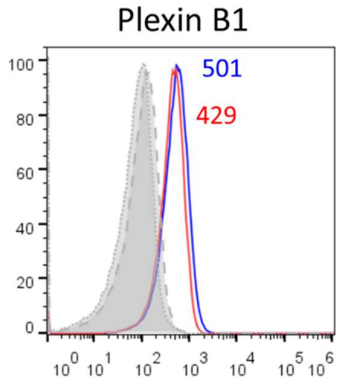

Figure 53 Expression profiles of surface Plexin B1 during VACV infection determined by FACS. HeLa cells were mock or infected with WT VACV at MOI 5 for 15 h. Cells were stained for surface expression of the indicated protein and the corresponding MFI is indicated next to the histogram curves, VACV-infected cells (red), mock cells (blue). Matching isotype Igg controls were used for mock (dotted line) and infected cells (dashed line). This data is representative of at least two independent experiments.

4.4.1 Refined analysis for classical HLA-I surface expression

HLA-I heavy chains associate with β2m to form an MHC-I complex. This complex is loaded with intracellular peptides and transported to the cell surface. The surface expression of a peptide bound to an MHC complex can be recognised by NK and T cell receptors. Both HLAs and T/NK cell receptors are highly polymorphic. Their expression correlates with disease outcomes, notably from viral infections such as HIV, HCV and HPV (reviewed in (Rajagopalan & Long 2005)). The high polymorphism of classical HLA-I (HLA-A, B, C) makes it difficult to assign HLA-derived peptides to the corresponding HLAs by mass spectrometry. Therefore, the PMP and WCL data for HLAs expression needed to be manually checked to ensure a correct assignment of the peptides to their corresponding HLAs.

To refine the temporal expression profile of surface HLA-I during VACV infection, the sequences of the raw peptides initially assigned to HLAs in the PMP/WCL screens were checked against the reference sequences of HLAs expressed by HFFF cells (HLA-A11:01, -A24:02, -B35:02 (Bw6), -B40:02 (Bw6), -C02:02 (C2), and -C04:01 (C2), -E, -F, -G (van der Ploeg *et al.* 2017). Only the peptides that were matching with one HLA chain type (A, B, C) were kept and used to generate 'cleaned-up profiles'.

Cleaned-up profiles for the PMP and the WCL datasets both showed that VACV infection caused mild downregulation of HLA-A and –B, and substantial downregulation of HLA-C (Figure 54). No peptides for HLA-E, F, G were detected in the PMP dataset which was expected because HLA-F is mostly intracellular, HLA-G is mostly expressed in the trophoblast, and HLA-E is expressed at low levels at the surface of most cells.

Flow cytometry validation for individual HLA-I surface expression is difficult because of the poor specificity of anti-HLA Abs. However, FACS staining of VACV-infected HFFF-TERTs with pan MHC-I, HLA-4E (HLA-B and -A) and DT9 mAbs (HLA-C and cross-reactivity with -E), support our proteomic data (Figure 55). Attempts with the anti-HLA-E Ab 3D12 did not show staining above control background on HFFF-TERT cells and therefore did not enable the level of HLA-E during VACV infection to be determined. These data support the fact that VACV might selectively down-regulate HLA-C surface expression.

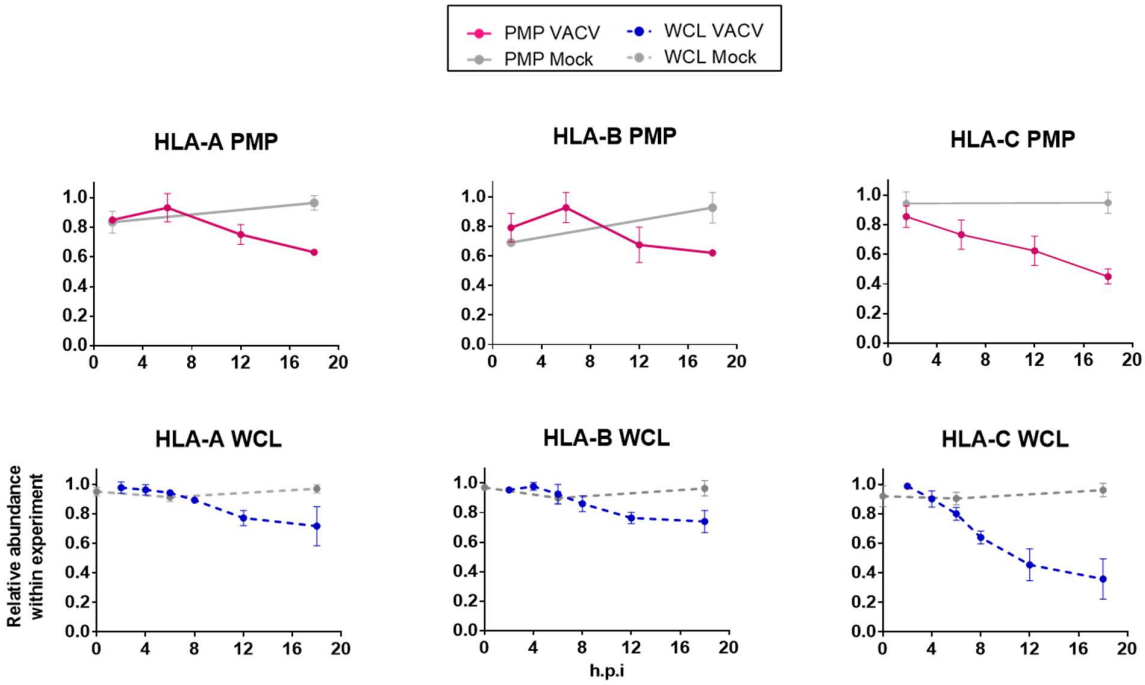

Figure 54 HLA cleaned-up temporal expression profiles during VACV infection at the cell surface (PMP) and whole-cell (WCL). HFFF-TERT cells were mock or VACV-infected at MOI 5 for the indicated time course. PM protein abundance was quantified by PMP screen. Whole-cell protein expression (WCL) data were extracted from (Soday et al., 2019). The sequences of the raw peptides initially assigned to HLAs in the PMP/WCL were manually checked against the reference sequences of HLAs that are expressed by HFFFs to ensure correct assignment. The temporal expression profile of the indicated proteins within each screen is shown. Data from the PMP (full line) and WCL (dotted line) for mock samples (grey), and VACV-infected sample (pink for PMP and blue for WCL) is shown. Error bars represent ± SD within independent PMP screens duplicates, and independent WCL screens triplicates.

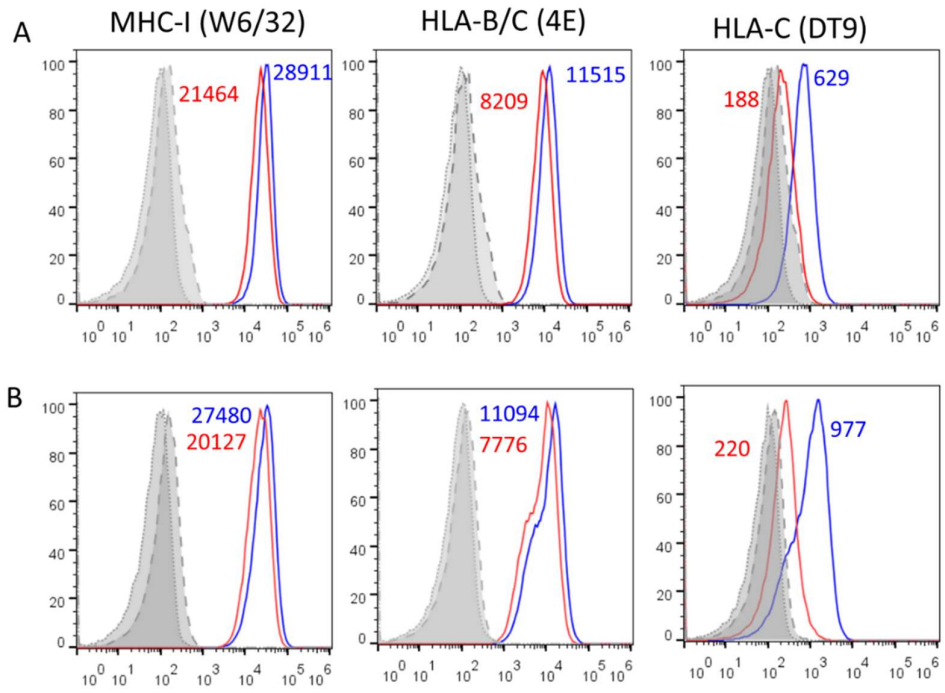

Figure 55 HLA-I surface expression during VACV infection determined by FACS. HFFF-TERTs (A) or HeLa cells (B) were mock or infected with WT VACV at MOI 5 for 15 h. Cells were stained for surface expression of the indicated protein and the corresponding MFI is indicated next to the histogram curves, VACV-infected cells (red), mock cells (blue). Matching isotype controls were used for mock (dotted line) and infected cells (dashed line). This data is representative of at least three independent experiments.

4.4.2 Search for putative NK ligands modulated during VACV infection

The NK field is relatively new and expanding, consequently, additional host proteins may be unknown NK ligands. To search for those, we took advantage of a common feature of known NK ligands. Most of the known NK ligands typically belong to one of the following families: cadherin, collagen, MHC, immunoglobulin, C-type lectin or TNF receptor (Vivier *et al.* 2008).

To search for new putative NK ligands, functional domain annotation from the InterPro database (Hunter *et al.* 2012; Weekes *et al.* 2014) were added to the PM proteins that were changed in abundance by more than 2-fold during viral infection. Results showed six upregulated (Table 12) and 20 downregulated (Table 13). host surface proteins with a functional domain typically found amongst known NK ligands. Some of these proteins were already described as NK ligands (COLEC12, nectin1, TNFSFR10D) and were expected to be found by this analysis. Among the downregulated proteins, the protocadherins stood out since multiple members of this family were downregulated, suggesting that VACV targets their expression. A similar analysis on the upregulated proteins did not highlight any group or family of proteins as being upregulated following VACV infection.

Table 12 Mining for putative NK ligands amongst proteins upregulated by>2 fold during VACV infection at the PM of infected cells

Uniprot ID	Gene Symbol	Protein Name	Mining Functional Domain	Known role as NK ligand
Q9NP84	TNFRSF12A	Tumour necrosis factor receptor superfamily member 12A	TNF	Binds to secreted TWEAK and leads to mild induction of apoptosis. Major role in NF-κB signalling (reviewed in Winkles et al., 2008)
Q9UBN6	TNFRSF10D	Tumour necrosis factor receptor superfamily member 10D	TNF	Decoy for TRAIL, evasion of apoptosis (Degli-Esposti *et al.* 1997a)
Q30201	HFE	Hereditary hemochromatosis protein	MHC, Ig	Tested; does not influence NK cell cytotoxicity (Pascolo *et al.* 2005)
Q5KU26	COLEC12	Collectin-12	Collagen, C-type lectin	Binds to inhibitory receptor PILRα (Sun *et al.* 2012)
O60449	LY75	Lymphocyte antigen 75	C-type lectin	None
P20908	COL5A1	Collagen α-1 (V) chain	Collagen	None

Table 13 Mining for putative NK ligands amongst proteins downregulated by > 2 fold at the PM of VACV-infected cells

Uniprot ID	Gene symbol	Protein name	Mining Functional Domain	Known role as NK ligand
O00300	TNFRSF11B	Tumour necrosis factor receptor superfamily member 11B	TNF	Inhibits osteoclastogenesis, could also be a decoy for TRAIL cytotoxicity (Emery *et al.* 1998; Liu *et al.* 2015)
P10721	KIT	Mast/stem cell growth factor receptor Kit	Immunoglobulin	None
Q06418	TYRO3	Tyrosine-protein kinase receptor TYRO3	Immunoglobulin	NK development (Caraux *et al.* 2006)
Q15262	PTPRK	Receptor-type tyrosine-protein phosphatase kappa	Immunoglobulin	None
Q13332	PTPRS	Receptor-type tyrosine-protein phosphatase S	Immunoglobulin	None
P30530	AXL	Tyrosine-protein kinase receptor UFO	Immunoglobulin	NK development (Caraux *et al.* 2006)
P11362	FGFR1	Fibroblast growth factor receptor 1	Immunoglobulin	Ligand for CD56, leads differentiation into cytotoxic NK cells (Chan et al., 2007)
Q15223	NECTIN1	Nectin-1	Immunoglobulin	Activating ligand for TACTILE (CD96) (Holmes *et al.* 2019; Seth *et al.* 2007)
P16234	PDGFRA	Platelet-derived growth factor receptor alpha	Immunoglobulin	None
Q9BRK3	MXRA8-2	Matrix-remodelling-associated protein 8	Immunoglobulin	None

P17948	FLT1 (VEGFR-1)	Vascular endothelial growth factor receptor 1	Immunoglobulin	None
Q9BRK3	MXRA8-2	Matrix-remodelling-associated protein 8	Immunoglobulin	None
O75326	SEMA7A	Semaphorin-7A	Immunoglobulin	Binds plexin C1, possibly involved in NK cell cytotoxicity (Lieu et al., 2010)
Q9HCU0	CD248	Endosialin	C-type lectin	None
O94985	CLSTN1	Calsyntenin-1	Cadherin	None
Q9Y5G7	PCDHGA6	Protocadherin gamma-A6	Cadherin	None
Q9UN70	PCDHGC3	Protocadherin gamma-C3	Cadherin	None
Q9Y5G0	PCDHGB5	Protocadherin gamma-B5	Cadherin	None
Q9Y5H3	PCDHGA10	Protocadherin gamma-A10	Cadherin	None
P55285	CDH6	Cadherin-6	Cadherin	Adhesion

4.4.3 Insight into the mechanistic modulation of NK ligands

To interpret our data further and understand the mechanism behind the changes observed at the PM (e.g. protein re-localisation to the PM, intracellular trapping, enhanced intracellular recycling, prevention of protein synthesis or proteasomal degradation), the PMP dataset was overlaid with the WCL dataset (Soday *et al.* 2019). Further, the expression of NK ligands was analysed in the samples treated with the proteasome inhibitor MG132.

Most proteins showed similar temporal expression profiles in the PMP and WCL datasets. Interestingly, some NK ligands showed a temporal expression profile that differed between the WCL and PMP datasets. Consequently, the overlaid PM/WCL profile of such proteins can reveal insights regarding the mechanism leading to their modulation.

During VACV infection, three NK ligands presented a temporal profile that differed substantially between the PMP and WCL datasets.

First, VIM was stably expressed at the total cell level, whilst it was substantially and gradually upregulated at the cell surface from 6 h onwards (Figure 48 B). Those temporal profiles analysed in

parallel suggest that VIM cell surface upregulation is due to the re-localisation of VIM to the cell surface from an intracellular pool.

Second, the COLEC12 temporal profile showed a gradual increase at the cell surface from 6 h onwards, whilst the total level gradually decreased (Figure 52 B). Taken together, these expression profiles suggest that during VACV infection, an intracellular pool of COLEC12 is being transported to the cell membrane and secreted.

Third, TNFRSF12A showed a mild upregulation at 3-8 h.p.i. followed by stable expression in the WCL dataset, whilst its surface expression gradually and substantially increased. This profile suggests that TNFSRF12A is produced between 3-8 h.p.i. and then gradually transported to the cell surface and secreted (Figure 50).

Cellular proteins can be degraded by two major pathways: the proteasome-ubiquitin or lysosomal proteolysis pathway. MG132 is an inhibitor of the proteasome and was added in a mock and a WT-VACV infected samples in our PMP screen to identify protein whose virus-induced downregulation is proteasome dependent.

An MG132 rescue ratio was calculated for proteins know to be NK ligands and whose expression was modulated during VACV infection. This ratio was calculated by comparing the protein abundance during VACV infection ± MG132 with the protein abundance during mock infection ± MG132. This ratio enabled the identification of NK ligands that are downregulated at the PM during VACV infection in a proteasome-dependent manner.

Table 14 NK ligands whose VACV-induced downregulation can be rescued by addition of MG132.

Host protein	PM1 rescue ratio	PM2 rescue ratio
Nectin1	3.211152	2.922048
LTBR	1.79626	1.194303

Results showed that LTBR and nectin1 were rescued by addition of MG132 by an average of 3 and 1.5-fold, respectively (Table 14). MG132 addition did not substantially rescued other previously discussed NK ligands. This implies that downregulation of other NK ligands during VACV relay on another pathway, such as lysosomal degradation, or that their protein synthesis is stopped upon VACV infection and their downregulation results from the natural half-life of the protein.

Together, these data suggest that VACV has evolved various strategies to modulate the expression of surface host proteins likely to impact on the interplay with NK cells.

4.5 Study of VACV proteins expressed at the host cell surface

Given the high number of proteins encoded by VACV and the limited availability of mAbs against VACV proteins, there is currently no extensive record of VACV proteins that are expressed at the surface of the infected cell. Identifying these proteins was one of the main objectives of this study. The results are presented hereafter.

4.5.1 Likelihood of VACV proteins to be expressed at the PM

Initial analysis showed that 49 viral proteins were detected in both PMP duplicates. To distinguish the viral proteins that are likely to be expressed at the PM during VACV infection from putative contaminants, we could not rely on the PM annotations for VACV proteins. Indeed, there is a poor annotation of VACV protein localisation in databases because studies of VACV surface proteins have been limited by the lack of reagents and the high number of VACV-encoded protein.

Consequently, to identify VACV surface proteins with high confidence, we took advantage of the host proteins and their much more reliable GO annotations to draw a cut-off value. This value is based on the ratio of the number peptides detected (peptide count) for a given protein during the PMP screen, versus the number of peptides detected for the same protein during the WCL screen. Such ratio was calculated for all the proteins detected in both PMP experiments.

These proteins were further separated into two groups, those with PM annotations and those without. Within those two groups, the number of proteins whose peptide count ratio falls within each 0.5 unit (Y-axis) was plotted (Figure 56). Figure 57 showed that the cut-off value where the proteins detected in the PMP screen are likely to be expressed at the PM (where pink bars are higher than grey bars) is situated between 0 and -1. By applying a cut-off value of 0, 95.7 % of the proteins that were detected in the PMP screen had a GO-annotation for PMP and are therefore high confidence hits.

Applying this cut-off value to all viral proteins detected in the PMP screens, we isolated 20 viral proteins whose peptide count ratio was greater than -1 (Figure 57). Such proteins are likely to be expressed at the PM with very high confidence. To have a better representation of each viral protein, the two components of the ratio (average peptide count in the PMP and average peptide count in the WCL) were plotted for each viral protein detected in the PMP screen (Figure 58). In figure 59, the cut-off value, as determined earlier, is represented by a dotted line and separates the viral proteins that are likely to be expressed at the PM (right of the axis) from the others (left of the axis).

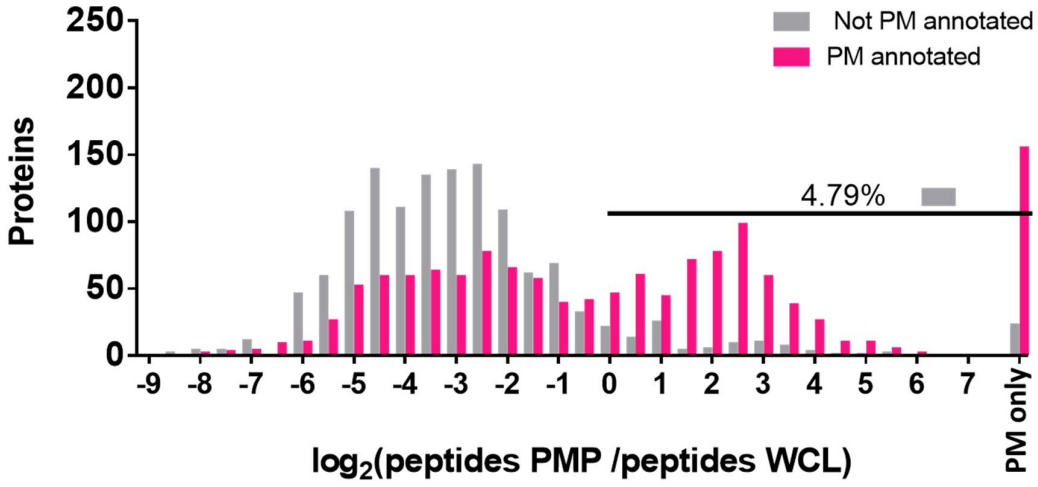

Figure 56 Definition of a cut-off value for the peptide count ratio (PMP/WCL) of all GO-annotated proteins quantified in PMP screens, corresponding to PM expression likelihood. HFFF-TERT cells were mock or VACV-infected at MOI 5, as described in Figure 42, and PM protein abundance was quantified by PMP screen. Whole-cell protein expression (WCL) data were extracted from (Soday et al., 2019). For each protein detected in the PMP screens, the corresponding peptide count (given by LC-MS3) detected in the PMP screens (duplicate) and WCL screens (triplicate) were isolated to calculate a ratio (average peptide count PMP/ average peptide count WCL). The histogram represents the number of proteins detected in the PMP screens falling in each 0.5 unit of the log_2 of the peptide count ratio. Proteins were separated according to their GO-annotations, pink bars represent proteins with a GO annotation for PM (PM, cell surface, extracellular or short GO) and grey bars represent proteins without PM GO-annotation. "PM only" represents proteins quantified only in the PMP screens but not in the WCL screens. The horizontal bar indicates that the proteins detected in the PMP without a GO PM annotation with a log_2 ratio greater to 0 represent 4.79 % of all host proteins quantified in the PMP experiments.

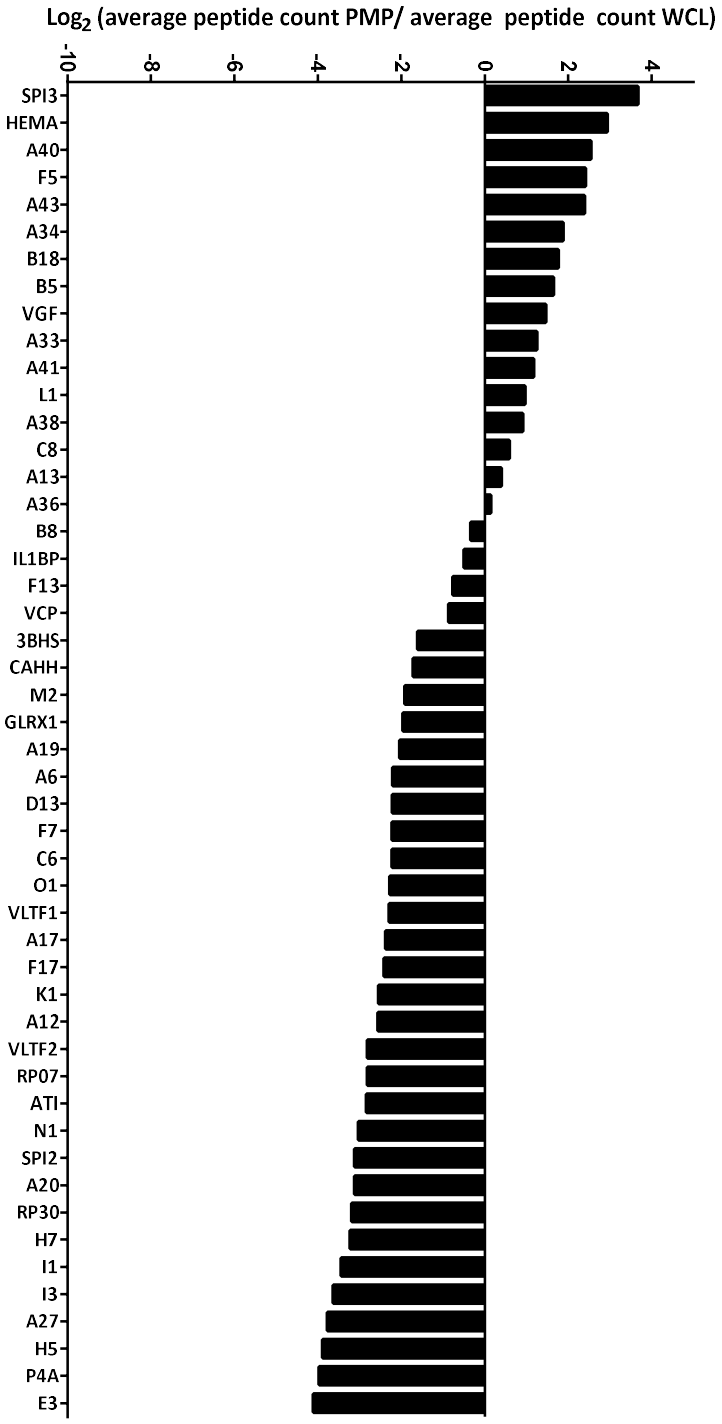

Figure 57 Histogram showing the VACV proteins quantified in the PMP screens and their respective "peptide count ratio". HFFF-TERT cells were infected with VACV WT at MOI5 as described in Figure 42, the surface protein abundance was analysed by PMP screen, and whole-cell protein abundance by WCL was extracted from (Soday et al., 2019). For each viral protein quantified in the PMP screens, the ratio of the average peptides count detected in the PMP versus the WCL is represented as log_2 on the Y-axis.

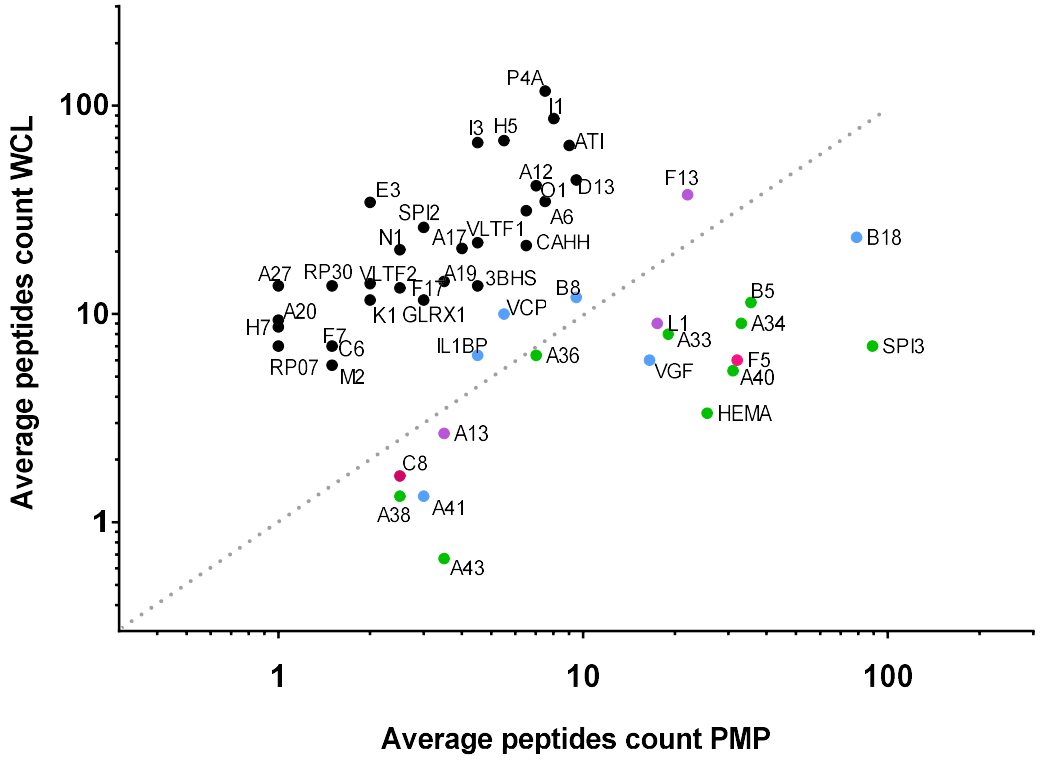

Figure 58 Graph representing the WCL and PMP average peptides count for VACV protein detected in both PMP screens. HFFF-TERT cells were mock or infected with VACV WT at MOI 5, as indicated in Figure 42. PM protein abundance was quantified by PMP screen, and whole-cell protein expression (WCL) data were extracted from (Soday et al., 2019). For each viral protein detected in the PMP screen, the average number of peptides detected in the PMP screens (X-axis), and the average peptide count detected for the same viral protein in the WCL screens (Y-axis), is shown. The dotted line corresponds to a peptide count ratio of 1, which represents the cut-off determined in Figure 57. For all viral proteins whose $\log_2$ (peptide count ratio) value is > -0.5, the colour indicates their location as described in the literature. Blue indicates secreted VACV proteins, green indicates VACV proteins known to be expressed at the plasma membrane, purple represents VACV proteins that are neither of the above and part of the IMV, and red represents proteins that are none of the above three categories.

Because we suspected that the viral proteins detected in the PMP screen could result from input virus, budding virions or disrupted virions, we included multiple controls in the PMP screens. One sample was infected with WT VACV for 90 min at 37 °C, to control for input viral proteins. We observed that all viral proteins detected in later time points were expressed at a much greater level suggesting that their detection in the latter did not result from contaminant from input virus (Figure 60).

Additionally, a sample was infected with WT VACV for 90 min at 4 °C to prevent virus entry and represent surface-bound virions-associated proteins. This sample showed that i) viral proteins had a much lower expression than at later time points, and ii) viral proteins were slightly more abundant than the sample incubated at for 90 min at 37 °C (data not shown). This suggests that virus proteins and virions in the inoculum were internalised after incubation at 37 °C.

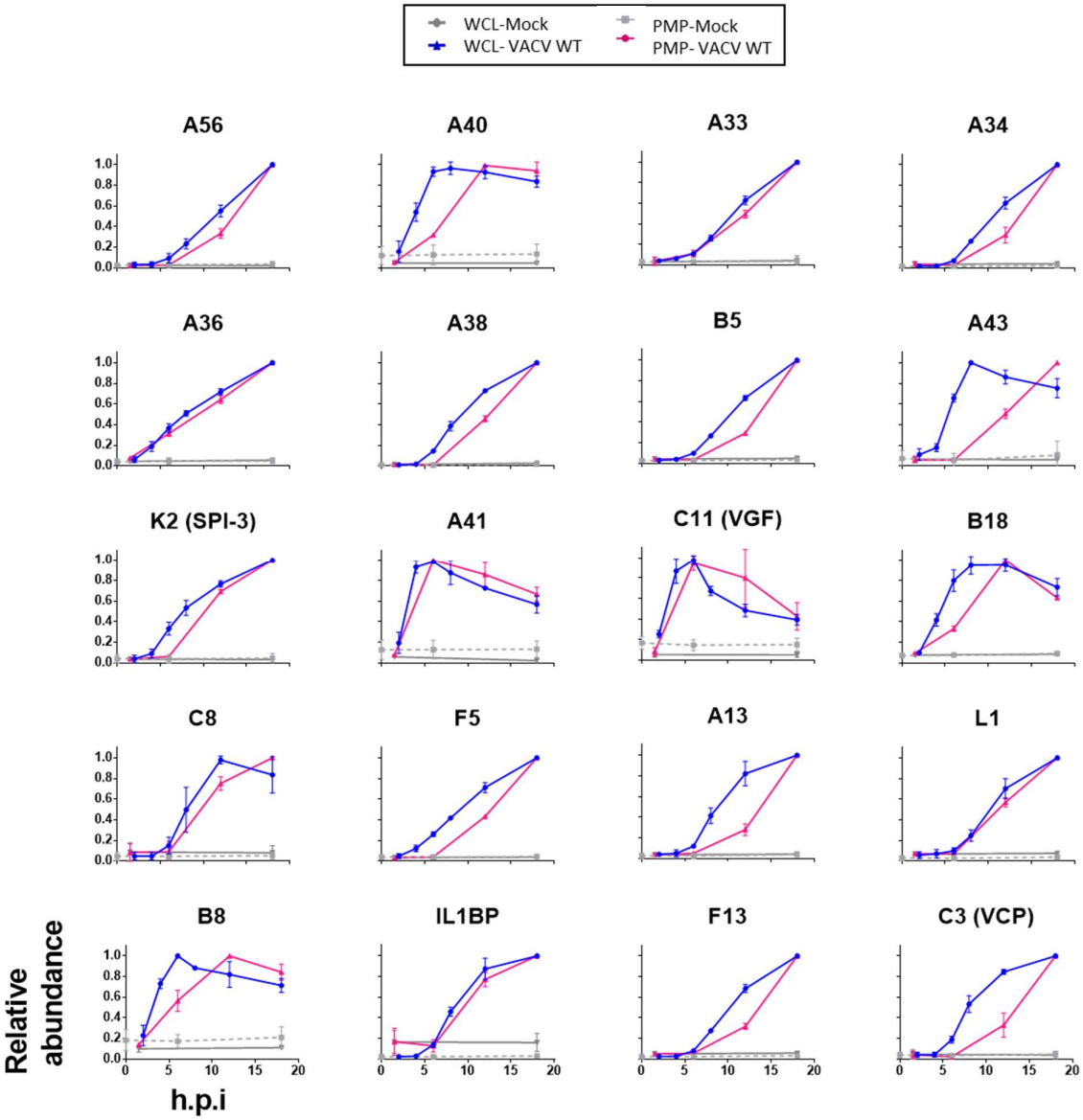

Figure 59 VACV proteins expressed at the PM as detected in the PMP screens. HFFF-TERT cells were mock or VACV-infected at MOI 5, as described in Figure 41. PM protein abundance was quantified by PMP screens. Whole-cell protein expression (WCL) data were extracted from (Soday et al., 2019). Viral proteins detected in the PMP screens were filtered based on their average peptide count ratio values (PMP/WCL), with the cut-off value determined in Figure 57. For each indicated viral protein, the average relative abundance within each screen (PMP or WCL) (Y-axis) is represented for the indicated time after infection (X-axis). Mock (grey) and VACV-infected samples (WCL in blue, PMP in pink). Data represent average (WCL triplicate, PMP duplicate) and error bars show t ± SD.

The PMP and WCL temporal profiles for the 20 high confidence VACV surface proteins were overlaid to get insight into their production and transport kinetics (Figure 59). A delay between the increased relative abundance at the total cell level and the cell surface was observed for proteins such as B8, VCP, A40, A43 and F13 (Figure 59). This may reflect the time needed for the transport of the protein to the cell surface. Besides, some known secreted proteins such as A41, VGF, B18 and B8, presented a peak followed by a diminution in the WCL dataset. This suggests that the viral protein is not produced in greater quantity but is transported to the cell surface to be secreted. Overall, Figure 59 shows that VACV surface proteins are produced at different times post-infection and gives insight into VACV life cycle and regulation of viral protein synthesis.

4.5.2 VACV surface proteins as candidate NK ligands

Since viral proteins are expressed at the cell surface, they are exposed to NK cells and could interact with their receptors. Hence, the mining strategy described earlier was applied to discover which VACV-surface proteins could potentially interact with NK cells. Analysis of the functional domains for the 20 VACV proteins found to be expressed at the PM showed that three VACV proteins possess a C-type lectin domain (A40, A33, A34), and three other possess and Ig-fold (A38, A56, F5) (Figure 60). Those viral proteins are candidates of choice for the study of VACV surface proteins with immune evasion functions, or for the study of VACV proteins that might be targets of cellular components of the immune system. One of those 6 proteins, A56, was chosen as a candidate NK ligand and its study is the object of the following results chapters of this thesis.

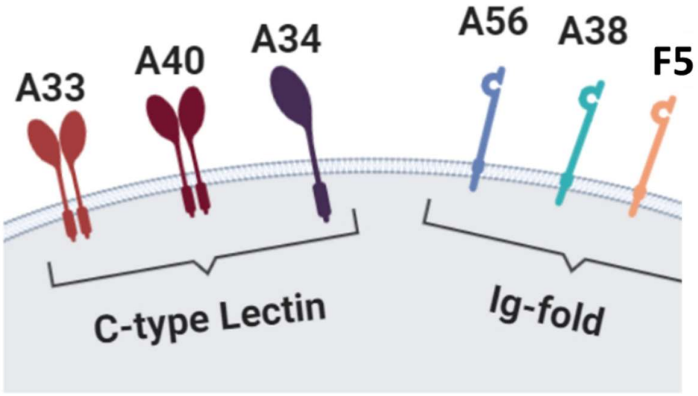

Figure 60 VACV surface proteins as described in the PMP screen with functional domains (here C-type lectin or Ig-fold) typically present in NK ligands. HFFF-TERT cells were mock or VACV-infected at MOI 5, PM protein abundance was quantified by PMP proteomics screen. The viral proteins detected at the PM as described in Figure 60 were analysed for the presence of a functional domain typically present in NK ligands (cadherin, collagen, MHC, C-type lectin, immunoglobulin, Ig, TNF).

4.6 Discussion: study of the host cell surface proteome during VACV infection

A proteomics-based screen was performed to get a comprehensive view of the changes occurring at the cell surface during VACV infection. The cell surface expression level of approximately 1100 human and 49 viral proteins was quantified over an infection time course. Even at late time p.i., a low number of host proteins were substantially modulated, suggesting selective manipulation and biological relevance. Further analysis showed that downregulated proteins were enriched in ephrins, protocadherins and tyrosine kinases. Interestingly, multiple members of these protein families are also substantially downregulated during HCMV infection (Weekes *et al.* 2014), suggesting that they might either trigger the immune response or act as viral restriction factors. Moreover, in recent studies, knockdown of protocadherin FAT1 in target cells led to decreased NK cell degranulation, therefore supporting the hypothesis that protocadherins might be NK cell activating ligands (Weekes *et al.* 2014). Further, Ephrin B2 was reported to co-stimulate T cells (Yu *et al.* 2003), which is relevant to NK cells, because many immune ligands engage both with T and NK cells, and suggests that ephrins might be targeted by viruses as an immune evasion strategy.

Amongst other heavily downregulated proteins, EGFR and IFNAR2 stood out. Targeting of IFNAR2 (receptor for type I IFNs), might be another strategy to add to the many that VACV uses to evade type I IFN response (Smith *et al.* 2018). Besides, EGFR, the receptor for epidermal growth factor, regulates many cellular processes (reviewed in (Wells 1999)) and is downregulated by multiple viruses, including HSV-1 and HCMV (Jafferji *et al.* 2009; Nakano *et al.* 2005; Weekes *et al.* 2014). However, VACV-mediated downregulation of EGFR might seem to contrast with a previous report suggesting that VACV hijacks EGFR signalling to promote its spread by enhancing cell motility via the binding of its own growth factor, VACV VGF (Beerli *et al.* 2018). A hypothesis to explain our data is that upon engagement with a ligand such as VGF, EGFR might be internalised, mediate cell motility and subsequently be degraded. A possible reason why EGFR is degraded rather than recycled to the cell surface might be to promote the binding of secreted VGF to surrounding cells that are not infected yet (and therefore express EGFR), to promote an optimal environment for VACV replication.

4.6.1 VACV infection impact on NK ligands expression

To identify how VACV affects NK ligands expression, the cell surface expression profile of 40 NK ligands was analysed. Interestingly, NKG2D ligands (MICA, MICB, ULBPs), were not upregulated following VACV infection while their expression is expected to be upregulated following stress such as viral infection (Raulet *et al.* 2013). This is in line with two previous studies, one reporting similar observations (Chisholm & Reyburn 2006), and the other suggesting that VACV E3, a dsRNA-binding protein, is key for the prevention of NKG2D ligands upregulation (Esteso *et al.* 2017). These data

suggest that VACV actively prevents NKG2D ligands upregulation, which constitutes an immune evasion strategy. This hypothesis is supported by the fact that NKG2D is a potent NK cell activating receptor and that preventing its activation is a common immune evasion strategy conserved among multiple viruses such as HCMV and HSV (Fielding *et al.* 2014, 2017; Reyburn *et al.* 2015). Similarly, B7-H6, a stress-induced ligand for the activating NKp30 receptor (Brandt *et al.* 2009; Matta *et al.* 2013), was not upregulated during VACV infection. Interestingly, B7-H6 is also targeted by HCMV (Fielding *et al.* 2017; Pignoloni *et al.* 2016), suggesting that its targeting might be a conserved immune evasion strategy also present in. Besides, MLL5, a ligand for the activating receptor NKp44 (Rajagopalan & Long 2013), was not upregulated during VACV infection but slightly downregulated. Interestingly, HIV Nef protein prevents MLL5 expression on infected CD4-T cells (Fausther-Bovendo *et al.* 2009), suggesting thatMLL5 might also be targeted by VACV to evade the NK cell response.

On the other hand, VIM, an activating ligand for NKp46, was upregulated at the PM during VACV infection, whilst its abundance was stable at the total cell level. This profile suggests that VIM is unlikely to be a 'stress ligand' but is rather re-localised to the PM during VACV infection. Garg and colleagues report that VIM is upregulated on the surface of human monocytes and macrophages following *Mycobacterium tuberculosis*-infected and enhances NK cell-mediated lysis (Garg *et al.* 2006). VIM upregulation at the surface of VACV-infected cells, would therefore be a disadvantage to the virus, which may seem paradoxical. However, the literature report that VIM is involved in the transport of adenovirus type 2 (Belin & Boulanger 1987) and that VIM interacts with VACV virions and facilitates their assembly (Risco *et al.* 2002). Taken together, those data suggest that VIM surface upregulation during VACV infection may result from the transport of virions to the cell surface and suggests that the immune system detect VACV-infected cells by the recognition of VIM.

Further, immune checkpoints were selectively modulated by VACV. Inhibitory checkpoints PD1-L1, PD-L2 and B7-H3 were stably expressed, which contrasts with PD-L1 upregulation during HCMV infection (Weekes *et al.* 2014). On the other hand, the activatory ICOS ligand was downregulated, which suggests a new strategy to evade NK cell response.

Another noteworthy result is the dramatic downregulation of nectin-1, a ligand for the CD96 receptor, also involved in cell-to-cell adhesion. Other related proteins such as poliovirus receptor (PVR, CD155), nectin-2 and nectin-3, for which multiple NKRs with opposite functions compete to form a regulatory system (Figure 61), remained largely unchanged. This suggests that nectin-1 is selectively targeted by VACV and contrasts with HCMV downregulation of nectin-2 and PVR (Prod'homme *et al.* 2010; Tomasec *et al.* 2005). Interestingly, nectin-1 was rescued by the addition of MG132, suggesting that its downregulation results from an active mechanism rather than protein natural turnover. Previous

studies report that nectin-1 overexpression increases NK-92 degranulation, suggesting that VACV-mediated nectin-1 downregulation might be an immune evasion strategy (Holmes *et al.* 2019). Interestingly, nectin-1 and related proteins are entry receptors for herpesviruses. For example, HSV-1 glycoprotein D binds nectin-1, which leads to its conformational change, triggers the viral fusion machinery, and leads to nectin-1 internalisation and low-pH dependent degradation (Stiles *et al.* 2008; Stiles & Krummenacher 2010). Moreover, HSV gD is reported to affect nectin-1 more globally through signalling, leading to its redistribution from the cellular junction (Bhargava *et al.* 2016). Together, HSV gD modulation of nectin-1 is thought to be a strategy to enhance viral spread by preventing superinfection and by disrupting cellular adherent junctions, which contributes to better dissemination. Importantly, VACV infection of K562 (which do not express nectin-1) is poor (unpublished data), which is in line with the hypothesis that nectin-1 could be used as an entry receptor for VACV. Together, these data suggest that VACV could downregulate nectin-1 to i) enhance its spread, ii) avoid CD96 activation, iii) enter the cells. Together, these hypotheses make of nectin-1 a very strong hit to be followed up.

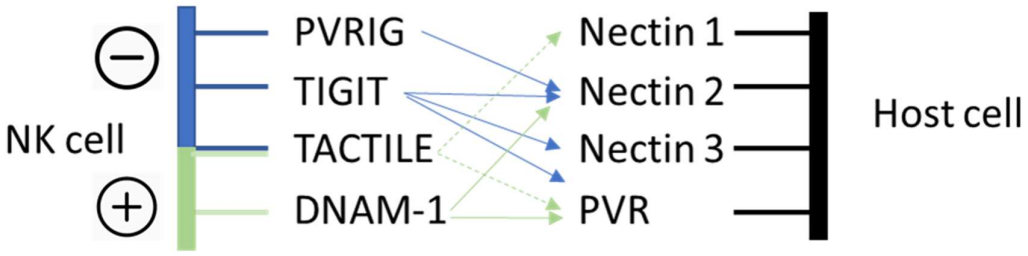

Figure 61 Nectins and PVR (CD155) host proteins interaction with NKRs, adapted from (Sanchez-Correa et al., 2019).

Another noteworthy change was COLEC12 total cell level downregulation while its surface expression gradually increased. This profile suggests that a pool of intracellular COLEC12 is transported to the cell surface, where a fraction might be secreted and another bind to the cell surface. Since COLEC12 is a binding partner of inhibitory receptor PILR-α (Sun *et al.* 2012), it suggests that its surface upregulation is a strategy by which VACV prevents NK cell activation.

Besides, analysis of molecules known to regulate lymphocyte-mediated apoptosis showed selective modulation during VACV infection. Downregulation of LTBR and TNFR1, as well as upregulation of TRAILR4 (TNFRSF10D), a decoy receptor for TRAIL, are likely to decrease sensitivity to apoptosis. Importantly, LTBR expression during VACV infection was rescued by the addition of the proteasome inhibitor MG132, suggesting that VACV has an active mechanism leading to LTBR degradation. Interestingly, the HCMV US12 family targets LTBR for degradation, suggesting that it might be a conserved immune evasion strategy. Conversely, upregulation of apoptosis inducer and NF-κB

activator TNFRSF12A, may sensitise the infected cell to lymphocyte-induced apoptosis. Expression levels of other surface proteins involved in apoptosis regulation, including FAS, TRAILR2, TRAILR3 and TNFR2 remained largely unchanged, suggesting that they do no influence susceptibility to VACV-infected cells. Together these data and the various apoptosis inhibitors encoded by VACV, highlight the importance of apoptosis evasion by VACV.

Another noteworthy result was the modest downregulation of HLA-A and -B, which is in line with the well-described VACV-specific T cell response, and the surprising dramatic downregulation of HLA-C. FACS analysis, in two different cell lines, indicated mild downregulation of total surface MHC-I and substantial downregulation of HLA-C, which is consistent, since HLA-A and -B account for the majority of total surface MHC-I. This is also in line with the literature, since it is well accepted that VACV leads to modest downregulation of surface MHC-I (Brooks *et al.* 2006; Chisholm & Reyburn 2006; Kirwan *et al.* 2006), and a previous study relying on transfection reports VACV-mediated substantial HLA-C downregulation (Kirwan *et al.* 2006). However, one report has shown substantial downregulation of MHC-I (HEK293 cells) (Kirwan *et al.* 2006). This discrepancy might reflect various experimental setting used or result from the differential expression of HLA allotypes by various cell lines and could highlight a stronger modulation of some allotypes by VACV. Further work is necessary to clarify whether VACV downregulates all HLA-C allotypes to a similar extent. A limitation of FACS surface staining data is the cross-reactivity of the anti-HLA-C mAb (DT9) with HLA-E, along with the fact that a study reports HLA-E downregulation during VACV infection in BCLC cells (Brooks *et al.* 2006). Thus, it could not be ruled out that HLA-E downregulation did not contribute to the observed phenotype for HLA-C by FACS. To clarify this, HFFF-TERTs cells were stained with anti-HLA-E mAbs MEM/02 and 3D12. No signal was observed, which is likely due to the very low abundance of HLA-E and is consistent with our proteomic data where HLA-E was not detected. This suggests that HLA-E is unlikely to have affected substantially our FACS data for HLA-C, and that VACV does not upregulate HLA-E surface expression which contrasts with HCMV (Tomasec *et al.* 2000).

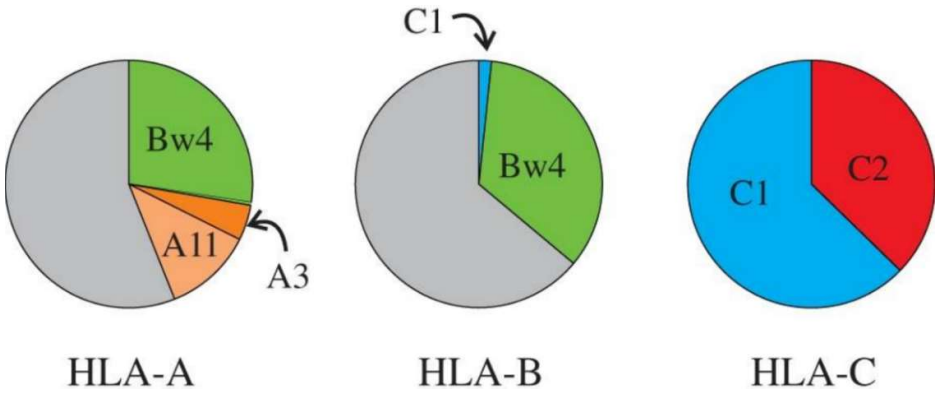

Figure 62 Pie charts representing the proportion of HLA- I allotypes that carry the epitopes A3, A11, Bw4, C1, C2, which allows their interactions with KIRs. Figure adapted from Parham et al., 2012.

Since HLA-C are all KIRs ligands while only a fraction of HLA-A -B have an epitope that allows such interaction (Figure 62) (Parham et al. 2012), our data suggests selective targeting of the NK cell response. A first hypothesis, to explain HLA-C downregulation is that it could prevent a HLA/KIR interaction restricted to a viral peptide. A second hypothesis is that it could lead to NK cell activation via a lack of KIR-mediated inhibitory signals and thus maintain an equilibrium between virulence and host survival, which ensure its transmission. Importantly, KIRs and HLA polymorphisms are linked to infectious disease outcome (reviewed in (Peter Parham & Guethlein, 2018)). If the selective modulation of HLA-C is conserved in other poxviruses such as VARV, this could have contributed to smallpox infection outcome. Given smallpox high mortality rate and prevalence through centuries, it raises the hypothesis that it may have imprinted the human MHC-I repertoire by leading to the selection of individuals with HLAs-KIRs combination favourable to the control of smallpox. The mechanism at the origin of HLA-C downregulation remains elusive. Our data indicates that it does not depend on a trapping mechanism or proteasomal degradation. Selective targeting of HLA-C could rely on lysosomal degradation or could occur at the mRNA level, HLA-C could be the target of a microRNA, similarly to what happens during HIV infection (Kulkarni *et al.* 2011). Alternatively, the cytoplasmic tail of HLA-C could be key for its selective downregulation and could be the target of a VACV protein, similarly to the laboratory-adapted HIV-1 strain Nef protein that selectively downregulates HLA-A and -B only by binding to a tyrosine motif in their cytoplasmic tails which is absent from HLA-C (Cohen *et al.* 1999; Williams *et al.* 2002). Lastly, VACV might disrupt a peptide loading pathway that is preferentially used by HLA-C, hence leading to its selective downregulation.

Further work is necessary to unravel whether VACV-mediated downregulation of HLA-C is restricted to a subset of HLA-C heavy chains, the mechanism by which the downregulation occurs, the functional impact of HLA-C downregulation on NK cell activation, and whether this is a conserved mechanism among orthopoxviruses.

In summary, the systematic analysis of changes in cell surface expression allowed to identify novel strategies by which VACV could manipulate the immune response or trigger an antiviral response. Although our analysis focuses on NK ligands modulation, our dataset can also be analysed to dissect T cell ligands modulation and others. A limitation to our study is the use of fibroblast cells which allowed comparison with previously published datasets but does not allow the detection of ligands typically expressed by other cells such as antigen-presenting or tumour cells. Hence, PMP studies could include different cell types in the future to comprehensively assess VACV modulation of the surface proteome in this context. Further, the consequences of the modulation of host proteins on the immune response remains to be determined. Noteworthy proteins to study further include HLA-C and nectin-1. Globally, our data inform host-pathogens interactions and of great interest to vaccine development and particularly VACV-based oncolytic virus therapy which design can benefit from VACV-induced immune ligands modulation.

4.6.2 VACV proteins expressed at the host PM

Aside from the surface expression of immune ligands, the PMP data allowed to establish, for the first time, a comprehensive list of VACV proteins expressed at the host PM. Our analyses revealed that 20 VACV proteins localise at the PM with high confidence. Out of those 20 proteins, 10 are reported in the literature as expressed at the host-cell surface; (VGF (C11) (Chang *et al.* 1988), A40 (Wilcock *et al.* 1999), A43 (Sood & Moss 2010), A36 (Parkinson & Smith 1994; Snetkov *et al.* 2016; van Eijl *et al.* 2000), SPI-3 (K2) (DeHaven *et al.* 2010), A33 (Roper *et al.* 1996), A34 (Duncan & Smith 1992), A38 (Parkinson *et al.* 1995), A56 (Ichihashi & Dales 1971), B5 (Engelstad *et al.* 1992; Isaacs *et al.* 1992), and five are reported as secreted and sometimes bound to the cell surface; VCP (Girgis *et al.* 2008), B18 (Alcami *et al.* 2000), A41 (Ng *et al.* 2001), IL-18 BP (Born *et al.* 2000) and B8 (Mossman *et al.* 1995). The robustness of our analysis is supported by the fact that all previously identified VACV proteins expressed at the cell surface were quantified in our assay.

In addition to established VACV surface proteins, five additional viral proteins were identified as potentially expressed at the PM by our filtering strategy. Among these, VACV proteins A13 and L1 are integral protein of the IMV membrane, and F13 is anchored onto the internal surface of the EEV external membrane (Hirt et al.; Jensen et al., 1996; Martin et al., 1997). Consequently, such proteins could have been quantified as a result of virion contamination. However, other viral proteins expressed at the IMV membrane (A9, A14, A26, A27, F9 and H3) or associated with the entry fusion

complex (A21, A28, G9, H2, J5, L5) (Resch, Hixson, Moore, Lipton, & Moss, 2007), were not quantified or did not qualify as high-confidence PM in our analysis. This suggests that L1, F13 or A13 are either expressed at the PM or very abundant and sticky. Alternatively, their PM expression could result from the interaction with another viral or host protein. For example, F13 interacts with A56 and B5, two other VACV PM proteins (Lorenzo, Sanchez-Puig, & Blasco, 2012; Oie, Shida, & Ichihashi, 1990). L1 is required for virus attachment and entry into the cell (Bisht *et al.* 2008), and interacts with the entry fusion complex. L1 might, therefore, be left at the PM after virion entry. A13 is required for virus assembly (Unger & Traktman 2004) but is not known to interact with other viral proteins. Thus far, our data does not suggest that the PM expression of these three viral proteins is highly likely and further characterisation of is required to determine whether A13, F13 and L1 are genuine PM proteins.

In addition to A13, F13 and L1, VACV proteins C8 and F5 were identified as putative PM proteins but are not part of the categories described above. Their likelihood to be expressed at the PM is supported by the fact that C8 and F5 are not detected in IMVs (Chung et al., 2006; Resch et al., 2007; Yoder et al., 2006) and have no known interaction with other VACV proteins (McCraith, Holtzman, Moss, & Fields, 2000). Our data complement a previous study suggesting that F5 is enriched at the PM in regions where cells are in contact with neighbouring cells (Dobson et al., 2014). Together with the fact that F5 has a transmembrane domain, these data strongly indicate that F5 is expressed at the PM. Regarding C8, there are no published data on its function or localisation, its sequence indicates the presence of a signal peptide, suggesting that C8 could be expressed at the PM as a precursor or bound to the PM after secretion rather than being a transmembrane protein. Interestingly, C8 sequence is found in many poxviruses such as horsepox, buffalopox, camelpox, rabbitpox, cowpox, skunkpox, rakoonpox, suggesting that it might have an important biological function. C8 may be involved in immune evasion or act as a virulence factor. Our data provides ground for future studies to characterise the role of C8 and F5 during VACV infection.

Taken together, the study of VACV proteins expressed at the PM is a useful resource for future studies with implications in vaccine design, as the viral proteins expressed at the cell surface are likely targets of the immune system. Implication might include therapeutics development since viral proteins are often the target of Abs. Moreover, this dataset constitutes a useful resource for the study of poxvirus biology and is an advancement for the field since, thus far, the literature reporting VACV surface proteins was fragmented in multiple studies, relying on different cell types, MOIs and time of infections and limited by the lack of specific mAbs.

5 Chapter 5: Study of VACV A56 and NKp46 in the context of VACV infection

In the previous chapter, we determined the modulation of VACV-induced host surface proteins and established a list of VACV proteins expressed at the host PM. This highlighted that six VACV proteins are putative NK ligands. Amongst them, VACV protein A56 stands out as the only VACV surface glycoprotein reported in the literature as being able to alter NK cell functions. Indeed, A56 enhances the binding of human and murine NCRs to VACV-infected cells and alters their signalling (Jarahian *et al.* 2011). Additionally, A56 is conserved amongst orthopoxviruses, and is a likely target for immune cells because of its abundant expression at the PM (section 1.6.2.3). Besides, the NKR NKp46, which is described to interact with VACV A56, is an activating receptor and is the only NCR conserved in both mice and humans. Importantly, NKp46 recognises influenza HA and is required for the control of influenza in mice (Gazit *et al.* 2006). Hence, we hypothesized that A56 and NKp46 could respectively be, the ligand and the receptor that trigger NK cell response during VACV infection, and could be involved in the control of VACV infection. We aimed to characterise the interaction of A56 and NKp46 *in vitro* and the impact of A56 and NKp46 on the immune response to VACV *in vivo*. The results of this study are presented in this chapter.

5.1 In vitro characterisation of a VACV deletion mutant for A56

To study VACV protein A56 and its possible impact on the NK cell response, but also more broadly on the immune response to VACV, three viruses were used: WT VACV (WR), a deletion mutant for A56 (ΔA56) and a revertant virus (RevA56) in which the *A56R* gene was reintroduced back into its natural locus. The deletion and Rev viruses for A56 were previously engineered by transient dominant selection by Geoffrey L. Smith (Sanderson *et al.* 1998). First, the genotype of these three viruses was verified by polymerase chain reaction (PCR) designed to allow for size-based amplicon discrimination (Figure 63). Data showed that amplicon size for ΔA56 corresponded to the absence of the *A56R* gene whilst the WT and Rev viruses amplicons corresponded to the full-size *A56R*. Further, the expression of A56 protein by these three viruses was studied by immunoblot following infection of BSC-1 cells. Data showed the absence of A56 protein in cells infected with ΔA56 virus whilst the WT and RevA56

viruses expressed the A56 protein at around 85 kDa, as expected when analysed by SDS-PAGE and immunoblotting (Shida & Dales 1981) (Figure 64).

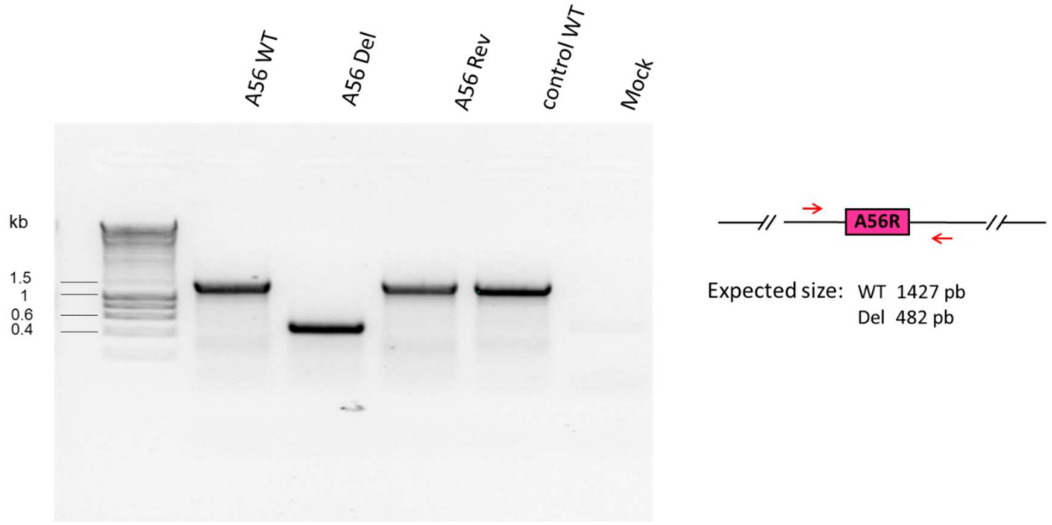

Figure 63 Genotyping of WT, Rev A56 and single deletion A56 viruses by amplicon-size based discriminative PCR. BSC-1 cells were infected with 1µl sucrose purified VACV overnight. Cells were lysed, and the lysate used to perform a PCR with primers designed in the flanking regions of A56R gene (right panel), allowing for amplicon size-based discrimination. PCR products were run on an agarose gel and separated by electrophoresis and imaged with Gel doc XR (Bio-Rad).

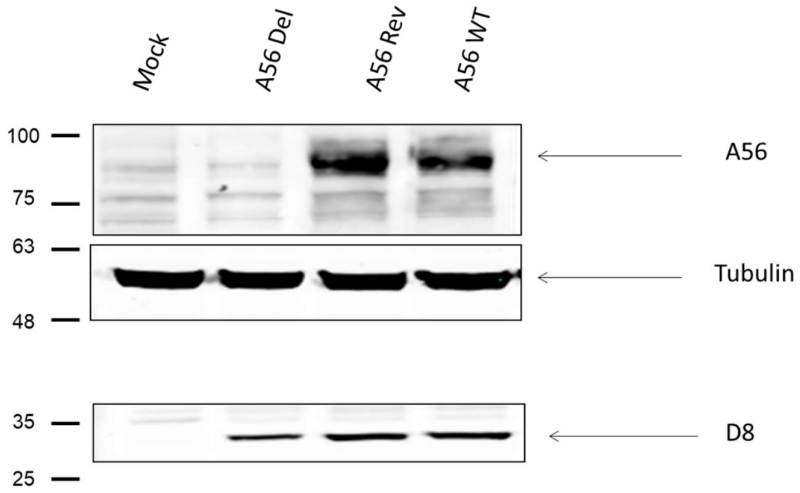

Figure 64 Study of VACV A56 protein expression in WT, Rev A56 and single deletion A56 viruses by immunoblotting. Monolayers of BSC-1 cells were infected overnight at MOI 10 with the indicated viruses. Cell lysates were analysed by immunoblotting with Abs against VACV proteins A56 (anti-A56 mAb from Shida and Dales., 1981), D8 (mAb AB1.1 Parkinson & Smith 1994) and alpha-tubulin. The position of molecular mass markers is shown on the left and expressed in kDa.

Next, the phenotype associated with the deletion of A56 was confirmed by studying the morphology of infected cells. As expected, cells infected with ΔA56 formed syncytia, whilst cells infected with RevA56 or WT VACV did not (Figure 65).

Further, the effect of A56 deletion on the plaque size resulting from CPE in the infected cell monolayer was studied. Deletion of A56 did not impact the plaque size in comparison to RevA56 and WTA56 (Figure 66), indicating that deletion of A56 does not affect the spread of the virus in culture.

Since the plaque size is not impacted by levels of CEV but enveloped virus are important for infecting neighbour cells (Blasco & Moss 1992), we tested whether A56 affected the release of EV by comet assay. The head of the comet being the initial plaque, and the tail resulting from secondary plaques (Appleyard *et al.* 1971). As a positive control, we used the international Health Department-J (IHD-J) virus that releases a higher amount of EEV in comparison to WT VACV and leads to the formation of comet-shaped plaques if incubated under a liquid overlay. A56 did not influence the formation of comets in comparison to WT and RevA56 viruses (Figure 67) indicating that A56 deletion does not impact the level of EV released from the infected cell.

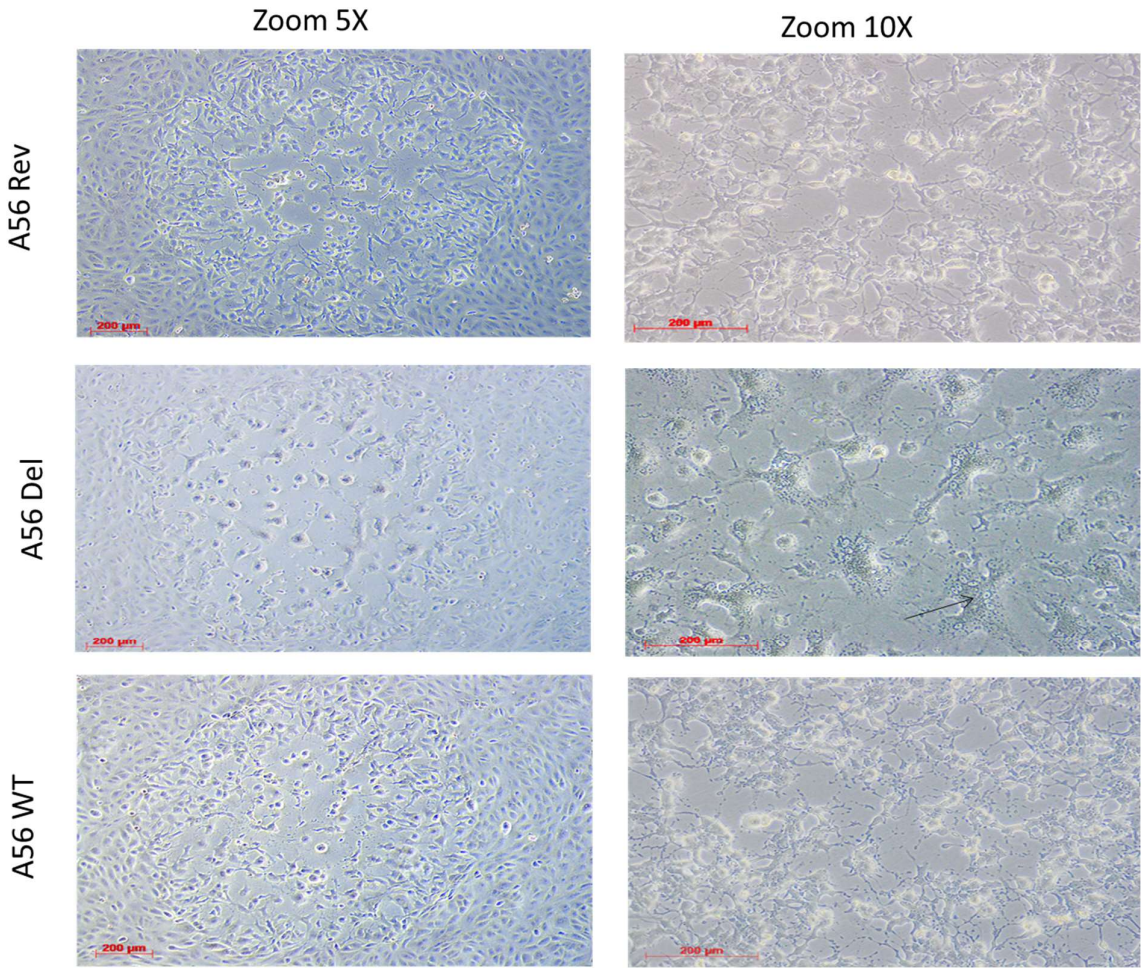

Figure 65 Plaque morphology of cells infected with WT, Rev A56 and single deletion A56 viruses. BSC1 monolayers were infected with the indicated virus at low MOI for 48 h under semi-liquid overlay. Plaque images were acquired using a Zeiss Axiovert 200 M microscope and the Axiovision 4.6 software with 5X magnification for the left panel or 10X magnification for the right panel. The arrow indicates a syncytium resulting from cell fusion.

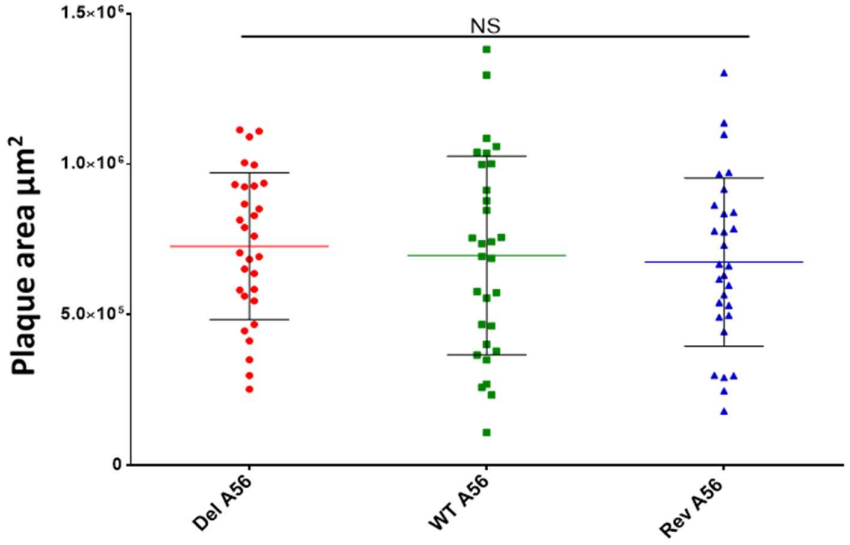

Figure 66 Plaque size after infection with WT, Rev A56 or single deletion A56 viruses. Monolayers of BSC-1 cells were infected with the indicated virus for 48 h. The surface area of >30 plaques was measured for each virus using a Zeiss Axiovert 200 M microscope and the Axiovision 4.6 software. Each measurement is represented as well as the mean and ±SD. Statistical significance was calculated using a Mann Whitney test (alpha 0.05). Statistical significance was defined as p<0.05. Data are representative of three independent experiments.

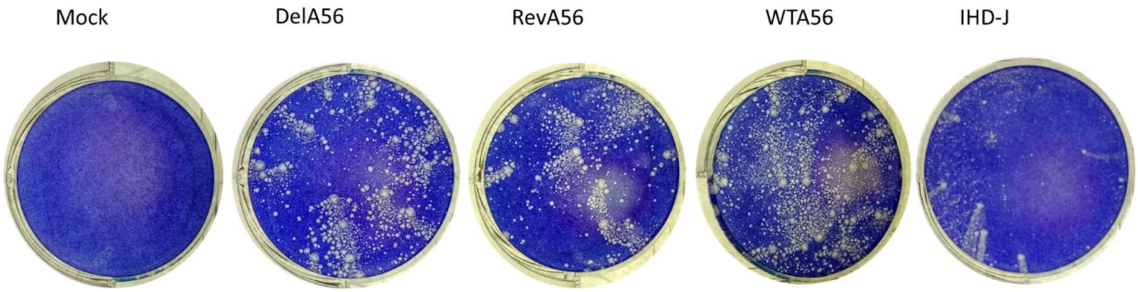

Figure 67 Comet formation after infection with WT, Rev A56 and single deletion A56 viruses infection. Monolayers of BSC-1 cells were infected with the indicated virus for 48 h under liquid overlay. Cells were stained with crystal violet and photographed. VACV IHD-J was used as a positive control for comet formation. Data are representative of three independent experiments.

5.2 Deletion of A56 influences the cytotoxic response of NK cells

Next, we studied the effect of A56 deletion on the cytotoxic response of murine NK cells primed with VACV using an *ex vivo* cytotoxic assay. Target cells were infected with WT, ΔA56, ΔA40 or mock-infected, labelled with ^{51}Cr and were co-incubated with murine NK cells isolated from WT VACV-immunised mice. The cytotoxicity of NK cells towards target cells was measured via ^{51}Cr release. Data showed that deletion of either A40 or A56 led to a significantly lower cytotoxicity of NK cells towards infected target cells in comparison to WT VACV(Figure 68). To control for equal infection, lysates of infected cells were analysed by immunoblotting using Abs against VACV structural protein D8. Equal loading of samples was analysed in parallel with Ab against *α*-tubulin. Data showed that the infection of target cells was equal amongst the three viruses, indicating that proteins A40 and A56 each affect the susceptibility of VACV-infected targets to VACV-primed NK cells.

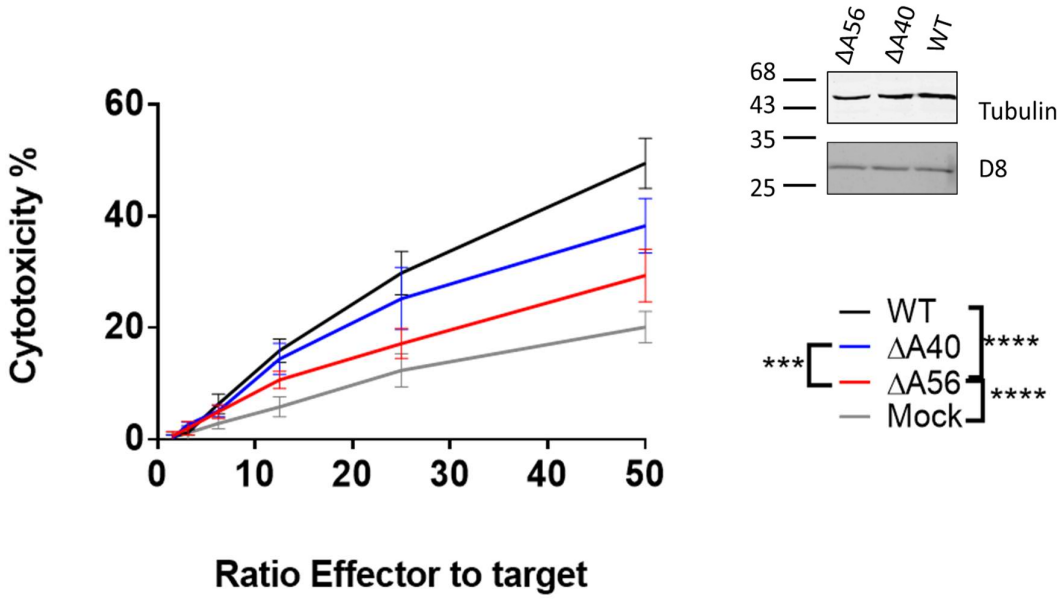

*Figure 68 Specific lysis of cells infected with WT, ΔA40, ΔA56 VACV viruses by VACV-primed NK cells. B6 mice were i.d. infected with 10^4 pfu/ear with VACV WT. One month p.i., splenic NK cells were purified and incubated at the indicated ratio for 4 h with ^{51}Cr-labelled P815 target cells that had been infected at MOI 10 for 10 h with the indicated viruses. The mean of 10 measurements of ^{51}Cr release is represented with ± SD. Statistical significance was determined by ANOVA2 (alpha 0.05), p<0.05 *, p<0.01 **, p<0.001***. Immunoblotting for VACV D8 and tubulin was performed on a fraction of the target cells used for the ^{51}Cr release assay. The positions of molecular mass marker are shown on the left (kDa) of the immunoblot. Data are representative of two independent experiments. This experiment was performed by Dr Hongwei Ren.*

After performing the cytotoxic assays described above, equipment failures prevented further cytotoxic chromium release assays to be performed. Due to the costs, hazards and organisational challenges related to working with radioactive material, efforts were invested in setting up of a non-radioactive cytotoxic assay.

First, a FACS-based degranulation assay was attempted to assess the cytotoxicity of murine NK cells towards target cells. Target cells typically used in degranulation assays such as YAC1, RMA-S and P815 cells were infected with WT VACV expressing GFP under a late VACV promoter to test how well VACV can infect these cells. YAC-1 and RMAS were poorly infected even at high MOI (10) for prolonged periods (18 h), which led to the choice of P815 cells as targets (Figure 69). The degranulation assay was set up using PMA/I (a potent T and NK cell activator) as a stimulant. However, when working with target cells, conclusive data were not obtained (data not shown). Technical difficulties with the yield of NK cells acquired during FACS analysis were encountered, and these were attributed to the duration of the experimental procedure which might have compromised NK cell viability.

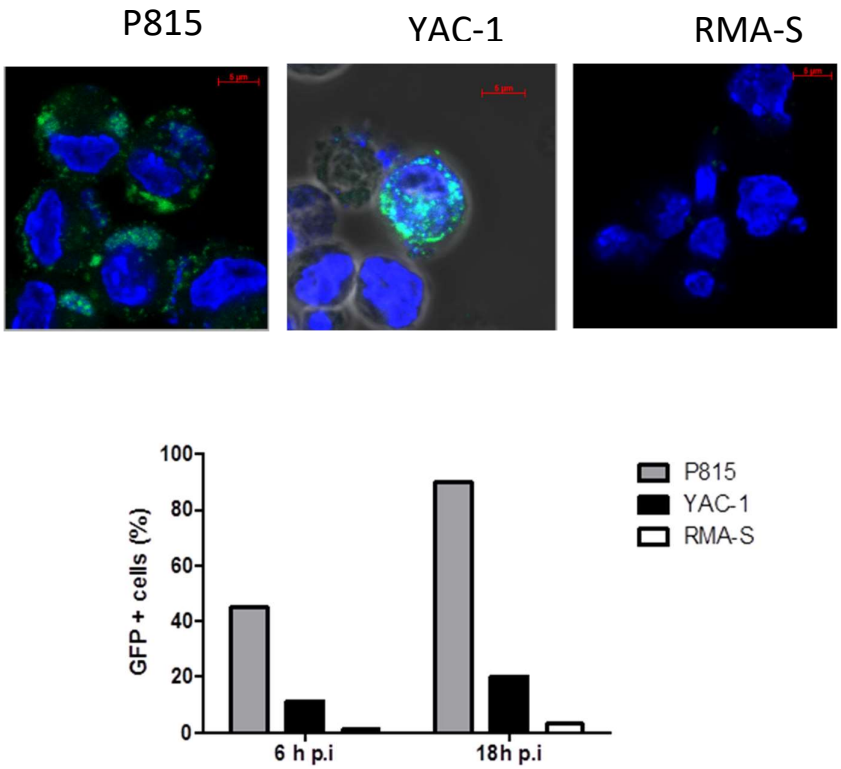

Figure 69 Infectivity by VACV of cell lines commonly used as targets in cytotoxic assays. YAC-1, RMA-S and P815 were infected with VACV expressing GFP at MOI 5, and GFP signal was measured at indicated times p.i.. Cells were stained with DAPI and imaged at 18 h.p.i. by confocal microscopy. The percentage of infected cells (expressing GFP) was analysed by FACS and is represented on the histogram at 6 and 18 h.p.i. for the indicated cell lines.

To reduce the time between sacrificing the mice and the acquisition of data, we attempted to set up a LDH assay. This assay is based on the quantification of the activity of the LDH that is released into the culture supernatant upon cell death. Despite successful training of the LDH assay with T cells in a collaborator's laboratory, conclusive data with NK cells were not obtained (data not shown). A highly variable signal was encountered, which we attributed to the fact that LDH activity is temperature-dependent and potential signal related to NK cells death LDH release.

In a third approach, we designed a murine splenocyte co-incubation assay, which is typically used to assess the cytotoxic response of CD8+ T cells. In this assay, single-cell suspensions of murine splenocytes were prepared, half of which were infected with VACV and served as target cells, whilst the other half served as effector cells (Figure 70). This method has the advantage of being an autologous system. It is, therefore, more physiologically relevant than cytotoxic assays that rely on the use of cancer cell lines or MHC-I negative cells. VACV-immunised mice were used, and a clear response of CD8+ T cells was observed as measured by higher degranulation and intracellular IFNγ production for CD8+ T cells incubated with VACV-infected splenocytes in comparison to uninfected cells (Figure 71). Enhanced degranulation of NK cells incubated with VACV-infected splenocytes in comparison to mock was also observed, however, the yield of NK cells acquired by FACS was too low to draw robust conclusions and suggested problems with NK cell viability. Further optimisations were undertaken but did not lead to improved outcomes. These technical difficulties prevented further functional cytotoxic assay to be performed.

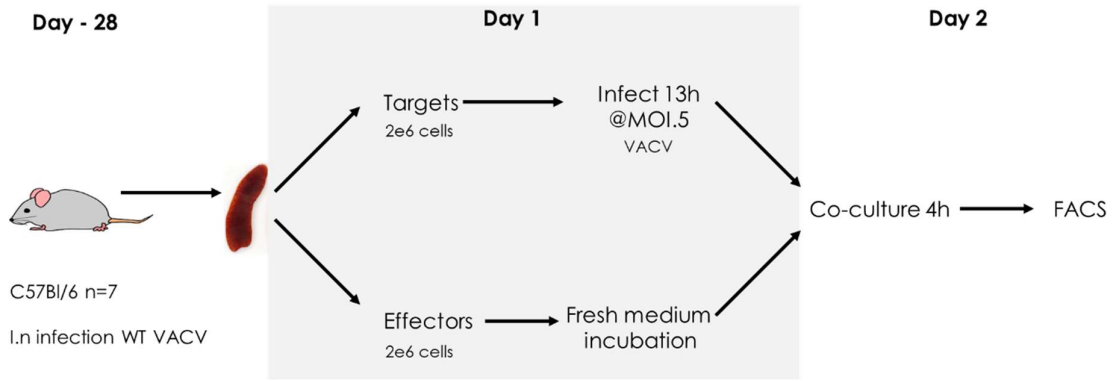

Figure 70 Schematic representing a splenocyte co-incubation assay. Spleens were collected from a group of B6 mice which have been mock or VACV-infected a month earlier. Spleens were converted into a single cell suspension, half of which was infected at the indicated MOI and for the specified time (target), whilst the other half was incubated in fresh medium (effectors). Targets and effectors were then incubated at ratio 1:1 for 4 h and then phenotyped by FACS.

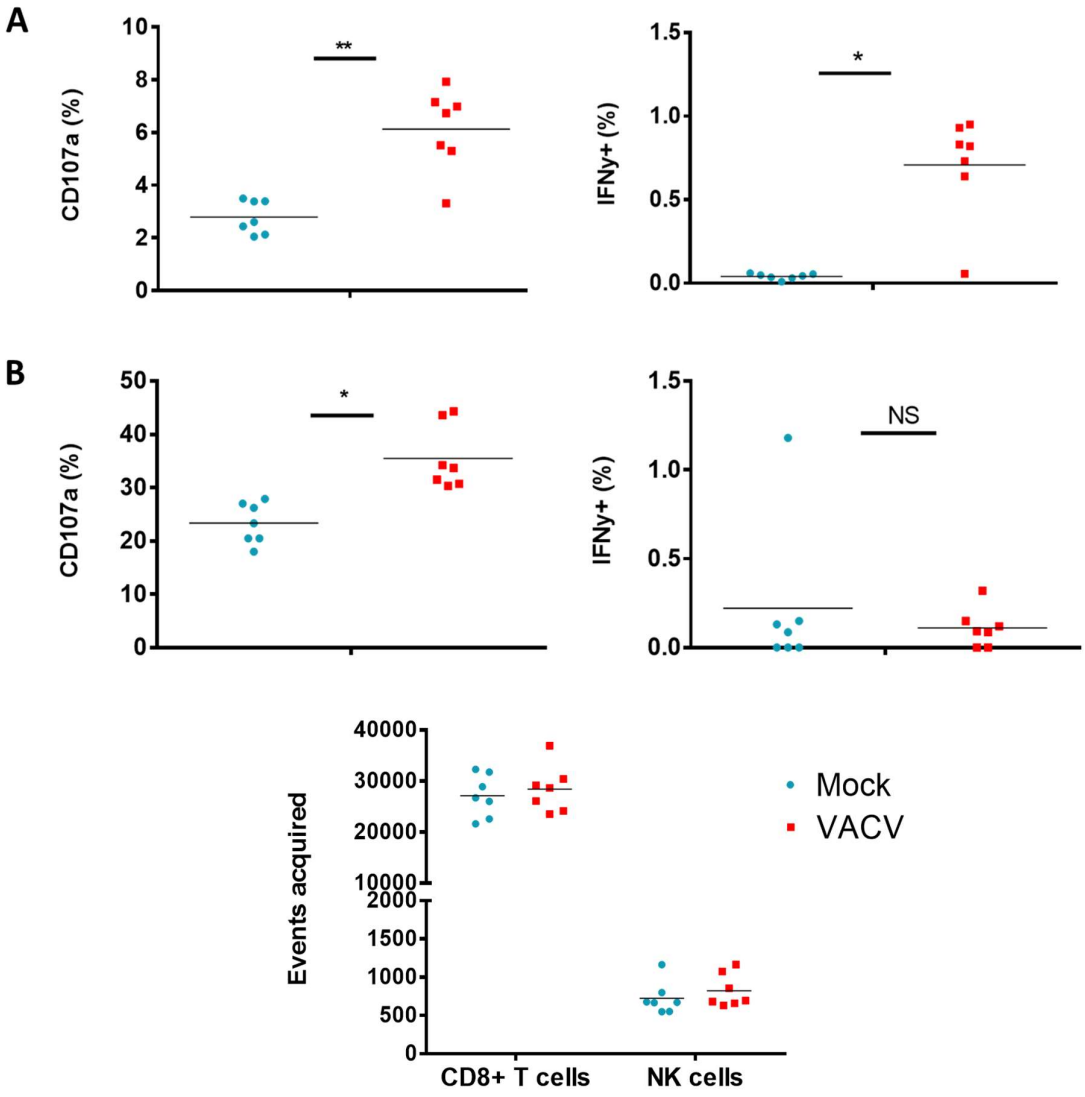

*Figure 71 Splenocytes co-incubation assay optimisation. Group B6 mice (n=7) were sacrificed a month post immunisation with VACV. Spleens were collected, and a single cell suspension prepared. A portion of these cells were mock or VACV-infected for 13 h at MOI 3 and served as autologous targets. The other portion of splenocytes were used as effectors and co-incubated with targets at ratio 1:1 for 4 h. Cell surface expression of CD107a and intracellular IFN-y was measured for CD8+ T cells (A) and NK cell (B). The number of events acquired within the same sample for CD8+ T cells and NK cells is shown (C). Statistical significance was measured by Wilcoxon test, p<0.05 *, p<0.01**, p<0.001***, NS unless otherwise indicated.*

5.3 Deletion of A56 influences the binding of soluble NKR to VACV-infected cells

In addition to cytotoxic assay optimisation, the contribution of A56 to the binding of soluble NKRs to VACV-infected cells was investigated for NKp30, NKp44, hNKp46 (human NKp46), mNKp46 (murine NKp46) and NKG2D. For this purpose, soluble chimeric Ig-NKRs were used (previously produced by Dr Kafai Leung from reagents kindly gifted by Dr Ofer Mandelboim).

First, to validate the functional qualities of these soluble receptors, their ability to bind to influenza-infected cells was assessed. Substantial binding of NKp44, hNKp46 and mNKp46 to influenza-infected cells was observed, as expected from the literature (Arnon *et al.* 2001) (Figure 72). Next, the binding of these soluble chimeric Ig-NCRs to VACV WT/ΔA56/mock-infected was tested in HFFF-TERTS and HeLa cells. In HFFF-TERTS, binding of NKp44, NKp30, hNKp46 and mNKp46 (but not NKG2D) to WT VACV-infected cells was observed (Figure 73), which is in line with previous observations made by Chisolm and colleagues (Chisholm & Reyburn 2006).

Our data also showed that in the absence of A56, the binding of such soluble receptors was much reduced in comparison to the binding observed to WT VACV-infected cells, suggesting that VACV A56 is required for efficient NCR binding to VACV-infected cells (Figure 74). In HeLa cells, the binding of NKG2D and NKp30 to uninfected cells was high, which is expected since HeLa cells constitutively express ligands for these receptors (Matta *et al.* 2013; Warren *et al.* 2005). Infection with WT VACV and ΔA56 led to a slight decrease in binding of NKG2D and NKp30 (Figure 74). NKp44, hNKp46 and mNKp46 binding to WT VACV-infected HeLa cells increased in comparison to uninfected cells. This binding was reduced in the absence of A56, suggesting that A56 contributes to the binding of soluble NCRs (NKp30, NKp44, hNKp46and mNKp46) (Figure 74).

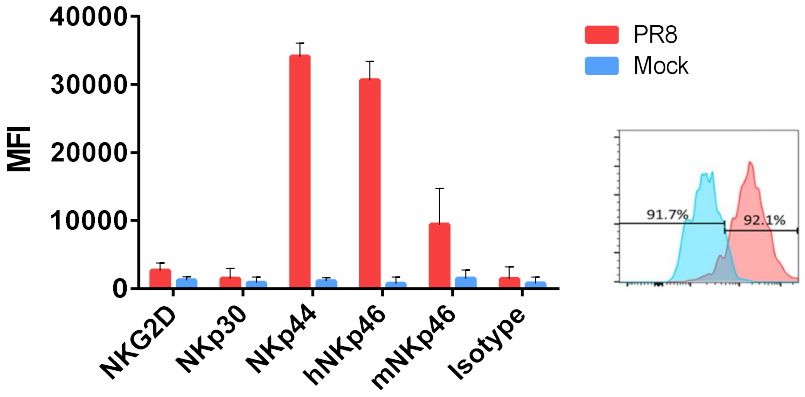

Figure 72 Validation of the binding capacity of the indicate soluble NCRs to influenza-infected cells. A549 cells were infected with influenza A/Puerto Rico/8/34 H1N1 (PR8) at MOI 5 for 14 h. Cells were incubated with 5 µg of the indicated soluble chimeric Ig receptor and then stained by FACS. The Y-axis represents the MFI of the indicated fusion protein. Infection level was monitored by surface staining with anti-HA H1N1 flu PR8 (clone 9B3.2) against influenza HA, and the percentage of infected cells is shown on the FACS histogram.

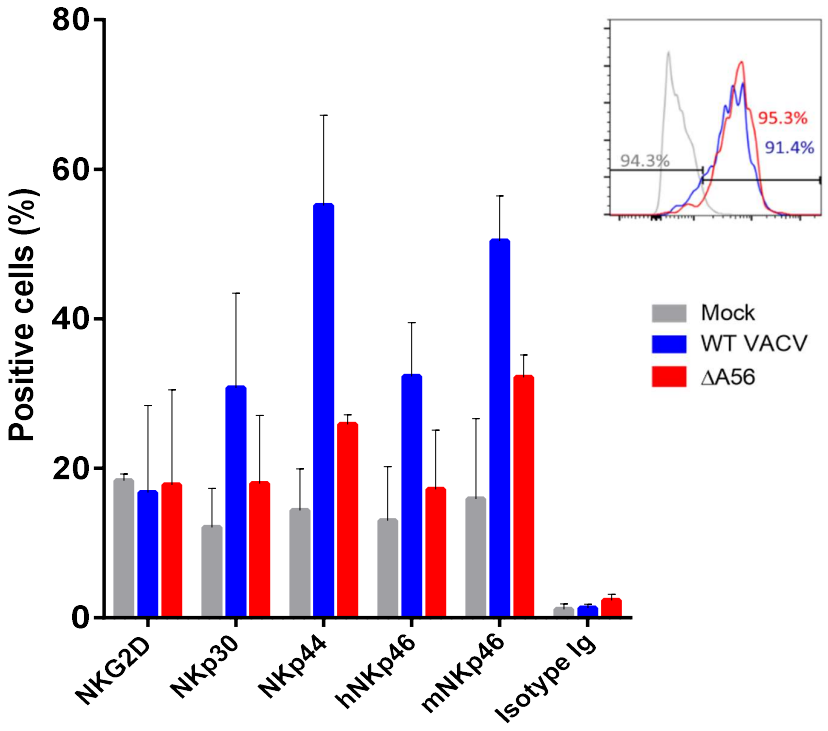

Figure 73 Binding of soluble chimeric Ig-NKRs to HFFF-TERTs cells infected with WT VACV, ΔA56 or mock. HFFF-TERTs cells were infected with the indicated virus at MOI 5 for 14 h and incubated with 5 µg of the indicated soluble chimeric Ig-NKRs. Binding of the soluble NKR to the cell surface was studied by FACS. Data shows the average of two independent experiments, error bars represent ±SD. Infection levels were monitored by intracellular staining for VACV protein D8. The percentage of infected cells is shown on the FACS histogram.

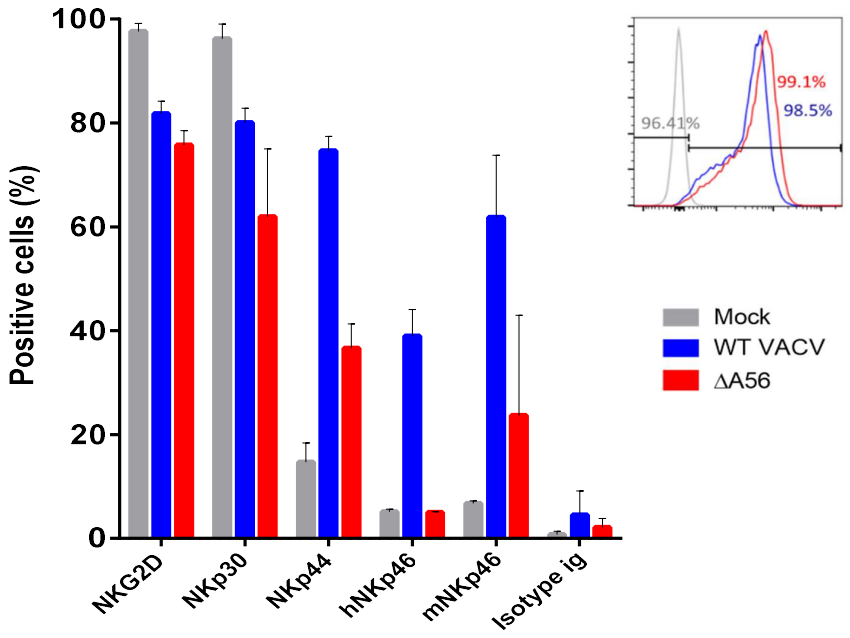

Figure 74 Binding of soluble chimeric Ig-NK receptors to HeLa cells infected with WT VACV, ΔA56 or mock. HeLa cells were infected with the indicated virus at MOI 5 for 14 h and incubated with 5 µg of the indicated soluble chimeric Ig- NKRs. Binding of the soluble NKR to the cell surface was studied by FACS. Data shows the average of 2 independent experiments and error bars represent SD. Infection levels were monitored by intracellular staining for VACV protein D8. The percentage of infected cells is shown on the FACS histogram.

5.4 Deletion of A56 influences the expression of other surface proteins

To clarify whether the phenotype associated with ΔA56 in the NKRs binding assay and NK cell cytotoxic assay is due to the PM expression of A56 itself or the presence of another PM protein whose expression is affected by A56, we compared the surface proteome of cells infected with ΔA56 and WT VACV. As a parallel interest, infection with ΔA38 was also performed. Data showed that the absence of A56 led to greatly reduced expression of K2 and VCP at the PM in comparison to infection with WT VACV (Figure 75A). This result was expected since A56 is known to anchor K2 and VCP at the PM (DeHaven *et al.* 2010, 2011; Girgis *et al.* 2008).

Interestingly, the expression of 5 other proteins was altered in the absence of A56 (Figure 75A). Analysis of the expression profile for those proteins (Figure 76) showed that differential expression in the absence of A56 is likely to be due to the high degree of variation in their expression profile, except for FGB (Fibrinogen beta chain). Only two peptides corresponding to FGB were quantified in each PM duplicate suggesting a low abundance, which makes expression profile validation by FACS difficult and

also increases the likelihood of a false positive hit (because quantification is less robust with low numbers of peptides).

Data acquired with ΔA38 served as a technical control for ΔA56 to estimate the noise signal that can be expected when a deletion mutant is compared to WT VACV. These data showed, as expected, the downregulation of A38 (Figure 75B) and highlighted that cell surface A13 protein was also downregulated in the absence of A38.

Proteins whose expression in the absence of A56 was altered by more than ± 2 FC in comparison to WT VACV, were analysed individually. This did not reveal a robust hit nor alteration of any protein known to interact with NK cells (Table 15). Together, these data suggest that the phenotype described earlier is likely to be due to the PM expression of A56 itself or its known binding partners K2 and VCP but not the altered expression of other host or viral proteins at the PM.

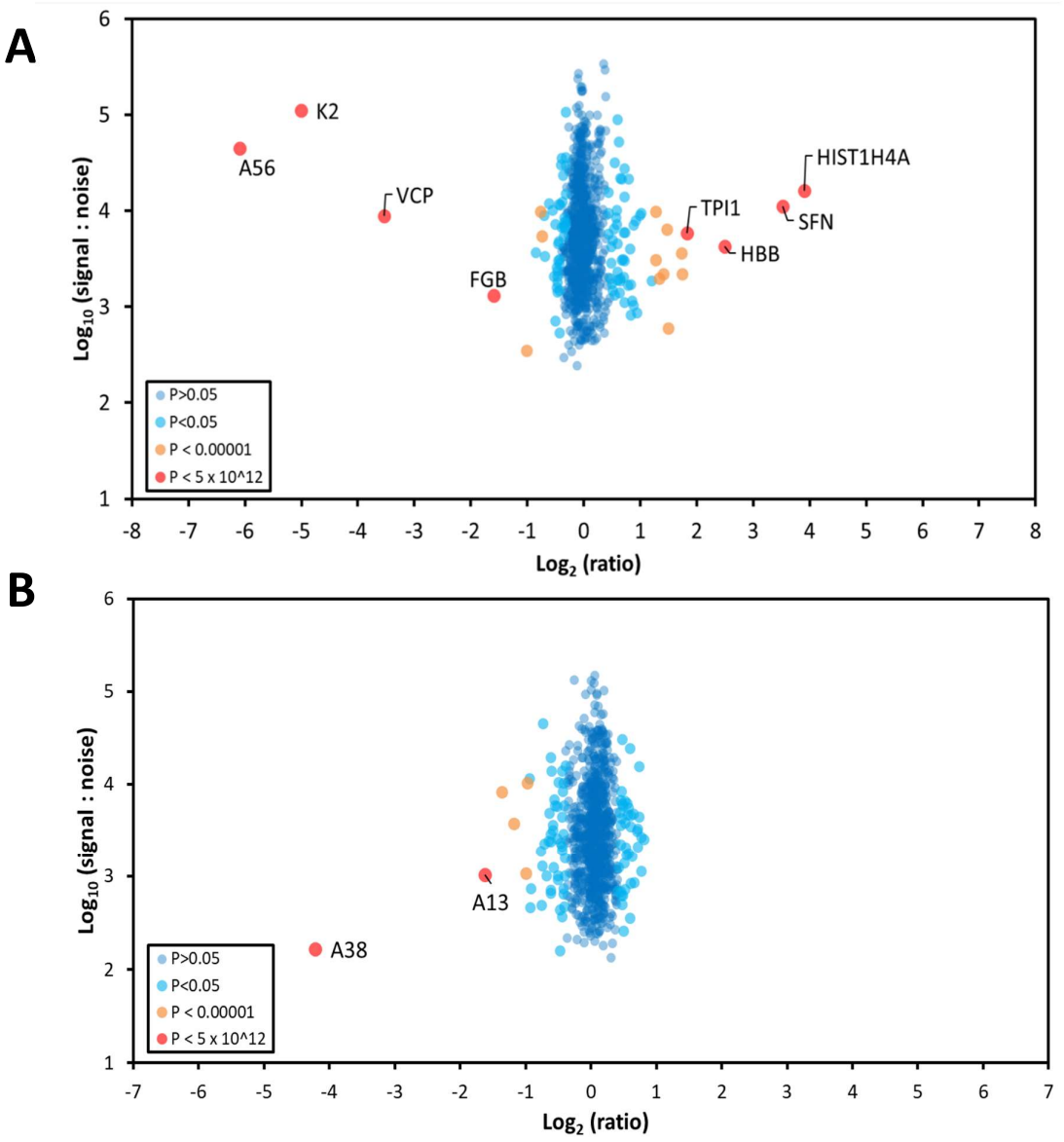

Figure 75 Dot plot representing the differential expression of PM proteins in HFFF-TERTs cells infected with VACV ΔA56 or ΔA38, in comparison to WT VACV. HFFF-TERTs cells were infected at MOI 5 with WT, ΔA56, ΔA38 for 18 h and the relative abundance of PM proteins studied in a PMP screen. The scatter plots show proteins quantified by at least two peptides in the PMP screen. FC of protein abundance is expressed as a ratio (deletion mutant vs WT VACV) and shown on the X-axis, expressed as log_2. The intensity with which proteins were quantified by mass spectrometry (also called signal: noise) is shown on the Y-axis, expressed as log_{10}. Proteins unaltered by the deletion of A56 or A38 are located at the centre of the plots, whereas proteins to the left or right of the centre of the graph represent proteins down- or upregulated by the A56 or A38 deletion. Significance A was used to estimate p values as described in (Cox et al., 2009).

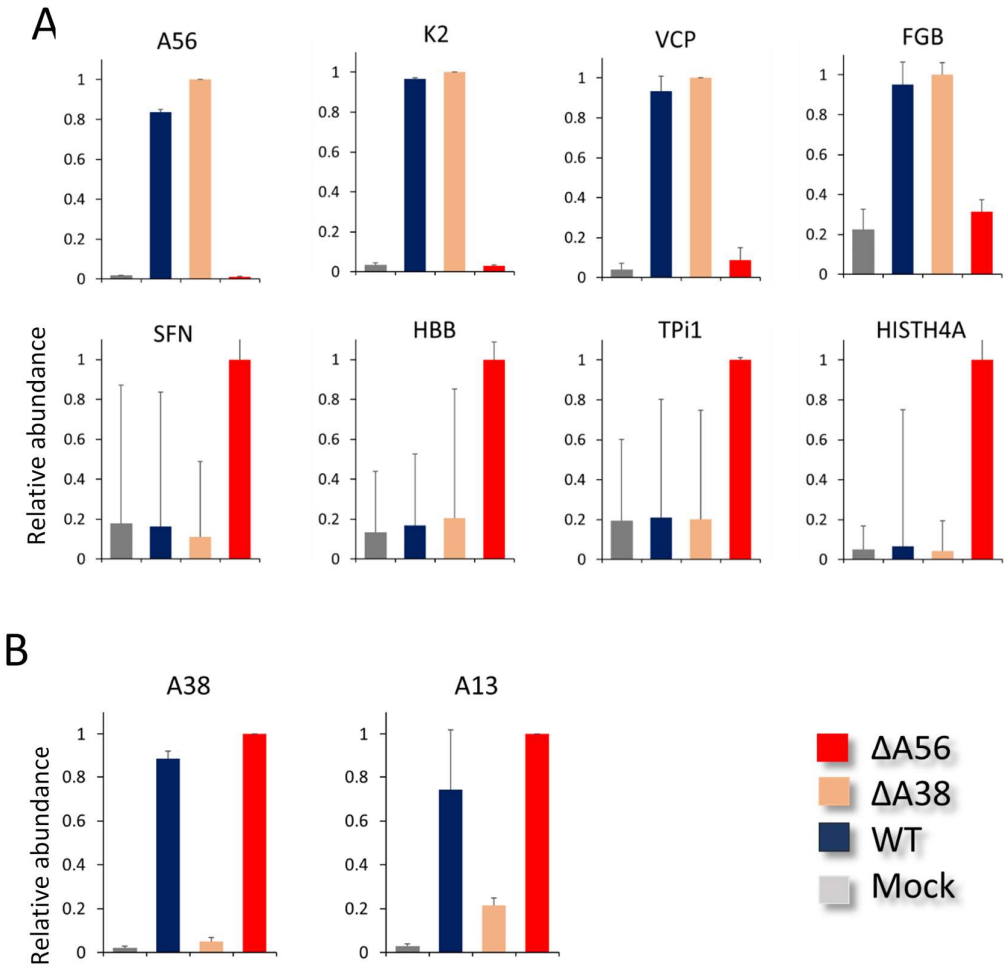

Figure 76 Relative abundance of PM proteins whose expression is altered during VACV infection, in the absence of A56 or A38 in comparison to WT VACV. HFFF-TERTs cells were infected at MOI 5 with the indicated viruses for 18 h. The relative abundance of PM proteins was assessed in a PMP screen, and proteins whose expression is modulated in the absence of A56 (A) or A38 (B) in comparison to WT VACV is shown (from Figure 75). The X-axis represents the average relative abundance of the indicated proteins. The error bars represent ± SD of two independent experiments.

Table 15 NK ligands mining in PM proteins whose expression is modulated (>± 2 FC) in the absence of A56 in comparison to WT VACV.

Uniprot	Gene Symbol	Description	Species	Average FC ΔA56 vs WT 18h	NK ligand similarity
Q01218	A56	Protein A56	VACV	0.01462	Yes
P18384	K2	Protein K2	VACV	0.031111	No
P68638	C3	Complement control protein C3	VACV	0.086466	No
P02675	FGB	Fibrinogen beta	HUMAN	0.331117	No
Q12866	MERTK	Tyrosine-protein kinase Mer	HUMAN	0.496732	No
P62805	HIST1H4A	Histone H4	HUMAN	15.01752	No
P31947	SFN	14-3-3 protein sigma	HUMAN	11.51171	No
P68871	HBB	Haemoglobin subunit beta	HUMAN	5.662245	No
P60174	TPI1	Triosephosphate isomerase	HUMAN	3.553203	No
P17066	HSPA6	Heat shock 70 kDa protein 6	HUMAN	3.338776	No
P09211	GSTP1	Glutathione S-transferase P	HUMAN	3.30362	No
P06576	ATP5B	ATP synthase subunit beta, mitochondrial	HUMAN	2.828031	No
P25705	ATP5A1	ATP synthase subunit alpha, mitochondrial	HUMAN	2.769105	No
P04080	CSTB	Cystatin-B	HUMAN	2.656404	No
O95274	LYPD3	Ly6/PLAUR domain-containing protein 3	HUMAN	2.515904	No
P04792	HSPB1	Heat shock protein beta-1	HUMAN	2.420734	No
P40926	MDH2	Malate dehydrogenase, mitochondrial	HUMAN	2.409112	No
P21796	VDAC1	Voltage-dependent anion-selective channel protein 1	HUMAN	2.295509	No
Q15149	PLEC	Plectin	HUMAN	2.012799	No

5.5 Characterisation of the impact of VACV A56 protein on the murine immune response to VACV infection

The literature and the results of our *in vitro* study on VACV A56 (described above) indicate that A56 i) anchors VCP and K2 at the PM, ii) alters the susceptibility of VACV-infected cells to NK-mediated killing, iii) enhances binding of soluble NCRs to VACV-infected cell surface, iv) and does not alter the surface expression of other NK ligands. Given that i) K2 and VCP are known to, respectively, protect the infected cell of the complement attack and contribute to viral spread by inhibiting superinfection, ii) and that A56 alters the NK cell response, we reasoned that deletion of A56 could affect the immune response to VACV.

Of note, the few studies that have assessed the contribution of A56 to VACV virulence in mouse models are inconsistent. These studies lack appropriate controls and rely on infection models that are poorly representative of physiologically relevant conditions. Consequently, we decided to characterise *in vivo,* the immune response to VACV ΔA56 in comparison to WT VACV, in the acute and the memory stage of two murine infection models. The results of this study are discussed sequentially below.

5.5.1 Experimental design

There are two infection models used routinely in our laboratory to study VACV virulence or immunogenicity; the i.n. infection model, which leads to a systemic infection (Turner, 1967; Williamson *et al.*, 1990a; Alcami and Smith, 1992; Rivera *et al.*, 2007; Chapman *et al.*, 2010; Bonduelle *et al.*, 2012) and the i.d. infection model, which is a local infection and mimics vaccination (Tscharke *et al.* 2002). Deletion of an individual VACV protein sometimes has a phenotype in comparison to WT VACV infection in only one of the two infection models (Tscharke *et al.* 2002). Consequently, both infection models were used to study the impact of VACV A56 deletion mutant during VACV infection in the mouse.

5.5.2 Study of A56 deletion impact on the pathology of VACV during i.n. infection

First, we studied the impact of A56 deletion on VACV infection in the i.n. model. The experimental design is represented in Figure 77. Weight loss and virus replication were analysed in the acute stage of infection. After the primary infection had resolved (memory stage), the level of anti-VACV neutralising Abs and anti-VACV specific $CD8^+$ T cells were analysed as well as the weight loss after a lethal challenge with WT VACV.

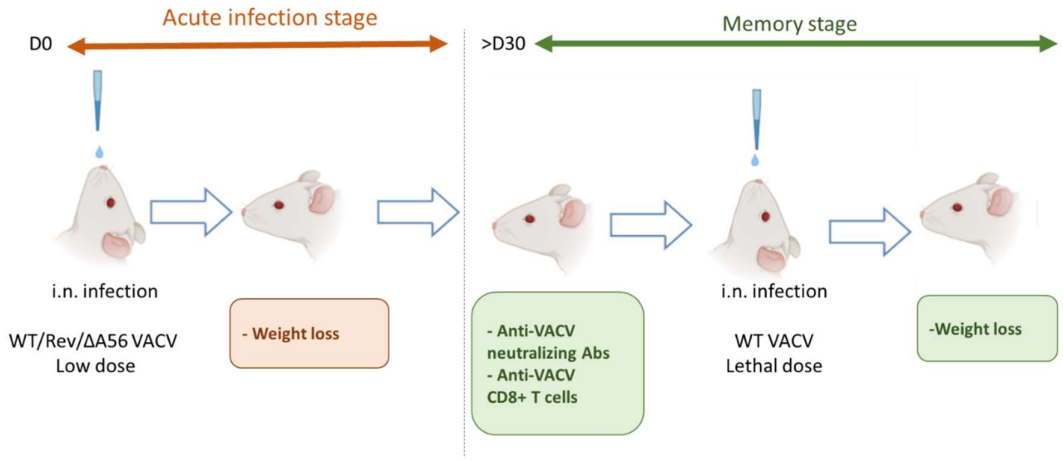

Figure 77 Schematic representing the experimental design for the study of VACV ΔA56 in the i.n. infection model**.** B6 female mice (6-8 weeks old) were i.n. infected with a low dose of VACV WR/ΔA56/RevA56. Weight loss was measured during the acute stage of infection (between 0 to 30 d.p.i.) until complete recovery. In the memory phase of infection (minimum 30 d.p.i.), the VACV-specific Abs and VACV-specific CD8+ T cell responses were measured, and another group of mice were challenged by i.n. infection with a lethal dose of WT VACV.

Results showed that, as expected, the control group that received control vehicle (PBS) did not lose weight whilst the three groups of mice infected with ΔA56, WT or RevA56 lost weight gradually from 4 to 7 d.p.i. and then recovered to their initial weight by d 14. Statistical analysis showed that there was no significant difference between the three infected groups of mice (Figure 78).

Next, we investigated whether the presence of VACV A56 during primary exposure to VACV impacted the generation of VACV-specific humoral and T cell memory. A month after primary i.n. infection with ΔA56, WT or RevA56, the serum was collected and tested for anti-VACV neutralising Abs, and splenic VACV-specific CD8+ T cells were measured by FACS dextramer staining. The absence of A56 did not affect the level of anti-VACV neutralising Abs (Figure 79) or the number of anti-VACV $CD8^+$ T cells (Figure 80) in comparison to WT VACV or Rev A56 when measured 10 weeks post-infection.

To investigate whether the absence of A56 during infection impacted the development of a protective immune response, mice in the memory stage of infection were challenged i.n. with 1×10^7 pfu of WT VACV (a lethal dose for non-immune animals) (Figure 81). Data showed that the group of mice which had received control vehicle (PBS) as primary injection lost weight and had to be sacrificed by 4 d.p.i. to comply with animal welfare guidance. All other groups did not lose weight showing that they were fully protected against challenge, and loss of A56 did not affect this. Taken together, those data suggest that in an i.n. infection model, the absence of A56 does not impact the virulence, or the development of a protective humoral and cellular immune response, or the degree of protection to VACV challenge.

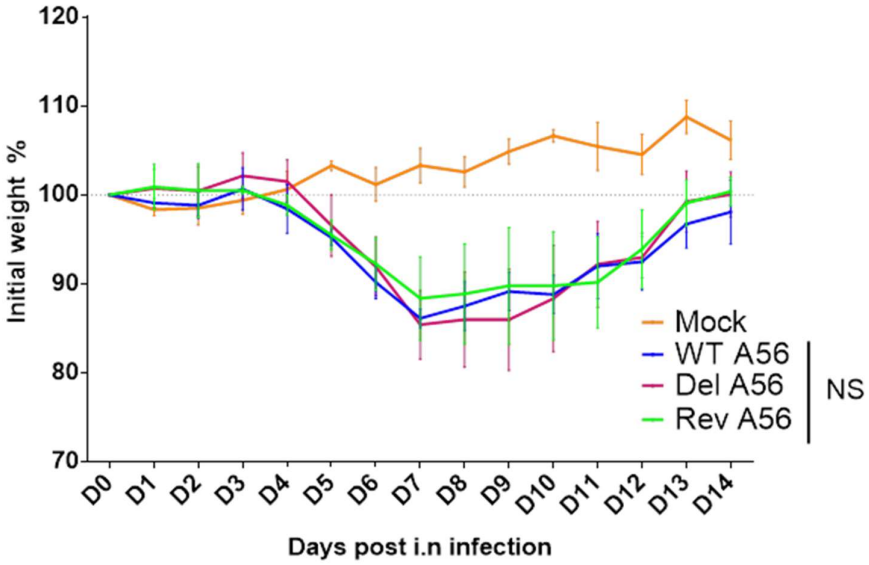

*Figure 78 Weight loss post i.n infection with mock, VACV WT, Rev or ΔA56. Female B6 mice (n=4 infected groups, n=3 mock) were i.n. infected with VACV at day 0 with 2*10^2 pfu, weight loss and signs of illness were monitored daily. Statistical significance was determined by ANOVA 2 (alpha 0.05), p<0.05. Error bars represent ± SD. Data are representative of two independent experiments.*

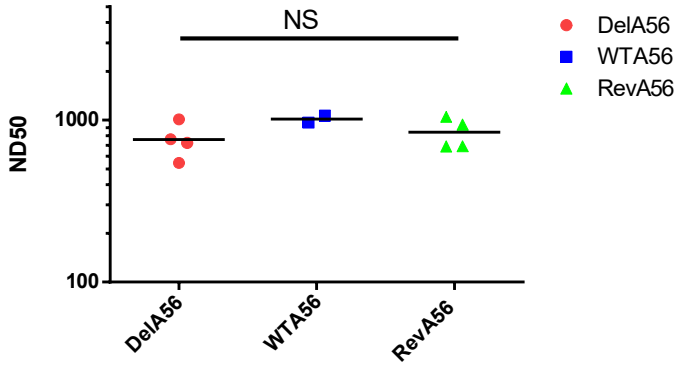

*Figure 79 Level of anti-VACV neutralising Abs in the memory phase after i.n infection with WT, Rev and ΔA56 viruses. Groups of 4 female B6 mice were i.n. infected with 2*10^2 pfu with the indicated virus. Ten weeks later, neutralising anti-VACV Abs levels were determined by plaque reduction neutralization test. A Mann-Whitney test was performed to assess significance between each group, p< 0.05 was considered significant. Note that there are only two mice in the WTA56 group because two mice had to be sacrificed because of a genetic abnormality and a paw injury.*

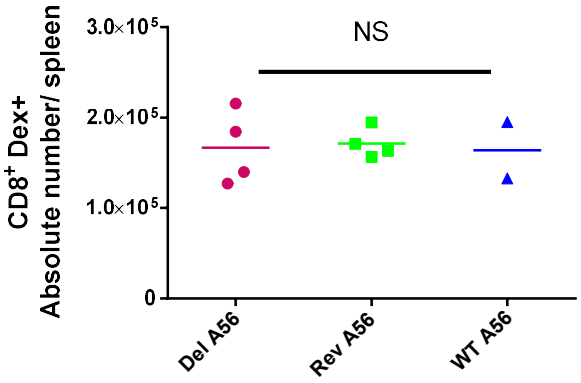

*Figure 80 Level of anti-VACV CD8+ T cells in the memory phase after i.n infection with WT, Rev and ΔA56 viruses. Groups of female B6 (n=5) were infected i.n. with 2*10^2 pfu of the indicated virus. Ten weeks post-infection, spleens were collected, and the total number of VACV-specific CD8+ T cells was assessed by FACS using anti-VACV dextramer staining. A Mann-Whitney test was performed to assess significance between each group, p< 0.05 was considered significant. Note that there are only two mice in the WTA56 group because two other mice had to be sacrificed because of a genetic abnormality and a paw injury.*

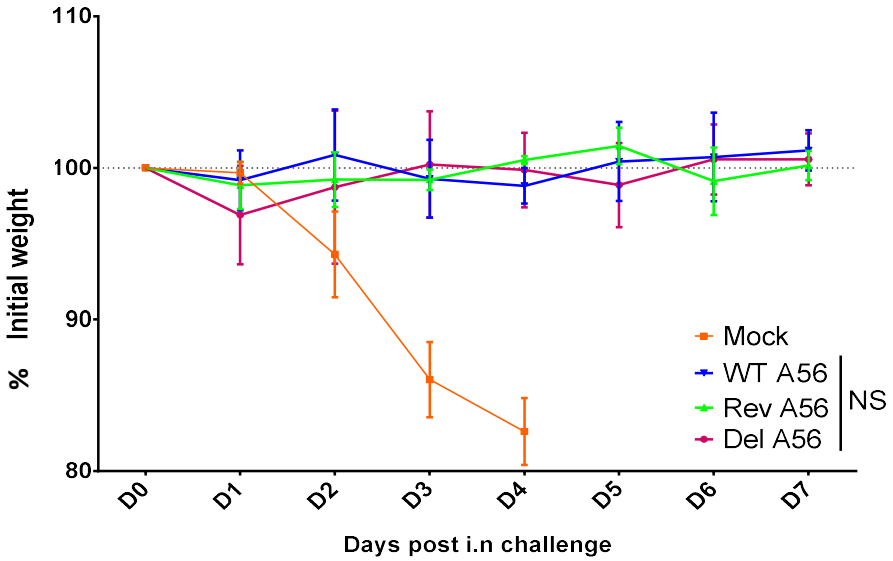

*Figure 81 Weight loss post lethal challenge with WT VACV in mice that had been previously i.n infected with mock, VACV WT, Rev or ΔA56. Group of 5 females B6 were infected i.n. with 2*10^2 pfu of the indicated virus two months before i.n challenge with 1*10^7 pfu of WT VACV (D0). Weight change was monitored daily. Error bars represent ±SD. Statistical significance was determined by ANOVA 2 (alpha 0.05), p<0.05 was considered significant.*

5.5.3 Study of VACV A56 deletion impact during VACV i.d. infection

As mentioned earlier, some VACV single deletion mutants show a phenotype in one infection model but not the other. The reason being that the two infection models are quite different, indeed, infection via the i.d. route, mimics vaccination and leads to local replication of the virus and to the development of lesion localised at the site of infection which appear 5-6 d.p.i. and resolves by 21 d.p.i. (Tscharke & Smith 1999). We followed the experimental design represented in Figure 82 to test whether the absence of A56 has an impact in comparison to WT VACV during i.d. infection in mice.

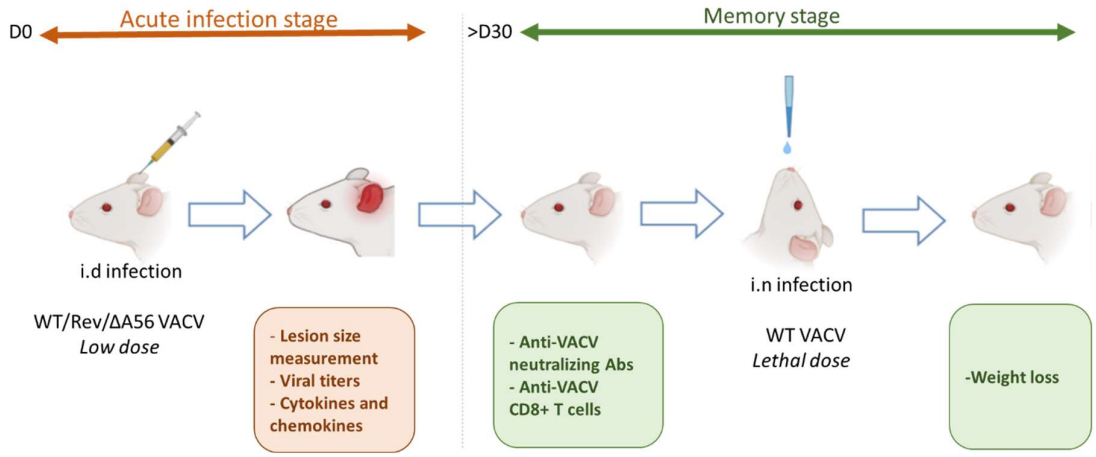

Figure 82 Schematic representing the experimental design for studying the impact of ΔA56 in comparison to WT VACV during murine i.d. infection**.** B6 female mice (6-8 weeks old) were i.d. infected with a low dose of VACV WR/ΔA56/RevA56. Lesion size, viral titres, and chemokines and cytokines were measured at various times during the acute stage of infection (between 0 to 30 d.p.i.). In the memory phase of infection (minimum 30 d.p.i.), the VACV-specific Abs and VACV-specific CD8+ T cell responses were measured, and another group of mice were challenged by i.n. infection with a high dose of WT VACV.

Results showed that the lesions developed gradually at the site of infection from 5 d.p.i. and had completely resolved by 22 d.p.i. (Figure 83). Statistical analysis showed that lesion development was not affected by the absence of A56 in comparison to WT or RevA56.

Further, the time course study of the viral load at the site of infection by plaque assay did not show any significant difference between any of the groups, suggesting that A56 does not influence the replication of VACV *in vivo* at the site of infection. Some variability in viral titre was observed at 9 d.p.i. , and this is due to the fact by this stage, the scab formed at the injection site falls off, which leads to variation in the total viral load recovered from the mice ears (Figure 84).

To assess whether A56 has any impact on the inflammatory environment in the tissue during infection, we used a cytokine bead array to measure the concentration of cytokines and chemokines locally

during infection (D1/D3/D6/D9) (Figure 85). These data showed that the temporal profiles for some cytokines/chemokines peaked at 6 d.p.i. (CCL2 (Chemokine (C-C motif) ligand), CCL5, CCL4, CCL7, CXCL1, CXCL10, TNF-α, IFNγ, LIX, IL-1b, IL-6, IL-10, Il-33) whilst the levels of others gradually increased until 9 d.p.i. (IL-4) or peaked at 3 d.p.i. (CCL20). Statistical analysis did not show a substantial difference between WT VACV and ΔA56 except for IL-33, CXCL2 at 3 d.p.i. and CCL5 at both 3d.p.i. and 9 d.p.i.. The temporary and small amplitude of these differences suggests that the biological relevance of those difference is low.

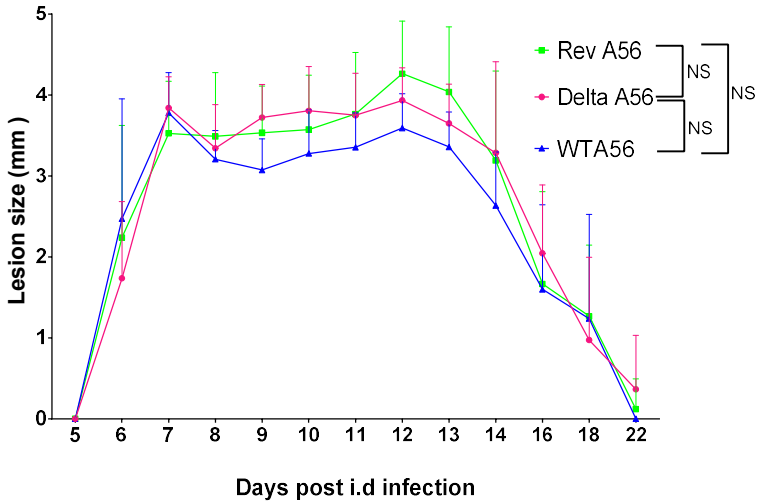

*Figure 83 Lesion size following i.d. infection with VACV WT, Rev or ΔA56. Groups of female B6 mice (n=10) were infected i.d. with 1.5*10⁴ pfu of the indicated viruses in both ear pinnae. Lesion sizes were measured daily with a micrometre and mean ± SD are represented. An ANOVA 2 (alpha 0.05) was performed between each group, and the significance of the virus effect is indicated, p<0.05 was considered significant. Data are representative of two independent experiments.*

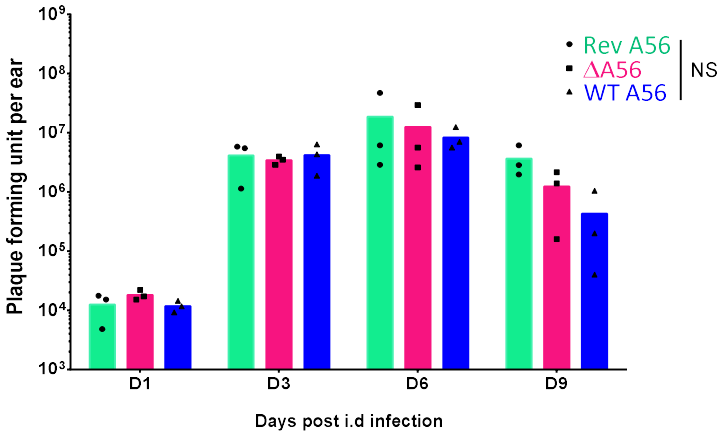

*Figure 84 Local viral titres after i.d. infection with VACV WT, Rev, ΔA56. Groups of female B6 mice (n=12) were infected i.d. with 1.5*10^4 pfu of the indicated viruses in both ear pinnae. Three mice of each group were sacrificed at the indicated time, and ear lobes were collected for viral titration by plaque assay. Bar graphs represent the mean, and individual samples are shown as dots. An ANOVA 2 (alpha 0.05) was performed between each group and p<0.05 was considered significant.*

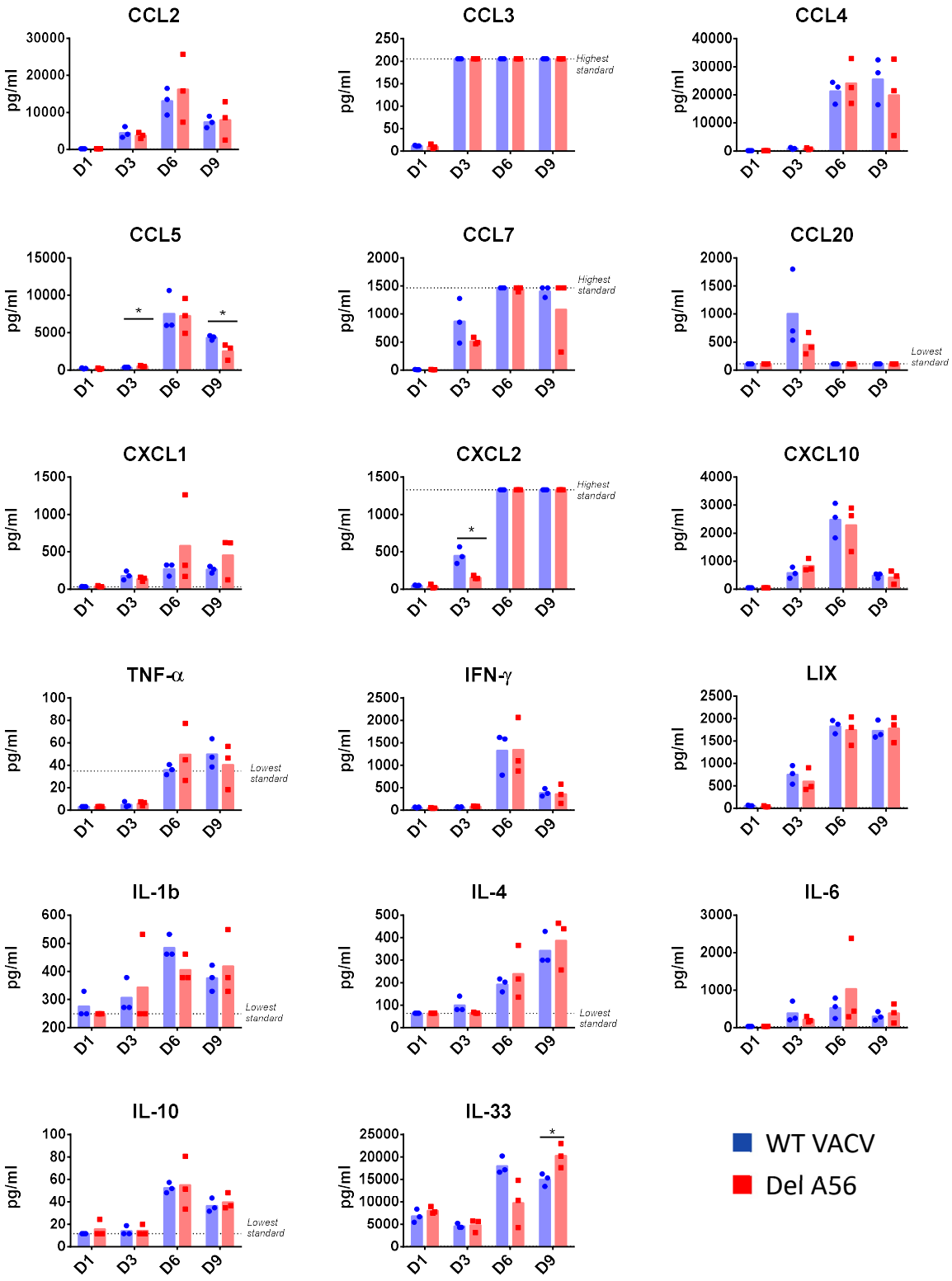

*Figure 85 Measurement of the local levels of cytokines and chemokines following i.d. infection with WT VACV or ΔA56. Groups of B6 mice (n=12) were vaccinated with 1.5*10^4 pfu of the indicated virus by i.d. injection at d 0. At the indicated d.p.i., 3 mice of each group were sacrificed, and ear tissues were collected. The level of the indicated cytokines/chemokines was measured by Luminex and is presented for each sample as well as the mean. A Mann-Whitney test for each time point (alpha 0.05) was performed/ Statistical significance is represented as followed: *p<0.05, **p<0.01, ***p<0.001, NS unless otherwise indicated.*

Furthermore, we investigated whether the absence of A56 during primary infection altered the development of a protective immune response to VACV in the i.d. infection model. Results showed that the levels of anti-VACV neutralising Abs (Figure 86) and the total number of VACV-specific $CD8^+$ T cells in the spleen (Figure 87) were not impacted by the absence of A56. Moreover, the weight loss of vaccinated mice after i.n. challenge with WT VACV led to equivalent weight loss in all groups (Figure 88). Taken together, those data suggest that the presence of VACV A56 does not affect the acute stage of infection, or the development of specific anti-VACV humoral and cellular immune response, or the protection degree to a lethal challenge with WT VACV, at least, in the conditions tested.

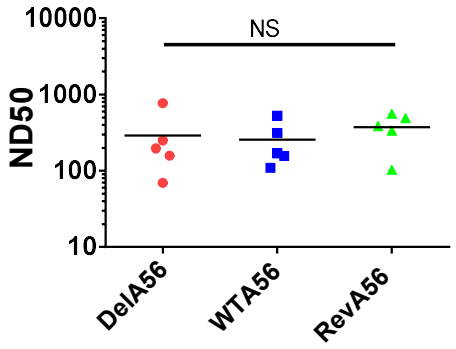

*Figure 86 Level of anti-VACV neutralising Abs after i.d. infection with VACV WT, Rev or ΔA56. Groups of five female B6 mice were infected with ~2*10⁴ pfu of the indicated virus in the ear pinnae. Serum was collected at 2.5 months pi and neutralising Abs levels were determined by plaque reduction neutralization test. ND50, is the minimum concentration required for 50 % plaque number reduction. A Mann-Whitney test was performed to assess significance, p<0.05 was considered significant.*

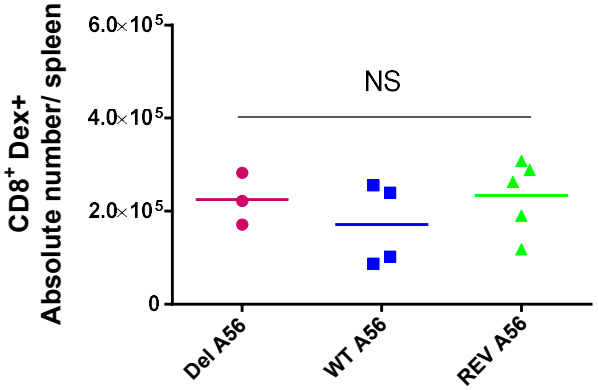

*Figure 87 Level of anti-VACV CD8+ T cells after i.d. infection with VACV WT, Rev or ΔA56. Groups of 5 female B6 mice were infected with ~2*10⁴ pfu of the indicated virus in the ear pinnae. Spleens were collected at 2.5 months p.i., and total anti-VACV $CD8^+$ T cells were determined by FACS using dextramer staining. A Mann-Whitney test was performed to assess significance, p<0.05 was considered significant. Note that two samples in ΔA56 and one in the WT group could not be represented because of technical failure during FACS acquisition.*

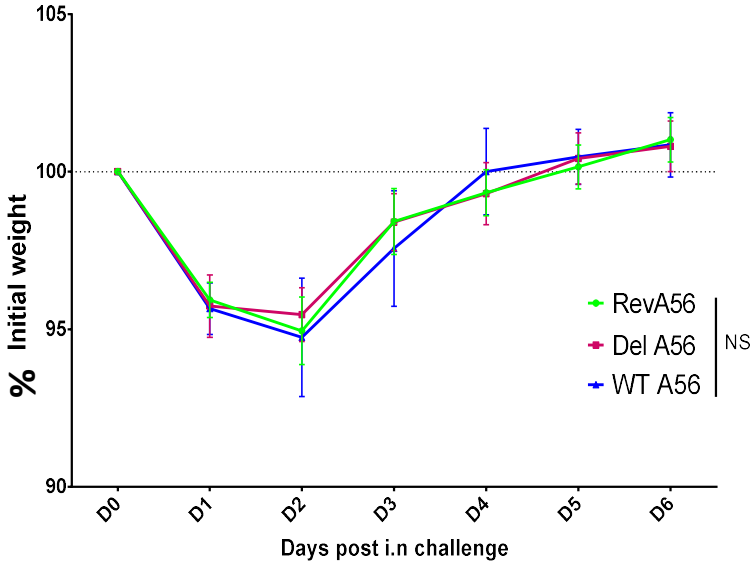

*Figure 88 Weight loss post lethal challenge with WT VACV, in mice that had been previously i.d. infected with mock, VACV WT, Rev or ΔA56. Groups of female B6 mice (n=10) were immunised with ~1.5*10^4 pfu of the indicated virus via i.d. route in the ear pinnae. At 30 d.p.i., mice were i.n. challenged with WT VACV (~2*10^7 pfu). Data means ± SEM are expressed as a percentage of the initial weight of each animal on day 0 (before i.n. injection). An ANOVA 2 (alpha 0.05) was performed between each group, and significance was considered when p<0.05.*

5.6 VACV infection in a mouse model lacking NKp46

NKp46 is an activating receptor expressed ubiquitously on NK cells and can trigger the cytotoxic response of NK cells directly. NKp46 is conserved in mice (where it is named mNKp46 or Ncr1) and humans, and binds multiple ligands expressed during infection; such as the influenza HA (Mandelboim *et al.* 2001), the adhesins of *Candida glabrata* (Vitenshtein *et al.* 2016), the sigma 1 protein of reovirus (Bar-On *et al.* 2017), the neuraminidase of Newcastle disease virus (Jarahian *et al.* 2009), the HA of Sendai virus (Mandelboim *et al.* 2001).

NKp46 is required for B6 mice to control influenza infection, and deletion of NKp46 leads to increased lethality of infection (Gazit *et al.* 2006). Importantly, human and murine NKp46 bind to VACV-infected cells (Chisholm & Reyburn 2006; Jarahian *et al.* 2011), and this interaction is promoted by the expression of VACV A56 (Jarahian *et al.* 2011). We also confirmed the binding of NKp46 to VACV-infected cells and the substantial reduction of this interaction in the absence of A56 (Figure 74 and Figure 73).

Considering those data together, we hypothesized that NKp46 might be involved in the control of VACV infection. To test this hypothesis, we used the NKp46 $^{GFP/GFP}$ mice in which the Ncr1 gene has

been replaced by GFP and compared their response to VACV infection in comparison to their WT counterpart.

The NKp46$^{GFP/GFP}$ mice were kindly provided by Ofer Mandelboim and were bred in house. Because the colony started with just a few animals and had poor breeding performances, the females were kept for expanding the colony, and the males were used for experimental procedures. Age and sex-matched B6 WT mice were always used for comparison. The experimental design shown in Figure 89 was followed to test our hypothesis with the available number of mice produced by our colony.

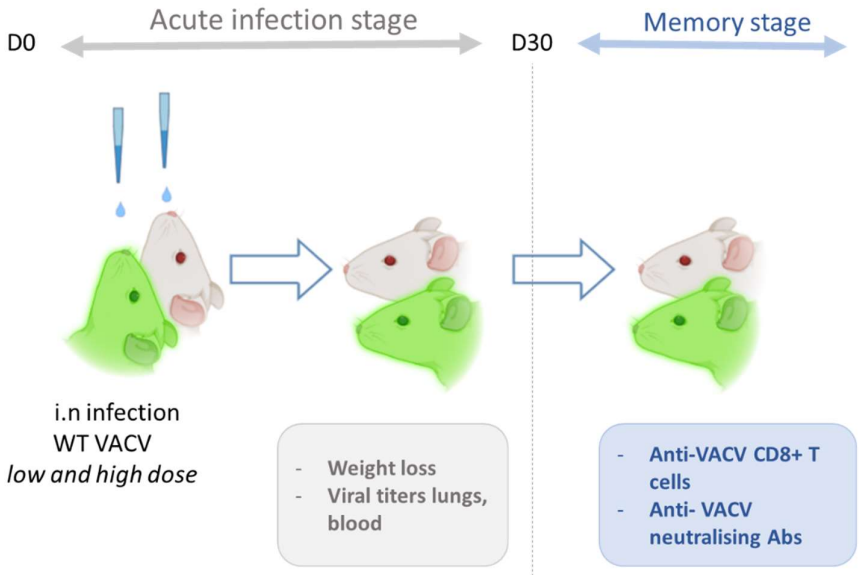

Figure 89 Schematic representing the experimental approach followed to study the effect of NKp46 deletion during VACV infection. Groups of NKp46 $^{GF/GFP}$ males were used in comparison to their WT counterpart, sex and aged-matched B6. Mice were i.n infected at a low or high dose with WT VACV. Weight loss, local and systemic viral titers were measured at various time points during the acute stage of infection (0-30 d.p.i.). In the memory phase (minimum 30 d.p.i.), the VACV-specific Abs and VACV-specific CD8+ T cell responses were measured.

Infection with a low dose of WT VACV i.n. showed that the group of mice with a deletion for NKp46 had a reduced weight gain over the two weeks following infection (Figure 90). Challenge with a high dose of WT VACV i.n. showed a similar result; groups of mice with a deletion for NKp46 showed a slightly enhanced weight loss in comparison to their WT counterpart (Figure 91). This trend was observed on multiple occasions, but statistical significance was not reached for overall group comparison, suggesting a minor effect.

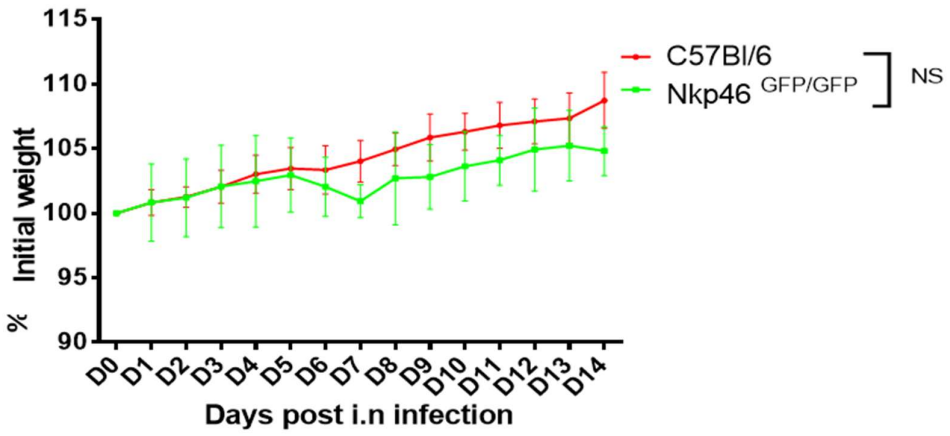

*Figure 90 Outcome of i.n. infection of B6 and NKp46 mice with a low dose of VACV. Groups of aged-matched males NKp46$^{GFP/GFP}$ and B6 (n=7) were infected intranasally with ~2*10^3 pfu WT VACV at day 0. Weight loss was monitored daily. Mean and error bars (± SD) are represented. Statistical significance between both groups was assessed with an ANOVA2, *p<0.05, **p<0.01, ***p<0.001, NS unless otherwise indicated. Data are representative of two independent experiments.*

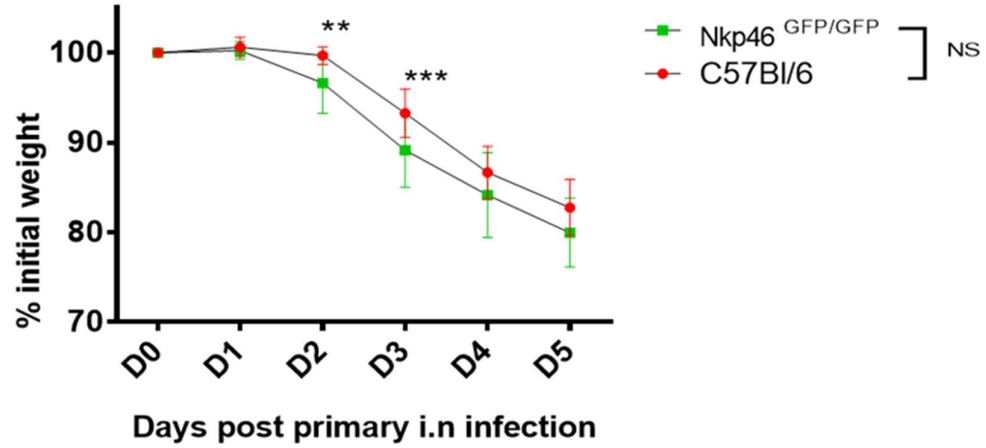

*Figure 91 Outcome of i.n. infection of B6 and NKp46 mice with a high dose of VACV. Groups of aged-matched males NKp46$^{GFP/GFP}$ and B6 mice were i.n. infected with ~1*10^6 pfu WT VACV at day 0. Weight loss was monitored daily. Mean and error bars (± SD) are represented. Statistical significance between both groups was assessed with an ANOVA2 (alpha 0.05), and between groups for each time point with a Holm-Sidak method, significance was defined as follows: *p<0.05, **p<0.01, ***p<0.001, NS unless unless otherwise indicated. Data are representative of two independent experiments.*

Further, the ability of VACV to replicate *in vivo* was compared between NKp46 $^{GFP/GFP}$ mice and their WT counterpart. Viral titres were measured in the lungs at multiple time points post i.n. infection (Figure 92). These data showed that VACV replicated rapidly in the lungs between D1 and D3 with a further modest increase between D3 and D5. Statistical analysis indicated that NKp46 deletion did not affect the total infectious particles found in the lungs after i.n. infection. Additionally, measurement of the viral load in the blood post i.n. infection showed a rapid increase of the viral load in the blood which did not show statistical significance between WT and NKp46 deletion (Figure 93), suggesting that NKp46 does not affect the VACV spread during a systemic infection.

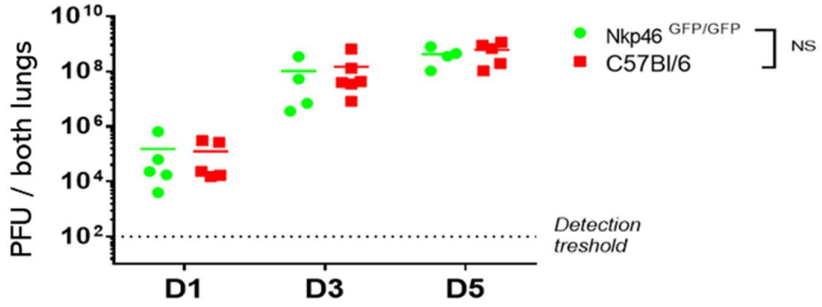

*Figure 92 Measure of virus titer in the lungs after VACV i.n infection in B6 and NKp46 $^{GFP/GFP}$ mice. Groups of age-matched males NKp46$^{GFP/GFP}$ and their WT counterpart were infected i.n. with ~1*10^6 pfu WT VACV at day 0. Subgroups of mice were sacrificed each day to collect organs for viral load measurement by plaque assay. Each replicate is shown as well as the mean. Statistical significance was assessed by ANOVA2 (alpha 0.05), p<0.05 was considered significant.*

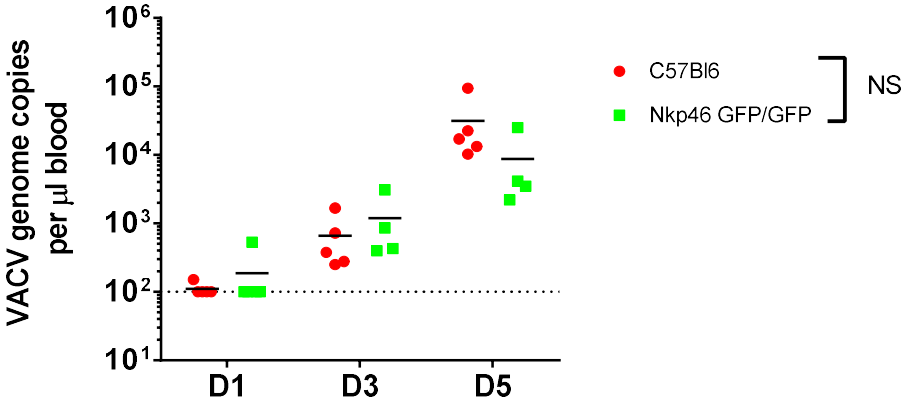

*Figure 93 Measure of virus titres in the blood after VACV i.n. infection in B6 and NKp46 $^{GFP/GFP}$ mice. Groups of age-matched males NKp46$^{GFP/GFP}$ and their WT counterpart were i.n. infected with ~1*10^6 pfu WT VACV at day 0. Subgroups of mice were sacrificed each day to collect organs for viral load measurement by plaque assay. Each replicate and mean are. Statistical significance was assessed by ANOVA2 (alpha 0.05), p<0.05 was considered significant.*

The comparison of humoral and cellular immune memory to WT VACV between NKp46$^{GFP/GFP}$ mice and their WT counterpart did not reveal any significant differences. The total number of anti-VACV CD8$^+$ T cells (Figure 94) and anti-VACV neutralizing Abs after i.n. challenge with WT VACV (Figure 95) were not significantly affected by the absence or presence of NKp46.

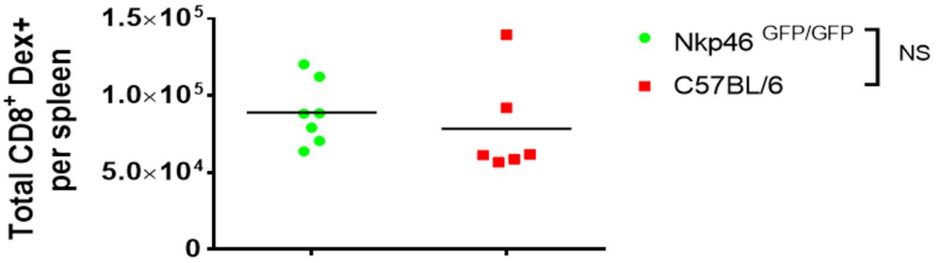

*Figure 94 Measure of anti-VACV memory CD8+ T cells in the spleen. Group of age and sex-matched B6 and NKp46$^{GFP/GFP}$ were i.n. infected with ~3*10^2 pfu. Four weeks p.i., spleens were collected, and the total number of CD8$^+$ T cells positive for anti-VACV dextramer staining was measured. Statistical significance was calculated with a Mann-Whitney test, p <0.05 was considered significant. Data are representative of two independent experiments.*

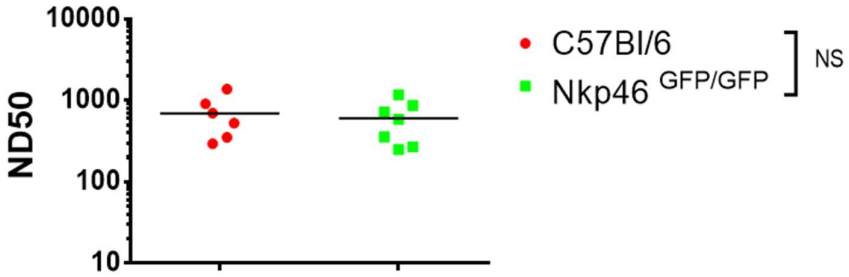

*Figure 95 Measure of VACV neutralising Ab titres in the memory phase of VACV i.n infection. Groups of age and sex-matched B6 and NKp46$^{GFP/GFP}$ mice were i.n. infected with ~3*10^2 pfu of WT VACV. Four weeks p.i., blood serum was harvested, and titre of anti-VACV Abs was calculated by plaque reduction assay. Statistical significance was calculated with a Man-Whitney test, p<0.05 was considered significant. Data are representative of 2 independent experiments.*

Together, those data suggest that, in sharp contrast with the influenza virus, NKp46 is not required for B6 mice to control i.n. VACV infection. B6 mice carrying a deletion for NKp46 showed a slightly greater weight loss after high dose infection, and a slightly delayed weight gain after low dose infection. However, the replication of VACV at the site of infection and the dissemination of VACV were not significantly affected in the absence of NKp46. Finally, the two groups of mice displayed similar VACV-specific humoral and cellular immune responses after a primary infection with WT VACV.

5.7 Discussion: study of VACV protein A56 and the NKR NKp46 in the context of VACV infection

5.7.1 *In vitro* study

To test the hypothesis that A56 and NKp46 could trigger NK cell recognition of VACV-infected cells and contribute to VACV infection control, studies were performed first *in vitro*. Deletion of A56 was associated with syncytium formation, as expected from the literature (Ichihashi & Dales 1971). No differences in plaque size or in comets formation were observed, suggesting that in cell culture, A56 does not affect VACV spread nor EEV release. This is consistent with a published study reporting no differences in plaque radius or virus spread rate in BSC1 cells infected with ΔA56 or WT VACV (Doceul *et al.* 2010). Further, absence of A56 correlated with reduced killing of VACV-infected cells by murine NK cells, suggesting A56 is activating. This result may seem to contrast with a previous study reporting that A56 absence leads to enhanced human NK cell-mediated killing, hence, suggesting A56 is inhibitory (Jarahian *et al.* 2011). However, this group also reports that A56-NKp46 interaction activates NK cells, whilst A56 blocks NKp30-mediated activation, which overrides A56-Nkp46 interaction (Jarahian *et al.* 2011). Since murine NK cells do not express NKp30, A56 may only engage with Nkp46 and therefore leads to murine NK cell activation, which is in line with our data.

Further, VACV A56 interaction with NKRs was studied in a binding assay with soluble chimeric Ig-NKRs. In line with the literature, WT VACV infection led to increased binding of NCRs but not NKG2D, in comparison to mock (Chisholm & Reyburn 2006; Jarahian *et al.* 2011). This is also consistent with our PMP dataset where NKG2DL surface expression did not increase during VACV infection. Further, A56 absence correlated with less NCR binding in comparison to WT VACV, which confirms the literature (Jarahian *et al.* 2011), although NKp44 binding in our assay was more pronounced than reported by Jarahian and colleagues. Parameters such as temperature, concentration, volumes, secondary Ab and the FACS instrument might be responsible for the difference observed. Besides, a caveat of their study is that NKp44 binding ability was not validated with a positive control such as we did with influenza-infected cells. Nevertheless, taken together these data indicate that VACV A56 contributes to soluble NCRs increased binding and enhanced NK cell-mediated killing.

To investigate whether these last results were due to A56 itself or its putative influence on other surface proteins expression, ΔA56 and WT VACV-infected cell surface proteome was compared by PMP. As expected from the literature, A56 absence led to a greatly reduced PM expression of K2 and VCP (Girgis *et al.* 2008; Turner & Moyer 2006). No NK ligands and no proteins with similarity to NK ligands were substantially modulated in absence of A56. A few other proteins seemed substantially altered in absence of A56, in comparison to WT VACV but further analysis revealed a high degree of

variation in their quantitation suggesting these were false positive. FGB signal was stable but it was quantified with only two peptides which increases the likelihood of a false positive hit. Further studies would be necessary to determine whether FGB differential expression in absence of A56 is genuine but would be complicated by FGB predicted low abundance.

Unfortunately, equipment failures did not allow to perform further ^{51}Cr release assay and efforts to set up alternative functional assays did not produce conclusive data, which was attributed to NK cell viability issue. We hypothesize that i) NK cells upon prolonged and close contact with infected target cells might become infected, which may compromise their viability, ii) NK cell intrinsic viability might be lower than other immune cells such as CD8+ T cells (for which conclusive data could be obtained). The first hypothesis is consistent with a previous study showing that NK cells can be infected during co-incubation with infected target cells (Kirwan *et al.* 2006). This study and others report that, *ex vivo*, NK cells are not infectable with VACV (Chahroudi *et al.* 2005) or only reach a modest infection level even when using a high MOI (>10), low serum concentration and small volumes (Kirwan *et al.* 2006; Sánchez-Puig *et al.* 2004; Yu *et al.* 2009a), suggesting that VACV is unlikely to infect NK cells *in vivo* where such conditions would not be met. Regardless of the reason for NK cell viability issue, our data suggest that NK cell functional studies in response to VACV should rely on a method for which the reading is not affected by NK cell viability, or that NK cells are isolated from VACV-infected host to be studied directly. Moreover, target cells such as cancer cells, which naturally express NK ligands that may be altered by VACV infection, should be avoided as well as the effector NK92 cell line which is not representative of a polyclonal NK cell response. Ideally, primary cells such as fibroblasts matched with donor NK cells should be used to perform these assays in physiologically relevant conditions.

In summary, *in vitro* study indicated that A56 does not affect virus spread, promotes NCRs binding to VACV-infected cells surface and leads to murine NK cell activation. This phenotype is likely due to A56 itself rather than another host protein under the influence of A56. Whether A56 glycans are involved in NCR binding and which region of A56 is required for binding, will require further work. Nevertheless, given that i) our *in vitro* data suggest that A56 modulates NK cell response, and ii) the innate immune response can impact the development of a memory immune response (Iwasaki & Medzhitov 2015), we next assessed A56 deletion impact *in vivo*, both in the acute and memory stage of VACV infection.

5.7.2 *In vivo* study

In the acute stage, our data did not show any significant difference for weight loss, local viral titres, lesions size, and local concentration of cytokines and chemokines except for CCL5, CXCL2 and IL-33. However, these changes were modest and not observed at all time points, suggesting that they were not sustained and might arise from background noise. Importantly, none of the cytokines produced by NK cells such as IFNγ, TNF-α, CXCL10 were differentially expressed. Taken together, these data suggest that A56 does not substantially alter VACV acute infection control and outcome, at least in the tested conditions. In the memory stage, there was no significant difference in anti-VACV specific CD8+ T cells level, anti-VACV neutralising Abs, and weight loss upon challenge with WT VACV. Together, these data indicate that A56 expression during first exposure to VACV is not required for the development of a VACV-specific adaptive immune response and does not significantly affect the degree of protection conferred by the adaptive immune response.

These data were somewhat surprising given that i) A56 expression correlates with enhanced murine NK cell killing and that, ii) A56 anchors VCP and K2 at the cell surface, which mediate respectively, protection of the infected cell against complement and prevent superinfection (DeHaven *et al.* 2010; Girgis *et al.* 2008; Turner & Moyer 2008; Wagenaar & Moss 2009). Hence, A56 deletion could have been expected to affect VACV infection outcome *in vivo*. Previous studies help distinguish the contribution of A56 and its two binding partners (VCP and K2) to VACV infection control. These studies can be compared with our data because they were performed with similar parameters such as mice and viral stain, and infection dose and models. DeHaven and colleagues showed that B6 mice infected with ΔVCP in comparison to WT developed smaller lesions (i.d. infection model) and a higher protection upon challenge (i.n. infection model) (DeHaven *et al.* 2010; Girgis *et al.* 2011), indicating that VCP is a virulence factor. Studies with ΔK2 and WT VACV in BALB/c mice (i.n. infection model) showed no substantial difference in the virulence (Law & Smith 1992), suggesting that K2 is not a virulence factor.

An hypothesis to explain why A56 deletion has no phenotype in our data is that it leads to loss of NKR-mediated activatory signals but at the same time absence of protection by surface-bound VCP. These 2 effects might balance out each other *in vivo*, resulting in no phenotype. Besides, our data suggests that secreted VCP rather than surface-bound VCP is involved in VACV virulence and responsible for the phenotype observed in DeHaven study. Further comparison of our data with other published studies assessing A56 contribution to VACV virulence is complicated by the different mice and viral strains used, and the multiple infection models employed. Flexner and colleagues report that ΔA56 (WR) is mildly attenuated (mortality reached later than WT) in an intracranial (i.c.) infection model in

nu/nu (athymic nude) mice (Flexner *et al.* 1987). Shida and colleagues report that disruption of *A56* gene (WR), leads to attenuation (higher viral load to reach 50 % mortality) in DDY mice (mice that develop spontaneous nephropathy (Imai *et al.* 1985), after i.c. infection (Shida *et al.* 1988). However, this group observed no phenotype for a similar study with the LC16mo VACV strain (temperature-sensitive VACV derived from Lister strain) (Shida *et al.* 1988). Additional studies, with the VACV NYCBH (New York City Board of Health) strain show attenuation (higher dose required for LD50) of ΔA56 after i.c. and i.n. infection in BalB/C mice (Lee *et al.* 1992). Finally, G. L. Smith reports no difference in the weight loss following i.n. infection with WT (WR), ΔA56 and Rev, in BAlb/C mice, and this at low and high doses (unpublished data).

Importantly, these studies present a few caveats i) no Rev viruses were used to control for potential off-target effects resulting from genetic manipulation of WT VACV, ii) the i.c. infection model is poorly representative of natural infection and fiddly, and iii) nu/nu mice and DDY mice are not immunocompetent animals. Together, this suggests that A56 deletion may have an impact that varies according to the infection model, mice and VACV strains used. A hypothesis arising from these data is that NK cell response might be redundant with another cell type *in vivo*. For example, the anti-viral immune response of T cell-deficient mice (nu/nu or RAG) might rely primarily on NK cells because these have more "immunological space" than in WT mice and consequently show a phenotype related to an altered NK cell response. Alternatively, the capacity of NK cells to make a substantial difference *in vivo* might be overcome by a high viral dose. Testing the impact of A56 deletion in other mice models such as $RAG^{-/-}$ mice cells would be valuable to clarify A56 role in different settings, although the implications of such data in VACV-based therapeutics development would be limited since they are not representative of immunocompetent individuals.

In parallel to A56 studies, NKp46 contribution to VACV infection outcome was assessed *in vivo* using a NKp46 murine deletion model and its WT counterpart. A mild increase in weight loss was observed in $NKp46^{GFP/GFP}$ mice, after low and high dose i.n. infections, suggesting a minor effect of NKp46. Local and systemic viral titres were unchanged, indicating that NKp46 does not substantially contribute to limiting VACV replication, *in vivo*. Further, in the memory stage, after primary i.n. infection with WT VACV, no substantial difference in anti-VACV neutralising Abs and anti-VACV CD8+ T cells levels were observed, suggesting that NKp46 is neither necessary nor has an influence on the development of protective adaptive immune response to VACV. Together, these data suggest that NKp46 has a mild contribution to the outcome of VACV following i.n. infection, which unlikely due to VACV replication control but instead could be related to NK cell secretion of cytokines such as IFNγ. Further studies by Luminex or ELISpot could shed light on this. Interestingly, the phenotype observed

in NKp46 $^{GFP/GFP}$ mice during VACV infection is in sharp contrast with influenza infection in such mice that leads to severe pathology and lethality (Gazit *et al.* 2006), suggesting that NKp46 is not required during VACV infection such as it is during influenza infection in B6 mice.

Overall, the study of A56 and NKp46 deletion impact during VACV infection *in vivo* showed no substantial differences. This suggests that despite A56 and NKp46 interacting with each other *in vitro*, they are unlikely to be a ligand: NKR couple crucially involved in the control of VACV infection, similarly to mCMV m157 and LY49H or influenza HA and NKp46. To determine whether another VACV ligand and/or NKR are specifically involved in VACV immune response requires further studies. Candidate NKRs defined in chapter 1 and VACV surface proteins defined in chapter 4 can guide future studies. Determining which NKR recognises VACV-infected cells could be exploited in cancer therapy for example by using VACV-based oncolytic virus in parallel with CAR-NK cells that highly expressing such receptor. Besides, our study of ΔA56 *in vivo* can inform vaccine design since the immunogenicity of VACV-based vaccine vectors is being improved by deletion of immunomodulatory genes. Additionally, the clarification of A56 contribution to the acute and adaptive immune response establishment is pertinent since MVA which is used in multiple clinical trials, expresses A56 and A56 is sometimes used as an insertion site for foreign antigens because of the advantage conferred by syncytium formation for selecting recombinant viruses. Globally, our study contributes to understanding how the innate immune system impacts the development of immune memory and enhances our ability to design better vaccines.

6 Conclusion

The results presented in this thesis have addressed important questions regarding the interplay between VACV and NK cells. The principal objective was to unravel which ligands are recognised by NK cells during VACV infection and via which NK cell receptors. This is a challenging question because of the great diversity of NKRs and host cell NK ligands, the absence of reagents for many of these proteins, the absence of a comprehensive list of VACV surface proteins and the fact that some NK ligands and receptors might not have been discovered yet. Hence, two strategies were employed to pursue our objectives; an unbiased screen-based method that overcomes such limitations, and in parallel, a literature-based study of putative candidates.

In the first results chapter, the responsiveness of murine NK cells to VACV infection *in vivo*, was studied at the transcriptomic level by RNA-seq and at the protein level by flow cytometry. This showed that during a systemic VACV infection, murine NK cells proliferate, are activated and upregulate the mediators necessary for a cytotoxic response, indicating that NK cells are involved in the immune response to VACV. Further, NK cells displayed a transcriptomic signature corresponding primarily with direct cell recognition, but also correlating with IL-12 and IL-18 stimulation and a response to IFNs. This indicates that NK cell activation is regulated by multiple stimuli and would be consistent with NK cells recognising one (or more) specific VACV-induced ligand.

Additionally, NK cells were shown to modify the surface expression of multiple receptors. No members of the murine receptors for MHC-I were seen to dominate the NK cell response in the way that Ly49H+ NK cells dominate the response to mCMV infection in B6 mice. However, the frequency of NK cells expressing Ly108 and CD319 increased substantially during VACV infection suggesting that these might be involved in the recognition of VACV-infected cells, possibly in a similar fashion than SLAM receptors recognise influenza HA and lead to NK cell co-stimulation.

Further, comparison with a transcriptomic study of NK cells during mCMV infection *in vivo* indicated that NKRP1F, NKRP1B and CD160 were substantially upregulated during systemic infection with VACV but not with mCMV, suggesting that such receptors may be NKRs that specifically engage with VACV-induced ligands. Interestingly, CD160 receptor was also upregulated in human NK cells post MVA-vaccination, suggesting that CD160 might be a NKR involved in the immune response to poxviruses, conserved in humans and mice.

Finally, the murine NK cell transcriptomic signature after VACV infection showed a substantial overlap with the human NK cell transcriptomic signature after vaccination with MVA, suggesting that NK cell response to VACV is at least partially conserved amongst humans and mice. This observation supports the use of B6 mice for research on NK cells and poxviruses that aims to translate into the human system.

In the second results chapter, a PMP screen of a time course of VACV-infected cells, unravelled how the host cell surface proteome changed during VACV infection. A focused analysis of proteins known to be NK cell ligands shed light on which host proteins are likely to contribute to NK cell response or to dampen it, and highlighted putative VACV immune evasion mechanisms. Mining host proteins that were substantially modulated during VACV infection for similarity with NK ligands highlighted putative new NK ligands. Analysis of a proteasome inhibitor-treated sample and comparison of our dataset with a previous study focusing on the WCL proteome during VACV infection enabled us to gain insights into the mechanisms behind surface protein modulation during VACV infection. The rather disparate literature on VACV-mediated influence on surface MHC-I expression was reassessed comprehensively. It showed that VACV only mildly reduced cell surface expression of total classical HLA-I, but selectively downmodulates HLA-C expression.
Additionally, a comprehensive list of VACV surface proteins was established and indicated that VACV F5, a suspected surface protein, and VACV C8, an uncharacterised protein, are likely expressed at the PM. Finally, six VACV surface proteins with structural similarity with known NK ligands were highlighted as potential NK ligands and are good candidates for future studies.

In the third chapter, the candidate NK ligands and receptors, VACV surface protein A56 and the NKR NKp46, were studied. First, this was done *in vitro* to validate and clarify the literature suggesting their interaction. Subsequently, this was analysed *in vivo* to define their contribution to the immune response to VACV infection. *In vitro* studies confirmed that VACV A56 prevents cell fusion, anchors VACV K2 and VCP at the cell surface and enhances the binding of human and murine NCRs to VACV-infected cells. Further, we showed that deletion of A56 did not affect plaque size or EEV release, did not alter the surface expression of known NK ligands during VACV infection, but led to a decreased NK-mediated killing of VACV-infected cells. Lastly, *in vivo* studies on the impact of the deletion of VACV A56 and NKp46 receptor during VACV infection in mice did not show a significant phenotype. This suggests that despite an interaction between A56 and NKp46, this receptor and ligand are not critical determinants in the control of VACV infection *in vivo*. Whether other NK ligand-receptor pairs exist and are involved in the control of VACV infection remains to be determined.

Overall, the data presented in this thesis constitute valuable resources for the study of VACV and NK cells. Data generated by these screening methods will allow future studies considering newly discovered candidate NK ligands and/or receptors. The potential VACV-specific NK ligands and NKRs have been reduced to a few candidates, which will help to guide future candidate-based studies. The

impact of VACV on host immune ligands and the putative VACV immune evasion highlighted in the PMP will be valuable for the design and optimisation of VACV-based oncolytic viruses and vaccines.

7 Bibliography

Abboud, G., Tahiliani, V., Desai, P., … Salek-Ardakani, S. (2016). Natural Killer Cells and Innate Interferon Gamma Participate in the Host Defense against Respiratory Vaccinia Virus Infection. *Journal of Virology*, **90**(1), 129–41.

Abrahão, J. S., Campos, R. K., Trindade, G. de S., Guimarães da Fonseca, F., Ferreira, P. C. P., & Kroon, E. G. (2015). Outbreak of Severe Zoonotic Vaccinia Virus Infection, Southeastern Brazil. *Emerging Infectious Diseases*, **21**(4), 695–698.

Adam, C., King, S., Allgeier, T., … Mocikat, R. (2005). DC-NK cell cross talk as a novel CD4+ T-cell–independent pathway for antitumor CTL induction. *Blood*, **106**(1), 338–344.

Addou-Klouche, L. (2017). NK Cells in Cancer Immunotherapy. In *Natural Killer Cells*, InTech. doi:10.5772/intechopen.71217

Adorno-Cruz, V., & Liu, H. (2019). Regulation and functions of integrin α2 in cell adhesion and disease. *Genes & Diseases*, **6**(1), 16–24.

Agrawal, S., & Prakash, S. (2020, July 1). Significance of KIR like natural killer cell receptors in autoimmune disorders. *Clinical Immunology*, Academic Press Inc., p. 108449.

Aguilar, O. A., Berry, R., Rahim, M. M. A., … Carlyle, J. R. (2017). A Viral Immunoevasin Controls Innate Immunity by Targeting the Prototypical Natural Killer Cell Receptor Family. *Cell*, **169**(1), 58-71.e14.

Alamri, A., Gounni, A. S., & Kung, S. K. P. (2017). View point: Semaphorin-3E: An emerging modulator of natural killer cell functions? *International Journal of Molecular Sciences*, **18**(11), 1–10.

Albarnaz, J. D., Torres, A. A., & Smith, G. L. (2018). Modulating Vaccinia Virus Immunomodulators to Improve Immunological Memory. *Viruses*, **10**(3), 101.

Alcami, A., Khanna, A., Paul, N. L., & Smith, G. L. (1999). Vaccinia virus strains Lister, USSR and Evans express soluble and cell- surface tumour necrosis factor receptors. *Journal of General Virology*, **80 (Pt 4)**(0022-1317 SB-M SB-X), 949–959.

Alcami, A., & Smith, G. L. (1992). A soluble receptor for interleukin-1β encoded by vaccinia virus: A novel mechanism of virus modulation of the host response to infection. *Cell*, **71**(1), 153–167.

Alcamí, A., & Smith, G. L. (1995). Vaccinia, cowpox, and camelpox viruses encode soluble gamma interferon receptors with novel broad species specificity. *Journal of Virology*, **69**(8), 4633–9.

Alcami, A., Symons, J. A., & Smith, G. L. (2000). The Vaccinia Virus Soluble Alpha/Beta Interferon (IFN) Receptor Binds to the Cell Surface and Protects Cells from the Antiviral Effects of IFN. *Journal of Virology*, **74**(23), 11230–11239.

Aldemir, H., Prod'homme, V., Dumaurier, M.-J., … Braud, V. M. (2005). Cutting Edge: Lectin-Like Transcript 1 Is a Ligand for the CD161 Receptor. *The Journal of Immunology*, **175**(12), 7791–7795.

Aldrich, C. J., DeCloux, A., Woods, A. S., Cotter, R. J., Soloski, M. J., & Forman, J. (1994). Identification of a tap-dependent leader peptide recognized by alloreactive T cells specific for a class Ib antigen. *Cell*, **79**(4), 649–658.

Alegre, E., Rizzo, R., Bortolotti, D., Fernandez-Landázuri, S., Fainardi, E., & González, A. (2014). Some Basic Aspects of HLA-G Biology. *Journal of Immunology Research*, **2014**, 1–10.

Alter, G., Malenfant, J. M., & Altfeld, M. (2004). CD107a as a functional marker for the identification

of natural killer cell activity. *Journal of Immunological Methods*, **294**(1–2), 15–22.

Alzhanova, D., Edwards, D. M., Hammarlund, E., … Früh, K. (2009). Cowpox Virus Inhibits the Transporter Associated with Antigen Processing to Evade T Cell Recognition. *Cell Host and Microbe*, **6**(5), 433–445.

Andre, P., Spertini, O., Guia, S., … Vivier, E. (2000). Modification of P-selectin glycoprotein ligand-1 with a natural killer cell-restricted sulfated lactosamine creates an alternate ligand for L-selectin. *Proceedings of the National Academy of Sciences*, **97**(7), 3400–3405.

Andrew M.Q. King. (2012). *Virus Taxonomy: Ninth Report of the International Comittee on Taxonomy of Viruses - Part II- The Double Stranded DNA Viruses- Family Poxviridae*. *Elsevier Inc.*, Elsevier Inc. doi:10.1016/B978-0-12-384684-6.00028-8

Aoyagi, M., Zhai, D., Jin, C., … Liddington, R. C. (2006). Vaccinia virus N1L protein resembles a B cell lymphoma-2 (Bcl-2) family protein. *Protein Science*, **16**(1), 118–124.

Appleyard, G., Hapel, A. J., & Boulter, E. A. (1971). An antigenic difference between intracellular and extracellular rabbitpox virus. *The Journal of General Virology*, **13**(1), 9–17.

Arase, H., Arase, N., & Saito, T. (1995). Fas-mediated cytotoxicity by freshly isolated natural killer cells. *The Journal of Experimental Medicine*, **181**(3), 1235–1238.

Arase, H., Mocarski, E. S., Campbell, A. E., Hill, A. B., & Lanier, L. L. (2002). Direct recognition of cytomegalovirus by activating and inhibitory NK cell receptors. *Science*, **296**(5571), 1323–1326.

Arase, N., Takeuchi, A., Unno, M., … Saito, T. (2005). Heterotypic interaction of CRTAM with Necl2 induces cell adhesion on activated NK cells and CD8+ T cells. *International Immunology*, **17**(9), 1227–1237.

Arita, I., Jezek, Z., Khodakevich, L., & Ruti, K. (1985). Human monkeypox: A newly emerged orthopoxvirus zoonosis in the tropical rain forests of Africa. *American Journal of Tropical Medicine and Hygiene*, **34**(4), 781–789.

Armstrong, J. A., Metz, D. H., & Young, M. R. (1973). The Mode of Entry of Vaccinia Virus into L Cells. *Journal of General Virology*, **21**(3), 533–537.

Arnon, T. I., Lev, M., Katz, G., Chernobrov, Y., Porgador, A., & Mandelboim, O. (2001). Recognition of viral hemagglutinins by NKp44 but not by NKp30. *European Journal of Immunology*, **31**(9), 2680–2689.

Assarsson, E., Greenbaum, J. A., Sundstrom, M., … Sette, A. (2008). Kinetic analysis of a complete poxvirus transcriptome reveals an immediate-early class of genes. *Proceedings of the National Academy of Sciences*, **105**(6), 2140–2145.

Augusto, D. G. (2016, June 28). The impact of KIR polymorphism on the risk of developing cancer: Not as strong as imagined? *Frontiers in Genetics*, Frontiers Research Foundation, p. 121.

Aust, J. G., Gays, F., Mickiewicz, K. M., Buchanan, E., & Brooks, C. G. (2009). The Expression and Function of the NKRP1 Receptor Family in C57BL/6 Mice. *The Journal of Immunology*, **183**(1), 106–116.

Azuma, M., Cayabyab, M., Buck, D., Phillips, J. H., & Lanier, L. L. (1992). Involvement of CD28 in MHC-unrestricted cytotoxicity mediated by a human natural killer leukemia cell line. *Journal of Immunology (Baltimore, Md. : 1950)*, **149**(4), 1115–23.

Babić, M., Krmpotić, A., & Jonjić, S. (2011). All is fair in virus–host interactions: NK cells and cytomegalovirus. *Trends in Molecular Medicine*, **17**(11), 677–685.

Bachtel, N. D., Umviligihozo, G., Pickering, S., … Apps, R. (2018). HLA-C downregulation by HIV-1 adapts to host HLA genotype. *PLOS Pathogens*, **14**(9), e1007257.

Bacon, L., Eagle, R. A., Meyer, M., Easom, N., Young, N. T., & Trowsdale, J. (2004). Two Human ULBP/RAET1 Molecules with Transmembrane Regions Are Ligands for NKG2D. *The Journal of Immunology*, **173**(2), 1078–1084.

Baker, J. L., & Ward, B. M. (2014). Development and comparison of a quantitative TaqMan-MGB real-time PCR assay to three other methods of quantifying vaccinia virions. *Journal of Virological Methods*, **196**(6), 126–132.

Balaji, K. N., Schaschke, N., Machleidt, W., Catalfamo, M., & Henkart, P. A. (2002). Surface Cathepsin B Protects Cytotoxic Lymphocytes from Self-destruction after Degranulation. *The Journal of Experimental Medicine*, **196**(4), 493–503.

Baltimore, D. (1971). Expression of animal virus genomes. *Bacteriological Reviews*, **35**(3), 235–241.

Bar-On, Y., Yoav Charpak-Amikam, A. G., Batya Isaacson, A., & Michal Mandelboim, O. M. A. D.-C. P. T. A. V. (2017). NKp46 Recognizes the Sigma1 Protein of Reovirus: Implications for Reovirus-Based Cancer Therapy. *Journal of Virology*, **91**(19), 1–15.

Barakonyi, A., Rabot, M., Marie-Cardine, A., … Le Bouteiller, P. (2004). Cutting Edge: Engagement of CD160 by its HLA-C Physiological Ligand Triggers a Unique Cytokine Profile Secretion in the Cytotoxic Peripheral Blood NK Cell Subset. *The Journal of Immunology*, **173**(9), 5349–5354.

Baraz, L., Khazanov, E., Condiotti, R., Kotler, M., & Nagler, A. (1999). Natural killer (NK) cells prevent virus production in cell culture. *Bone Marrow Transplantation*, **24**(2), 179–189.

Barber, D. F., Faure, M., & Long, E. O. (2004). LFA-1 Contributes an Early Signal for NK Cell Cytotoxicity. *The Journal of Immunology*, **173**(6), 3653–3659.

Barber, D. F., & Long, E. O. (2003). Coexpression of CD58 or CD48 with Intercellular Adhesion Molecule 1 on Target Cells Enhances Adhesion of Resting NK Cells. *The Journal of Immunology*, **170**(1), 294–299.

Bartel, Y., Bauer, B., & Steinle, A. (2013). Modulation of NK Cell Function by Genetically Coupled C-Type Lectin-Like Receptor/Ligand Pairs Encoded in the Human Natural Killer Gene Complex. *Frontiers in Immunology*, **4**, 362.

Barten, R., Torkar, M., Haude, A., Trowsdale, J., & Wilson, M. J. (2001). Divergent and convergent evolution of NK-cell receptors. *Trends in Immunology*, **22**(1), 52–57.

Bauer, S. (1999). Activation of NK Cells and T Cells by NKG2D, a Receptor for Stress-Inducible MICA. *Science*, **285**(5428), 727–729.

Baxby, D. (1981). *Jenner's smallpox vaccine: the riddle of vaccinia virus and its origin*, Heinemann Educational Publishers.

BAXBY, D., BENNETT, M., & GETTY, B. (1994). Human cowpox 1969–93: a review based on 54 cases. *British Journal of Dermatology*, **131**(5), 598–607.

Beauchamp, N. M., Busick, R. Y., & Alexander-Miller, M. A. (2010). Functional Divergence among CD103+ Dendritic Cell Subpopulations following Pulmonary Poxvirus Infection. *Journal of Virology*, **84**(19), 10191–10199.

Beer, E. M., & Rao, V. B. (2019). A systematic review of the epidemiology of human monkeypox outbreaks and implications for outbreak strategy. *PLOS Neglected Tropical Diseases*, **13**(10), e0007791.

Beerli, C., Yakimovich, A., Kilcher, S., … Mercer, J. (2018). Vaccinia virus hijacks EGFR signalling to enhance virus spread through rapid and directed infected cell motility. *Nature Microbiology*. doi:10.1038/s41564-018-0288-2

Belin, M. T., & Boulanger, P. (1987). Processing of vimentin occurs during the early stages of adenovirus infection. *Journal of Virology*, **61**(8), 2559–2566.

Bell, E., Shamim, M., Whitbeck, J. C., Sfyroera, G., Lambris, J. D., & Isaacs, S. N. (2004). Antibodies against the extracellular enveloped virus B5R protein are mainly responsible for the EEV neutralizing capacity of vaccinia immune globulin. *Virology*, **325**(2), 425–431.

Belongia, E. A., & Naleway, A. L. (2003). Smallpox Vaccine: The Good, the Bad, and the Ugly. *Clinical Medicine & Research*, **1**(2), 87–92.

Benfield, C. T. O. O., Ren, H., Lucas, S. J., Bahsoun, B., & Smith, G. L. (2013). Vaccinia virus protein K7 is a virulence factor that alters the acute immune response to infection. *Journal of General Virology*, **94**(7), 1647–1657.

Benhnia, M. R.-E.-I., Maybeno, M., Blum, D., … Crotty, S. (2013). Unusual Features of Vaccinia Virus Extracellular Virion Form Neutralization Resistance Revealed in Human Antibody Responses to the Smallpox Vaccine. *Journal of Virology*, **87**(3), 1569–1585.

Benson, D. M., Bakan, C. E., Mishra, A., … Caligiuri, M. A. (2010). The PD-1/PD-L1 axis modulates the natural killer cell versus multiple myeloma effect: a therapeutic target for CT-011, a novel monoclonal anti-PD-1 antibody. *Blood*, **116**(13), 2286–2294.

Bera, B. C., Shanmugasundaram, K., Barua, S., … Singh, R. K. (2011). Zoonotic cases of camelpox infection in India. *Veterinary Microbiology*, **152**(1–2), 29–38.

Bezman, N. A., Kim, C. C., Sun, J. C., … Lanier, L. L. (2012). Molecular definition of the identity and activation of natural killer cells. *Nature Immunology*, **13**(10), 1000–1009.

Bhargava, A. K., Rothlauf, P. W., & Krummenacher, C. (2016). Herpes simplex virus glycoprotein D relocates nectin-1 from intercellular contacts. *Virology*, **499**, 267–277.

Bhatt, P. N., & Jacoby, R. O. (1987). Mousepox in inbred mice innately resistant or susceptible to lethal infection with ectromelia virus. I. Clinical responses. *Laboratory Animal Science*, **37**(1), 11–5.

Bianchi, G., Sironi, M., Ghibaudi, E., … Mantovani, A. (1993). Migration of natural killer cells across endothelial cell monolayers. *Journal of Immunology (Baltimore, Md. : 1950)*, **151**(10), 5135–44.

Billadeau, D. D., & Leibson, P. J. (2002). ITAMs versus ITIMs: striking a balance during cell regulation. *Journal of Clinical Investigation*, **109**(2), 161–168.

Biron, C. A., & Brossay, L. (2001). NK cells and NKT cells in innate defense against viral infections. *Current Opinion in Immunology*, **13**(4), 458–464.

Biron, C. A., Byron, K. S., & Sullivan, J. L. (1989). Severe Herpesvirus Infections in an Adolescent without Natural Killer Cells. *New England Journal of Medicine*, **320**(26), 1731–1735.

Biron, C. A., Nguyen, K. B., Pien, G. C., Cousens, L. P., & Salazar-Mather, T. P. (1999). NATURAL KILLER CELLS IN ANTIVIRAL DEFENSE: Function and Regulation by Innate Cytokines. *Annual Review of Immunology*, **17**(1), 189–220.

Biron, C. A., Young, H. A., & Kasaian, M. T. (1990). Interleukin 2-induced proliferation of murine natural killer cells in vivo. *The Journal of Experimental Medicine*, **171**(1), 173–188.

Bisht, H., Weisberg, A. S., & Moss, B. (2008). Vaccinia Virus L1 Protein Is Required for Cell Entry and Membrane Fusion. *Journal of Virology*, **82**(17), 8687–8694.

Björkström, N. K., Svensson, A., Malmberg, K.-J., Eriksson, K., & Ljunggren, H.-G. (2011). Characterization of Natural Killer Cell Phenotype and Function during Recurrent Human HSV-2 Infection. *PLoS ONE*, **6**(11), e27664.

Blackman, K. E., & Bubel, H. C. (1972). Origin of the Vaccinia Virus Hemagglutinin 1. *Journal of Virology*, **9**(2), 290–296.

Blackwell, J. M., Jamieson, S. E., & Burgner, D. (2009, April 1). HLA and infectious diseases. *Clinical Microbiology Reviews*, American Society for Microbiology Journals, pp. 370–385.

Blasco, R., & Moss, B. (1992). Role of cell-associated enveloped vaccinia virus in cell-to-cell spread. *Journal of Virology*, **66**(7), 4170–4179.

Boles, K. S. (2005). The tumor suppressor TSLC1/NECL-2 triggers NK-cell and CD8+ T-cell responses through the cell-surface receptor CRTAM. *Blood*, **106**(3), 779–786.

Boles, K. s., Nakajima, H., Colonna, M., … Mathew, P. a. (1999). Molecular characterization of a novel human natural killer cell receptor homologous to mouse 2B4. *Tissue Antigens*, **54**(1), 27–34.

Bonduelle, O., Duffy, D., Verrier, B., Combadière, C., & Combadière, B. (2012). Cutting Edge: Protective Effect of CX3CR1 + Dendritic Cells in a Vaccinia Virus Pulmonary Infection Model. *The Journal of Immunology*, **188**(3), 952–956.

Born, T. L., Morrison, L. A., Esteban, D. J., … Buller, R. M. (2000). A poxvirus protein that binds to and inactivates IL-18, and inhibits NK cell response. *Journal of Immunology*, **164**(6), 3246–54.

Borrego, F., Ulbrecht, M., Weiss, E. H., Coligan, J. E., & Brooks, A. G. (1998). Recognition of Human Histocompatibility Leukocyte Antigen (HLA)-E Complexed with HLA Class I Signal Sequence–derived Peptides by CD94/NKG2 Confers Protection from Natural Killer Cell–mediated Lysis. *Journal of Experimental Medicine*, **187**(5), 813–818.

Bottino, C., Castriconi, R., Pende, D., … Moretta, A. (2003). Identification of PVR (CD155) and Nectin-2 (CD112) as Cell Surface Ligands for the Human DNAM-1 (CD226) Activating Molecule. *The Journal of Experimental Medicine*, **198**(4), 557–567.

Boulter, E. A., & Appleyard, G. (1973). Differences between extracellular and intracellular forms of poxvirus and their implications. *Progress in Medical Virology*, **16**, 86–108.

Brandstadter, J. D., Huang, X., & Yang, Y. (2014). NK cell-extrinsic IL-18 signaling is required for efficient NK-cell activation by vaccinia virus. *European Journal of Immunology*, **44**(9), 2659–66.

Brandstadter, J. D., & Yang, Y. (2011). Natural Killer Cell Responses to Viral Infection. *Journal of Innate Immunity*, **3**(3), 274–279.

Brandt, C. S., Baratin, M., Yi, E. C., … Levin, S. D. (2009). The B7 family member B7-H6 is a tumor cell ligand for the activating natural killer cell receptor NKp30 in humans. *The Journal of Experimental Medicine*, **206**(7), 1495–1503.

Braud, V. M., Allan, D. S. J. J., O'Callaghan, C. A., … McMichael, A. J. (1998a). HLA-E binds to natural killer cell receptors CD94/NKG2A, B and C. *Nature*, **391**(6669), 795–799.

Braud, V. M., Allan, D. S. J., Wilson, D., & McMichael, A. J. (1998b). TAP- and tapasin-dependent HLA-E surface expression correlates with the binding of an MHC class I leader peptide. *Current Biology*, **8**(1), 1–10.

Brooks, C. R., Elliott, T., Parham, P., & Khakoo, S. I. (2006). The Inhibitory Receptor NKG2A Determines Lysis of Vaccinia Virus-Infected Autologous Targets by NK Cells. *The Journal of Immunology*, **176**(2), 1141–1147.

Brown, M. H., Boles, K., Anton Van Der Merwe, P., Kumar, V., Mathew, P. A., & Barclay, A. N. (1998). *2B4, the Natural Killer and T Cell Immunoglobulin Superfamily Surface Protein, Is a Ligand for CD48*. *J. Exp. Med*, Vol. 188.

Brutkiewicz, R. R., Klaus, S. J., & Welsh, R. M. (1992). Window of vulnerability of vaccinia virus-infected cells to natural killer (NK) cell-mediated cytolysis correlates with enhanced NK cell triggering and is concomitant with a decrease in H-2 class I antigen expression. *Natural Immunity*, **11**(4), 203–14.

Bryk, P., Brewer, M. G., & Ward, B. M. (2018). Vaccinia Virus Phospholipase Protein F13 Promotes Rapid Entry of Extracellular Virions into Cells. *Journal of Virology*, **92**(11). doi:10.1128/jvi.02154-17

Bukowski, J. F., Mcintyre, K. W., Yang, H., & Welsh, R. M. (1987). *Natural Killer Cells Are Not Required for Interferon-mediated Prophylaxis Against Vaccinia or Murine Cytomegalovirus Infections*. *J. gen. Virol*, Vol. 68.

Bukowski, J. F., Woda, B. A., & Welsh, R. M. (1984). Pathogenesis of murine cytomegalovirus infection in natural killer cell-depleted mice. *Journal of Virology*, **52**(1), 119–28.

Bukowski, W. J. F., Woda, B. A., Habu, S., … Welsh, R. M. (1983). Natural killer cell depletion enhances virus synthesis and virus-induced hepatitis in vivo. *J Immunol The Journal of Immunology by Guest on March THE JOURNAL OF LMMUNOLOGY*, **131**(3), 1531–1538.

Buller, R. M. L., Chakrabarti, S., Moss, B., & Fredricksont, T. (1988). Cell proliferative response to vaccinia virus is mediated by VGF. *Virology*, **164**(1), 182–192.

Burrack, K. S., Hart, G. T., & Hamilton, S. E. (2019, September 18). Contributions of natural killer cells to the immune response against Plasmodium. *Malaria Journal*, BioMed Central Ltd., p. 321.

Byun, M., Verweij, M. C., Pickup, D. J., Wiertz, E. J. H. J., Hansen, T. H., & Yokoyama, W. M. (2009). Two Mechanistically Distinct Immune Evasion Proteins of Cowpox Virus Combine to Avoid Antiviral CD8 T Cells. *Cell Host & Microbe*, **6**(5), 422–432.

Byun, M., Wang, X., Pak, M., Hansen, T. H., & Yokoyama, W. M. (2007). Cowpox Virus Exploits the Endoplasmic Reticulum Retention Pathway to Inhibit MHC Class I Transport to the Cell Surface. *Cell Host and Microbe*, **2**(5), 306–315.

Cairns, J. (1960). The initiation of vaccinia infection. *Virology*, **11**(3), 603–623.

Campbell, J. A., Trossman, D. S., Yokoyama, W. M., & Carayannopoulos, L. N. (2007). Zoonotic orthopoxviruses encode a high-affinity antagonist of NKG2D. *The Journal of Experimental Medicine*, **204**(6), 1311–1317.

Campe, H., Zimmermann, P., Glos, K., … Sing, A. (2009). Cowpox Virus Transmission from Pet Rats to Humans, Germany. *Emerging Infectious Diseases*, **15**(5), 777–780.

Cann, J. A., Jahrling, P. B., Hensley, L. E., & Wahl-Jensen, V. (2013). Comparative Pathology of Smallpox and Monkeypox in Man and Macaques. *Journal of Comparative Pathology*, **148**(1), 6–21.

Caraux, A., Lu, Q., Fernandez, N., … Roth, C. (2006). Natural killer cell differentiation driven by Tyro3 receptor tyrosine kinases. *Nature Immunology*, **7**(7), 747–754.

Carayannopoulos, L. N., Naidenko, O. V., Fremont, D. H., & Yokoyama, W. M. (2002). Cutting Edge: Murine UL16-Binding Protein-Like Transcript 1: A Newly Described Transcript Encoding a High-Affinity Ligand for Murine NKG2D. *The Journal of Immunology*, **169**(8), 4079–4083.

Carbone, E., Ruggiero, G., Terrazzano, G., … Zappacosta, S. (1997). A new mechanism of NK cell cytotoxicity activation: the CD40-CD40 ligand interaction. *The Journal of Experimental Medicine*, **185**(12), 2053–60.

Carrara, G., Saraiva, N., Parsons, M., … Smith, G. L. (2015). Golgi Anti-apoptotic Proteins Are Highly Conserved Ion Channels That Affect Apoptosis and Cell Migration. *Journal of Biological Chemistry*, **290**(18), 11785–11801.

Carrillo-Bustamante, P., Keşmir, C., & de Boer, R. J. (2016, January 21). The evolution of natural killer cell receptors. *Immunogenetics*, Springer Berlin Heidelberg, pp. 3–18.

Carter, G. C., Law, M., Hollinshead, M., & Smith, G. L. (2005). Entry of the vaccinia virus intracellular mature virion and its interactions with glycosaminoglycans. *Journal of General Virology*, **86**(5), 1279–1290.

Carter, G. C., Rodger, G., Murphy, B. J., … Smith, G. L. (2003). Vaccinia virus cores are transported on microtubules. *Journal of General Virology*, **84**(9), 2443–2458.

Cassidy, S. A., Cheent, K. S., & Khakoo, S. I. (2014). Effects of Peptide on NK Cell-Mediated MHC I Recognition. *Frontiers in Immunology*, **5**(MAR), 133.

Castriconi, R., Dondero, A., Augugliaro, R., … Bottino, C. (2004). Identification of 4Ig-B7-H3 as a neuroblastoma-associated molecule that exerts a protective role from an NK cell-mediated lysis. *Proceedings of the National Academy of Sciences of the United States of America*, **101**(34), 12640.

Cerwenka, A., Bakker, A. B. H., McClanahan, T., … Lanier, L. L. (2000). Retinoic Acid Early Inducible Genes Define a Ligand Family for the Activating NKG2D Receptor in Mice. *Immunity*, **12**(6), 721–727.

Chahroudi, A., Chavan, R., Kozyr, N., … Feinberg, M. B. (2005). Vaccinia virus tropism for primary hematolymphoid cells is determined by restricted expression of a unique virus receptor. *Journal of Virology*, **79**(16), 10397–407.

Chambers, B. J., Salcedo, M., & Ljunggren, H.-G. (1996). Triggering of Natural Killer Cells by the Costimulatory Molecule CD80 (B7-1). *Immunity*, **5**(4), 311–317.

Chan, C. J., Martinet, L., Gilfillan, S., … Smyth, M. J. (2014). The receptors CD96 and CD226 oppose each other in the regulation of natural killer cell functions. *Nature Immunology*, **15**(5), 431–438.

Chan, J. R., Hyduk, S. J., & Cybulsky, M. I. (2000). α 4 β 1 Integrin/VCAM-1 Interaction Activates α L β 2 Integrin-Mediated Adhesion to ICAM-1 in Human T Cells. *The Journal of Immunology*, **164**(2), 746–753.

Chang, W., Lim, J. G., Hellström, I., & Gentry, L. E. (1988). Characterization of vaccinia virus growth factor biosynthetic pathway with an antipeptide antiserum. *Journal of Virology*, **62**(3), 1080–3.

Chapman, J. L., Nichols, D. K., Martinez, M. J., & Raymond, J. W. (2010). Animal Models of Orthopoxvirus Infection. *Veterinary Pathology*, **47**(5), 852–870.

Chicheportiche, Y., Bourdon, P. R., Xu, H., … Browning, J. L. (1997). TWEAK, a New Secreted Ligand in the Tumor Necrosis Factor Family That Weakly Induces Apoptosis. *Journal of Biological Chemistry*, **272**(51), 32401–32410.

Chiossone, L., Chaix, J., Fuseri, N., Roth, C., Vivier, E., & Walzer, T. (2010). Maturation of Mouse NK Cells is a Four-stage Developmental Program. *Clinical Immunology*, **135**(22), S48.

Chisholm, S., & Reyburn, H. (2006). Recognition of vaccinia virus-infected cells by human natural killer cells depends on natural cytotoxicity receptors. *Journal of Virology*, **80**(5), 2225–2233.

Chiu, W.-L., Lin, C.-L., Yang, M.-H., Tzou, D.-L. M., & Chang, W. (2007). Vaccinia Virus 4c (A26L) Protein on Intracellular Mature Virus Binds to the Extracellular Cellular Matrix Laminin. *Journal of Virology*, **81**(5), 2149–2157.

Chong, A. S.-F., Boussy, I. A., Jiang, X. L., Lamas, M., & Graf, L. H. (1994). CD54/ICAM-1 Is a Costimulator of NK Cell-Mediated Cytotoxicity. *Cellular Immunology*, **157**(1), 92–105.

Chung, C.-S., Hsiao, J.-C., Chang, Y.-S., & Chang, W. (1998). A27L Protein Mediates Vaccinia Virus Interaction with Cell Surface Heparan Sulfate. *Journal of Virology*, **72**(2), 1577–1585.

Cibrián, D., & Sánchez-Madrid, F. (2017). CD69: from activation marker to metabolic gatekeeper. *European Journal of Immunology*, **47**(6), 946–953.

Cohen, G. B., Gandhi, R. T., Davis, D. M., … Baltimore, D. (1999). The Selective Downregulation of Class I Major Histocompatibility Complex Proteins by HIV-1 Protects HIV-Infected Cells from NK Cells. *Immunity*, **10**(6), 661–671.

Cohnen, A., Chiang, S. C., Stojanovic, A., … Watzl, C. (2013). Surface CD107a / LAMP-1 protects natural killer cells from degranulation-associated damage. *Immunobiology*, **122**(8), 1411–1418.

Colamonici, O. R., Domanski, P., Sweitzer, S. M., Larner, A., & Buller, R. M. L. (1995). Vaccinia Virus B18R Gene Encodes a Type I Interferon-binding Protein That Blocks Interferon α Transmembrane Signaling. *Journal of Biological Chemistry*, **270**(27), 15974–15978.

Colucci, F. (2017). The role of KIR and HLA interactions in pregnancy complications. *Immunogenetics*, **69**(8–9), 557–565.

Cooper, M. A., Bush, J. E., Fehniger, T. A., … Caligiuri, M. A. (2002). In vivo evidence for a dependence on interleukin 15 for survival of natural killer cells. *Blood*, **100**(10), 3633–3638.

Cooper, M. A., Elliott, J. M., Keyel, P. A., Yang, L., Carrero, J. A., & Yokoyama, W. M. (2009). Cytokine-induced memory-like natural killer cells. *Proceedings of the National Academy of Sciences*, **106**(6), 1915–1919.

Cooray, S., Bahar, M. W., Abrescia, N. G. A., … Smith, G. L. (2007). Functional and structural studies of the vaccinia virus virulence factor N1 reveal a Bcl-2-like anti-apoptotic protein. *Journal of General Virology*, **88**(6), 1656–1666.

Cosman, D., Müllberg, J., Sutherland, C. L., … Chalupny, N. J. (2001). ULBPs, Novel MHC Class I–Related Molecules, Bind to CMV Glycoprotein UL16 and Stimulate NK Cytotoxicity through the NKG2D Receptor. *Immunity*, **14**(2), 123–133.

Costanzo, M. C., Kim, D., Creegan, M., … Eller, M. A. (2018). Transcriptomic signatures of NK cells suggest impaired responsiveness in HIV-1 infection and increased activity post-vaccination. *Nature Communications*, **9**(1), 1212.

Cox, J., & Mann, M. (2008). MaxQuant enables high peptide identification rates, individualized p.p.b.-range mass accuracies and proteome-wide protein quantification. *Nature Biotechnology*, **26**(12), 1367–1372.

Cox, S., Trifonov, V., Bohl, B., … Barrow, A. D. (2017). Natural Killer Cells Control Tumor Growth by Sensing a Growth Factor. *Cell*, **172**(3), 534-548.e19.

Crespo, Â. C., Mulik, S., Dotiwala, F., … Lieberman, J. (2020). Decidual NK Cells Transfer Granulysin to Selectively Kill Bacteria in Trophoblasts. *Cell*, **182**(5), 1125-1139.e18.

Crotta, S., Stilla, A., Wack, A., … Valiante, N. M. (2002). Inhibition of Natural Killer Cells through Engagement of CD81 by the Major Hepatitis C Virus Envelope Protein. *The Journal of Experimental Medicine*, **195**(1), 35–42.

Crotty, S., Felgner, P., Davies, H., Glidewell, J., Villarreal, L., & Ahmed, R. (2003). Cutting Edge: Long-Term B Cell Memory in Humans after Smallpox Vaccination. *The Journal of Immunology*, **171**(10), 4969–4973.

Czerny, C.-P., Eis-Hübinger, A. M., Mayr, A., Schneweis, K. E., & Pfeiff, B. (1991). Animal poxviruses transmitted from cat to man: current event with lethal end. *Journal of Veterinary Medicine, Series B*, **38**(1–10), 421–431.

de Andrade, L. F., Smyth, M. J., & Martinet, L. (2014). DNAM-1 control of natural killer cells functions through nectin and nectin-like proteins. *Immunology and Cell Biology*, **92**(3), 237–244.

de Souza Trindade, G., Drumond, B. P., Guedes, M. I. M. C., … Kroon, E. G. (2007). Zoonotic Vaccinia Virus Infection in Brazil: Clinical Description and Implications for Health Professionals. *Journal of Clinical Microbiology*, **45**(4), 1370–1372.

Degli-Esposti, M. A., Dougall, W. C., Smolak, P. J., Waugh, J. Y., Smith, C. A., & Goodwin, R. G. (1997a). The Novel Receptor TRAIL-R4 Induces NF-κB and Protects against TRAIL-Mediated Apoptosis, yet Retains an Incomplete Death Domain. *Immunity*, **7**(6), 813–820.

Degli-Esposti, M. A., Smolak, P. J., Walczak, H., … Smith, C. A. (1997b). Cloning and Characterization of TRAIL-R3, a Novel Member of the Emerging TRAIL Receptor Family. *The Journal of Experimental Medicine*, **186**(7), 1165–1170.

DeHaven, B. C., Girgis, N. M., Xiao, Y., … Isaacs, S. N. (2010). Poxvirus Complement Control Proteins Are Expressed on the Cell Surface through an Intermolecular Disulfide Bridge with the Viral A56 Protein. *Journal of Virology*, **84**(21), 11245–11254.

DeHaven, B. C., Gupta, K., & Isaacs, S. N. (2011). The vaccinia virus A56 protein: a multifunctional transmembrane glycoprotein that anchors two secreted viral proteins. *Journal of General Virology*, **92**(9), 1971–1980.

DeLange, A. M., & McFadden, G. (1987). Efficient resolution of replicated poxvirus telomeres to native hairpin structures requires two inverted symmetrical copies of a core target DNA sequence. *Journal of Virology*, **61**(6), 1957–1963.

Delano, M. L., & Brownstein, D. G. (1995a). Innate resistance to lethal mousepox is genetically linked to the NK gene complex on chromosome 6 and correlates with early restriction of virus replication by cells with an NK phenotype. *Journal of Virology*, **69**(9), 5875–5877.

Delano, M. L., & Brownstein, D. G. (1995b). Innate resistance to lethal mousepox is genetically linked to the NK gene complex on chromosome 6 and correlates with early restriction of virus replication by cells with an NK phenotype. *J Virol*, **69**(9), 5875–5877.

Della Chiesa, M., Falco, M., Podestà, M., … Moretta, A. (2012). Phenotypic and functional heterogeneity of human NK cells developing after umbilical cord blood transplantation: A role for human cytomegalovirus? *Blood*, **119**(2), 399–410.

Deng, L., Yang, X., Fan, J., … Hu, Z. (2020). An Oncolytic Vaccinia Virus Armed with GM-CSF and IL-24 Double Genes for Cancer Targeted Therapy. *OncoTargets and Therapy*, **Volume 13**, 3535–3544.

Diefenbach, A., Jamieson, A. M., Liu, S. D., Shastri, N., & Raulet, D. H. (2000). Ligands for the murine

NKG2D receptor: expression by tumor cells and activation of NK cells and macrophages. *Nature Immunology*, **1**(2), 119–126.

Doceul, V., Hollinshead, M., van der Linden, L., & Smith, G. L. (2010). Repulsion of Superinfecting Virions: A Mechanism for Rapid Virus Spread. *Science*, **327**(5967), 873–876.

Dokun, A. O., Kim, S., Smith, H. R., Kang, H.-S. P., Chu, D. T., & Yokoyama, W. M. (2001). Specific and nonspecific NK cell activation during virus infection. *Nature Immunology*, **2**(10), 951–956.

Drews, E., Adam, A., Htoo, P., Townsley, E., & Mathew, A. (2018). Upregulation of HLA-E by dengue and not Zika viruses. *Clinical & Translational Immunology*, **7**(9), e1039.

Duev-cohen, A., Bar-On, Y., Glasner, A., … Mandelboim, O. (2015). The human 2B4 and NTB-A receptors bind the influenza viral hemagglutinin and co-stimulate NK cell cytotoxicity. *Oncotarget*, **7**(11), 13093–13105.

Duncan, S. A., & Smith, G. L. (1992). Identification and characterization of an extracellular envelope glycoprotein affecting vaccinia virus egress. *Journal of Virology*, **66**(3), 1610–1621.

Dustin, M. L. (1987). Purified lymphocyte function-associated antigen 3 binds to CD2 and mediates T lymphocyte adhesion. *Journal of Experimental Medicine*, **165**(3), 677–692.

Eagle, R. A., Traherne, J. A., Hair, J. R., Jafferji, I., & Trowsdale, J. (2009). ULBP6/RAET1L is an additional human NKG2D ligand. *European Journal of Immunology*, **39**(11), 3207–3216.

Elhaik-Goldman, S., Kafka, D., Yossef, R., … Porgador, A. (2011). The Natural Cytotoxicity Receptor 1 Contribution to Early Clearance of Streptococcus pneumoniae and to Natural Killer-Macrophage Cross Talk. *PLoS ONE*, **6**(8), e23472.

Emery, J. G., McDonnell, P., Burke, M. B., … Young, P. R. (1998). Osteoprotegerin Is a Receptor for the Cytotoxic Ligand TRAIL. *Journal of Biological Chemistry*, **273**(23), 14363–14367.

Engelstad, M., Howard, S. T., & Smith, G. L. (1992). A constitutively expressed vaccinia gene encodes a 42-kDa glycoprotein related to complement control factors that forms part of the extracellular virus envelope. *Virology*, **188**(2), 801–810.

Essbauer, S., & Meyer, H. (2007). Genus Orthopoxvirus: Cowpox virus. In *Poxviruses*, Basel: Birkhäuser Basel, pp. 75–88.

Esteso, G., Guerra, S., Valés-Gómez, M., & Reyburn, H. T. (2017). Innate immune recognition of double-stranded RNA triggers increased expression of NKG2D ligands after virus infection. *Journal of Biological Chemistry*, **292**(50), 20472–20480.

Etzioni, A., Eidenschenk, C., Katz, R., Beck, R., Casanova, J. L., & Pollack, S. (2005). Fatal varicella associated with selective natural killer cell deficiency. *Journal of Pediatrics*, **146**(3), 423–425.

Falco, M., Biassoni, R., Bottino, C., … Moretta, A. (1999). Identification and Molecular Cloning of P75/Airm1, a Novel Member of the Sialoadhesin Family That Functions as an Inhibitory Receptor in Human Natural Killer Cells. *The Journal of Experimental Medicine*, **190**(6), 793–802.

Falkner, F. G., & Moss, B. (1988). Escherichia coli gpt gene provides dominant selection for vaccinia virus open reading frame expression vectors. *Journal of Virology*, **62**(6), 1849–1854.

Fang, M., Lanier, L. L., & Sigal, L. J. (2008a). A role for NKG2D in NK cell-mediated resistance to poxvirus disease. *PLoS Pathogens*, **4**(2), e30.

Fang, M., Lanier, L. L., & Sigal, L. J. (2008b). A Role for NKG2D in NK Cell–Mediated Resistance to Poxvirus Disease. *PLoS Pathogens*, **4**(2), e30.

Fang, M., Orr, M. T., Spee, P., Egebjerg, T., Lanier, L. L., & Sigal, L. J. (2011). CD94 Is Essential for NK Cell-Mediated Resistance to a Lethal Viral Disease. *Immunity*, **34**(4), 579–589.

Farré, D., Martínez-Vicente, P., Engel, P., & Angulo, A. (2017). Immunoglobulin superfamily members encoded by viruses and their multiple roles in immune evasion. *European Journal of Immunology*, **47**(5), 780–796.

Fauquet, C., Mayo, M., Maniloff, J., Desselberger, U., & Ball, L. (2005). *Virus Taxonomy: VIIIth Report of the International Committee on Taxonomy of Viruses*. (U. Academic Press (Elsevier); London, Ed.).

Fausther-Bovendo, H., Sol-Foulon, N., Candotti, D., … Vieillard, V. (2009). HIV escape from natural killer cytotoxicity: Nef inhibits NKp44L expression on CD4+ T cells. *AIDS*, **23**(9), 1077–1087.

Fenner, F., Henderson, D. A., Arita, I., JeZek, Z., & I. D. Ladnyi. (1988). Smallpox and its eradication. *Geneva: World Health Organization*, **43**(1), 92–92.

Fielding, C. A., Aicheler, R., Stanton, R. J., … Tomasec, P. (2014). Two Novel Human Cytomegalovirus NK Cell Evasion Functions Target MICA for Lysosomal Degradation. *PLoS Pathogens*, **10**(5), e1004058.

Fielding, C. A., Weekes, M. P., Nobre, L. V, … Wilkinson, G. W. G. (2017). Control of immune ligands by members of a cytomegalovirus gene expansion suppresses natural killer cell activation. *ELife*, **6**. doi:10.7554/eLife.22206

Fisicaro, P., Rossi, M., Vecchi, A., … Boni, C. (2019). The Good and the Bad of Natural Killer Cells in Virus Control: Perspective for Anti-HBV Therapy. *International Journal of Molecular Sciences*, **20**(20), 5080.

Flexner, C., Hügin, A., & Moss, B. (1987). Prevention of vaccinia virus infection in imiminodeficient mice by vector-directed IL-2 expression. *Nature*, **330**(6145), 259–262.

Fogel, L. A. (2016). *The Resolution Phase of NK Cell Proliferation and IFN Production Following Viral Infection Are Highly Regulated Processes.*

Fogel, L. A., Sun, M. M., Geurs, T. L., Carayannopoulos, L. N., & French, A. R. (2013a). Markers of Nonselective and Specific NK Cell Activation. *The Journal of Immunology*, **190**(12), 6269–6276.

Fogel, L. A., Yokoyama, W. M., & French, A. R. (2013b). Natural killer cells in human autoimmune disorders. *Arthritis Research & Therapy*, **15**(4), 216.

Franksson, L., Sundbäck, J., Achour, A., Bernlind, J., Glas, R., & Kärre, K. (1999). Peptide dependency and selectivity of the NK cell inhibitory receptor Ly-49C. *European Journal of Immunology*, **29**(9), 2748–2758.

Fu, B., Wang, F., Sun, R., Ling, B., Tian, Z., & Wei, H. (2011). CD11b and CD27 reflect distinct population and functional specialization in human natural killer cells. *Immunology*, **133**(3), 350–359.

Fuchs, A., Cella, M., Giurisato, E., Shaw, A. S., & Colonna, M. (2004). Cutting Edge: CD96 (Tactile) Promotes NK Cell-Target Cell Adhesion by Interacting with the Poliovirus Receptor (CD155). *The Journal of Immunology*, **172**(7), 3994–3998.

Gaggero, S., Bruschi, M., Petretto, A., … Cantoni, C. (2018). Nidogen-1 is a novel extracellular ligand for the NKp44 activating receptor. *OncoImmunology*, **7**(9), e1470730.

Gardiner, C. M. (2015). NK cell function and receptor diversity in the context of HCV infection. *Frontiers in Microbiology*, **6**(SEP), 1061.

Garg, A., Barnes, P. F., Porgador, A., … Vankayalapati, R. (2006). Vimentin Expressed on Mycobacterium tuberculosis -Infected Human Monocytes Is Involved in Binding to the NKp46 Receptor. *The Journal of Immunology*, **177**(9), 6192–6198.

Gazit, R., Gruda, R., Elboim, M., … Mandelboim, O. (2006). Lethal influenza infection in the absence of the natural killer cell receptor gene Ncr1. *Nature Immunology*, **7**(5), 517–23.

Geshelin, P., & Berns, K. I. (1974). Characterization and localization of the naturally occurring cross-links in vaccinia virus DNA. *Journal of Molecular Biology*, **88**(4), 785–796.

Gewurz, B. E., Wang, E. W., Tortorella, D., Schust, D. J., & Ploegh, H. L. (2001). Human Cytomegalovirus US2 Endoplasmic Reticulum-Lumenal Domain Dictates Association with Major Histocompatibility Complex Class I in a Locus-Specific Manner. *Journal of Virology*, **75**(11), 5197–5204.

Gherardi, M. M. (2003). IL-12 and IL-18 act in synergy to clear vaccinia virus infection: involvement of innate and adaptive components of the immune system. *Journal of General Virology*, **84**(8), 1961–1972.

Ghiotto, M., Gauthier, L., Serriari, N., … Olive, D. (2010). PD-L1 and PD-L2 differ in their molecular mechanisms of interaction with PD-1. *International Immunology*, **22**(8), 651–660.

Ghofrani, J., Lucar, O., Dugan, H., Reeves, R. K., & Jost, S. (2019). Semaphorin 7A modulates cytokine-induced memory-like responses by human natural killer cells. *European Journal of Immunology*, **49**(8), eji.201847931.

Ghosh, S., Nandi, M., Pal, S., … Datta, S. (2016). Natural killer cells contribute to hepatic injury and help in viral persistence during progression of hepatitis B e-antigen-negative chronic hepatitis B virus infection. *Clinical Microbiology and Infection*, **22**(8), 733.e9-733.e19.

Gillard, G. O., Bivas-Benita, M., Hovav, A. H., … Letvin, N. L. (2011). Thy1 + nk cells from vaccinia virus-primed mice confer protection against vaccinia virus challenge in the absence of adaptive lymphocytes. *PLoS Pathogens*, **7**(8). doi:10.1371/journal.ppat.1002141

Girgis, N. M., DeHaven, B. C., Fan, X., Viner, K. M., Shamim, M., & Isaacs, S. N. (2008). Cell Surface Expression of the Vaccinia Virus Complement Control Protein Is Mediated by Interaction with the Viral A56 Protein and Protects Infected Cells from Complement Attack. *Journal of Virology*, **82**(9), 4205–4214.

Girgis, N. M., DeHaven, B. C., Xiao, Y., Alexander, E., Viner, K. M., & Isaacs, S. N. (2011). The Vaccinia Virus Complement Control Protein Modulates Adaptive Immune Responses during Infection. *Journal of Virology*, **85**(6), 2547–2556.

Glimcher, L., Shen, F. W., & Cantor, H. (1977). Identification of a cell-surface antigen selectively expressed on the natural killer cell. *The Journal of Experimental Medicine*, **145**(1), 1–9.

Golden-Mason, L., Stone, A. E. L., Bambha, K. M., Cheng, L., & Rosen, H. R. (2012). Race- and gender-related variation in natural killer p46 expression associated with differential anti-hepatitis c virus immunity. *Hepatology*, **56**(4), 1214–1222.

Gomez, C., Najera, J., Krupa, M., & Esteban, M. (2008). The Poxvirus Vectors MVA and NYVAC as Gene Delivery Systems for Vaccination Against Infectious Diseases and Cancer. *Current Gene Therapy*, **8**(2), 97–120.

Goodier, M. R., Jonjić, S., Riley, E. M., & Juranić Lisnić, V. (2018). CMV and natural killer cells: shaping the response to vaccination. *European Journal of Immunology*, **48**(1), 50–65.

Goulding, J., Bogue, R., Tahiliani, V., Croft, M., & Salek-Ardakani, S. (2012). CD8 T Cells Are Essential

for Recovery from a Respiratory Vaccinia Virus Infection. *The Journal of Immunology*, **189**(5), 2432–2440.

Graham, S. C., Bahar, M. W., Abrescia, N. G. A., Smith, G. L., Stuart, D. I., & Grimes, J. M. (2007). Structure of CrmE, a Virus-encoded Tumour Necrosis Factor Receptor. *Journal of Molecular Biology*, **372**(3), 660–671.

Grell, M., Wajant, H., Zimmermann, G., & Scheurich, P. (1998). The type 1 receptor (CD120a) is the high-affinity receptor for soluble tumor necrosis factor. *Proceedings of the National Academy of Sciences*, **95**(2), 570–575.

Griewank, K., Borowski, C., Rietdijk, S., … Bendelac, A. (2007). Homotypic Interactions Mediated by Slamf1 and Slamf6 Receptors Control NKT Cell Lineage Development. *Immunity*, **27**(5), 751–762.

Gu, X., Laouar, A., Wan, J., … Manjunath, N. (2003). The gp49B1 Inhibitory Receptor Regulates the IFN- Responses of T Cells and NK Cells. *The Journal of Immunology*, **170**(8), 4095–4101.

Gubser, C., Bergamaschi, D., Hollinshead, M., Lu, X., van Kuppeveld, F. J. M., & Smith, G. L. (2007). A New Inhibitor of Apoptosis from Vaccinia Virus and Eukaryotes. *PLoS Pathogens*, **3**(2), e17.

Gubser, C., & Smith, G. L. (2002). The sequence of camelpox virus shows it is most closely related to variola virus, the cause of smallpox Accession numbers: AY009089 and AY037935. *Journal of General Virology*, **83**(4), 855–872.

Guerin, J.-L., Gelfi, J., Boullier, S., … Messud-Petit, F. (2002). Myxoma Virus Leukemia-Associated Protein Is Responsible for Major Histocompatibility Complex Class I and Fas-CD95 Down-Regulation and Defines Scrapins, a New Group of Surface Cellular Receptor Abductor Proteins. *Journal of Virology*, **76**(6), 2912–2923.

Gumá, M., Budt, M., Sáez, A., … López-Botet, M. (2006). Expansion of CD94/NKG2C+ NK cells in response to human cytomegalovirus-infected fibroblasts. *Blood*, **107**(9), 3624–3631.

Gunn, B. M., Yu, W.-H., Karim, M. M., … Alter, G. (2018). A Role for Fc Function in Therapeutic Monoclonal Antibody-Mediated Protection against Ebola Virus. *Cell Host & Microbe*, **24**(2), 221-233.e5.

Guo, Z. S., Lu, B., Guo, Z. S., … Bartlett, D. L. (2019, January 9). Vaccinia virus-mediated cancer immunotherapy: Cancer vaccines and oncolytics. *Journal for ImmunoTherapy of Cancer*, BioMed Central Ltd., pp. 1–21.

Gwozdowicz, S., Nestorowicz, K., Graczyk-Pol, E., … Nowak, J. (2019). KIR specificity and avidity of standard and unusual C1, C2, Bw4, Bw6 and A3/11 amino acid motifs at entire HLA:KIR interface between NK and target cells, the functional and evolutionary classification of HLA class I molecules. *International Journal of Immunogenetics*, **46**(4), 217–231.

Haddad, D. (2017). Genetically Engineered Vaccinia Viruses As Agents for Cancer Treatment, Imaging, and Transgene Delivery. *Frontiers in Oncology*, **7**(MAY), 1.

Haeryfar, S. M. M., & Hoskin, D. W. (2004). Thy-1: More than a Mouse Pan-T Cell Marker. *The Journal of Immunology*, **173**(6), 3581–3588.

Hammarlund, E., Lewis, M. W., Hansen, S. G., … Slifka, M. K. (2003). Duration of antiviral immunity after smallpox vaccination. *Nature Medicine*, **9**(9), 1131–1137.

Hammer, Q., Rückert, T., Borst, E. M., … Romagnani, C. (2018). Peptide-specific recognition of human cytomegalovirus strains controls adaptive natural killer cells. *Nature Immunology*, **19**(5), 453–463.

Hanke, T., Takizawa, H., McMahon, C. W., … Raulet, D. H. (1999). Direct assessment of MHC class I binding by seven Ly49 inhibitory NK cell receptors. *Immunity*, **11**(1), 67–77.

Hanson, D., & Diven, D. G. (2003). Molluscum contagiosum. *Dermatology Online Journal*, **9**(2), 2.

Harvey, I. B., Wang, X., & Fremont, D. H. (2019). Molluscum contagiosum virus MC80 sabotages MHC-I antigen presentation by targeting tapasin for ER-associated degradation. *PLOS Pathogens*, **15**(4), e1007711.

Hatfield, S. D., Daniels, K. A., O'Donnell, C. L., Waggoner, S. N., & Welsh, R. M. (2018). Weak vaccinia virus-induced NK cell regulation of CD4 T cells is associated with reduced NK cell differentiation and cytolytic activity. *Virology*, **519**, 131–144.

Hayakawa, Y., & Smyth, M. J. (2006). CD27 Dissects Mature NK Cells into Two Subsets with Distinct Responsiveness and Migratory Capacity. *The Journal of Immunology*, **176**(3), 1517–1524.

Hayes, R. L., Koslow, M., Hiesiger, E. M., … Ransohoff, J. (1995). Improved long term survival after intracavitary interleukin-2 and lymphokine-activated killer cells for adults with recurrent malignant glioma. *Cancer*, **76**(5), 840–852.

He, Y., Guo, Y., Fan, C., … Jia, Z. (2017). Interferon-α-Enhanced CD100/Plexin-B1/B2 Interactions Promote Natural Killer Cell Functions in Patients with Chronic Hepatitis C Virus Infection. *Frontiers in Immunology*, **8**, 1435.

Hecht, M.-L., Rosental, B., Horlacher, T., … Seeberger, P. H. (2009). Natural Cytotoxicity Receptors NKp30, NKp44 and NKp46 Bind to Different Heparan Sulfate/Heparin Sequences. *Journal of Proteome Research*, **8**(2), 712–720.

Hendricks, D. W., Balfour, H. H., Dunmire, S. K., Schmeling, D. O., Hogquist, K. A., & Lanier, L. L. (2014). Cutting Edge: NKG2C hi CD57 + NK Cells Respond Specifically to Acute Infection with Cytomegalovirus and Not Epstein–Barr Virus. *The Journal of Immunology*, **192**(10), 4492–4496.

Henney, C. S., Kuribayashi, K., Kern, D. E., & Gillis, S. (1981). Interleukin-2 augments natural killer cell activity. *Nature*, **291**(5813), 335–338.

Herberman, R. B., Nunn, M. E., Holden, H. T., & Lavrin, D. H. (1975). Natural cytotoxic reactivity of mouse lymphoid cells against syngeneic and allogeneic tumors. II. Characterization of effector cells. *International Journal of Cancer*, **16**(2), 230–239.

Hesslein, D. G. T., & Lanier, L. L. (2011). Transcriptional Control of Natural Killer Cell Development and Function. In *Advances in Immunology*, Vol. 109, Academic Press Inc., pp. 45–85.

Hill, C., & Carlisle, R. (2019). Achieving systemic delivery of oncolytic viruses. *Expert Opinion on Drug Delivery*, **16**(6), 607–620.

Hiller, G., & Weber, K. (1985). Golgi-derived membranes that contain an acylated viral polypeptide are used for vaccinia virus envelopment. *Journal of Virology*, **55**(3), 651–659.

Hinman, A. R. (1998). Global progress in infectious disease control. *Vaccine*, **16**(11–12), 1116–1121.

Hirst, C. E., Buzza, M. S., Bird, C. H., … Bird, P. I. (2003). The Intracellular Granzyme B Inhibitor, Proteinase Inhibitor 9, Is Up-Regulated During Accessory Cell Maturation and Effector Cell Degranulation, and Its Overexpression Enhances CTL Potency. *The Journal of Immunology*, **170**(2), 805–815.

Hollinshead, M., Rodger, G., Van Eijl, H., … Smith, G. L. (2001). Vaccinia virus utilizes microtubules for movement to the cell surface. *Journal of Cell Biology*, **154**(2), 389–402.

Hollyoake, M. (2005). NKp30 (NCR3) is a Pseudogene in 12 Inbred and Wild Mouse Strains, but an Expressed Gene in Mus caroli. *Molecular Biology and Evolution*, **22**(8), 1661–1672.

Holmes, T. D., & Bryceson, Y. T. (2016). Natural killer cell memory in context. *Seminars in Immunology*, **28**(4), 368–376.

Holmes, V. M., Maluquer de Motes, C., Richards, P. T., … Krummenacher, C. (2019). Interaction between nectin-1 and the human natural killer cell receptor CD96. *PLOS ONE*, **14**(2), e0212443.

Horton, N. C., Mathew, S. O., & Mathew, P. A. (2013). Novel Interaction between Proliferating Cell Nuclear Antigen and HLA I on the Surface of Tumor Cells Inhibits NK Cell Function through NKp44. *PLoS ONE*, **8**(3), e59552.

Hosomi, S., Chen, Z., Baker, K., … Blumberg, R. S. (2013). CEACAM1 on activated NK cells inhibits NKG2D-mediated cytolytic function and signaling. *European Journal of Immunology*, **43**(9), 2473–2483.

Houchins, J. P., Lanier, L. L., Niemi, E. C., Phillips, J. H., & Ryan, J. C. (1997). Natural killer cell cytolytic activity is inhibited by NKG2-A and activated by NKG2-C. *Journal of Immunology (Baltimore, Md. : 1950)*, **158**(8), 3603–9.

Howard, A. R., Senkevich, T. G., & Moss, B. (2008). Vaccinia Virus A26 and A27 Proteins Form a Stable Complex Tethered to Mature Virions by Association with the A17 Transmembrane Protein. *Journal of Virology*, **82**(24), 12384–12391.

Hsiao, J.-C., Chung, C.-S., & Chang, W. (1999). Vaccinia Virus Envelope D8L Protein Binds to Cell Surface Chondroitin Sulfate and Mediates the Adsorption of Intracellular Mature Virions to Cells. *Journal of Virology*, **73**(10), 8750–8761.

Hunter, S., Jones, P., Mitchell, A., … Yong, S. Y. (2012). InterPro in 2011: New developments in the family and domain prediction database. *Nucleic Acids Research*, **40**(D1). doi:10.1093/nar/gkr948

Hutchens, M. A., Luker, K. E., Sonstein, J., Núñez, G., Curtis, J. L., & Luker, G. D. (2008a). Protective Effect of Toll-like Receptor 4 in Pulmonary Vaccinia Infection. *PLoS Pathogens*, **4**(9), e1000153.

Hutchens, M., Luker, K. E., Sottile, P., … Luker, G. D. (2008b). TLR3 Increases Disease Morbidity and Mortality from Vaccinia Infection. *The Journal of Immunology*, **180**(1), 483–491.

Ichihashi, Y., & Dales, S. (1971). Biogenesis of poxviruses: Interrelationship between hemagglutinin production and polykaryocytosis. *Virology*, **46**(3), 533–543.

Ichihashi, Y., Matsumoto, S., & Dales, S. (1971). Biogenesis of poxviruses: Role of A-type inclusions and host cell membranes in virus dissemination. *Virology*, **46**(3), 507–532.

Iizuka, K., Naidenko, O. V., Plougastel, B. F. M., Fremont, D. H., & Yokoyama, W. M. (2003). Genetically linked C-type lectin-related ligands for the NKRP1 family of natural killer cell receptors. *Nature Immunology*, **4**(8), 801–807.

Imai, H., Nakamoto, Y., Asakura, K., Miki, K., Yasuda, T., & Miura, A. B. (1985). Spontaneous glomerular IgA deposition in ddY mice: An animal model of IgA nephritis. *Kidney International*, **27**(5), 756–761.

Imai, K., Matsuyama, S., Miyake, S., Suga, K., & Nakachi, K. (2000). Natural cytotoxic activity of peripheral-blood lymphocytes and cancer incidence: An 11-year follow-up study of a general population. *Lancet*, **356**(9244), 1795–1799.

Isaacs, S. N., Wolffe, E. J., Payne, L. G., & Moss, B. (1992). Characterization of a vaccinia virus-

encoded 42-kilodalton class I membrane glycoprotein component of the extracellular virus envelope. *Journal of Virology*, **66**(12), 7217–24.

Ishido, S., Choi, J.-K., Lee, B.-S., … Jung, J. U. (2000a). Inhibition of Natural Killer Cell–Mediated Cytotoxicity by Kaposi's Sarcoma–Associated Herpesvirus K5 Protein. *Immunity*, **13**(3), 365–374.

Ishido, S., Wang, C., Lee, B.-S., Cohen, G. B., & Jung, J. U. (2000b). Downregulation of Major Histocompatibility Complex Class I Molecules by Kaposi's Sarcoma-Associated Herpesvirus K3 and K5 Proteins. *Journal of Virology*, **74**(11), 5300–5309.

Ito, M., Maruyama, T., Saito, N., Koganei, S., Yamamoto, K., & Matsumoto, N. (2006). Killer cell lectin-like receptor G1 binds three members of the classical cadherin family to inhibit NK cell cytotoxicity. *The Journal of Experimental Medicine*, **203**(2), 289–295.

Iwasaki, A., & Medzhitov, R. (2015). Control of adaptive immunity by the innate immune system. *Nature Immunology*, **16**(4), 343–353.

Jacobs, B. L., Langland, J. O., Kibler, K. V., … Baskin, C. R. (2009). Vaccinia virus vaccines: Past, present and future. *Antiviral Research*, **84**(1), 1–13.

Jacobs, N., Bartlett, N. W., Clark, R. H., & Smith, G. L. (2008). Vaccinia virus lacking the Bcl-2-like protein N1 induces a stronger natural killer cell response to infection. *Journal of General Virology*, **89**(11), 2877–2881.

Jacobs, N., Chen, R. a-J., Gubser, C., Najarro, P., & Smith, G. L. (2006). Intradermal immune response after infection with Vaccinia virus. *The Journal of General Virology*, **87**(Pt 5), 1157–61.

Jacoby, R. O., Bhatt, P. N., & Brownstein, D. G. (1989). Evidence that NK cells and interferon are required for genetic resistance to lethal infection with ectromelia virus. *Archives of Virology*, **108**(1–2), 49–58.

Jafferji, I., Bain, M., King, C., & Sinclair, J. H. (2009). Inhibition of epidermal growth factor receptor (EGFR) expression by human cytomegalovirus correlates with an increase in the expression and binding of Wilms' Tumour 1 protein to the EGFR promoter. *Journal of General Virology*, **90**(7), 1569–1574.

Jan Chalupny, N., Sutherland, C. L., Lawrence, W. A., Rein-Weston, A., & Cosman, D. (2003). ULBP4 is a novel ligand for human NKG2D. *Biochemical and Biophysical Research Communications*, **305**(1), 129–135.

Jarahian, M., Fiedler, M., Cohnen, A., … Momburg, F. (2011). Modulation of nkp30- and nkp46-mediated natural killer cell responses by poxviral hemagglutinin. *PLoS Pathogens*, **7**(8). doi:10.1371/journal.ppat.1002195

Jarahian, M., Watzl, C., Fournier, P., … Momburg, F. (2009). Activation of Natural Killer Cells by Newcastle Disease Virus Hemagglutinin-Neuraminidase. *Journal of Virology*, **83**(16), 8108–8121.

Jezek, Z., Grab, B., Szczeniowski, M. V., Paluku, K. M., & Mutombo, M. (1988). Human monkeypox: secondary attack rates. *Bulletin of the World Health Organization*, **66**(4), 465–70.

Joller, N., Hafler, J. P., Brynedal, B., … Kuchroo, V. K. (2011). Cutting Edge: TIGIT Has T Cell-Intrinsic Inhibitory Functions. *The Journal of Immunology*, **186**(3), 1338–1342.

Jones, E. Y. (1997). MHC class I and class II structures. *Current Opinion in Immunology*, **9**(1), 75–79.

Jonjić, S., Babić, M., Polić, B., & Krmpotić, A. (2008). Immune evasion of natural killer cells by viruses.

Current Opinion in Immunology, **20**(1), 30–38.

Jost, S., & Altfeld, M. (2013). Control of Human Viral Infections by Natural Killer Cells. *Annual Review of Immunology*, **31**(1), 163–194.

Kaiserman, D., Stewart, S. E., Plasman, K., Gevaert, K., Van Damme, P., & Bird, P. I. (2014). Identification of Serpinb6b as a Species-specific Mouse Granzyme A Inhibitor Suggests Functional Divergence between Human and Mouse Granzyme A. *Journal of Biological Chemistry*, **289**(13), 9408–9417.

Karlhofer, F. M., Ribaudo, R. K., & Yokoyama, W. M. (1992). The interaction of Ly-49 with H-2Dd globally inactivates natural killer cell cytolytic activity. *Transactions of the Association of American Physicians*, **105**, 72–85.

Kärre, K. (2008). Natural killer cell recognition of missing self. *Nature Immunology*, **9**(5), 477–480.

Kastenmayer, R. J., Maruri-Avidal, L., Americo, J. L., Earl, P. L., Weisberg, A. S., & Moss, B. (2014). Elimination of A-type inclusion formation enhances cowpox virus replication in mice: Implications for orthopoxvirus evolution. *Virology*, **452–453**, 59–66.

Kayagaki, N., Yamaguchi, N., Nakayama, M., … Yagita, H. (1999). Expression and function of TNF-related apoptosis-inducing ligand on murine activated NK cells. *Journal of Immunology (Baltimore, Md. : 1950)*, **163**(4), 1906–1913.

Kelley, J., Walter, L., & Trowsdale, J. (2005). Comparative Genomics of Natural Killer Cell Receptor Gene Clusters. *PLoS Genetics*, **1**(2), e27.

Kennedy, M. K., Glaccum, M., Brown, S. N., … Peschon, J. J. (2000). Reversible Defects in Natural Killer and Memory Cd8 T Cell Lineages in Interleukin 15–Deficient Mice. *The Journal of Experimental Medicine*, **191**(5), 771–780.

Kennedy, R., & Poland, G. A. (2007). T-Cell epitope discovery for variola and vaccinia viruses. *Reviews in Medical Virology*, **17**(2), 93–113.

Kettle, S., Alcamí, A., Khanna, A., Ehret, R., Jassoy, C., & Smith, G. L. (1997). Vaccinia virus serpin B13R(SPI-2) inhibits interleukin-1β-converting enzyme and protects virus-infected cells from TNF- and Fas-mediated apoptosis, but does not prevent IL-1β-induced fever. *Journal of General Virology*, **78**(3), 677–685.

Khakoo, S. I., & Carrington, M. (2006). KIR and disease: a model system or system of models? *Immunological Reviews*, **214**(1), 186–201.

Kielczewska, A., Pyzik, M., Sun, T., … Vidal, S. M. (2009). Ly49P recognition of cytomegalovirus-infected cells expressing H2-D k and CMV-encoded m04 correlates with the NK cell antiviral response. *The Journal of Experimental Medicine*, **206**(3), 515–523.

Kiessling, R., Klein, E., & Wigzell, H. (1975). „Natural" killer cells in the mouse. I. Cytotoxic cells with specificity for mouse Moloney leukemia cells. Specificity and distribution according to genotype. *European Journal of Immunology*, **5**(2), 112–117.

Kim, M. J., Lee, J.-C., Lee, J.-J., … Heo, D. S. (2008). Association of CD47 with Natural Killer Cell-Mediated Cytotoxicity of Head-and-Neck Squamous Cell Carcinoma Lines. *Tumor Biology*, **29**(1), 28–34.

Kim, S., Iizuka, K., Kang, H.-S. P., … Yokoyama, W. M. (2002). In vivo developmental stages in murine natural killer cell maturation. *Nature Immunology*, **3**(6), 523–528.

Kirwan, S., Merriam, D., Barsby, N., McKinnon, A., & Burshtyn, D. N. (2006). Vaccinia virus

modulation of natural killer cell function by direct infection. *Virology*, **347**(1), 75–87.

Knight, J. C., Goldsmith, C. S., Tamin, A., Regnery, R. L., Regnery, D. C., & Esposito, J. J. (1992). Further analyses of the orthopoxviruses volepox virus and raccoon poxvirus. *Virology*, **190**(1), 423–433.

Koch, T., Dahlke, C., Fathi, A., … Addo, M. M. (2020). Safety and immunogenicity of a modified vaccinia virus Ankara vector vaccine candidate for Middle East respiratory syndrome: an open-label, phase 1 trial. *The Lancet Infectious Diseases*, **20**(7), 827–838.

Kogure, A., Shiratori, I., Wang, J., Lanier, L. L., & Arase, H. (2011). PANP is a novel O-glycosylated PILRα ligand expressed in neural tissues. *Biochemical and Biophysical Research Communications*, **405**(3), 428–433.

Koka, R., Burkett, P., Chien, M., Chai, S., Boone, D. L., & Ma, A. (2004). Cutting Edge: Murine Dendritic Cells Require IL-15Rα to Prime NK Cells. *The Journal of Immunology*, **173**(6), 3594–3598.

Kubin, M., Cassiano, L., Chalupny, J., … Armitage, R. (2001). ULBP1, 2, 3: novel MHC class I-related molecules that bind to human cytomegalovirus glycoprotein UL16, activate NK cells. *European Journal of Immunology*, **31**(5), 1428–1437.

Kulkarni, S., Savan, R., Qi, Y., … Carrington, M. (2011). Differential microRNA regulation of HLA-C expression and its association with HIV control. *Nature*, **472**(7344), 495–498.

Kumar, S. (2018). Natural killer cell cytotoxicity and its regulation by inhibitory receptors. *Immunology*, **154**(3), 383–393.

Kumaresan, P. R., Lai, W. C., Chuang, S. S., Bennett, M., & Mathew, P. A. (2002). CS1, a novel member of the CD2 family, is homophilic and regulates NK cell function. *Molecular Immunology*, **39**(1–2), 1–8.

Kundu, K., Ghosh, S., Sarkar, R., … Porgador, A. (2019). Inhibition of the NKp44-PCNA Immune Checkpoint Using a mAb to PCNA. *Cancer Immunology Research*, **7**(7), 1120–1134.

Kuroki, K., Furukawa, A., & Maenaka, K. (2012). Molecular Recognition of Paired Receptors in the Immune System. *Frontiers in Microbiology*, **3**, 429.

Kvansakul, M., Yang, H., Fairlie, W. D., … Colman, P. M. (2008). Vaccinia virus anti-apoptotic F1L is a novel Bcl-2-like domain-swapped dimer that binds a highly selective subset of BH3-containing death ligands. *Cell Death & Differentiation*, **15**(10), 1564–1571.

Lanier, L. L. (1998). *NK CELL RECEPTORS*. *Annu. Rev. Immunol*, Vol. 16.

Lanier, L. L. (2003). Natural killer cell receptor signaling. *Current Opinion in Immunology*, **15**(3), 308–314.

Lanier, L. L. (2008). Up on the tightrope: natural killer cell activation and inhibition. *Nature Immunology*, **9**(5), 495–502.

Lanier, L. L., Corliss, B., Wu, J., & Phillips, J. H. (1998). Association of DAP12 with Activating CD94/NKG2C NK Cell Receptors. *Immunity*, **8**(6), 693–701.

Lanier, L. L., Le, A. M., Civin, C. I., Loken, M. R., & Phillips, J. H. (1986a). The relationship of CD16 (Leu-11) and Leu-19 (NKH-1) antigen expression on human peripheral blood NK cells and cytotoxic T lymphocytes. *Journal of Immunology (Baltimore, Md. : 1950)*, **136**(12), 4480–6.

Lanier, L. L., Phillips, J. H., Hackett, J., Tutt, M., & Kumar, V. (1986b). Natural killer cells: definition of a cell type rather than a function. *Journal of Immunology (Baltimore, Md. : 1950)*, **137**(9), 2735–

9.

Latchman, Y., Mckay, P. F., & Reiser, H. (1998). *Molecule as a Counter-Receptor for CD48 Cutting Edge: Identification of the 2B4*.

Law, K. M., & Smith, G. L. (1992). A vaccinia serine protease inhibitor which prevents virus-induced cell fusion. *Journal of General Virology*, **73**(3), 549–557.

Law, M., Carter, G. C. G., Roberts, K. L., Hollinshead, M., & Smith, G. L. (2006). Ligand-induced and nonfusogenic dissolution of a viral membrane. *Proceedings of the National Academy of Sciences of the United States of America*, **103**(15), 5989–5994.

Law, M., & Smith, G. L. (2001). Antibody Neutralization of the Extracellular Enveloped Form of Vaccinia Virus. *Virology*, **280**(1), 132–142.

Lazear, E., Peterson, L. W., Nelson, C. A., & Fremont, D. H. (2013). Crystal Structure of the Cowpox Virus-Encoded NKG2D Ligand OMCP. *Journal of Virology*, **87**(2), 840–850.

Le Bouteiller, P., Tabiasco, J., Polgar, B., … Jabrane-Ferrat, N. (2011). CD160: A unique activating NK cell receptor. *Immunology Letters*, **138**(2), 93–96.

Lebbink, R. J., de Ruiter, T., Adelmeijer, J., … Meyaard, L. (2006). Collagens are functional, high affinity ligands for the inhibitory immune receptor LAIR-1. *The Journal of Experimental Medicine*, **203**(6), 1419–1425.

Lee, K. H., Ono, M., Inui, M., Yuasa, T., & Takai, T. (2000). Stimulatory Function of gp49A, a Murine Ig-Like Receptor, in Rat Basophilic Leukemia Cells. *The Journal of Immunology*, **165**(9), 4970–4977.

Lee, M. S., Roos, J. M., McGuigan, L. C., … Payne, L. G. (1992). Molecular attenuation of vaccinia virus: mutant generation and animal characterization. *Journal of Virology*, **66**(5), 2617–2630.

Lee, N., Llano, M., Carretero, M., … Geraghty, D. E. (1998). HLA-E is a major ligand for the natural killer inhibitory receptor CD94/NKG2A. *Proceedings of the National Academy of Sciences*, **95**(9), 5199–5204.

Lefkowitz, E. J., Wang, C., & Upton, C. (2006). Poxviruses: Past, present and future. *Virus Research*, **117**(1), 105–118.

Lenac Rovis, T., Kucan Brlic, P., Kaynan, N., … Jonjic, S. (2016). Inflammatory monocytes and NK cells play a crucial role in DNAM-1–dependent control of cytomegalovirus infection. *The Journal of Experimental Medicine*, **213**(9), 1835–1850.

Li, M., Xia, P., Du, Y., … Fan, Z. (2014). T-cell Immunoglobulin and ITIM Domain (TIGIT) Receptor/Poliovirus Receptor (PVR) Ligand Engagement Suppresses Interferon-γ Production of Natural Killer Cells via β-Arrestin 2-mediated Negative Signaling. *Journal of Biological Chemistry*, **289**(25), 17647–17657.

Lin, C.-L., Chung, C.-S., Heine, H. G., & Chang, W. (2000). Vaccinia Virus Envelope H3L Protein Binds to Cell Surface Heparan Sulfate and Is Important for Intracellular Mature Virion Morphogenesis and Virus Infection In Vitro and In Vivo. *Journal of Virology*, **74**(7), 3353–3365.

Lisnić, B., Lisnić, V. J., & Jonjić, S. (2015). NK cell interplay with cytomegaloviruses. *Current Opinion in Virology*, **15**, 9–18.

Liu, W., Garrett, S. C., Fedorov, E. V, … Almo, S. C. (2019). Structural Basis of CD160:HVEM Recognition. *Structure*, **27**(8), 1286-1295.e4.

Liu, W., Xu, C., Zhao, H., … Liu, Z. (2015). Osteoprotegerin induces apoptosis of osteoclasts and osteoclast precursor cells via the fas/fas ligand pathway. *PLoS ONE*, **10**(11). doi:10.1371/journal.pone.0142519

Ljunggren, H.-G., & Kärre, K. (1990). In search of the 'missing self': MHC molecules and NK cell recognition. *Immunology Today*, **11**(C), 237–244.

Lopez-Vergès, S., Milush, J. M., Schwartz, B. S., … Lanier, L. L. (2011). Expansion of a unique CD57 +NKG2C hi natural killer cell subset during acute human cytomegalovirus infection. *Proceedings of the National Academy of Sciences of the United States of America*, **108**(36), 14725–14732.

Lucas, M., Schachterle, W., Oberle, K., Aichele, P., & Diefenbach, A. (2007). Dendritic Cells Prime Natural Killer Cells by trans-Presenting Interleukin 15. *Immunity*, **26**(4), 503–517.

Luevano, M., Madrigal, A., & Saudemont, A. (2012). Transcription factors involved in the regulation of natural killer cell development and function: an update. *Frontiers in Immunology*, **3**(OCT), 319.

Lundstrom, K. (2018). New frontiers in oncolytic viruses: optimizing and selecting for virus strains with improved efficacy. *Biologics: Targets and Therapy*, **Volume 12**, 43–60.

Luque, I., Reyburn, H., & Strominger, J. L. (2000). Expression of the CD80 and CD86 molecules enhances cytotoxicity by human natural killer cells. *Human Immunology*, **61**(8), 721–728.

Machold, R. P., Wiertz, E. J. H. J., Jones, T. R., & Ploegh, H. L. (1997). The HCMV Gene Products US11 and US2 Differ in Their Ability to Attack Allelic Forms of Murine Major Histocompatibility Complex (MHC) Class I Heavy Chains. *The Journal of Experimental Medicine*, **185**(2), 363–366.

Mack, E. A., Kallal, L. E., Demers, D. A., & Biron, C. A. (2011). Type 1 Interferon Induction of Natural Killer Cell Gamma Interferon Production for Defense during Lymphocytic Choriomeningitis Virus Infection. *MBio*, **2**(4). doi:10.1128/mBio.00169-11

Maeda, M., Carpenito, C., Russell, R. C., … Takei, F. (2005). Murine CD160, Ig-Like Receptor on NK Cells and NKT Cells, Recognizes Classical and Nonclassical MHC Class I and Regulates NK Cell Activation. *The Journal of Immunology*, **175**(7), 4426–4432.

Maeda, T., Suetake, H., Odaka, T., & Miyadai, T. (2018). Original Ligand for LTβR Is LIGHT: Insight into Evolution of the LT/LTβR System. *The Journal of Immunology*, **201**(1), 202–214.

Maki, J., Guiot, A.-L., Aubert, M., … Lankau, E. W. (2017). Oral vaccination of wildlife using a vaccinia–rabies-glycoprotein recombinant virus vaccine (RABORAL V-RG®): a global review. *Veterinary Research*, **48**(1), 57.

Maksyutov, R. A., Gavrilova, E. V., Meyer, H., & Shchelkunov, S. N. (2015). Real-time PCR assay for specific detection of cowpox virus. *Journal of Virological Methods*, **211**, 8–11.

Malnati, M., Peruzzi, M., Parker, K., … Long, E. (1995). Peptide specificity in the recognition of MHC class I by natural killer cell clones. *Science*, **267**(5200), 1016–1018.

Maloy, K. J., Burkhart, C., Junt, T. M., … Hengartner, H. (2000). Cd4+ T Cell Subsets during Virus Infection. *The Journal of Experimental Medicine*, **191**(12), 2159–2170.

Mandal, A., & Viswanathan, C. (2015). Natural killer cells: In health and disease. *Hematology/Oncology and Stem Cell Therapy*, **8**(2), 47–55.

Mandelboim, O., Lieberman, N., Lev, M., … Porgador, A. (2001). Recognition of haemagglutinins on virus-infected cells by NKp46 activates lysis by human NK cells. *Nature*, **409**(6823), 1055–1060.

Mandelboim, O., Malik, P., Davis, D. M., Jo, C. H., Boyson, J. E., & Strominger, J. L. (1999). Human CD16 as a lysis receptor mediating direct natural killer cell cytotoxicity. *Proceedings of the National Academy of Sciences*, **96**(10), 5640–5644.

Markel, G., Lieberman, N., Katz, G., … Mandelboim, O. (2002). CD66a Interactions Between Human Melanoma and NK Cells: A Novel Class I MHC-Independent Inhibitory Mechanism of Cytotoxicity. *The Journal of Immunology*, **168**(6), 2803–2810.

Marsh, S. G. E., Parham, P., Dupont, B., … Wain, H. (2003). Killer-cell immunoglobulin-like receptor (KIR) nomenclature report, 2002. *Immunogenetics*, **55**(4), 220–226.

Martín-Fontecha, A., Lord, G. M., & Brady, H. J. M. (2011). Transcriptional control of natural killer cell differentiation and function. *Cellular and Molecular Life Sciences*, **68**(21), 3495–3503.

Martín-Fontecha, A., Thomsen, L. L., Brett, S., … Sallusto, F. (2004). Induced recruitment of NK cells to lymph nodes provides IFN-γ for TH1 priming. *Nature Immunology*, **5**(12), 1260–1265.

Martinez, J., Huang, X., & Yang, Y. (2008). Direct Action of Type I IFN on NK Cells Is Required for Their Activation in Response to Vaccinia Viral Infection In Vivo. *The Journal of Immunology*, **180**(3), 1592–1597.

Martinez, J., Huang, X., & Yang, Y. (2010a). Direct TLR2 Signaling Is Critical for NK Cell Activation and Function in Response to Vaccinia Viral Infection. *PLoS Pathogens*, **6**(3), e1000811.

Martinez, J., Huang, X., & Yang, Y. (2010b). Toll-like receptor 8-mediated activation of murine plasmacytoid dendritic cells by vaccinia viral DNA. *Proceedings of the National Academy of Sciences*, **107**(14), 6442–6447.

Mason, L. H., Anderson, S. K., Yokoyama, W. M., Smith, H. R. C., Winkler-Pickett, R., & Ortaldo, J. R. (1996). The Ly-49D Receptor Activates Murine Natural Killer Cells. *Journal of Experimental Medicine*, **184**(6), 2119–2128.

Mastrangelo, M. J., Maguire, H. C., Eisenlohr, L. C., … Lattime, E. C. (1999). Intratumoral recombinant GM-CSF-encoding virus as gene therapy in patients with cutaneous melanoma. *Cancer Gene Therapy*, **6**(5), 409–422.

Matta, J., Baratin, M., Chiche, L., … Vivier, E. (2013). Induction of B7-H6, a ligand for the natural killer cell-activating receptor NKp30, in inflammatory conditions. *Blood*, **122**(3), 394–404.

Mayr, A., Hochstein-Mintzel, V., & Stickl, H. (1975). Abstammung, Eigenschaften und Verwendung des attenuierten Vaccinia-Stammes MVA. *Infection*, **3**(1), 6–14.

Mayrink de Oliveira, D., Marques Campos, J., de Oliveira Silva, S., & Norma Melo, M. (2019). Vaccinia Virus-Derived Vectors in Leishmaniases Vaccine Development. In *Vaccines - the History and Future*, IntechOpen. doi:10.5772/intechopen.85302

McAlister, G. C., Huttlin, E. L., Haas, W., … Gygi, S. P. (2012). Increasing the Multiplexing Capacity of TMTs Using Reporter Ion Isotopologues with Isobaric Masses. *Analytical Chemistry*, **84**(17), 7469–7478.

McAlister, G. C., Nusinow, D. P., Jedrychowski, M. P., … Gygi, S. P. (2014). MultiNotch MS3 Enables Accurate, Sensitive, and Multiplexed Detection of Differential Expression across Cancer Cell Line Proteomes. *Analytical Chemistry*, **86**(14), 7150–7158.

McCollum, A. M., & Damon, I. K. (2014). Human Monkeypox. *Clinical Infectious Diseases*, **58**(2), 260–267.

McCoy, W. H., Wang, X., Yokoyama, W. M., Hansen, T. H., & Fremont, D. H. (2012). Structural

Mechanism of ER Retrieval of MHC Class I by Cowpox. *PLoS Biology*, **10**(11), e1001432.

McKelvey, T. A., Andrews, S. C., Miller, S. E., Ray, C. A., & Pickup, D. J. (2002). Identification of the Orthopoxvirus p4c Gene, Which Encodes a Structural Protein That Directs Intracellular Mature Virus Particles into A-Type Inclusions. *Journal of Virology*, **76**(22), 11216–11225.

McLysaght, A., Baldi, P. F., & Gaut, B. S. (2003). Extensive gene gain associated with adaptive evolution of poxviruses. *Proceedings of the National Academy of Sciences*, **100**(26), 15655–15660.

Melo-Silva, C. R., Tscharke, D. C., Lobigs, M., … Regner, M. (2011). The Ectromelia Virus SPI-2 Protein Causes Lethal Mousepox by Preventing NK Cell Responses. *Journal of Virology*, **85**(21), 11170–11182.

Meng, R. D., McDonald, E. R., Sheikh, M. S., Fornace, A. J., & El-Deiry, W. S. (2000). The TRAIL Decoy Receptor TRUNDD (DcR2, TRAIL-R4) Is Induced by Adenovirus-p53 Overexpression and Can Delay TRAIL-, p53-, and KILLER/DR5-Dependent Colon Cancer Apoptosis. *Molecular Therapy*, **1**(2), 130–144.

Mercer, J., & Helenius, A. (2008). Vaccinia virus uses macropinocytosis and apoptotic mimicry to enter host cells. *Science*, **320**(5875), 531–535.

Meyer, H., Ehmann, R., & Smith, G. L. (2020). Smallpox in the post-eradication Era. *Viruses*, **12**(2), 1–11.

Miller, J. S., Soignier, Y., Panoskaltsis-Mortari, A., … McGlave, P. B. (2005). Successful adoptive transfer and in vivo expansion of human haploidentical NK cells in patients with cancer. *Blood*, **105**(8), 3051–3057.

Minev, B. R., Lander, E., Feller, J. F., … Szalay, A. A. (2019). First-in-human study of TK-positive oncolytic vaccinia virus delivered by adipose stromal vascular fraction cells. *Journal of Translational Medicine*, **17**(1), 271.

Mizrahi, S., Markel, G., Porgador, A., Bushkin, Y., & Mandelboim, O. (2007). CD100 on NK Cells Enhance IFNγ Secretion and Killing of Target Cells Expressing CD72. *PLoS ONE*, **2**(9), e818.

Mocikat, R., Braumüller, H., Gumy, A., … Röcken, M. (2003). Natural Killer Cells Activated by MHC Class ILow Targets Prime Dendritic Cells to Induce Protective CD8 T Cell Responses. *Immunity*, **19**(4), 561–569.

Montel, A. H., Bochan, M. R., Hobbs, J. A., Lynch, D. H., & Brahmi, Z. (1995a). Fas Involvement in Cytotoxicity Mediated by Human NK Cells. *Cellular Immunology*, **166**(2), 236–246.

Montel, A. H., Morse, P. A., & Brahmi, Z. (1995b). Upregulation of B7 molecules by the Epstein—Barr virus enhances susceptibility to lysis by a human NK-like cell line. *Cellular Immunology*, **160**(1), 104–114.

Morandi, B., Bougras, G., Muller, W. A., Ferlazzo, G., & Münz, C. (2006). NK cells of human secondary lymphoid tissues enhance T cell polarizationvia IFN-γ secretion. *European Journal of Immunology*, **36**(9), 2394–2400.

Morandi, B., Bramanti, P., Bonaccorsi, I., … Ferlazzo, G. (2008, January). Role of natural killer cells in the pathogenesis and progression of multiple sclerosis. *Pharmacological Research*, Pharmacol Res, pp. 1–5.

Mori, M., Leitman, E., Walker, B., Ndung'u, T., Carrington, M., & Goulder, P. (2019). Impact of HLA Allele-KIR Pairs on HIV Clinical Outcome in South Africa. *The Journal of Infectious Diseases*, **219**(9), 1456–1463.

Moss, B. (2007). *Poxviridae: the viruses and their replicaton*. (D. E. FIELDS, B. N., KNIPE, D. M., HOWLEY, P. M., GRIFFIN, Ed.), Fiels viro, Lippincott Williams & Wilkins.

Moss, B. (2012). Poxvirus Cell Entry: How Many Proteins Does it Take? *Viruses*, **4**(5), 688–707.

Moss, B. (2013). Poxvirus DNA Replication. *Cold Spring Harbor Perspectives in Biology*, **5**(9), a010199–a010199.

Moss, B., Fuerst, T. R., Flexner, C., & Hugin, A. (1988). Roles of vaccinia virus in the development of new vaccines. *Vaccine*, **6**(2), 161–163.

Moss, B., & Rosenblum, E. N. (1973). Protein cleavage and poxvirus morphogenesis: Tryptic peptide analysis of core precursors accumulated by blocking assembly with rifampicin. *Journal of Molecular Biology*, **81**(2), 267–269.

Mossman, K., Upton, C., Buller, R. M. L., & McFadden, G. (1995). Species Specificity of Ectromelia Virus and Vaccinia Virus Interferon-γ Binding Proteins. *Virology*, **208**(2), 762–769.

Moussa, P., Marton, J., Vidal, S. M., & Fodil-Cornu, N. (2013). Genetic dissection of NK cell responses. *Frontiers in Immunology*, **3**(JAN), 1–11.

Muller, W. A., Weigl, S. A., Deng, X., & Phillips, D. M. (1993). PECAM-1 is required for transendothelial migration of leukocytes. *The Journal of Experimental Medicine*, **178**(2), 449–460.

Nabekura, T., Kanaya, M., Shibuya, A., Fu, G., Gascoigne, N. R. J., & Lanier, L. L. (2014). Costimulatory Molecule DNAM-1 Is Essential for Optimal Differentiation of Memory Natural Killer Cells during Mouse Cytomegalovirus Infection. *Immunity*, **40**(2), 225–234.

Nagler, F. P. O. (1942). APPLICATION OF HIRST'S PHENOMENON TO THE TITRATION OF VACCINIA VIRUS AND VACCINIA IMMUNE SERUM. *Medical Journal of Australia*, **1**(10), 281–283.

Naiyer, M. M., Cassidy, S. A., Magri, A., … Khakoo, S. I. (2017). KIR2DS2 recognizes conserved peptides derived from viral helicases in the context of HLA-C. *Science Immunology*, **2**(15), eaal5296.

Nakano, K., Asano, R., Tsumoto, K., … Glorioso, J. C. (2005). Herpes Simplex Virus Targeting to the EGF Receptor by a gD-Specific Soluble Bridging Molecule. *Molecular Therapy*, **11**(4), 617–626.

Natuk, R. J., & Welsh, R. M. (1986). Accumulation and chemotaxis of natural killer / large granular lymphocytes at sites of virus replication . *The Journal of Immunology*, **138**(3), 877–883.

Nelson, J. B. (1938). THE BEHAVIOR OF POX VIRUSES IN THE RESPIRATORY TRACT. *The Journal of Experimental Medicine*, **68**(3), 401–412.

Ng, A., Smith, G. L., Tscharke, D. C., & Reading, P. C. (2001). The vaccinia virus A41L protein is a soluble 30 kDa glycoprotein that affects virus virulence. *Journal of General Virology*, **82**(9), 2095–2105.

Nguyen, K. B., Salazar-Mather, T. P., Dalod, M. Y., … Biron, C. A. (2002). Coordinated and Distinct Roles for IFN-αβ, IL-12, and IL-15 Regulation of NK Cell Responses to Viral Infection. *The Journal of Immunology*, **169**(8), 4279–4287.

Nicoll, G., Ni, J., Liu, D., … Crocker, P. R. (1999). Identification and Characterization of a Novel Siglec, Siglec-7, Expressed by Human Natural Killer Cells and Monocytes. *Journal of Biological Chemistry*, **274**(48), 34089–34095.

Nightingale, K., Lin, K.-M., Ravenhill, B. J., … Weekes, M. P. (2018). High-Definition Analysis of Host

Protein Stability during Human Cytomegalovirus Infection Reveals Antiviral Factors and Viral Evasion Mechanisms. *Cell Host & Microbe*, **24**(3), 447-460.e11.

Nikzad, R., Angelo, L. S., Aviles-Padilla, K., … Paust, S. (2019). Human natural killer cells mediate adaptive immunity to viral antigens. *Science Immunology*, **4**(35), eaat8116.

Ninove, L., Domart, Y., Vervel, C., … Charrel, R. N. (2009). Cowpox Virus Transmission from Pet Rats to Humans, France. *Emerging Infectious Diseases*, **15**(5), 781–784.

Notario, L., Alari-pahissa, E., Molina, A. De, De Molina, A., Lauzurica, P., & Molina, A. De. (2016). CD69 Deficiency Enhances the Host Response to Vaccinia Virus Infection through Altered NK Cell Homeostasis. *Journal of Virology*, **90**(14), 6464–6474.

Nowak, I., Wilczyńska, K., Wilczyński, J. R., … Kuśnierczyk, P. (2017). KIR, LILRB and their Ligands' Genes as Potential Biomarkers in Recurrent Implantation Failure. *Archivum Immunologiae et Therapiae Experimentalis*, **65**(5), 391–399.

O'Leary, J. G., Goodarzi, M., Drayton, D. L., & von Andrian, U. H. (2006). T cell– and B cell–independent adaptive immunity mediated by natural killer cells. *Nature Immunology*, **7**(5), 507–516.

O'Sullivan, T. E., Sun, J. C., & Lanier, L. L. (2015). Natural Killer Cell Memory. *Immunity*, **43**(4), 634–645.

Ogasawara, K., Yoshinaga, S. K., & Lanier, L. L. (2002). Inducible Costimulator Costimulates Cytotoxic Activity and IFN-γ Production in Activated Murine NK Cells. *The Journal of Immunology*, **169**(7), 3676–3685.

Ogbomo, H., & Mody, C. H. (2017, January 11). Granule-dependent natural killer cell cytotoxicity to fungal pathogens. *Frontiers in Immunology*, Frontiers Media S.A., p. 11.

Okeke, M. I., Adekoya, O. A., Moens, U., Tryland, M., Traavik, T., & Nilssen, Ø. (2009). Comparative sequence analysis of A-type inclusion (ATI) and P4c proteins of orthopoxviruses that produce typical and atypical ATI phenotypes. *Virus Genes*, **39**(2), 200–209.

Orange, J. S. (2013). Natural killer cell deficiency. *Journal of Allergy and Clinical Immunology*, **132**(3), 515–525.

Orange, J. S. (2020). How I Manage Natural Killer Cell Deficiency. *Journal of Clinical Immunology*, **40**(1), 13–23.

Orange, J. S., Fassett, M. S., Koopman, L. A., Boyson, J. E., & Strominger, J. L. (2002). Viral evasion of natural killer cells. *Nature Immunology*, **3**(11), 1006–1012.

Orbelyan, G. A., Tang, F., Sally, B., … Jabri, B. (2014). Human NKG2E Is Expressed and Forms an Intracytoplasmic Complex with CD94 and DAP12. *The Journal of Immunology*, **193**(2), 610–616.

Ortaldo, J. R., Winkler-Pickett, R., Wigginton, J., … Young, H. A. (2006). Regulation of ITAM-positive receptors: role of IL-12 and IL-18. *Blood*, **107**(4), 1468–1475.

Osborne, J. D., Da Silva, M., Frace, A. M., … Esposito, J. J. (2007). Genomic differences of Vaccinia virus clones from Dryvax smallpox vaccine: The Dryvax-like ACAM2000 and the mouse neurovirulent Clone-3. *Vaccine*, **25**(52), 8807–8832.

Osterrieder, N., Meyer, H., & Pfeffer, M. (1994). Characterization of the gene encoding the A-type inclusion body protein of mousepox virus. *Virus Genes*, **8**(1), 125–135.

Pahl, J. H. W., Cerwenka, A., & Ni, J. (2018). Memory-Like NK Cells: Remembering a Previous

Activation by Cytokines and NK Cell Receptors. *Frontiers in Immunology*, **9**, 2796.

Pan, G., O'Rourke, K., Chinnaiyan, A. M., … Dixit, V. M. (1997). The receptor for the cytotoxic ligand TRAIL. *Science*, **276**(5309), 111–113.

Paolini, R., Bernardini, G., Molfetta, R., & Santoni, A. (2015). NK cells and interferons. *Cytokine & Growth Factor Reviews*, **26**(2), 113–120.

Parham, P. (2015). *The immune System- Fourth Edition*.

Parham, P., Barnstable, C. J., & Bodmer, W. F. (1979). Use of a monoclonal antibody (W6/32) in structural studies of HLA-A,B,C, antigens. *Journal of Immunology*, **123**(1), 342–9.

Parham, P., & Moffett, A. (2013). Variable NK cell receptors and their MHC class I ligands in immunity, reproduction and human evolution. *Nature Reviews Immunology*, **13**(2), 133–144.

Parham, P., Norman, P. J., Abi-Rached, L., & Guethlein, L. A. (2012). Human-specific evolution of killer cell immunoglobulin-like receptor recognition of major histocompatibility complex class I molecules. *Philosophical Transactions of the Royal Society B: Biological Sciences*, **367**(1590), 800–811.

Parker, A. K., Parker, S., Yokoyama, W. M., Corbett, J. A., & Buller, R. M. L. (2007a). Induction of Natural Killer Cell Responses by Ectromelia Virus Controls Infection. *Journal of Virology*, **81**(8), 4070–4079.

Parker, R. F., Bronson, L. H., & Green, R. H. (1941). FURTHER STUDIES OF THE INFECTIOUS UNIT OF VACCINIA. *The Journal of Experimental Medicine*, **74**(3), 263–281.

Parker, S., Nuara, A., Buller, R. M. L., & Schultz, D. A. (2007b). Human monkeypox: an emerging zoonotic disease. *Future Microbiology*, **2**(1), 17–34.

Parkinson, J. E., Sanderson, C. M., & Smith, G. L. (1995). The Vaccinia Virus A38L Gene Product Is a 33-kDa Integral Membrane Glycoprotein. *Virology*, **214**(1), 177–188.

Parkinson, J. E., & Smith, G. L. (1994). Vaccinia Virus Gene A36R Encodes a Mr 43-50 K Protein on the Surface of Extracellular Enveloped Virus. *Virology*, **204**(1), 376–390.

Parry, D. A., Holmes, T. D., Gamper, N., … Mighell, A. J. (2016). A homozygous STIM1 mutation impairs store-operated calcium entry and natural killer cell effector function without clinical immunodeficiency. *Journal of Allergy and Clinical Immunology*, **137**(3), 955-957.e8.

Pascolo, S., Ginhoux, F., Laham, N., … Rammensee, H.-G. (2005). The non-classical HLA class I molecule HFE does not influence the NK-like activity contained in fresh human PBMCs and does not interact with NK cells. *International Immunology*, **17**(2), 117–122.

Pastoret, P., Brochier, B., Languet, B., … Et, A. (1988). First field trial of fox vaccination against rabies using a vaccinia-rabies recombinant virus. *Veterinary Record*, **123**(19), 481–483.

Patel, D. D., Pickup, D. J., & Joklik, W. K. (1986). Isolation of cowpox virus a-type inclusions and characterization of their major protein component. *Virology*, **149**(2), 174–189.

Paul, S., & Lal, G. (2017). The Molecular Mechanism of Natural Killer Cells Function and Its Importance in Cancer Immunotherapy. *Frontiers in Immunology*, **8**(SEP), 1124.

Paust, S., Gill, H. S., Wang, B.-Z., … von Andrian, U. H. (2010). Critical role for the chemokine receptor CXCR6 in NK cell–mediated antigen-specific memory of haptens and viruses. *Nature Immunology*, **11**(12), 1127–1135.

Payne, L. G. (1980). Significance of Extracellular Enveloped Virus in the in vitro and in vivo

Dissemination of Vaccinia. *Journal of General Virology*, **50**(1), 89–100.

Payne, L. G., & Norrby, E. (1976). Presence of Haemagglutinin in the Envelope of Extracellular Vaccinia Virus Particles. *Journal of General Virology*, **32**(1), 63–72.

Pelin, A., Boulton, S., Tamming, L. A., Bell, J. C., & Singaravelu, R. (2020). Engineering vaccinia virus as an immunotherapeutic battleship to overcome tumor heterogeneity. *Expert Opinion on Biological Therapy*, **0**(0), 1.

Pende, D., Parolini, S., Pessino, A., … Moretta, A. (1999). Identification and Molecular Characterization of Nkp30, a Novel Triggering Receptor Involved in Natural Cytotoxicity Mediated by Human Natural Killer Cells. *The Journal of Experimental Medicine*, **190**(10), 1505–1516.

Peng, Y., Luo, G., Zhou, J., … Wu, J. (2013). CD86 Is an Activation Receptor for NK Cell Cytotoxicity against Tumor Cells. *PLoS ONE*, **8**(12), e83913.

Perez-Villar, J. J., Zapata, J. M., Melero, I., Postigo, A., & Sanchez-Madrid, F. (1996). *Expression and function of a4/b7 integrin on human natural killer cells*. *Immunology*, Vol. 89.

Perkus, M. E., Taylor, J., Tartaglia, J., … Paoletti, E. (1995). Live attenuated vaccinia and other poxviruses as delivery systems: public health issues. *Annals of the New York Academy of Sciences*, **754**(1), 222–33.

Piccioli, D., Sbrana, S., Melandri, E., & Valiante, N. M. (2002). Contact-dependent Stimulation and Inhibition of Dendritic Cells by Natural Killer Cells. *The Journal of Experimental Medicine*, **195**(3), 335–341.

Pignoloni, B., Fionda, C., Dell'Oste, V., … Cerboni, C. (2016). Distinct Roles for Human Cytomegalovirus Immediate Early Proteins IE1 and IE2 in the Transcriptional Regulation of MICA and PVR/CD155 Expression. *The Journal of Immunology*, **197**(10), 4066–4078.

Pogge von Strandmann, E., Simhadri, V. R., von Tresckow, B., … Engert, A. (2007). Human Leukocyte Antigen-B-Associated Transcript 3 Is Released from Tumor Cells and Engages the NKp30 Receptor on Natural Killer Cells. *Immunity*, **27**(6), 965–974.

Prlic, M., Gibbs, J., & Jameson, S. C. (2005). Characteristics of NK cell migration early after vaccinia infection. *Journal of Immunology (Baltimore, Md. : 1950)*, **175**(4), 2152–7.

Prod'homme, V., Sugrue, D. M., Stanton, R. J., … Tomasec, P. (2010). Human cytomegalovirus UL141 promotes efficient downregulation of the natural killer cell activating ligand CD112. *Journal of General Virology*, **91**(8), 2034–2039.

Pütz, M. M., Midgley, C. M., Law, M., & Smith, G. L. (2006). Quantification of antibody responses against multiple antigens of the two infectious forms of Vaccinia virus provides a benchmark for smallpox vaccination. *Nature Medicine*, **12**(11), 1310–1315.

Pyzik, M., Charbonneau, B., Gendron-Pontbriand, E.-M., … Vidal, S. M. (2011). Distinct MHC class I–dependent NK cell–activating receptors control cytomegalovirus infection in different mouse strains. *The Journal of Experimental Medicine*, **208**(5), 1105–1117.

Quoix, E., Lena, H., Losonczy, G., … Limacher, J.-M. (2016). TG4010 immunotherapy and first-line chemotherapy for advanced non-small-cell lung cancer (TIME): results from the phase 2b part of a randomised, double-blind, placebo-controlled, phase 2b/3 trial. *The Lancet Oncology*, **17**(2), 212–223.

Rabin, E. M., Gordon, K., Knoppers, M. H., … Dwyer, D. S. (1993). Inhibition of T Cell Activation and Adhesion Functions by Soluble CD2 Protein. *Cellular Immunology*, **149**(1), 24–38.

Rahim, M. M. A., Chen, P., Mottashed, A. N., … Makrigiannis, A. P. (2015). The mouse NKR-P1B:Clr-b recognition system is a negative regulator of innate immune responses. *Blood*, **125**(14), 2217–2227.

Rajagopalan, S., & Long, E. O. (2005). Understanding how combinations of HLA and KIR genes influence disease. *The Journal of Experimental Medicine*, **201**(7), 1025–1029.

Rajagopalan, S., & Long, E. O. (2013). Found: a cellular activating ligand for NKp44. *Blood*, **122**(17), 2921–2922.

Raulet, D. H., Gasser, S., Gowen, B. G., Deng, W., & Jung, H. (2013). Regulation of Ligands for the NKG2D Activating Receptor. *Annual Review of Immunology*, **31**(1), 413–441.

Ravetch, J. V. (2000). Immune Inhibitory Receptors. *Science*, **290**(5489), 84–89.

Reading, P. C., & Smith, G. L. (2003). Vaccinia Virus Interleukin-18-Binding Protein Promotes Virulence by Reducing Gamma Interferon Production and Natural Killer and T-Cell Activity. *Journal of Virology*, **77**(18), 9960–9968.

Reeves, R. K., Li, H. H., Jost, S., … Barouch, D. H. (2015). Antigen-specific NK cell memory in rhesus macaques. *Nature Immunology*, **16**(9), 927–932.

Reyburn, H., Esteso, G., Ashiru, O., & Vales-Gomez, M. (2015). Viral strategies to modulate NKG2D-ligand expression in Human Cytomegalovirus infection. *New Horizons in Translational Medicine*, **2**(6–7), 159–166.

Ricordel, M., Foloppe, J., Pichon, C., … Erbs, P. (2018). Oncolytic properties of non-vaccinia poxviruses. *Oncotarget*, **9**(89), 35891–35906.

Riedel, S. (2005). Edward Jenner and the History of Smallpox and Vaccination. *Baylor University Medical Center Proceedings*, **18**(1), 21–25.

Risco, C., Rodriguez, J. R., Lopez-Iglesias, C., Carrascosa, J. L., Esteban, M., & Rodriguez, D. (2002). Endoplasmic Reticulum-Golgi Intermediate Compartment Membranes and Vimentin Filaments Participate in Vaccinia Virus Assembly. *Journal of Virology*, **76**(4), 1839–1855.

Rivera, R., Hutchens, M., Luker, K. E., Sonstein, J., Curtis, J. L., & Luker, G. D. (2007). Murine alveolar macrophages limit replication of vaccinia virus. *Virology*, **363**(1), 48–58.

Robbins, S. H., Tessmer, M. S., Mikayama, T., & Brossay, L. (2004). Expansion and Contraction of the NK Cell Compartment in Response to Murine Cytomegalovirus Infection. *The Journal of Immunology*, **173**(1), 259–266.

Roberts, K. L., & Smith, G. L. (2008). Vaccinia virus morphogenesis and dissemination. *Trends in Microbiology*, **16**(10), 472–479.

Rooney, I. A., Butrovich, K. D., Glass, A. A., … Ware, C. F. (2000). The Lymphotoxin-β Receptor Is Necessary and Sufficient for LIGHT-mediated Apoptosis of Tumor Cells. *Journal of Biological Chemistry*, **275**(19), 14307–14315.

Roper, R. L., Payne, L. G., & Moss, B. (1996). Extracellular vaccinia virus envelope glycoprotein encoded by the A33R gene. *Journal of Virology*, **70**(6), 3753–3762.

Rosen, D. B., Bettadapura, J., Alsharifi, M., Mathew, P. A., Warren, H. S., & Lanier, L. L. (2005). Cutting Edge: Lectin-Like Transcript-1 Is a Ligand for the Inhibitory Human NKR-P1A Receptor. *The Journal of Immunology*, **175**(12), 7796–7799.

Rosenberg, S. A. (1984). Immunotherapy of cancer by systemic administration of lymphoid cells plus

interleukin-2. *Journal of Biological Response Modifiers*, **3**(5), 501–511.

Rosental, B., Brusilovsky, M., Hadad, U., … Porgador, A. (2011). Proliferating Cell Nuclear Antigen Is a Novel Inhibitory Ligand for the Natural Cytotoxicity Receptor NKp44. *The Journal of Immunology*, **187**(11), 5693–5702.

Sadasiv, E. C., Chang, P. W., & Gulka, G. (1985). Morphogenesis of canary poxvirus and its entrance into inclusion bodies. *American Journal of Veterinary Research*, **46**(2), 529–535.

Sánchez-Puig, J. M., Sánchez, L., Roy, G., & Blasco, R. (2004). Susceptibility of different leukocyte cell types to Vaccinia virus infection. *Virology Journal*, **1**(1), 10.

Sanderson, C. M., Frischknecht, F., Way, M., Hollinshead, M., & Smith, G. L. (1998). Roles of vaccinia virus EEV-specific proteins in intracellular actin tail formation and low pH-induced cell-cell fusion. *Journal of General Virology*, **79**(6), 1415–1425.

Sanderson, C. M., Hollinshead, M., & Smith, G. L. (2000). The vaccinia virus A27L protein is needed for the microtubule-dependent transport of intracellular mature virus particles. *Journal of General Virology*, **81**(1), 47–58.

Saphire, E. O., Schendel, S. L., Fusco, M. L., … Dye, J. M. (2018a). Systematic Analysis of Monoclonal Antibodies against Ebola Virus GP Defines Features that Contribute to Protection. *Cell*, **174**(4), 938-952.e13.

Saphire, E. O., Schendel, S. L., Gunn, B. M., Milligan, J. C., & Alter, G. (2018b). Antibody-mediated protection against Ebola virus. *Nature Immunology*, **19**(11), 1169–1178.

Saunders, P. M., MacLachlan, B. J., Pymm, P., … Brooks, A. G. (2020). The molecular basis of how buried human leukocyte antigen polymorphism modulates natural killer cell function. *Proceedings of the National Academy of Sciences*, 201920570.

Schmelz, M., Sodeik, B., Ericsson, M., … Griffiths, G. (1994). Assembly of vaccinia virus: the second wrapping cisterna is derived from the trans Golgi network. *Journal of Virology*, **68**(1), 130–47.

Schmidt, F. I., Bleck, C. K. E., Helenius, A., & Mercer, J. (2011). Vaccinia extracellular virions enter cells by macropinocytosis and acid-activated membrane rupture. *The EMBO Journal*, **30**(17), 3647–3661.

Schuster, I. S., Coudert, J. D., Andoniou, C. E., & Degli-Esposti, M. A. (2016). "Natural Regulators": NK Cells as Modulators of T Cell Immunity. *Frontiers in Immunology*, **7**(JUN), 235.

Šedý, J. R., Bjordahl, R. L., Bekiaris, V., … Benedict, C. A. (2013). CD160 activation by herpesvirus entry mediator augments inflammatory cytokine production and cytolytic function by NK cells. *Journal of Immunology*, **191**(2), 828–836.

Seitz, R. (2010, December). Orthopox viruses: Infections in humans. *Transfusion Medicine and Hemotherapy*, Karger Publishers, pp. 351–364.

Seki, M., Oie, M., Ichihashi, Y., & Shida, H. (1990). Hemadsorption and fusion inhibition activities of hemagglutinin analyzed by vaccinia virus mutants. *Virology*, **175**(2), 372–384.

Selvaraj, P., Plunkett, M. L., Dustin, M., Sanders, M. E., Shaw, S., & Springer, T. A. (1987). The T lymphocyte glycoprotein CD2 binds the cell surface ligand LFA-3. *Nature*, **326**(6111), 400–403.

Senkevich, T. G., & Moss, B. (1998). Domain Structure, Intracellular Trafficking, and β2-Microglobulin Binding of a Major Histocompatibility Complex Class I Homolog Encoded by Molluscum Contagiosum Virus. *Virology*, **250**(2), 397–407.

Seth, S., Maier, M. K., Qiu, Q., … Bernhardt, G. (2007). The murine pan T cell marker CD96 is an adhesion receptor for CD155 and nectin-1. *Biochemical and Biophysical Research Communications*, **364**(4), 959–965.

Sheridan J P, Marsters S A, Pitti R M, … Ashkenazi A. (1997). Control of TRAIL-induced apoptosis by a family of signaling and decoy receptors. *Science*, **277**(5327), 818–821.

Shi, L., Li, K., Guo, Y., … Krupnick, A. S. (2018). Modulation of NKG2D, NKp46, and Ly49C/I facilitates natural killer cell-mediated control of lung cancer. *Proceedings of the National Academy of Sciences*, **115**(46), 11808–11813.

Shida, H. (1986). Nucleotide sequence of the vaccinia virus hemagglutinin gene. *Virology*, **150**(2), 451–462.

Shida, H. (1989). Vaccinia virus hemagglutinin. *Sub-Cellular Biochemistry*, Springer, Boston, MA, pp. 405–440.

Shida, H., & Dales, S. (1981). Biogenesis of vaccinia: Carbohydrate of the hemagglutinin molecule. *Virology*, **111**(1), 56–72.

Shida, H., & Dales, S. (1982). Biogenesis of vaccinia: Molecular basis for the hemagglutination-negative phenotype of the IHD-W strain. *Virology*, **117**(1), 219–237.

Shida, H., Hinuma, Y., Hatanaka, M., … Kitamura, R. (1988). Effects and virulences of recombinant vaccinia viruses derived from attenuated strains that express the human T-cell leukemia virus type I envelope gene. *Journal of Virology*, **62**(12), 4474–80.

Shiroishi, M., Kuroki, K., Rasubala, L., … Maenaka, K. (2006). Structural basis for recognition of the nonclassical MHC molecule HLA-G by the leukocyte Ig-like receptor B2 (LILRB2/LIR2/ILT4/CD85d). *Proceedings of the National Academy of Sciences*, **103**(44), 16412–16417.

Shiroishi, M., Tsumoto, K., Amano, K., … Maenaka, K. (2003). Human inhibitory receptors Ig-like transcript 2 (ILT2) and ILT4 compete with CD8 for MHC class I binding and bind preferentially to HLA-G. *Proceedings of the National Academy of Sciences*, **100**(15), 8856–8861.

Simonetta, F., Alvarez, M., & Negrin, R. S. (2017, April 25). Natural killer cells in graft-versus-host-disease after allogeneic hematopoietic cell transplantation. *Frontiers in Immunology*, Frontiers Research Foundation, p. 25.

Sivori, S., Vitale, M., Morelli, L., … Moretta, A. (1997). p46, a Novel Natural Killer Cell–specific Surface Molecule That Mediates Cell Activation. *The Journal of Experimental Medicine*, **186**(7), 1129–1136.

Skálová, T., Kotýnková, K., Dušková, J., … Dohnálek, J. (2012). Mouse Clr-g, a Ligand for NK Cell Activation Receptor NKR-P1F: Crystal Structure and Biophysical Properties. *The Journal of Immunology*, **189**(10), 4881–4889.

Sklenovská, N., & Van Ranst, M. (2018). Emergence of Monkeypox as the Most Important Orthopoxvirus Infection in Humans. *Frontiers in Public Health*, **6**, 241.

Smith, G. L., Benfield, C. T. O., Maluquer de Motes, C., … Sumner, R. P. (2013). Vaccinia virus immune evasion: mechanisms, virulence and immunogenicity. *Journal of General Virology*, **94**(11), 2367–2392.

Smith, G. L., Chan, Y. S., & Howard, S. T. (1991). Nucleotide sequence of 42 kbp of vaccinia virus strain WR from near the right inverted terminal repeat. *Journal of General Virology*, **72**(6), 1349–1376.

Smith, G. L., Mackett, M., & Moss, B. (1983a). Infectious vaccinia virus recombinants that express hepatitis B virus surface antigen. *Nature*, **302**(5908), 490–495.

Smith, G. L., & Moss, B. (1983). Infectious poxvirus vectors have capacity for at least 25 000 base pairs of foreign DNA. *Gene*, **25**(1), 21–28.

Smith, G. L., Murphy, B. R., & Moss, B. (1983b). Construction and characterization of an infectious vaccinia virus recombinant that expresses the influenza hemagglutinin gene and induces resistance to influenza virus infection in hamsters. *Proceedings of the National Academy of Sciences*, **80**(23), 7155–7159.

Smith, G. L., Talbot-Cooper, C., & Lu, Y. (2018). How Does Vaccinia Virus Interfere With Interferon? In *Advances in virus research*, Vol. 100, pp. 355–378.

Smith, G. L., Vanderplasschen, A., & Law, M. (2002a). The formation and function of extracellular enveloped vaccinia virus. *Journal of General Virology*, **83**(12), 2915–2931.

Smith, H., Heusel, J. W., Mehta, I. K., … Yokoyama, W. M. (2002b). Recognition of a virus-encoded ligand by a natural killer cell activation receptor. *Proceedings of the National Academy of Sciences*, **99**(13), 8826–8831.

Snetkov, X., Weisswange, I., Pfanzelter, J., Humphries, A. C., & Way, M. (2016). NPF motifs in the vaccinia virus protein A36 recruit intersectin-1 to promote Cdc42:N-WASP-mediated viral release from infected cells. *Nature Microbiology*, **1**(10), 16141.

Soday, L., Lu, Y., Albarnaz, J. D., … Smith, G. L. (2019). Quantitative Temporal Proteomic Analysis of Vaccinia Virus Infection Reveals Regulation of Histone Deacetylases by an Interferon Antagonist Resource Quantitative Temporal Proteomic Analysis of Vaccinia Virus Infection Reveals Regulation of Histone Deacety. *CellReports*, **27**(6), 1920-1933.e7.

Sojka, D. K., Tian, Z., & Yokoyama, W. M. (2014). Tissue-resident natural killer cells and their potential diversity. *Seminars in Immunology*, **26**(2), 127–131.

Sood, C. L., & Moss, B. (2010). Vaccinia virus A43R gene encodes an orthopoxvirus-specific late non-virion type-1 membrane protein that is dispensable for replication but enhances intradermal lesion formation. *Virology*, **396**(1), 160–168.

Spreu, J., Kuttruff, S., Stejfova, V., Dennehy, K. M., Schittek, B., & Steinle, A. (2010). Interaction of C-type lectin-like receptors NKp65 and KACL facilitates dedicated immune recognition of human keratinocytes. *Proceedings of the National Academy of Sciences*, **107**(11), 5100–5105.

Stanietsky, N., Simic, H., Arapovic, J., … Mandelboim, O. (2009). The interaction of TIGIT with PVR and PVRL2 inhibits human NK cell cytotoxicity. *Proceedings of the National Academy of Sciences*, **106**(42), 17858–17863.

Stegmann, K. A., Björkström, N. K., Ciesek, S., … Wedemeyer, H. (2012). Interferon α–Stimulated Natural Killer Cells From Patients With Acute Hepatitis C Virus (HCV) Infection Recognize HCV-Infected and Uninfected Hepatoma Cells via DNAX accessory molecule-1. *The Journal of Infectious Diseases*, **205**(9), 1351–1362.

Steinle, A., Li, P., Morris, D. L., … Spies, T. (2001). Interactions of human NKG2D with its ligands MICA, MICB, and homologs of the mouse RAE-1 protein family. *Immunogenetics*, **53**(4), 279–87.

Stephensen, C. B. (2001). V ITAMIN A, I NFECTION , AND I MMUNE F UNCTION *. *Annual Review of Nutrition*, **21**(1), 167–192.

Stern, N., Markel, G., Arnon, T. I., … Mandelboim, O. (2005). Carcinoembryonic Antigen (CEA) Inhibits

NK Killing via Interaction with CEA-Related Cell Adhesion Molecule 1. *The Journal of Immunology*, **174**(11), 6692–6701.

Stiles, K. M., & Krummenacher, C. (2010). Glycoprotein D actively induces rapid internalization of two nectin-1 isoforms during herpes simplex virus entry. *Virology*, **399**(1), 109–119.

Stiles, K. M., Milne, R. S. B., Cohen, G. H., Eisenberg, R. J., & Krummenacher, C. (2008). The herpes simplex virus receptor nectin-1 is down-regulated after trans-interaction with glycoprotein D. *Virology*, **373**(1), 98–111.

Sun, J. C., Beilke, J. N., & Lanier, L. L. (2009a). Adaptive immune features of natural killer cells. *Nature*, **457**. doi:10.1038/nature07665

Sun, J. C., Beilke, J. N., & Lanier, L. L. (2010). Immune memory redefined: characterizing the longevity of natural killer cells. *Immunological Reviews*, **236**(1), 83–94.

Sun, J. C., Beilke, J. N., Lanier, L. L., & Francisco, S. (2009b). Adaptive Immune Features of Natural Killer Cells Joseph. *Nature*, **457**(7229), 557–561.

Sun, Y., Senger, K., Baginski, T. K., … Zarrin, A. A. (2012). Evolutionarily Conserved Paired Immunoglobulin-like Receptor α (PILRα) Domain Mediates Its Interaction with Diverse Sialylated Ligands. *Journal of Biological Chemistry*, **287**(19), 15837–15850.

Symons, J. A., Adams, E., Tscharke, D. C., Reading, P. C., Waldmann, H., & Smith, G. L. (2002). The vaccinia virus C12L protein inhibits mouse IL-18 and promotes virus virulence in the murine intranasal model. *Journal of General Virology*, **83**(11), 2833–2844.

Symons, J. A., Alcami, A., Smith, G. L., & William, S. (1995). Vaccinia Virus Encodes a Soluble Type I Interferon Receptor of Novel Structure and Broad Species Specificity. *Cell*, **61**, 551–560.

Tahara-Hanaoka, S. (2004). Functional characterization of DNAM-1 (CD226) interaction with its ligands PVR (CD155) and nectin-2 (PRR-2/CD112). *International Immunology*, **16**(4), 533–538.

Tahara-Hanaoka, S., Miyamoto, A., Hara, A., Honda, S., Shibuya, K., & Shibuya, A. (2005). Identification and characterization of murine DNAM-1 (CD226) and its poliovirus receptor family ligands. *Biochemical and Biophysical Research Communications*, **329**(3), 996–1000.

Takeda, K., Hayakawa, Y., Smyth, M. J., … Okumura, K. (2001). Involvement of tumor necrosis factor-related apoptosis-inducing ligand in surveillance of tumor metastasis by liver natural killer cells. *Nature Medicine*, **7**(1), 94–100.

Takeda, K., Oshima, H., Hayakawa, Y., … Okumura, K. (2000). CD27-Mediated Activation of Murine NK Cells. *The Journal of Immunology*, **164**(4), 1741–1745.

Tanaka-Kataoka, M., Kunikata, T., Takayama, S., Ohashi, K., Ikeda, M., & Kurimoto, M. (1999). In vivo antiviral effect of interleukin 18 in a mouse model of vaccinia virus infection. *Cytokine*, **11**(8), 593–599.

Tangye, S. G., Phillips, J. H., & Lanier, L. L. (2000). The CD2-subset of the Ig superfamily of cell surface molecules: receptor–ligand pairs expressed by NK cells and other immune cells. *Seminars in Immunology*, **12**(2), 149–157.

Tangye, S. G., Phillips, J. H., Lanier, L. L., & Nichols, K. E. (2000). Cutting Edge: Functional Requirement for SAP in 2B4-Mediated Activation of Human Natural Killer Cells as Revealed by the X-Linked Lymphoproliferative Syndrome. *The Journal of Immunology*, **165**(6), 2932–2936.

Tessmer, M. S., Fugere, C., Stevenaert, F., … Brossay, L. (2007). KLRG1 binds cadherins and preferentially associates with SHIP-1. *International Immunology*, **19**(4), 391–400.

Tewari, M., & Dixit, V. M. (1995). Fas- and Tumor Necrosis Factor-induced Apoptosis Is Inhibited by the Poxvirus crmA Gene Product. *Journal of Biological Chemistry*, **270**(7), 3255–3260.

Titus, J. A., Perez, P., Kaubisch, A., Garrido, M. A., & Segal, D. M. (1987). Human K/natural killer cells targeted with hetero-cross-linked antibodies specifically lyse tumor cells in vitro and prevent tumor growth in vivo. *Journal of Immunology (Baltimore, Md. : 1950)*, **139**(9), 3153–8.

Tolonen, N., Doglio, L., Schleich, S., & Locker, J. K. (2001). Vaccinia Virus DNA Replication Occurs in Endoplasmic Reticulum-enclosed Cytoplasmic Mini-Nuclei. *Molecular Biology of the Cell*, **12**(7), 2031–2046.

Tomasec, P., Braud, V. M., Rickards, C., … Wilkinson, G. W. G. (2000). Surface Expression of HLA-E, an Inhibitor of Natural Killer Cells, Enhanced by Human Cytomegalovirus gpUL40. *Science*, **287**(5455), 1031–1033.

Tomasec, P., Wang, E. C. Y., Davison, A. J., … Wilkinson, G. W. G. (2005). Downregulation of natural killer cell–activating ligand CD155 by human cytomegalovirus UL141. *Nature Immunology*, **6**(2), 181–188.

Tooze, J., Hollinshead, M., Reis, B., Radsak, K., & Kern, H. (1993). Progeny vaccinia and human cytomegalovirus particles utilize early endosomal cisternae for their envelopes. *European Journal of Cell Biology*, **60**(1), 163–178.

Torres-Domínguez, L. E., & McFadden, G. (2019). Poxvirus oncolytic virotherapy. *Expert Opinion on Biological Therapy*, **19**(6), 561–573.

Townsley, A. C., & Moss, B. (2007). Two Distinct Low-pH Steps Promote Entry of Vaccinia Virus. *Journal of Virology*, **81**(16), 8613–8620.

Townsley, A. C., Weisberg, A. S., Wagenaar, T. R., & Moss, B. (2006). Vaccinia Virus Entry into Cells via a Low-pH-Dependent Endosomal Pathway. *Journal of Virology*, **80**(18), 8899–8908.

Townsley, E., O'Connor, G., Cosgrove, C., … Mathew, A. (2016). Interaction of a dengue virus NS1-derived peptide with the inhibitory receptor KIR3DL1 on natural killer cells. *Clinical & Experimental Immunology*, **183**(3), 419–430.

Trinchieri, G. (1989). Biology of Natural Killer Cells. In *Advances in Immunology*, Vol. 47, Academic Press, pp. 187–376.

Tscharke, D. C., Reading, P. C., & Smith, G. L. (2002). Dermal infection with vaccinia virus reveals roles for virus proteins not seen using other inoculation routes. *Journal of General Virology*, **83**(8), 1977–1986.

Tscharke, D. C., & Smith, G. L. (1999). A model for vaccinia virus pathogenesis and immunity based on intradermal injection of mouse ear pinnae. *Journal of General Virology*, **80**(10), 2751–2755.

Tsutsui, K., Uno, F., Akatsuka, K., & Nii, S. (1983). Electron microscopic study on vaccinia virus release. *Archives of Virology*, **75**(3), 213–218.

Tu, T. C., Brown, N. K., Kim, T.-J. J., … Fu, Y.-X. X. (2015). CD160 is essential for NK-mediated IFN-γ production. *The Journal of Experimental Medicine*, **212**(3), 415–429.

Turner, G. S. (1967). Respiratory Infection of Mice with Vaccinia Virus. *Journal of General Virology*, **1**(3), 399–402.

Turner, P. C., & Moyer, R. W. (2006). The cowpox virus fusion regulator proteins SPI-3 and hemagglutinin interact in infected and uninfected cells. *Virology*, **347**(1), 88–99.

Turner, P. C., & Moyer, R. W. (2008). The vaccinia virus fusion inhibitor proteins SPI-3 (K2) and HA (A56) expressed by infected cells reduce the entry of superinfecting virus. *Virology*, **380**(2), 226–233.

Ulbrecht, M., Martinozzi, S., Grzeschik, M., … Weiss, E. H. (2000). Cutting Edge: The Human Cytomegalovirus UL40 Gene Product Contains a Ligand for HLA-E and Prevents NK Cell-Mediated Lysis. *The Journal of Immunology*, **164**(10), 5019–5022.

Umer, B. A., Noyce, R. S., Franczak, B. C., … Evans, D. H. (2020). Deciphering the Immunomodulatory Capacity of Oncolytic Vaccinia Virus to Enhance the Immune Response to Breast Cancer. *Cancer Immunology Research*, **8**(5), 618–631.

Unger, B., & Traktman, P. (2004). Vaccinia Virus Morphogenesis: A13 Phosphoprotein Is Required for Assembly of Mature Virions. *Journal of Virology*, **78**(16), 8885–8901.

van der Ploeg, K., Chang, C., Ivarsson, M. A., Moffett, A., Wills, M. R., & Trowsdale, J. (2017). Modulation of Human Leukocyte Antigen-C by Human Cytomegalovirus Stimulates KIR2DS1 Recognition by Natural Killer Cells. *Frontiers in Immunology*, **8**, 298.

van Eijl, H., Hollinshead, M., & Smith, G. L. (2000). The Vaccinia Virus A36R Protein Is a Type Ib Membrane Protein Present on Intracellular but Not Extracellular Enveloped Virus Particles. *Virology*, **271**(1), 26–36.

Vance, R. E., Jamieson, A. M., & Raulet, D. H. (1999). Recognition of the Class Ib Molecule Qa-1b by Putative Activating Receptors Cd94/Nkg2c and Cd94/Nkg2e on Mouse Natural Killer Cells. *The Journal of Experimental Medicine*, **190**(12), 1801–1812.

Vanderplasschen, A., Hollinshead, M., & Smith, G. L. (1997). Antibodies against vaccinia virus do not neutralize extracellular enveloped virus but prevent virus release from infected cells and comet formation. *Journal of General Virology*, **78**(8), 2041–2048.

Vanderplasschen, A., Mathew, E., Hollinshead, M., Sim, R. B., & Smith, G. L. (1998). Extracellular enveloped vaccinia virus is resistant to complement because of incorporation of host complement control proteins into its envelope. *Proceedings of the National Academy of Sciences*, **95**(13), 7544–7549.

Vanderplasschen, A., & Smith, G. L. (1997). A novel virus binding assay using confocal microscopy: demonstration that the intracellular and extracellular vaccinia virions bind to different cellular receptors. *Journal of Virology*, **71**(5), 4032–4041.

VanSlyke, J. K., & Hruby, D. E. (1990). Posttranslational modification of vaccinia virus proteins. *Current Topics in Microbiology and Immunology*, Springer, Berlin, Heidelberg, pp. 185–206.

Veillette, A. (2010). SLAM-Family Receptors: Immune Regulators with or without SAP-Family Adaptors. *Cold Spring Harbor Perspectives in Biology*, **2**(3), a002469–a002469.

Vély, F., Barlogis, V., Vallentin, B., … Vivier, E. (2016). Evidence of innate lymphoid cell redundancy in humans. *Nature Immunology*, **17**(11), 1291–1299.

Veyer, D. L., Carrara, G., Maluquer de Motes, C., & Smith, G. L. (2017). Vaccinia virus evasion of regulated cell death. *Immunology Letters*, **186**, 68–80.

Vitale, M., Bottino, C., Sivori, S., … Moretta, A. (1998). NKp44, a novel triggering surface molecule specifically expressed by activated natural killer cells, is involved in non-major histocompatibility complex-restricted tumor cell lysis. *Journal of Experimental Medicine*, **187**(12), 2065–2072.

Vitenshtein, A., Charpak-Amikam, Y., Yamin, R., … Mandelboim, O. (2016). NK Cell Recognition of

Candida glabrata through Binding of NKp46 and NCR1 to Fungal Ligands Epa1, Epa6, and Epa7. *Cell Host and Microbe*, **20**(4), 527–534.

Vivier, E. (2004). Natural Killer Cell Signaling Pathways. *Science*, **306**(5701), 1517–1519.

Vivier, E., Tomasello, E., Baratin, M., Walzer, T., & Ugolini, S. (2008). Functions of natural killer cells. *Nature Immunology*, **9**(5), 503–510.

Vogler, I., & Steinle, A. (2011). Vis-à-Vis in the NKC: Genetically Linked Natural Killer Cell Receptor/Ligand Pairs in the Natural Killer Gene Complex (NKC). *Journal of Innate Immunity*, **3**(3), 227–235.

Voigt, S., Sandford, G. R., Ding, L., & Burns, W. H. (2001). Identification and Characterization of a Spliced C-Type Lectin-Like Gene Encoded by Rat Cytomegalovirus. *Journal of Virology*, **75**(2), 603–611.

Wagenaar, T. R., & Moss, B. (2007). Association of Vaccinia Virus Fusion Regulatory Proteins with the Multicomponent Entry/Fusion Complex. *Journal of Virology*, **81**(12), 6286–6293.

Wagenaar, T. R., & Moss, B. (2009). Expression of the A56 and K2 proteins is sufficient to inhibit vaccinia virus entry and cell fusion. *Journal of Virology*, **83**(4), 1546–54.

Wagenaar, T. R., Ojeda, S., & Moss, B. (2008). Vaccinia Virus A56/K2 Fusion Regulatory Protein Interacts with the A16 and G9 Subunits of the Entry Fusion Complex. *Journal of Virology*, **82**(11), 5153–5160.

Waibler, Z., Anzaghe, M., Ludwig, H., … Kalinke, U. (2007). Modified Vaccinia Virus Ankara Induces Toll-Like Receptor-Independent Type I Interferon Responses. *Journal of Virology*, **81**(22), 12102–12110.

Walczak, H., Degli-Esposti, M. A., Johnson, R. S., … Rauch, C. T. (1997). TRAIL-R2: a novel apoptosis-mediating receptor for TRAIL. *The EMBO Journal*, **16**(17), 5386–5397.

Walter, L., & Ansari, A. A. (2015). MHC and KIR Polymorphisms in Rhesus Macaque SIV Infection. *Frontiers in Immunology*, **6**(OCT), 540.

Wang, J., Sanmamed, M. F., Datar, I., … Chen, L. (2019). Fibrinogen-like Protein 1 Is a Major Immune Inhibitory Ligand of LAG-3. *Cell*, **176**(1–2), 334-347.e12.

Wang, L. L., Chu, D. T., Dokun, A. O., & Yokoyama, W. M. (2000). Inducible Expression of the gp49B Inhibitory Receptor on NK Cells. *The Journal of Immunology*, **164**(10), 5215–5220.

Wang, W., Jiang, J., & Wu, C. (2020). CAR-NK for tumor immunotherapy: Clinical transformation and future prospects. *Cancer Letters*, **472**, 175–180.

Warren, H. S., Jones, A. L., Freeman, C., Bettadapura, J., & Parish, C. R. (2005). Evidence That the Cellular Ligand for the Human NK Cell Activation Receptor NKp30 Is Not a Heparan Sulfate Glycosaminoglycan. *The Journal of Immunology*, **175**(1), 207–212.

Wasilenko, S. T., Meyers, A. F. A., Vander Helm, K., & Barry, M. (2001). Vaccinia Virus Infection Disarms the Mitochondrion-Mediated Pathway of the Apoptotic Cascade by Modulating the Permeability Transition Pore. *Journal of Virology*, **75**(23), 11437–11448.

Wasilenko, S. T., Stewart, T. L., Meyers, A. F. A., & Barry, M. (2003). Vaccinia virus encodes a previously uncharacterized mitochondrial-associated inhibitor of apoptosis. *Proceedings of the National Academy of Sciences*, **100**(24), 14345–14350.

Watt, S., Fawcett, J., Murdoch, S., … Simmons, D. (1994). CD66 identifies the biliary glycoprotein

(BGP) adhesion molecule: cloning, expression, and adhesion functions of the BGPc splice variant. *Blood*, **84**(1), 200–210.

Weekes, M. P., Antrobus, R., Lill, J. R., Duncan, L. M., Hör, S., & Lehner, P. J. (2010). Comparative analysis of techniques to purify plasma membrane proteins. *Journal of Biomolecular Techniques*, **21**(3), 108–115.

Weekes, M. P., Antrobus, R., Talbot, S., … Lehner, P. J. (2012). Proteomic plasma membrane profiling reveals an essential role for gp96 in the cell surface expression of LDLR family members, including the LDL receptor and LRP6. *Journal of Proteome Research*, **11**(3), 1475–84.

Weekes, M. P., Tomasec, P., Huttlin, E. L., … Gygi, S. P. (2014). Quantitative Temporal Viromics: An Approach to Investigate Host-Pathogen Interaction. *Cell*, **157**(6), 1460–1472.

Wells, A. (1999). EGF receptor. *International Journal of Biochemistry and Cell Biology*, **31**(6), 637–643.

Welte, S., Kuttruff, S., Waldhauer, I., & Steinle, A. (2006). Mutual activation of natural killer cells and monocytes mediated by NKp80-AICL interaction. *Nature Immunology*, **7**(12), 1334–1342.

Wight, A., Mahmoud, A. B., Scur, M., … Makrigiannis, A. P. (2018). Critical role for the Ly49 family of class I MHC receptors in adaptive natural killer cell responses. *Proceedings of the National Academy of Sciences*, **115**(45), 11579–11584.

Wilcock, D., Duncan, Stephen A.Traktman, P., Zhang, W.-H., & Smith, G. L. (1999). The vaccinia virus A40R gene product is a nonstructural, type II membrane glycoprotein that is expressed at the cell surface. *Journal of General Virology*, **80**(8), 2137–2148.

Williams, K. J. N. N., Eaton, H. E., Jones, L., Rengan, S., & Burshtyn, D. N. (2016). Vaccinia virus Western Reserve induces rapid surface expression of a host molecule detected by the antibody 4C7 that is distinct from CLEC2D. *Microbiology and Immunology*, **60**(11), 754–769.

Williams, K. J. N., Wilson, E., Davidson, C. L., … Burshtyn, D. N. (2012). Poxvirus Infection-Associated Downregulation of C-Type Lectin-Related-b Prevents NK Cell Inhibition by NK Receptor Protein-1B. *The Journal of Immunology*, **188**(10), 4980–4991.

Williams, M., Roeth, J. F., Kasper, M. R., Fleis, R. I., Przybycin, C. G., & Collins, K. L. (2002). Direct Binding of Human Immunodeficiency Virus Type 1 Nef to the Major Histocompatibility Complex Class I (MHC-I) Cytoplasmic Tail Disrupts MHC-I Trafficking. *Journal of Virology*, **76**(23), 12173–12184.

Williamson, J. D., Reith, R. W., Jeffrey, L. J., Arrand, J. R., & Mackett, M. (1990). Biological characterization of recombinant vaccinia viruses in mice infected by the respiratory route. *Journal of General Virology*, **71**(11), 2761–2767.

Winkles, J. A. (2008). The TWEAK–Fn14 cytokine–receptor axis: discovery, biology and therapeutic targeting. *Nature Reviews Drug Discovery*, **7**(5), 411–425.

Wu, J., Song, Y., Bakker, A. B. H., … Phillips, J. H. (1999). An activating immunoreceptor complex formed by NKG2D and DAP10. *Science*, **285**(5428), 730–732.

Xu, F., Sunderland, A., Zhou, Y., Schulick, R. D., Edil, B. H., & Zhu, Y. (2017). Blockade of CD112R and TIGIT signaling sensitizes human natural killer cell functions. *Cancer Immunology, Immunotherapy*, **66**(10), 1367–1375.

Yammani, R. D., Pejawar-Gaddy, S., Gurley, T. C., Weimer, E. T., Hiltbold, E. M., & Alexander-Miller, M. A. (2008). Regulation of maturation and activating potential in CD8+ versus CD8− dendritic cells following in vivo infection with vaccinia virus. *Virology*, **378**(1), 142–150.

Yang, Q., Goding, S. R., Hokland, M. E., & Basse, P. H. (2006). Antitumor Activity of NK Cells. *Immunologic Research*, **36**(1–3), 13–26.

Yang, S., Wang, J., Brand, D. D., & Zheng, S. G. (2018). Role of TNF–TNF Receptor 2 Signal in Regulatory T Cells and Its Therapeutic Implications. *Frontiers in Immunology*, **9**(APR). doi:10.3389/fimmu.2018.00784

Yang, S. Y., Morishima, Y., Collins, N. H., … Dupont, B. (1984). Comparison of one-dimensional IEF patterns for serologically detectable HLA-A and B allotypes. *Immunogenetics*, **19**(3), 217–231.

Yewdell, J. W., Bennink, J. R., Smith, G. L., & Moss, B. (1985). Influenza A virus nucleoprotein is a major target antigen for cross-reactive anti-influenza A virus cytotoxic T lymphocytes. *Proceedings of the National Academy of Sciences*, **82**(6), 1785–1789.

Yu, G., Luo, H., Wu, Y., & Wu, J. (2003). Ephrin B2 Induces T Cell Costimulation. *The Journal of Immunology*, **171**(1), 106–114.

Yu, J., Freud, A. G., & Caligiuri, M. A. (2013). Location and cellular stages of natural killer cell development. *Trends in Immunology*, **34**(12), 573–582.

Yu, Q., Hu, N., & Ostrowski, M. (2009a). Poxvirus Tropism for Primary Human Leukocytes and Hematopoietic Cells. In *Methods in molecular biology (Clifton, N.J.)*, pp. 309–328.

Yu, X., Harden, K., Gonzalez, L. C., … Grogan, J. L. (2009b). The surface protein TIGIT suppresses T cell activation by promoting the generation of mature immunoregulatory dendritic cells. *Nature Immunology*, **10**(1), 48–57.

Yutoku, M., Grossberg, A. L., & Pressman, D. (1974). A cell surface antigenic determinant present on mouse plasmacytes and only about half of mouse thymocytes. *Journal of Immunology (Baltimore, Md. : 1950)*, **112**(5), 1774–81.

Zhou, Y., Xu, X., Tian, Z., & Wei, H. (2017). "Multi-Omics" Analyses of the Development and Function of Natural Killer Cells. *Frontiers in Immunology*, **8**. doi:10.3389/fimmu.2017.01095

Zhu, J., Martinez, J., Huang, X., & Yang, Y. (2007). Innate immunity against vaccinia virus is mediated by TLR2 and requires TLR-independent production of IFN-β. *Blood*, **109**(2), 619–625.

Zhu, Y., Paniccia, A., Schulick, A. C., … Edil, B. H. (2016). Identification of CD112R as a novel checkpoint for human T cells. *The Journal of Experimental Medicine*, **213**(2), 167–176.